Thick-skinned tectonics and basement-involved shortening in foreland fold-thrust belts : how the basement (and deeper lithospheric levels) controls geometry, kinematics and mechanics

Professeur Olivier LACOMBE

UPMC SORBONNE UNIVERSITÉS
cnrs
Institut des Sciences de la Terre de Paris ISTeP SORBONNE UNIVERSITÉS

The fold-and-thrust belt / foreland system

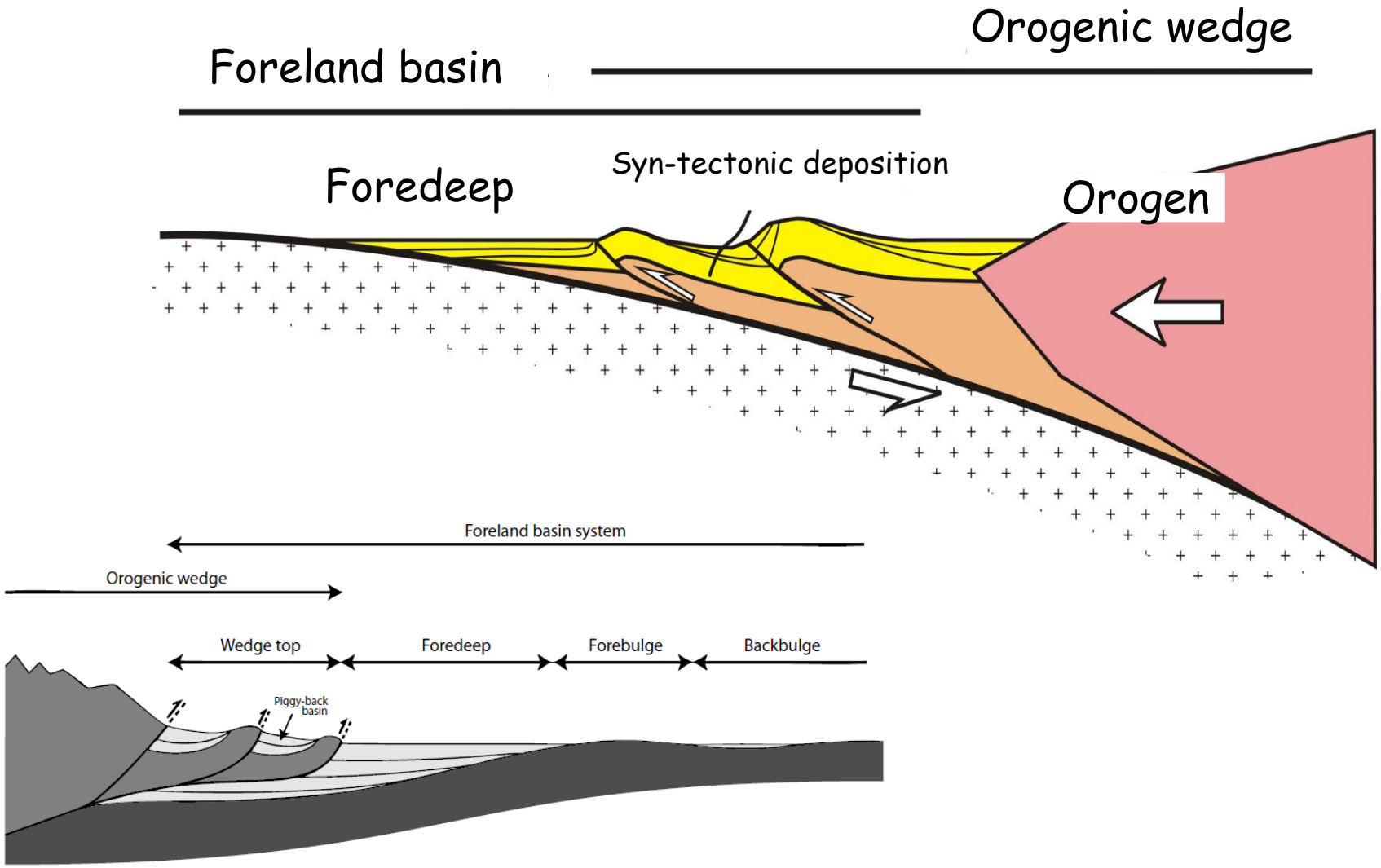

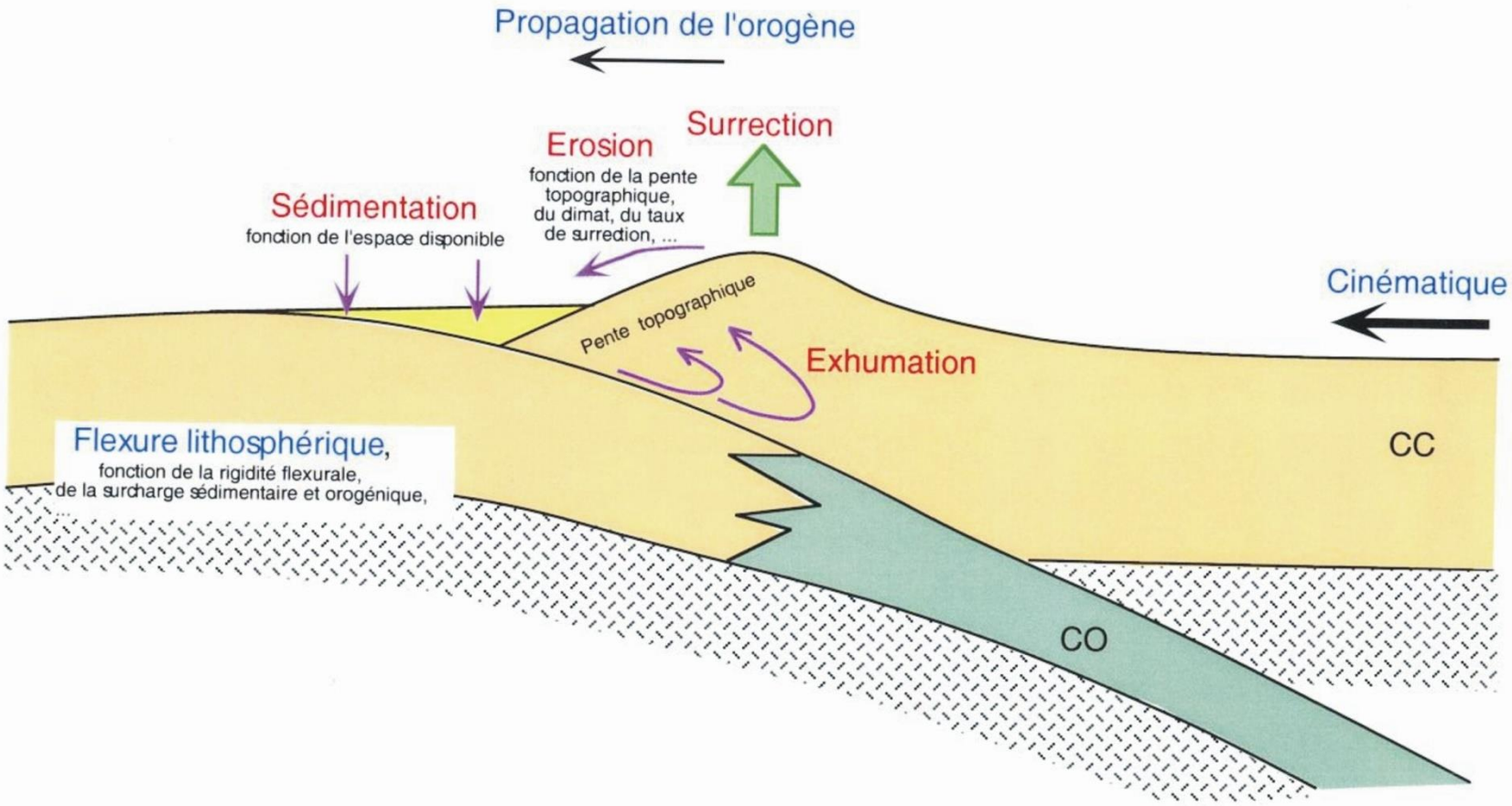
Propagation de l'orogène
Surrection
Erosion
fonction de la pente topographique, du dimat, du taux de surrection, ...
Sédimentation
fonction de l'espace disponible
Cinématique
Pente topographique
Exhumation
Flexure lithosphérique,
fonction de la rigidité flexurale, de la surcharge sédimentaire et orogénique, ...
CC
CO

Defining the structural style of fold-thrust belts and understanding the controlling factors are necessary steps toward prediction of their long-term and short-term dynamics, including seismic hazard, and to assess their potential in terms of hydrocarbon exploration.

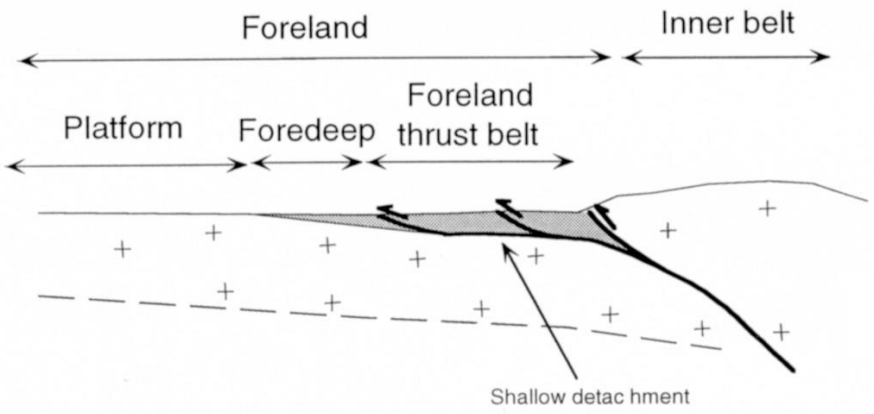

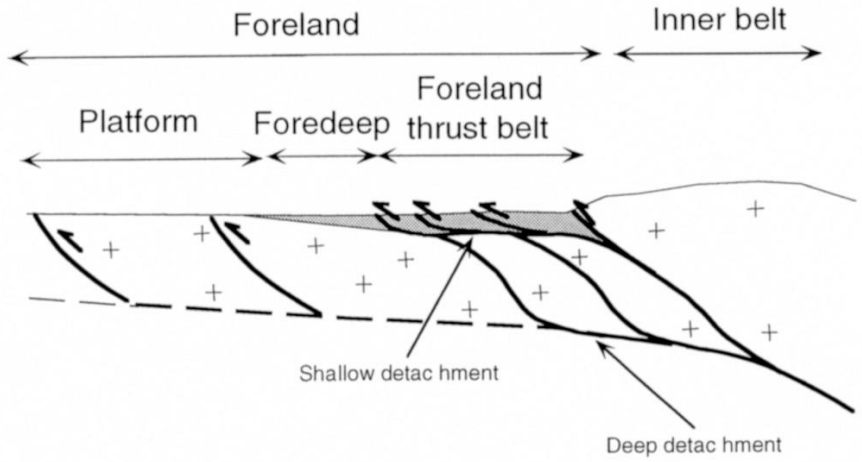

(Lacombe and Mouthereau, 2002)

simple-shear style "subduction"

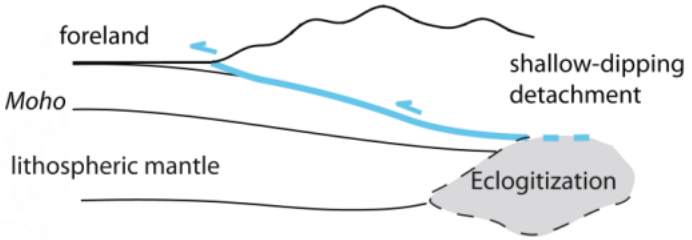

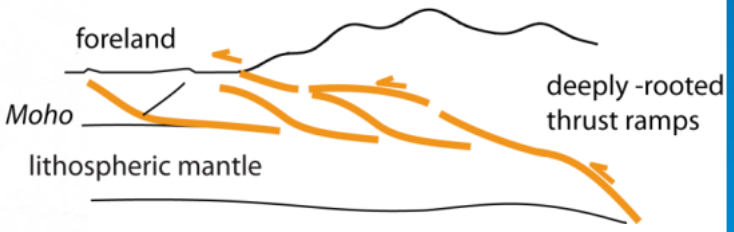

pure-shear style "inversion"

Mouthereau et al,, 2013)

Internal thickening until critical angle α is reached

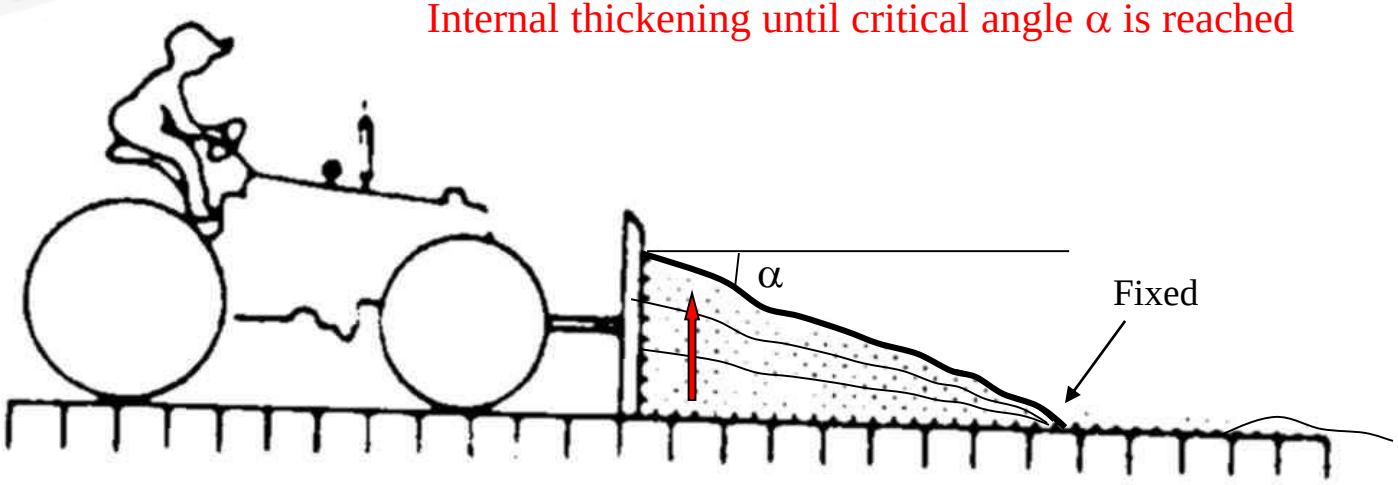

1. Basal sliding without internal thickening, then
2. New snow is incorporated in the wedge, α is lowered, then
3. The wedge will deform internally until α is reached again, and so on

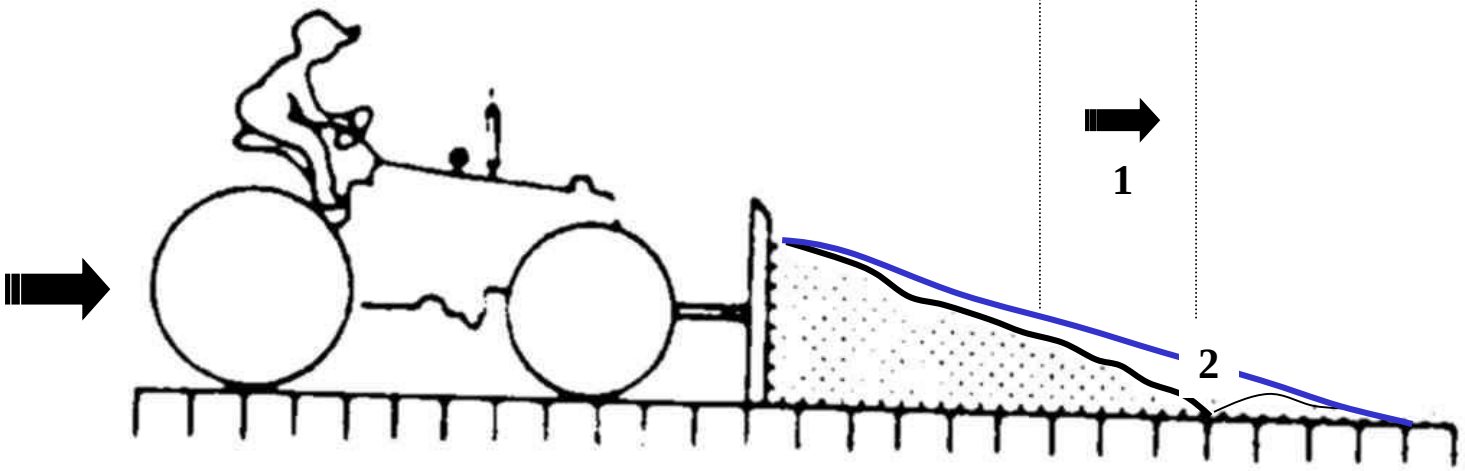

Davis et al. (1983)

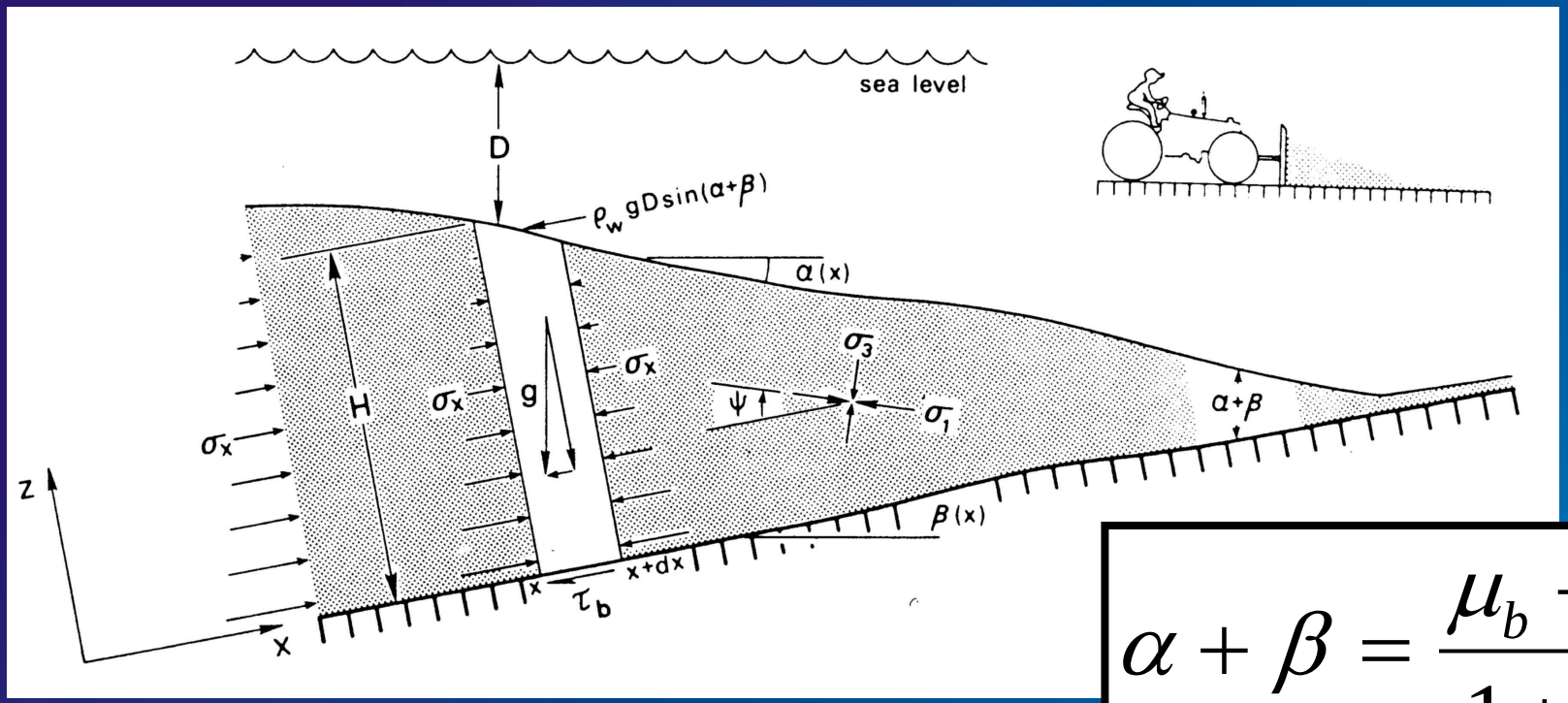

$$\alpha + \beta = \frac{\mu_b + \beta}{1 + K}$$

for a non-cohesive sub-aerial wedge

$$\rho g H \beta + \rho_w g D(\alpha + \beta) + \tau_b + \frac{d}{dx}\int_0^H \sigma_x dz = 0$$

Weight of sedimentary column (lithostatic pressure)

Weight of water column

Basal frictional shear strength)

Sum of lateral push forces

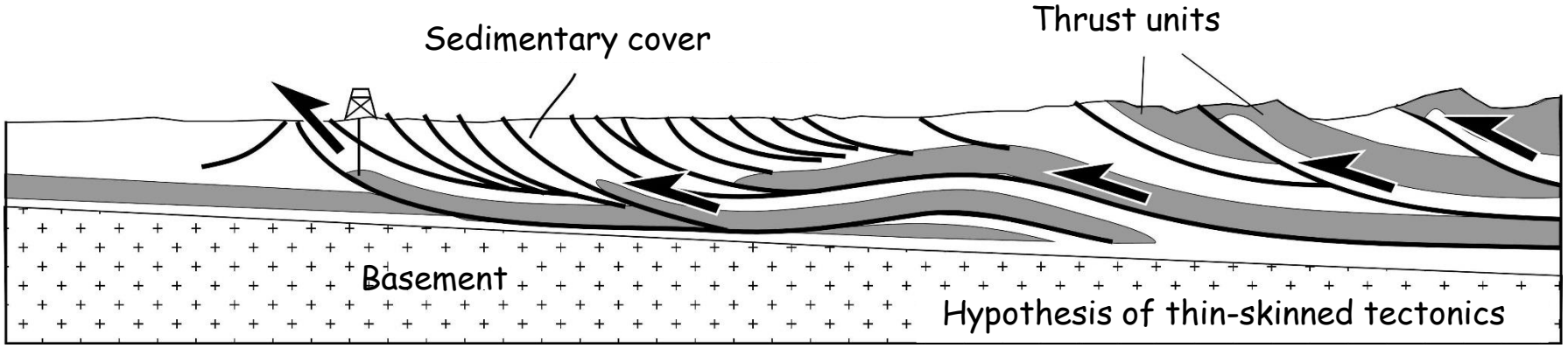

Shortening is accommodated in the upper part of the crust above a basal décollement dipping toward the hinterland

Implicit assumption of « thin-skinned » tectonic style

Topographic slope and dip of basal décollement define the orogenic wedge

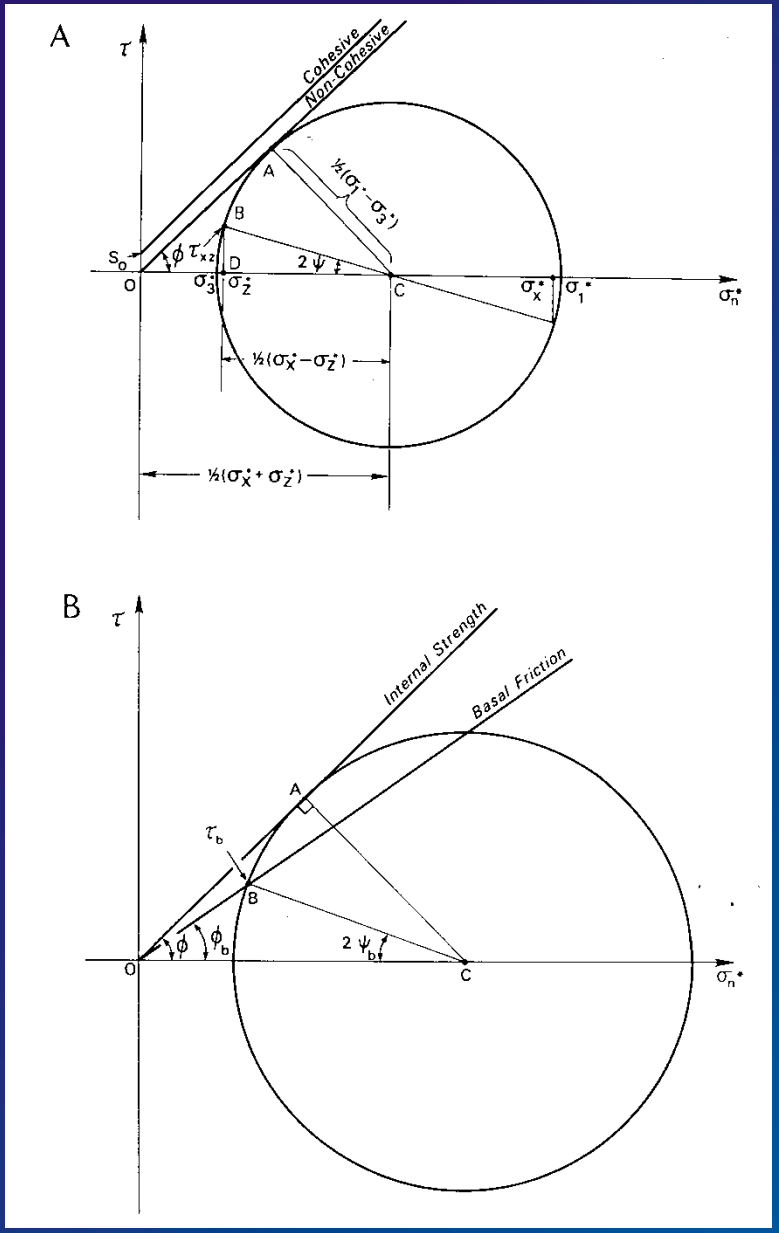

Conditions de fracturation et état critique

Dans le prisme

→ ***Critère de néorupture (Mohr-Coulomb)***

$$\tau_i = C_o + \mu_c \sigma_n$$

$$\tau_b = C_f + \mu_f \sigma_n$$

avec $\mu_f < \mu_c$

Le prisme est à l'état critique lorsque le cercle tangente la droite de néorupture

Base du prisme

→ ***Critère de friction***

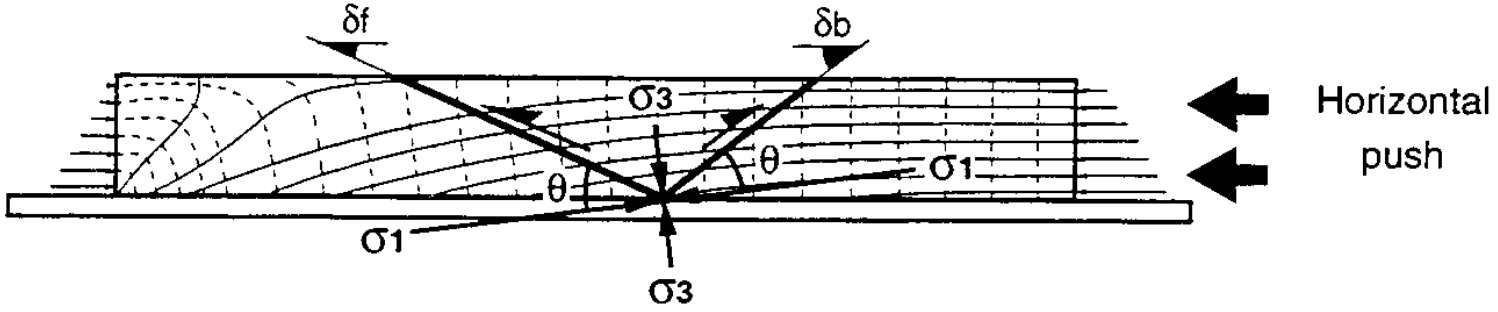

$$tg\ 2\theta = 2\ .\tau b\ /\ (\sigma h - \sigma v)$$

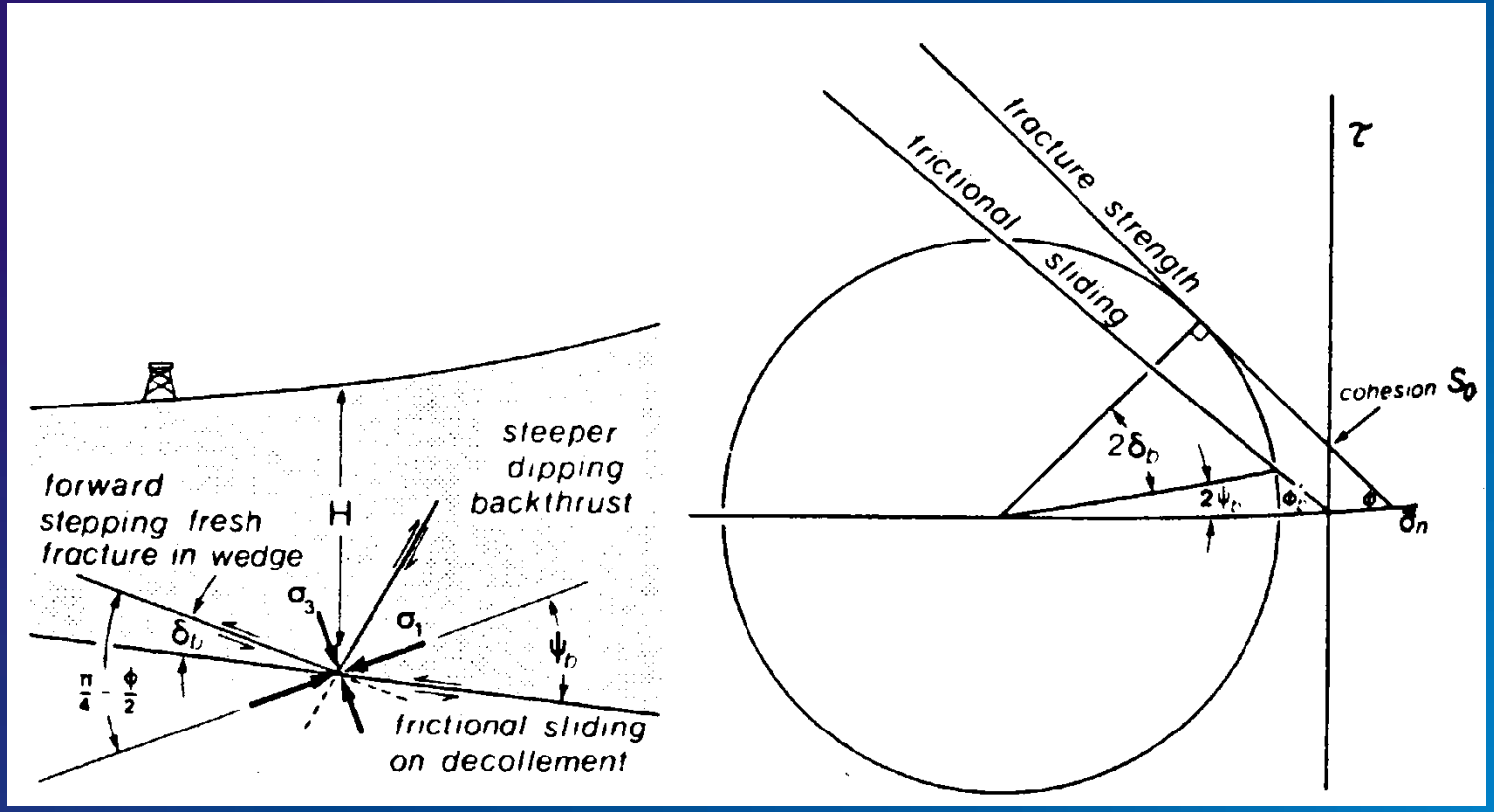
steeper
dipping
backthrust
forward
stepping fresh
fracture in wedge
H
σ_3
σ_1
δ_b
ψ_b
$\frac{\pi}{4} - \frac{\phi}{2}$
frictional sliding
on decollement
fracture strength
frictional
sliding
τ
cohesion S_0
$2\delta_b$
$2\psi_b$
ϕ_i
ϕ
σ_n

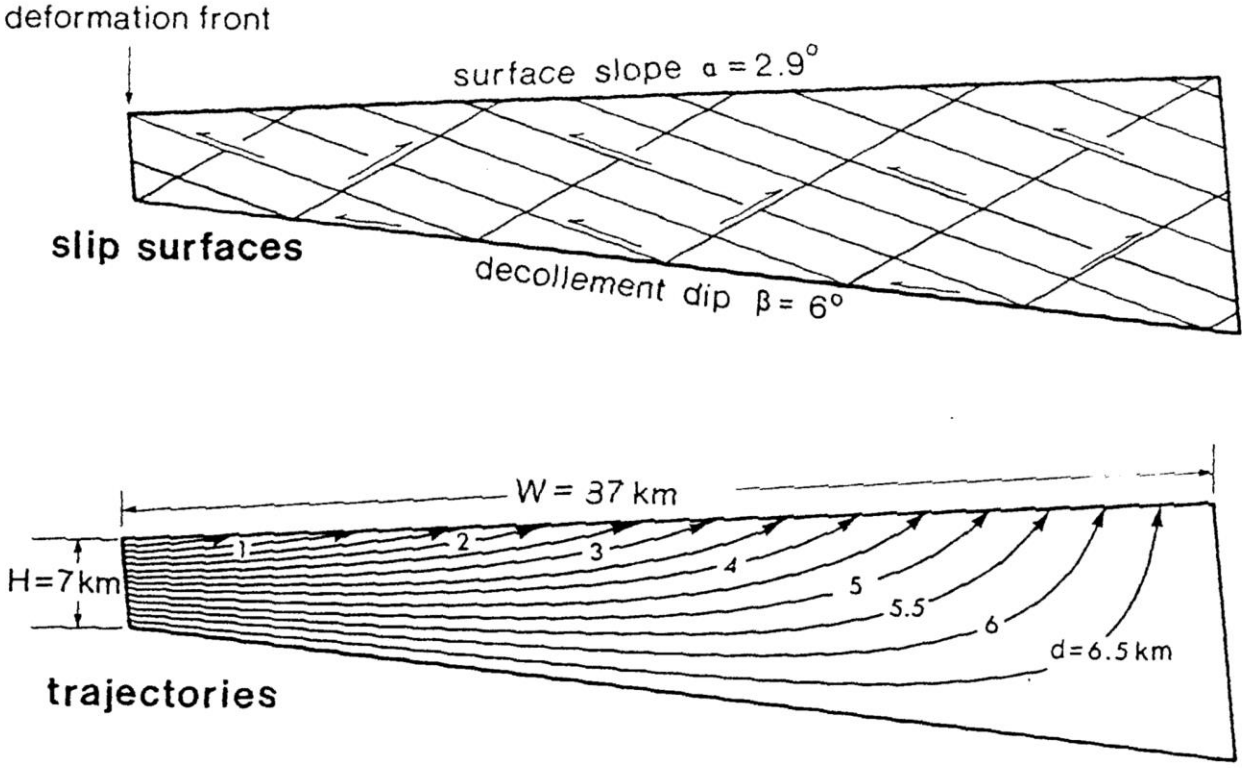

Figure 14. Theoretical slip surfaces and rock trajectories in the critically tapered Taiwan wedge, assuming $\mu = 0.85$.

Dahlen et Suppe, 1988

Le prisme est dit « stable » lorsqu'il ne se déforme pas (pas de changement de sa topographie)

- il glisse passivement

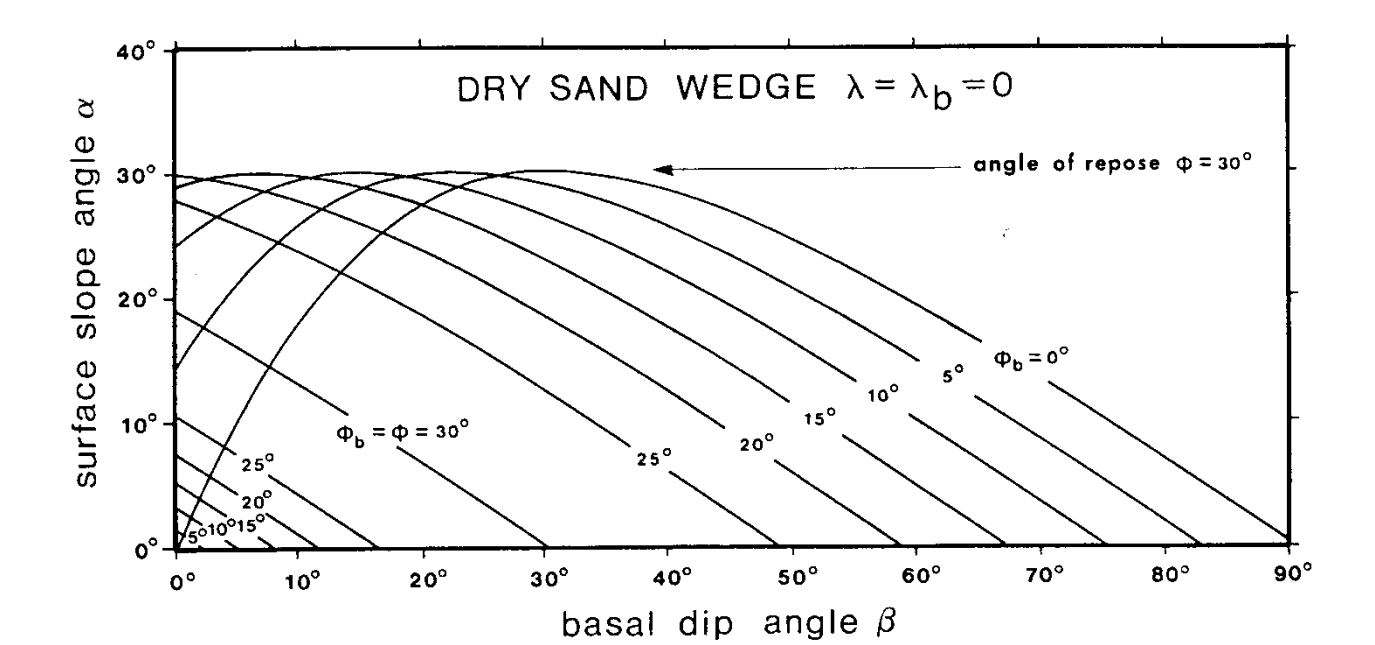

Enveloppes de stabilité

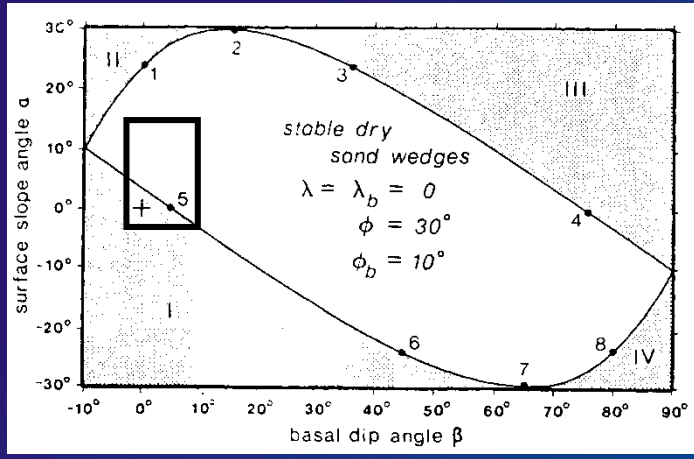

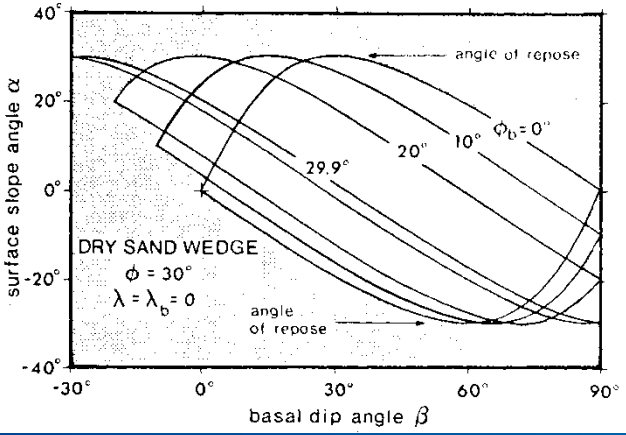

EXAMPLES OF CRITICAL DRY SAND WEDGES

1. *normal faulting and downslope flow*

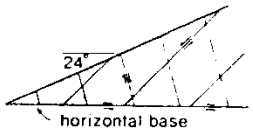

2. *surface at angle of repose*

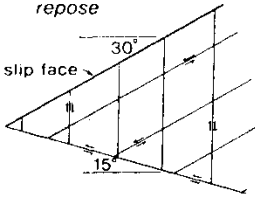

3. *combined normal and thrust faulting*

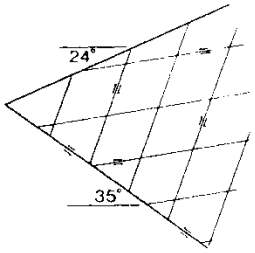

4. *thrust faulting*

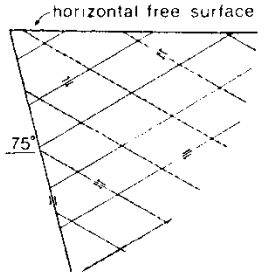

5. *accretionary wedge fails by thrusting*

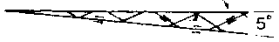

6. *combined normal and thrust faulting*

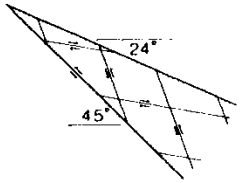

7. *surface at angle of repose*

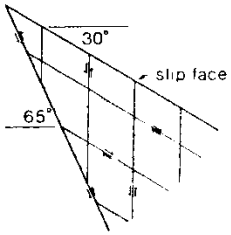

8. *normal faulting*

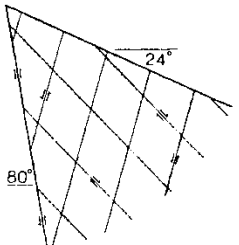

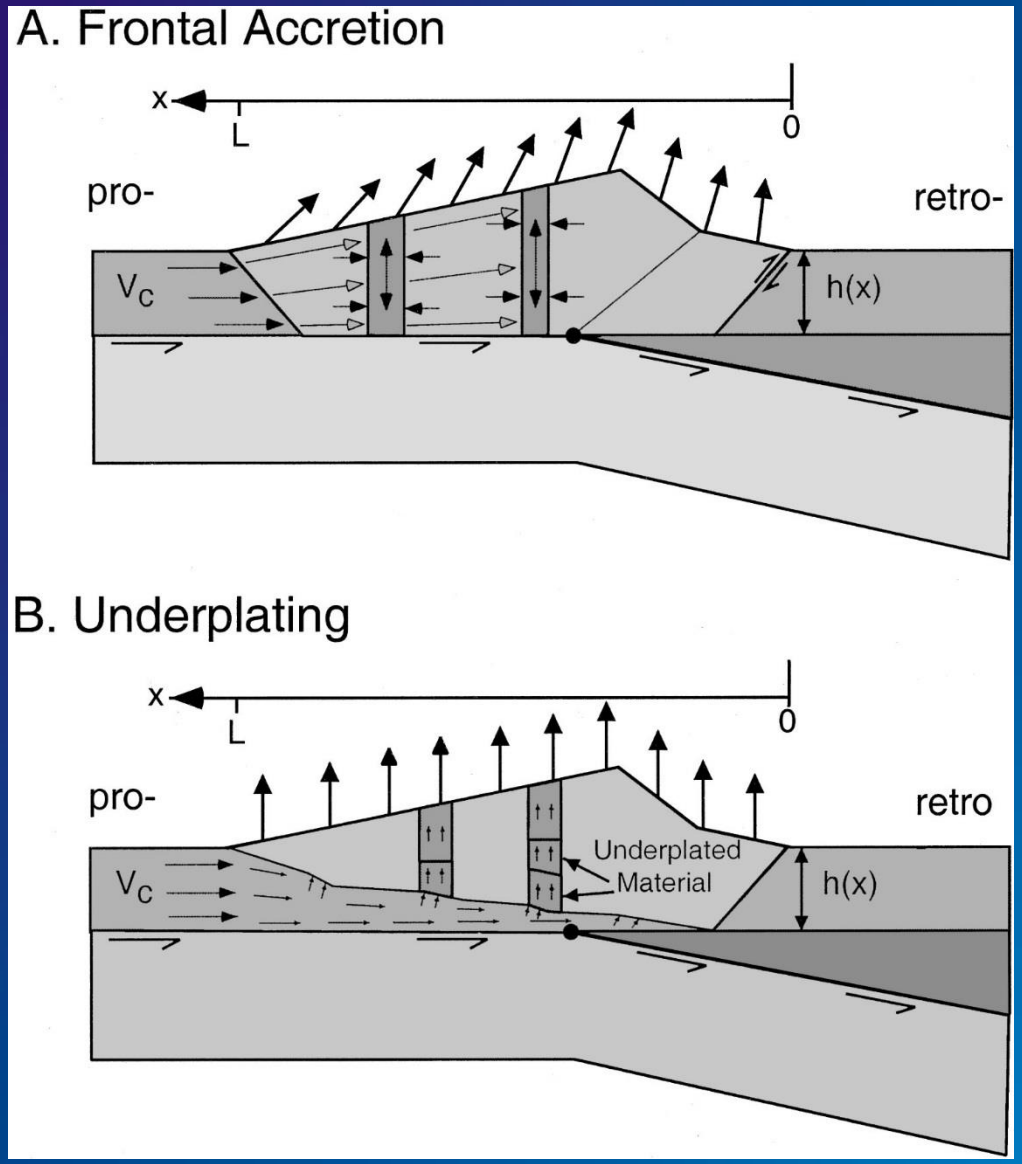

Willett et al., 2001

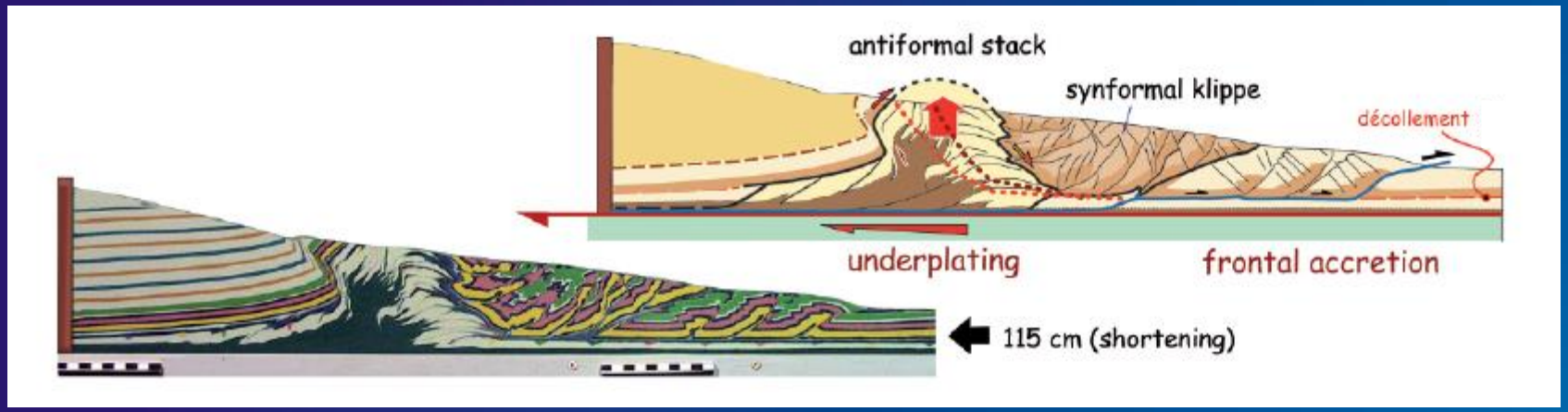
antiformal stack
synformal klippe
décollement
underplating
frontal accretion
115 cm (shortening)

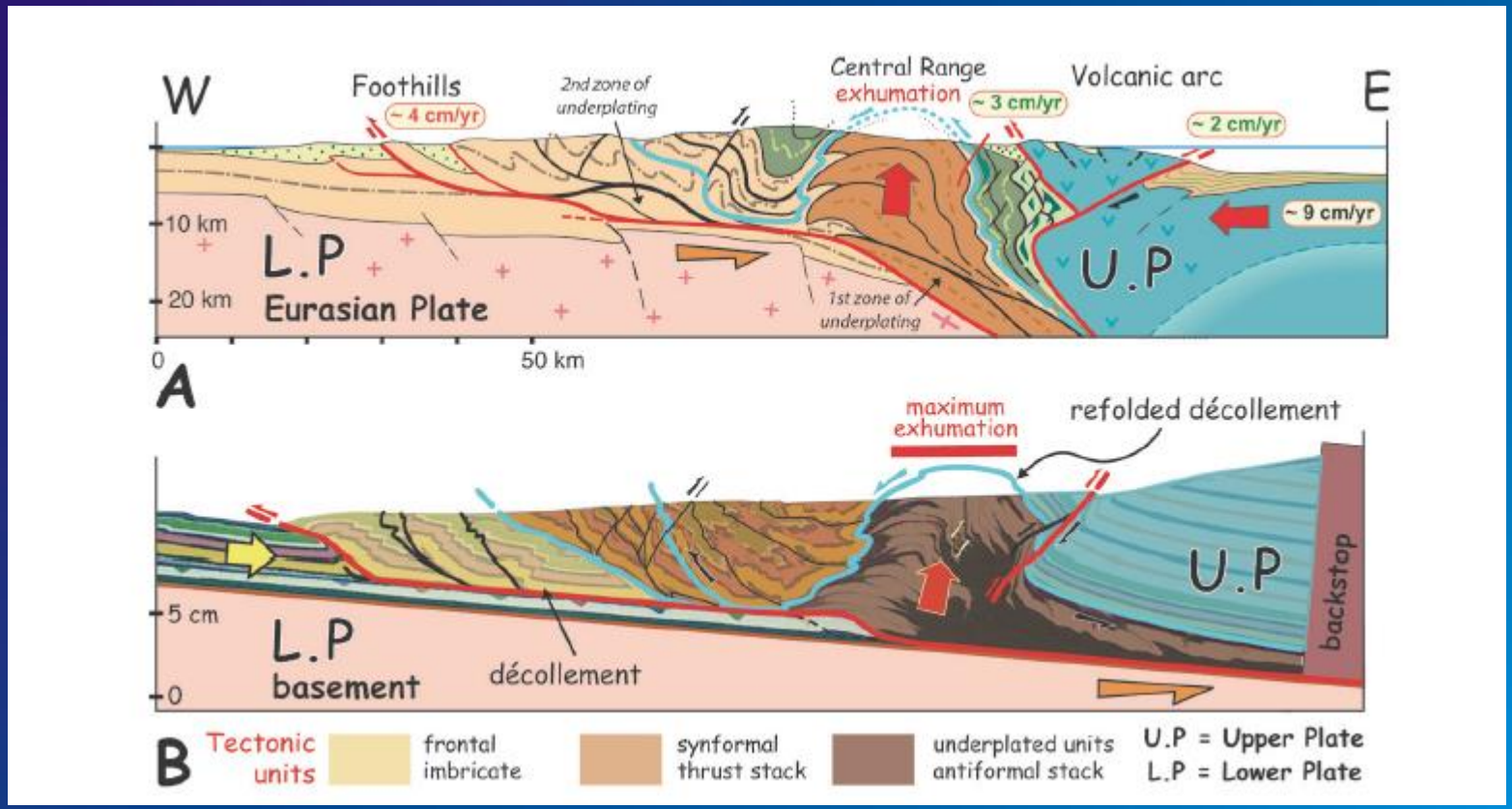
W
Foothills
~ 4 cm/yr
2nd zone of underplating
Central Range exhumation
~ 3 cm/yr
Volcanic arc
~ 2 cm/yr
E
~ 9 cm/yr
10 km
20 km
L.P
Eurasian Plate
U.P
1st zone of underplating
0
50 km
A
maximum exhumation
refolded décollement
5 cm
0
L.P
basement
décollement
U.P
backstop
B
Tectonic units
frontal imbricate
synformal thrust stack
underplated units antiformal stack
U.P = Upper Plate
L.P = Lower Plate

Basement involvement in fold-and-thrust belts : what are the evidence?

Davis et al. (1983) model however fundamentally meets several main restrictions.

A first one is related to the assumed homogeneous nature of the material of the wedge, so that widespread reactivation of preexisting faults in the cover is not generally considered.

A second one lies in the assumed rigid and undeformable behaviour of the substratum below the basal décollement, leading generally to implicitely favor thin-skin tectonics styles, so that basement-involved shortening is not accounted for.

Reactivation/inversion of basement faults widespreadly occurs during orogenic evolution of collided passive margins and this process is known to exert a strong control on the evolution of orogen

Number of regional studies have demonstrated the compressional reactivation of preexisting extensional structures within the cover and the basement of foreland thrust belts (e.g., Alps, Urals, Andes, Zagros, Rockies, Taiwan, …).

Signature of basement-involved shortening in foreland thrust belts ?

Basement fault reactivation may induce :

-localization of thrusts and folds in the developing shallow thrust wedge;
-inversion of extensional faults and development of crystalline thrust sheets;
- out-of-sequence thrusting and refolding of shallow nappes;
- development of accommodation structures such as lateral ramps;
- development of basement uplifts.

In foreland thrust belts of young but no longer active orogens (e.g., Pyrenees-Provence), these signatures can therefore be identified in some places by careful structural investigations of the relationships between cover and basement.

In more recent orogens (e.g., western Alps), active basement uplifts recognized by geodesy or gravimetric investigations may complement structural analyses in demonstrating deep basement thrusting.

In still active orogens (e.g., Taiwan, Zagros), seismicity combined with structural analyses provides first-order constraints on deep crustal deformation.

In all cases, the study of inversion of preexisting basement (normal) faults is generally much easier in forelands than in inner parts of orogens where the initial relationships between the basement and its sedimentary cover have generally not been preserved and the initial attitude of the faults has been strongly modified or erased by later evolution.

Tertiary fold-thrust belts

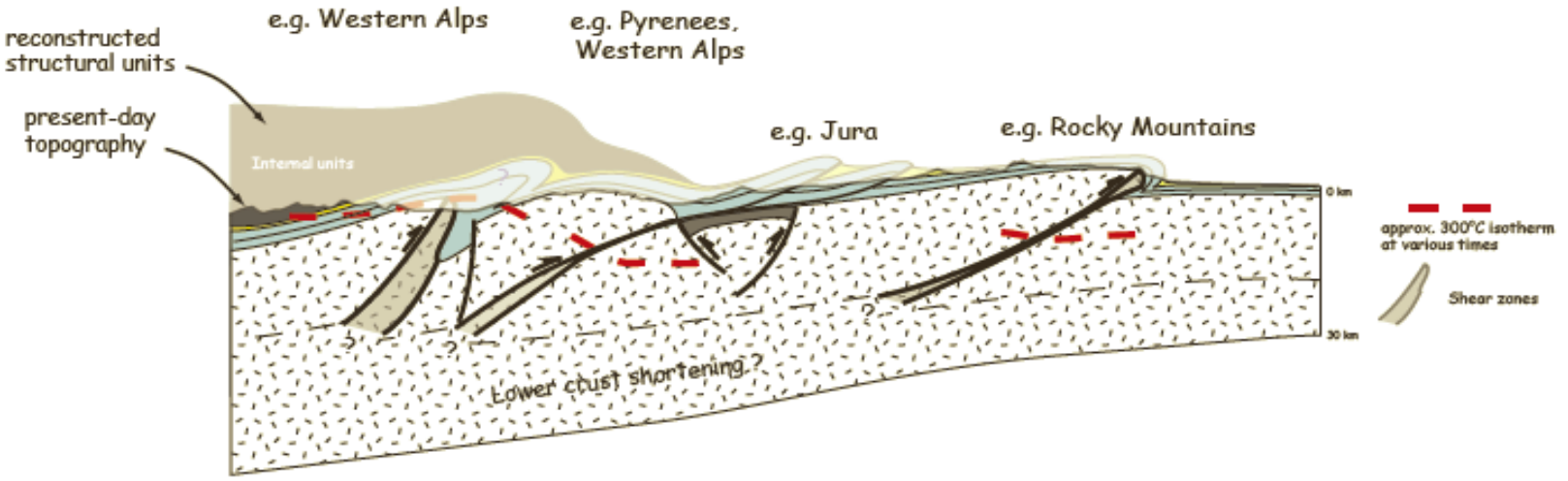

Active fold-thrust belts

e.g. Sierras Pampeanas

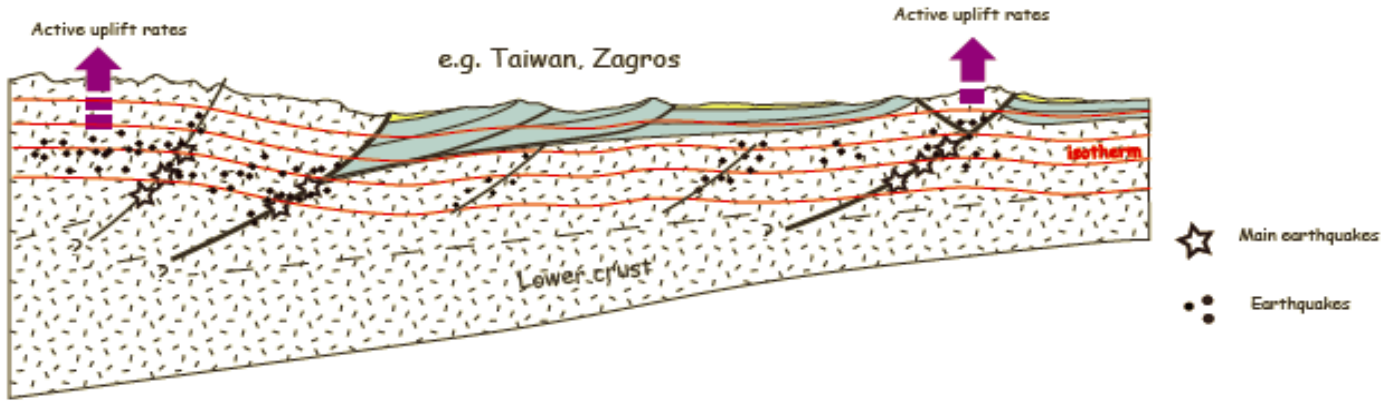

Basement-involved shortening in the upper plate above an oceanic flat-slab subduction zone

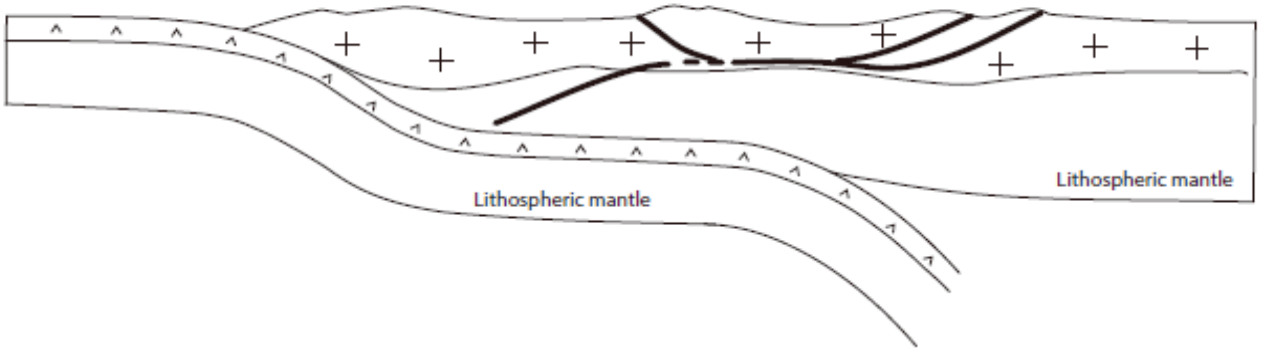

'Classical' basement-involved shortening in the lower/upper plate

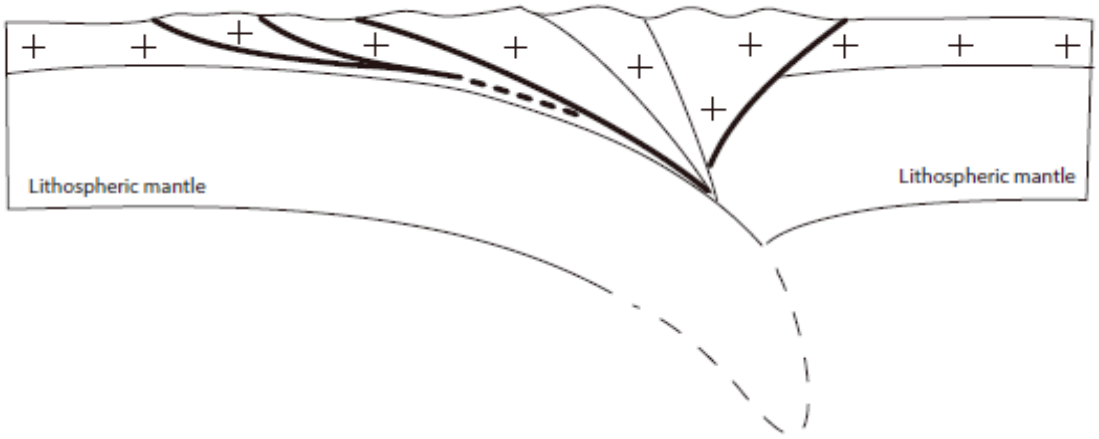

Oisans (western Alps) - style :
distributed shearing within the basement reflecting basement underplating then frontal accretion/exhumation thanks to crustal thrust ramps

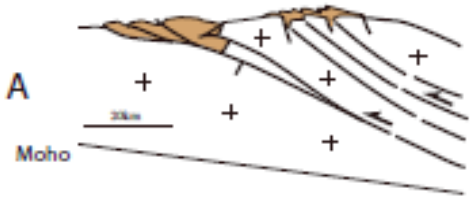

Mont Blanc (western Alps) - style :
Stacking of crustal slices at the rear of the thin-skinned fold-thrust belt as a result of basement underplating and localized exhumation then frontal accretion/exhumation thanks to crustal thrust ramps

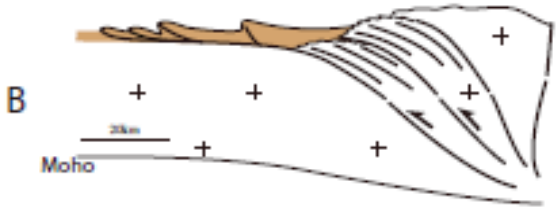

Zagros -style : superimposed thin-skinned and thick-skinned tectonic styles.
The basement deforms by both seismogenic faulting and ductile aseismic shearing below the deforming detached cover

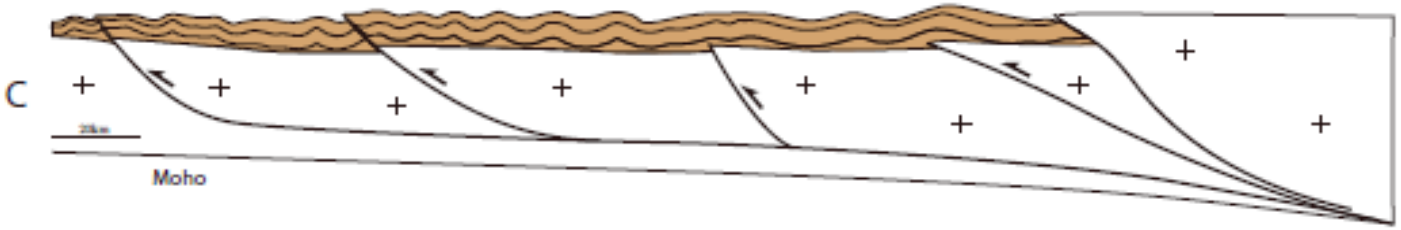

Sierras Pampeanas-Laramide - style : the basement is involved in the foreland of the thin-skinned belt (basement uplifts).

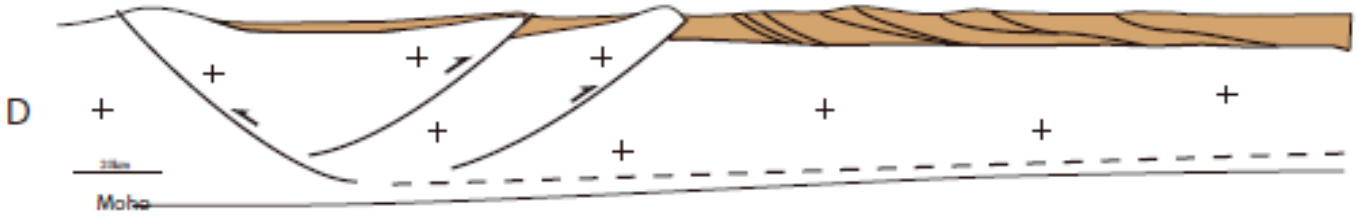

Basement control on the late evolution of fold-and-thrust belts : the Jura case

CARTE GÉOLOGIQUE DE LA FRANCE

à l'échelle du millionième

6e édition

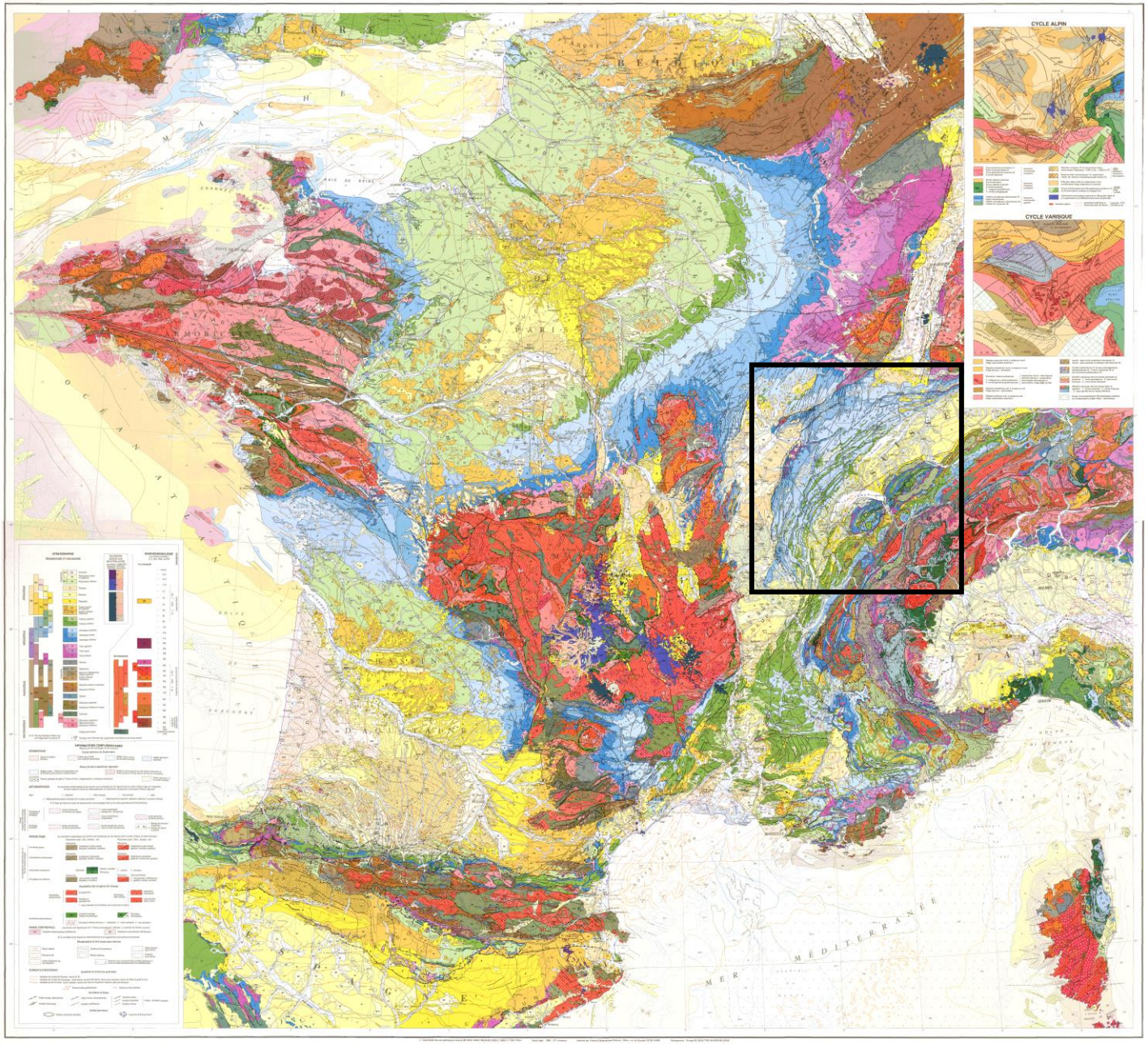

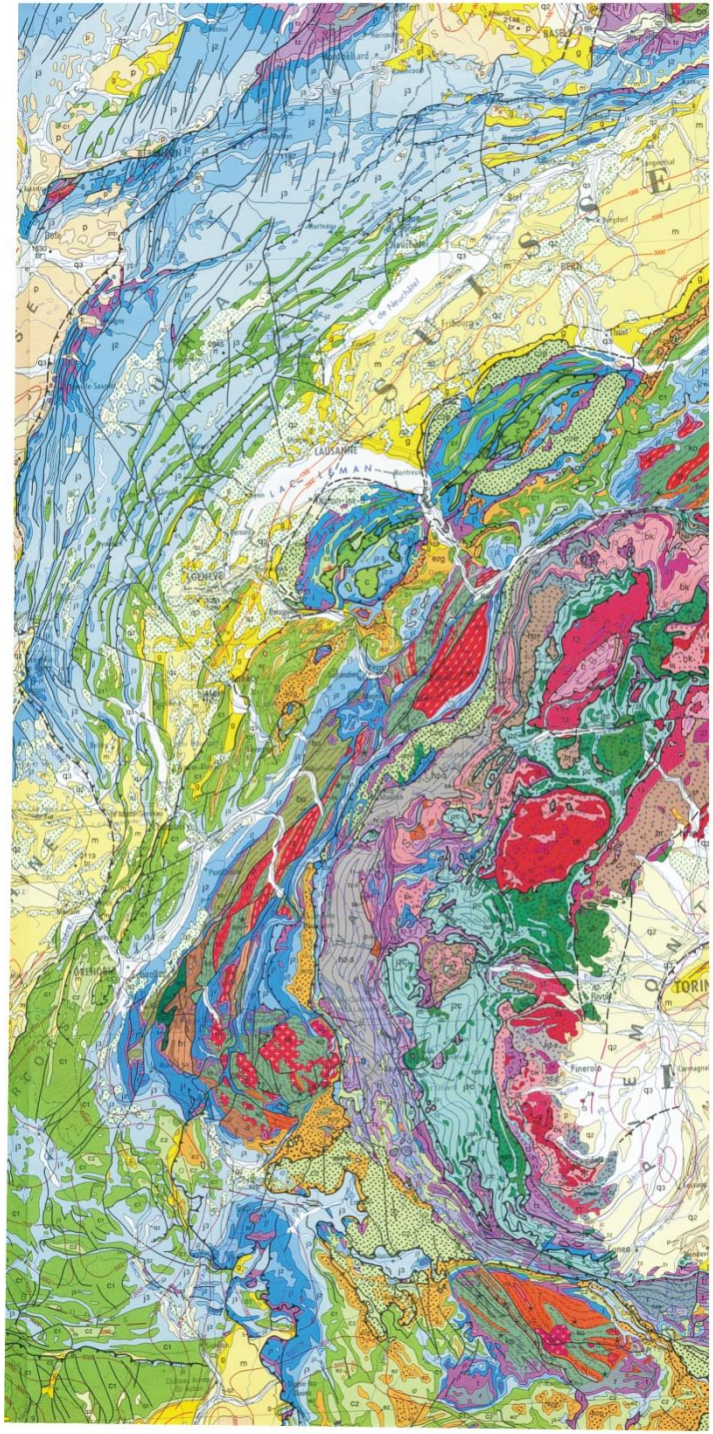
BASEL
BERN
LAUSANNE
LAC LÉMAN
GENÈVE
TORINO

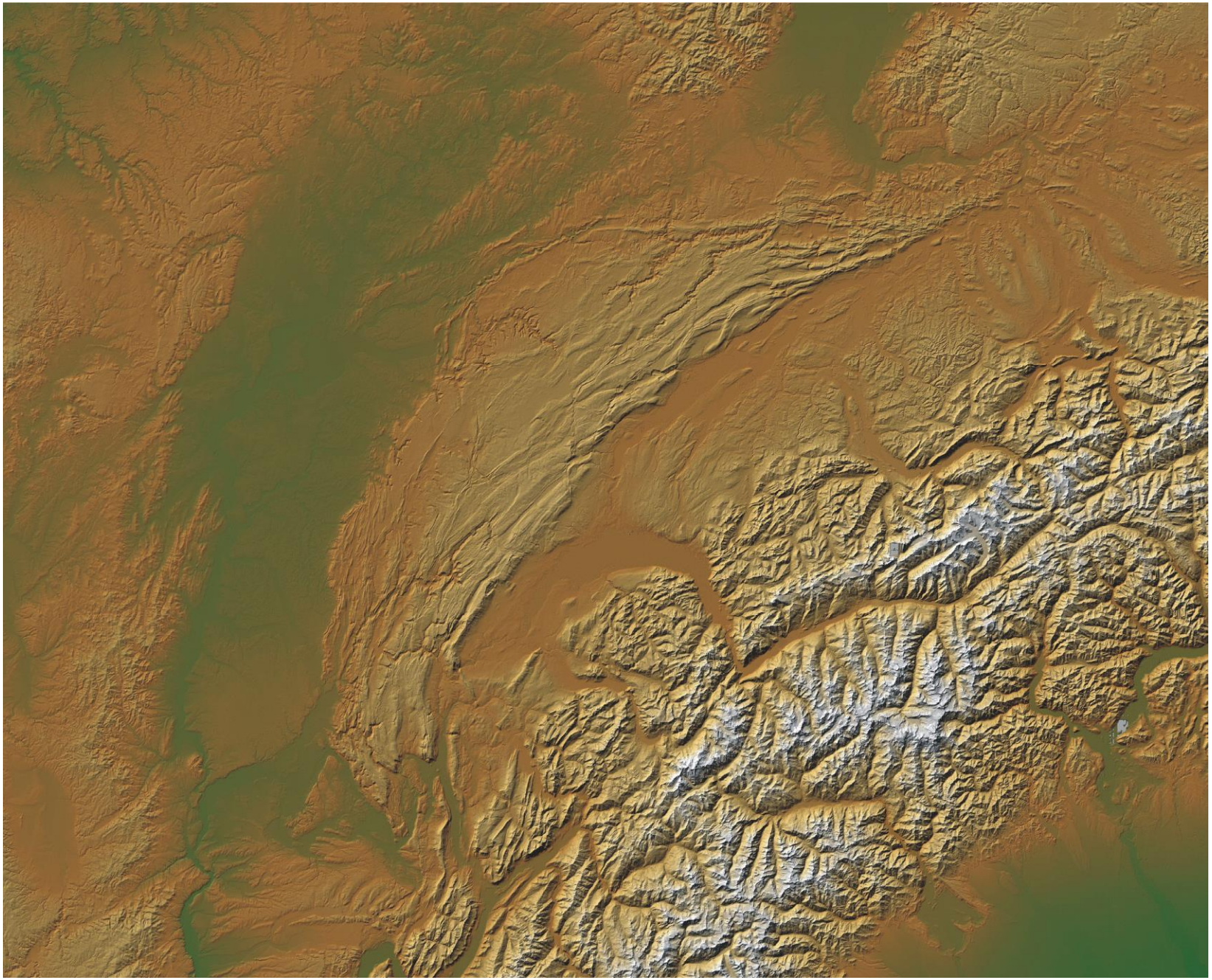

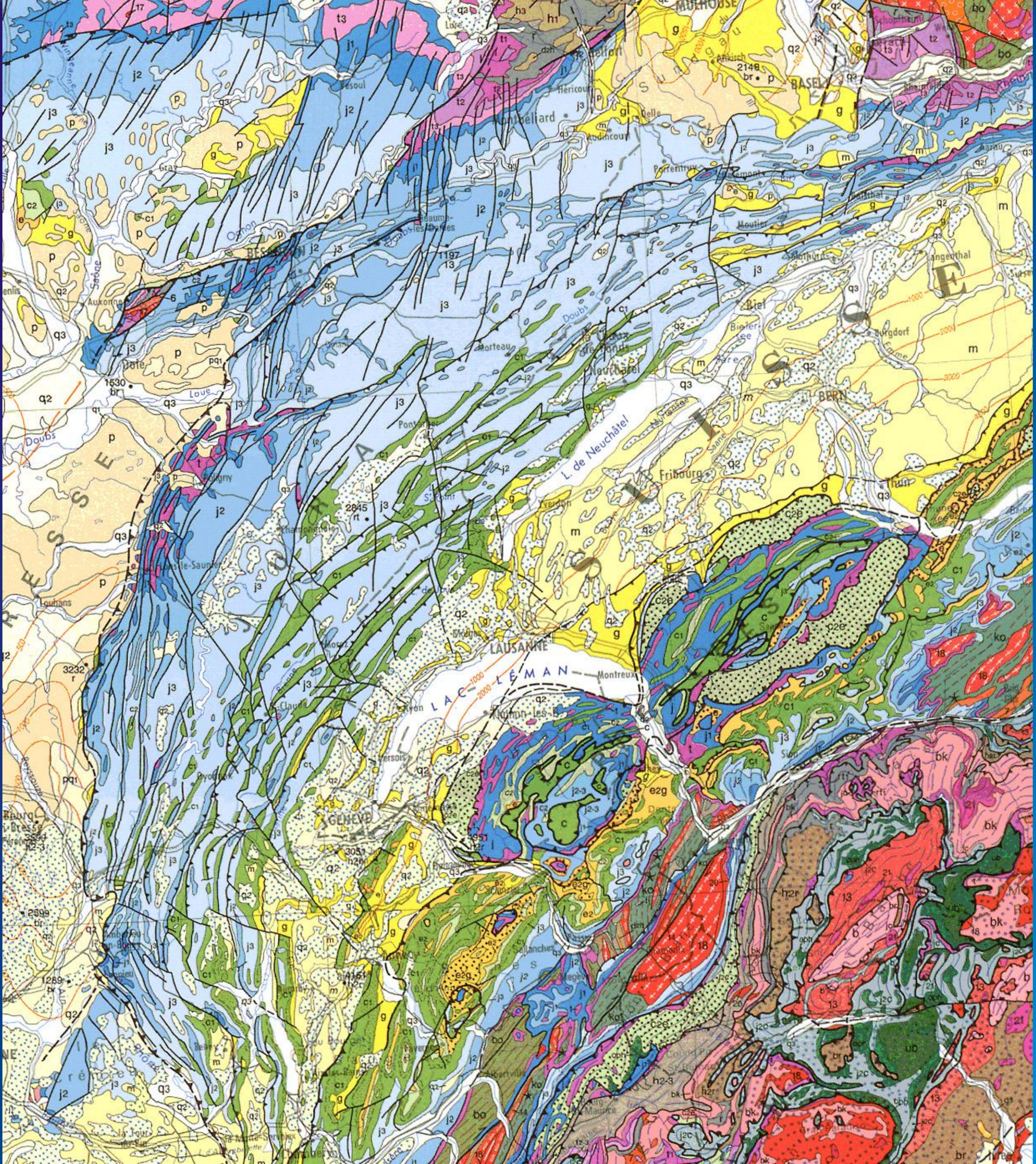
MULHOUSE
BASEL
Montbéliard
Porrentruy
Biel
Burgdorf
Langenthal
BERN
Neuchâtel
L. de Neuchâtel
Fribourg
Yverdon
Thun
Doubs
Loue
Dole
LAUSANNE
LAC LÉMAN
Montreux
Thonon-les-B.
Nyon
GENÈVE
Sion

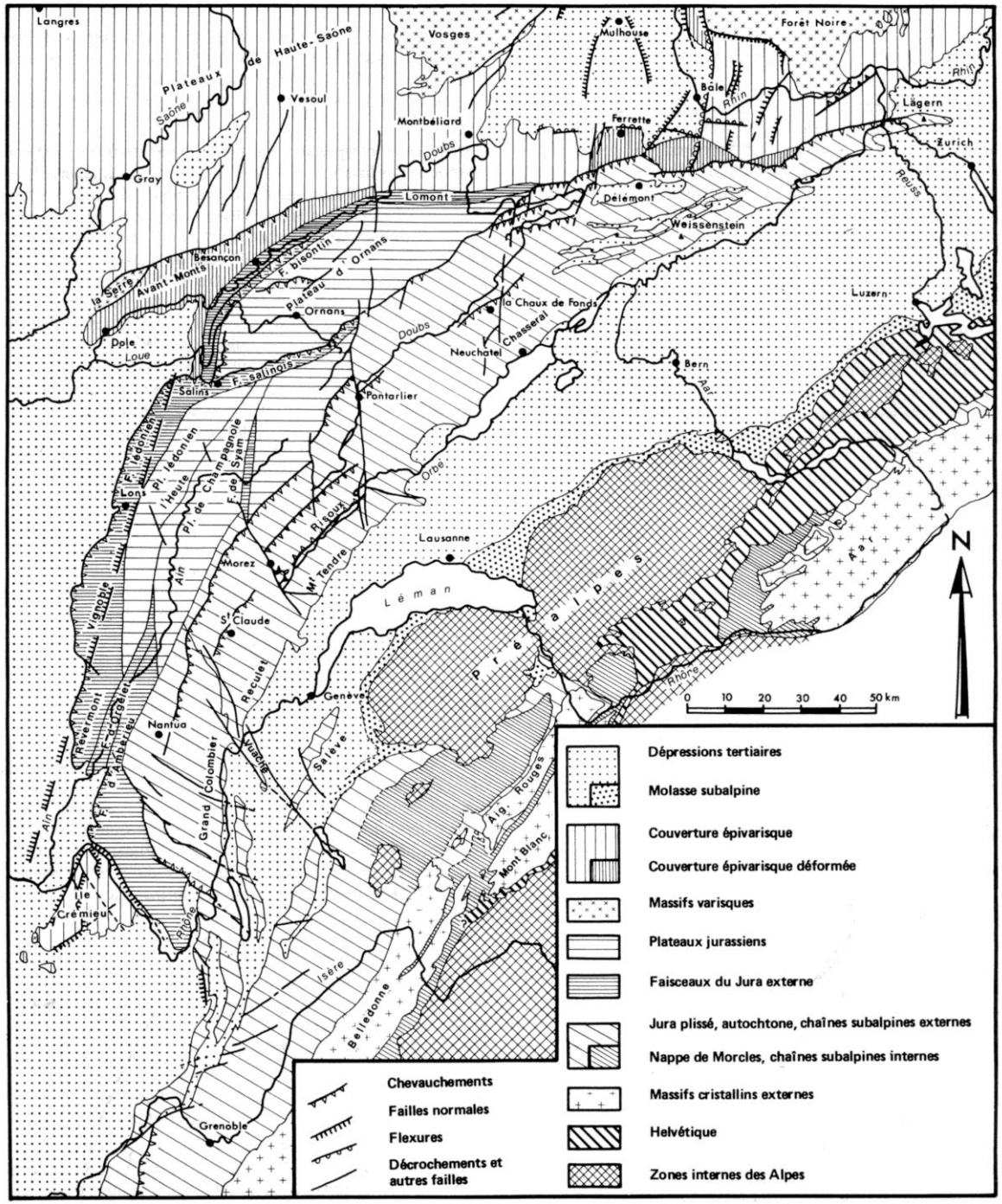
Langres
Vosges
Mulhouse
Forêt Noire
Plateaux de Haute-Saône
Saône
Vesoul
Bâle
Rhin
Lägern
Montbéliard
Ferrette
Zurich
Doubs
Gray
Lomont
Delémont
Reuss
Weissenstein
la Serre
Avant-Monts
Besançon
F. bisontin
Plateau d'Ornans
Luzern
Ornans
La Chaux de Fonds
Chasseral
Doubs
Dole
Loue
Neuchatel
Bern
F. salinois
Salins
Pontarlier
Aar
Orbe
Lons
Pl. lédonien
l'Heute
Pl. de Champagnole
F. de Syam
Risoux
Lausanne
Morez
Mt Tendre
Ain
Léman
Préalpes
St Claude
Vignoble
Reculet
Genève
Rhône
Nantua
Colombier
Vuache
Salève
Alp. Rouges
Mont Blanc
Grand
Ain
Crémieu
Isère
Belledonne
Grenoble
N
0 10 20 30 40 50 km
Dépressions tertiaires
Molasse subalpine
Couverture épivarisque
Couverture épivarisque déformée
Massifs varisques
Plateaux jurassiens
Faisceaux du Jura externe
Jura plissé, autochtone, chaînes subalpines externes
Nappe de Morcles, chaînes subalpines internes
Massifs cristallins externes
Helvétique
Zones internes des Alpes
Chevauchements
Failles normales
Flexures
Décrochements et autres failles

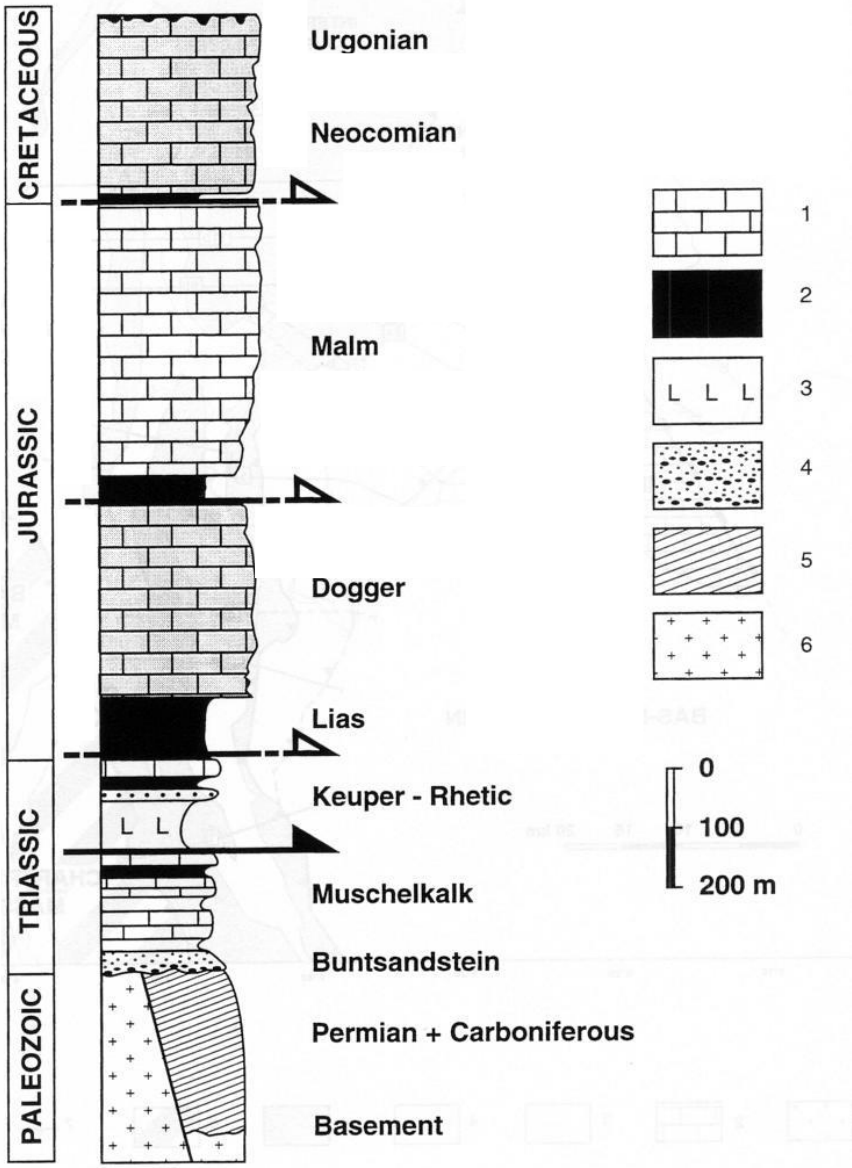
CRETACEOUS
JURASSIC
TRIASSIC
PALEOZOIC
Urgonian
Neocomian
Malm
Dogger
Lias
Keuper - Rhetic
Muschelkalk
Buntsandstein
Permian + Carboniferous
Basement
L L
L L L
1
2
3
4
5
6
0
100
200 m

Distribution of Triassic evaporites below the Jura

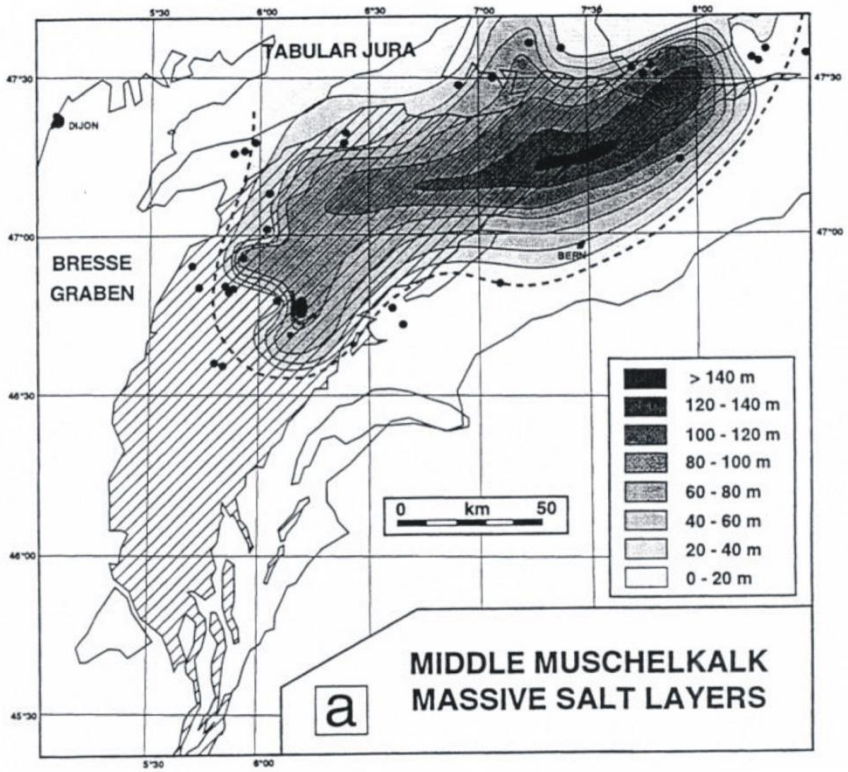

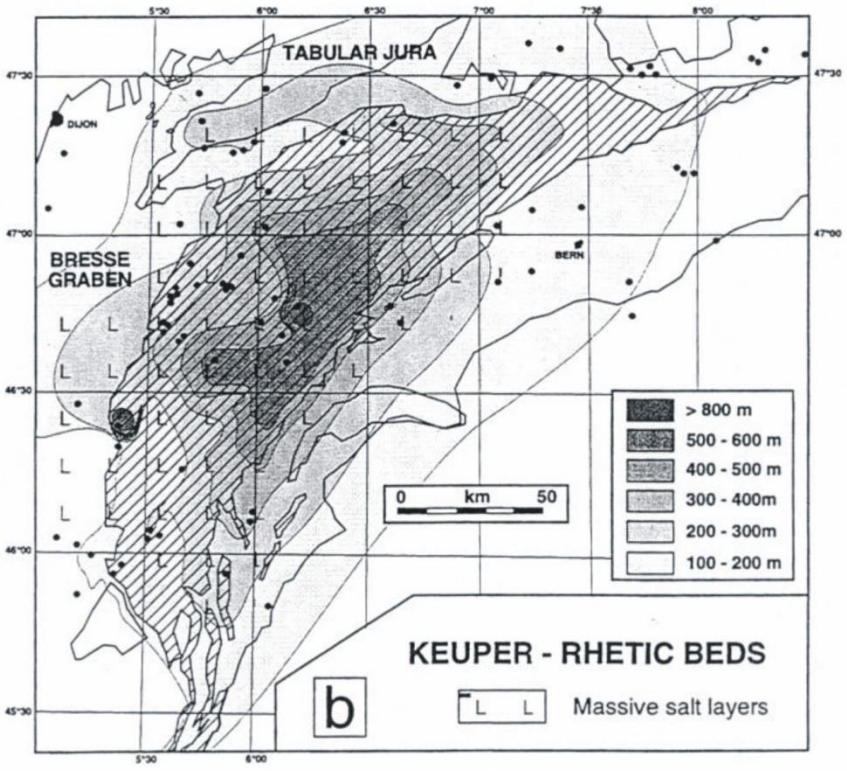

(Lienhard, 1984)

(Philippe, 1995)

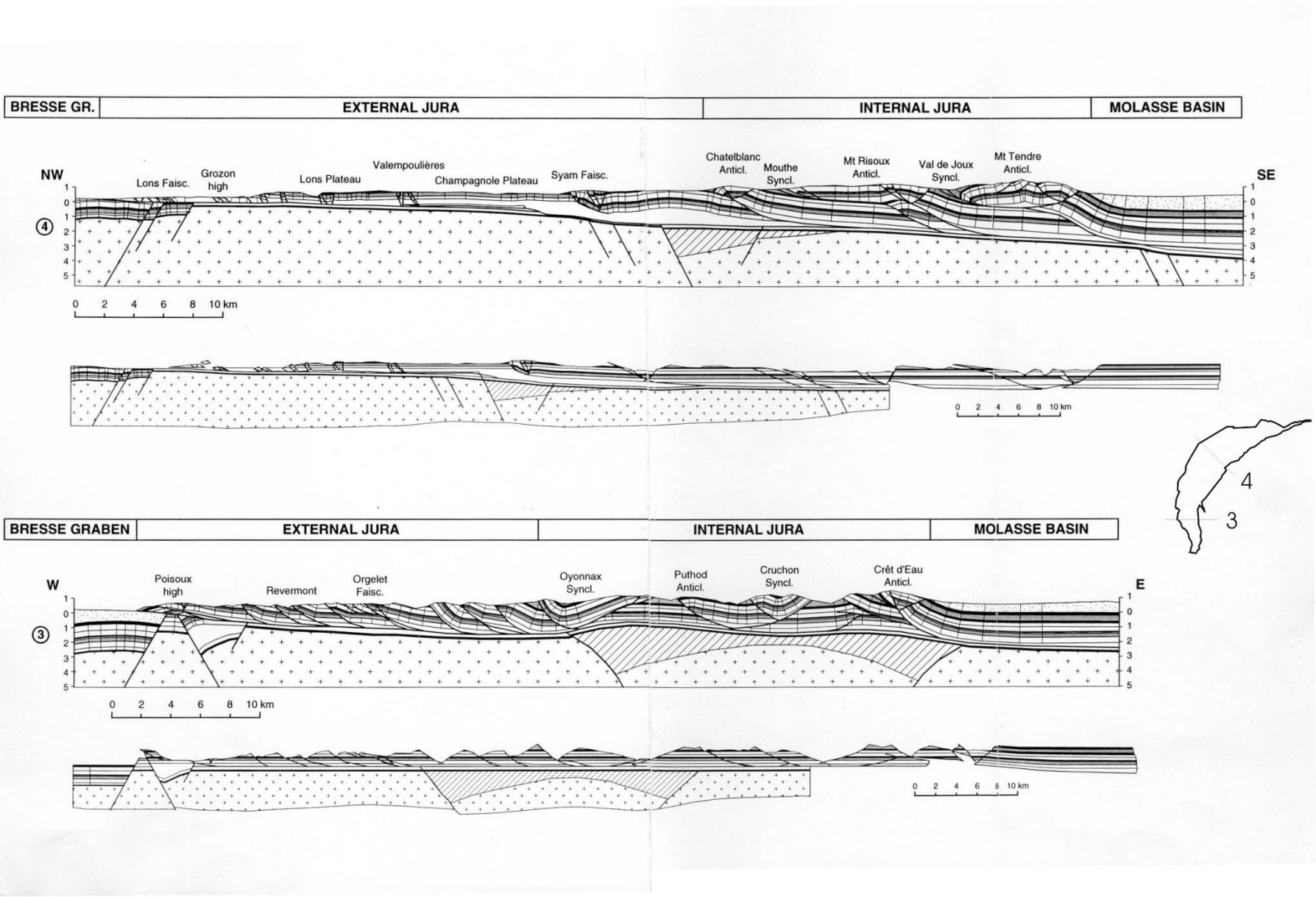

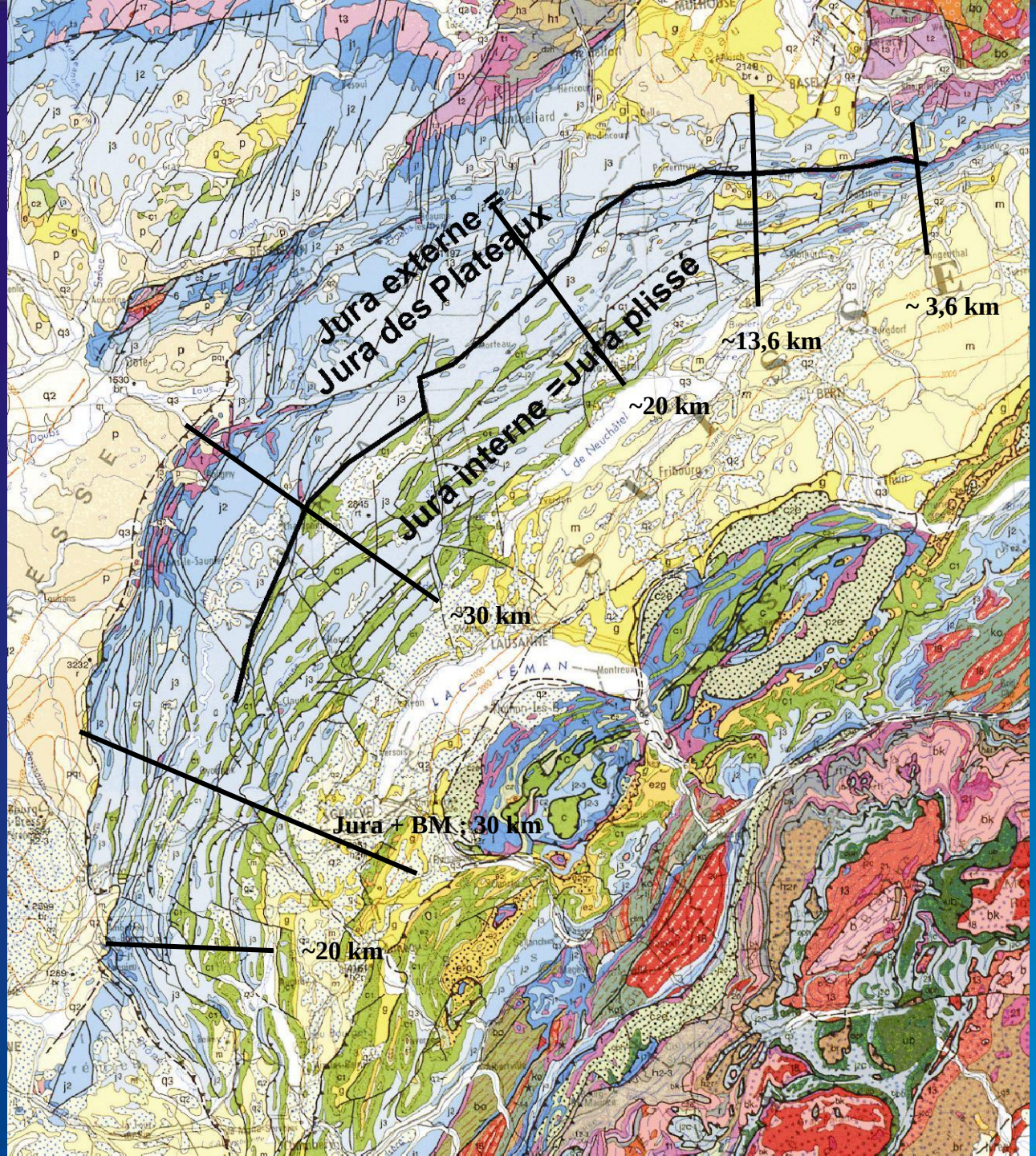
Jura externe =
Jura des Plateaux
Jura interne =Jura plisse
~ 3,6 km
~13,6 km
~20 km
~30 km
Jura + BM : 30 km
~20 km

Most authors consider the formation of the thin-skinned Jura fold-and-thrust belt as a rather short-lived event.

Near its northern rim a maximum age for the onset of thin-skinned deformation is inferred from the Bois de Raube formation, which reveals a biostratigraphic age between 13.8 and 10.5 Ma years and whose sedimentation predates thin-skinned Jura folding in that area.
A maximum age of 9 Ma can be inferred from the western front of the Jura where this fold-and-thrust belt thrusted the Bresse Graben.

Termination of thin-skinned Jura folding is less well constrained. Undeformed karst sediments have been detected in a fold limb located in the central part of the fold-and-thrust belt; their biostratigraphic age implies that folding terminated before some 4.2–3.2 Ma ago in this area. In the case that propagation of the fold-and-thrust belt toward the foreland was in sequence, thin-skinned deformation may have operated longer in the more external parts of the fold-and-thrust belt.

Evidence for ongoing deformation from the northern and northwestern front of the fold-and-thrust-belt is indeed provided by studies in tectonic geomorphology

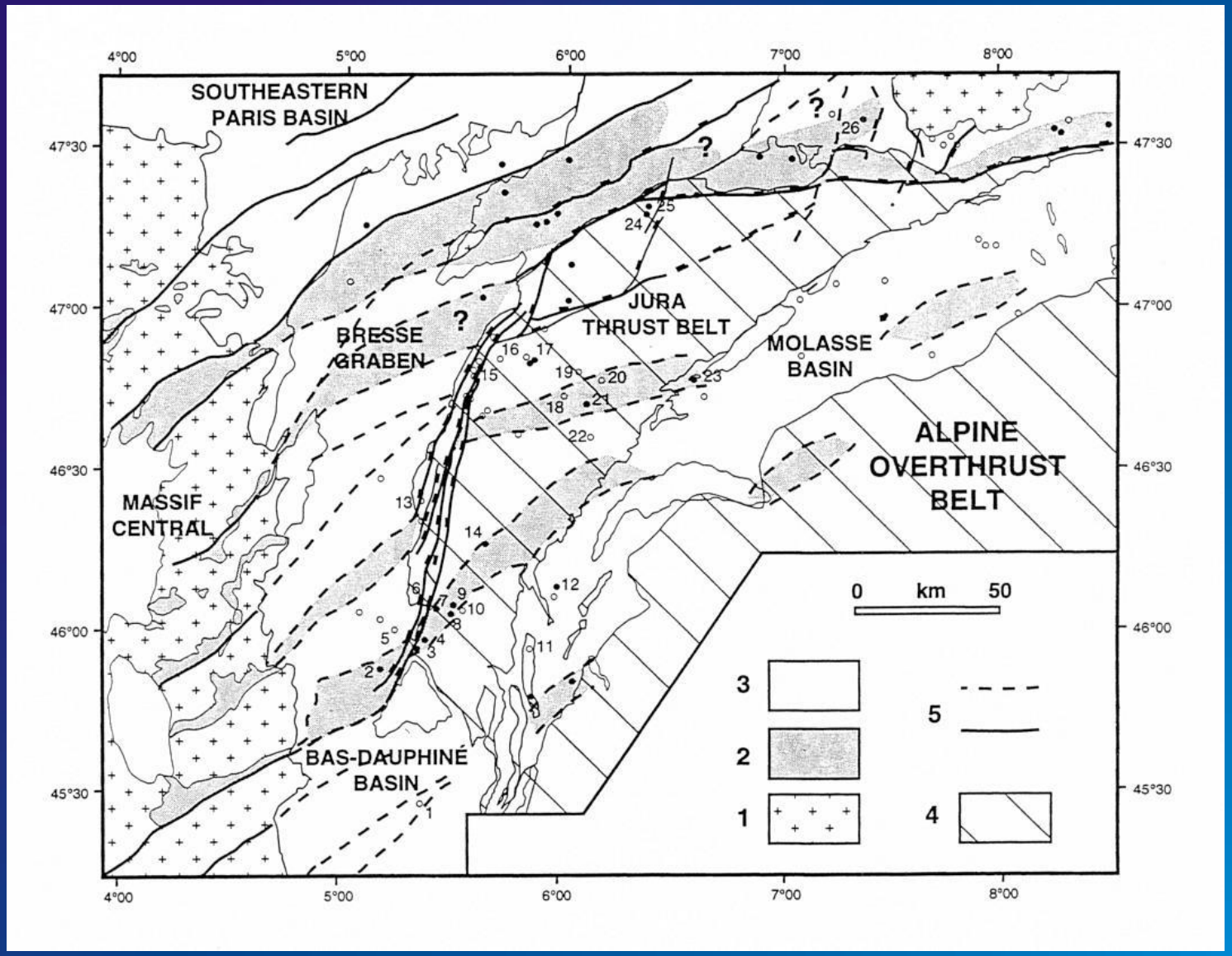

(BRGM, 1980; Truffert et al., 1990)

(Philippe, 1995)

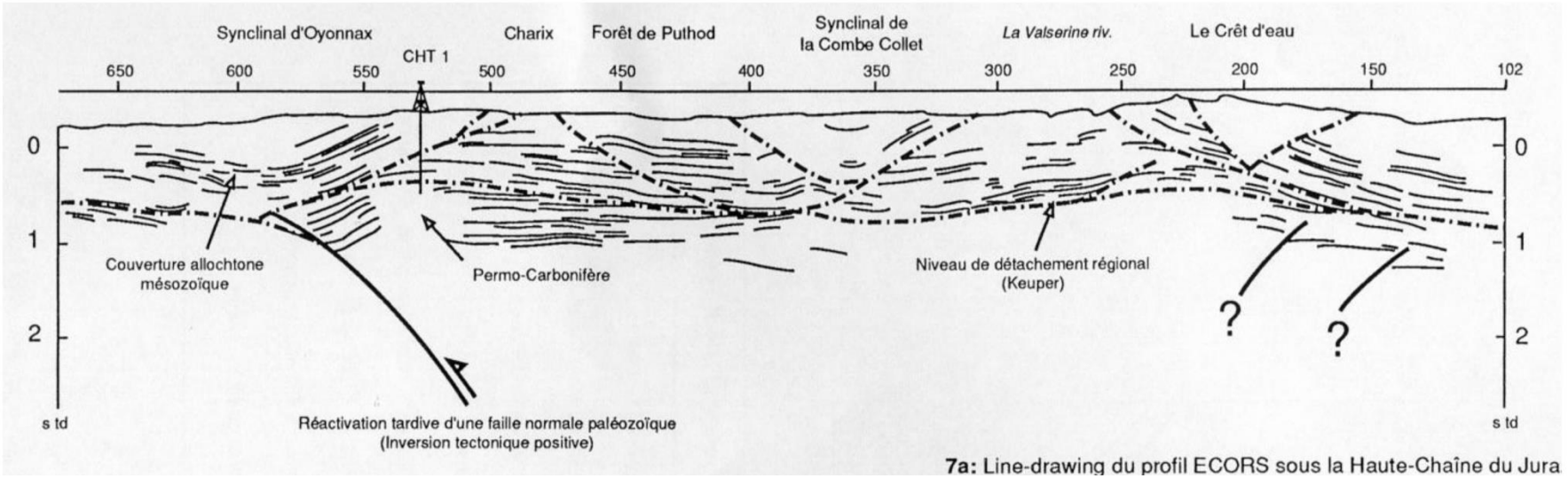

7a: Line-drawing du profil ECORS sous la Haute-Chaîne du Jura

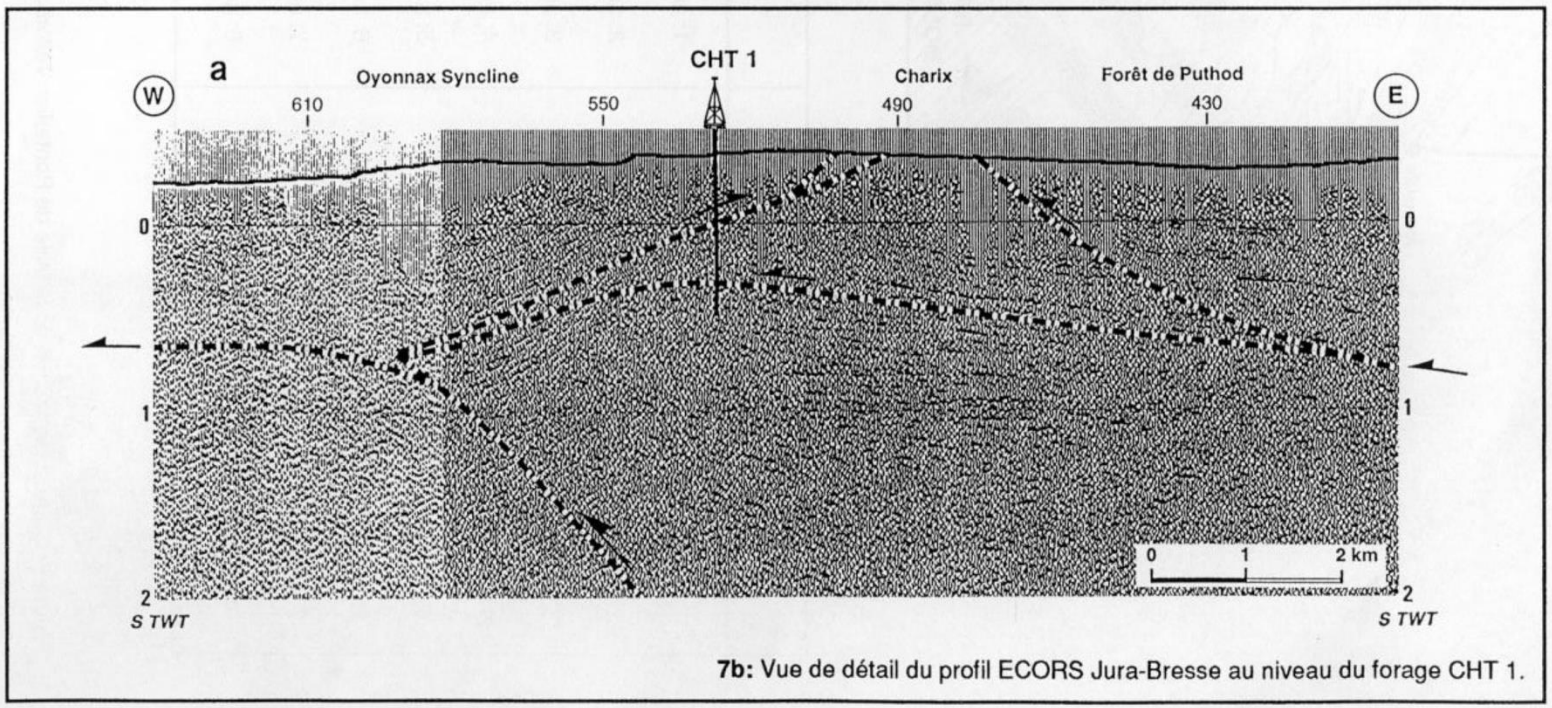

7b: Vue de détail du profil ECORS Jura-Bresse au niveau du forage CHT 1.

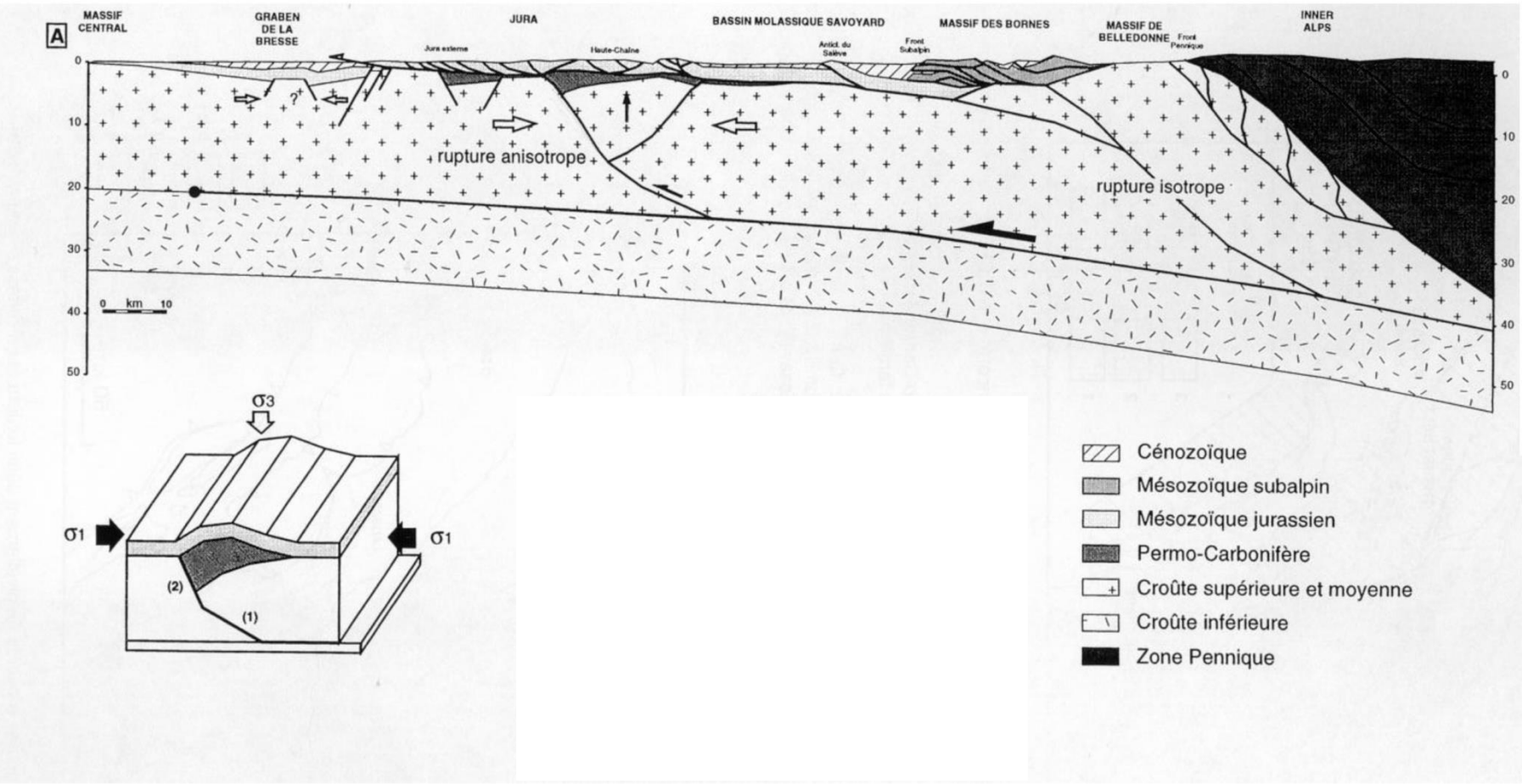

(Philippe, 1995)

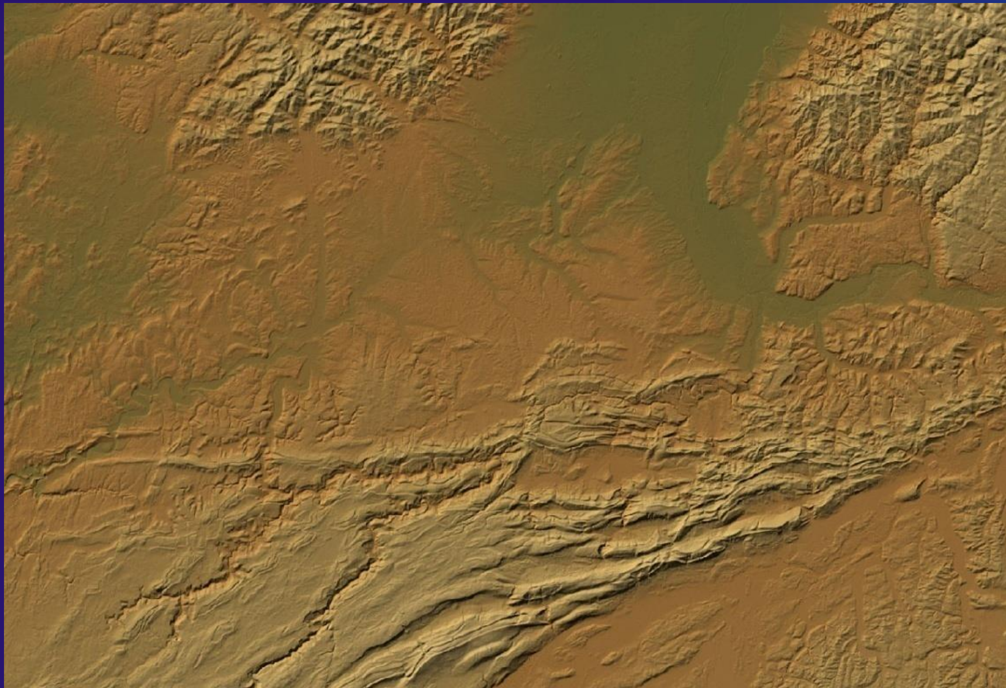

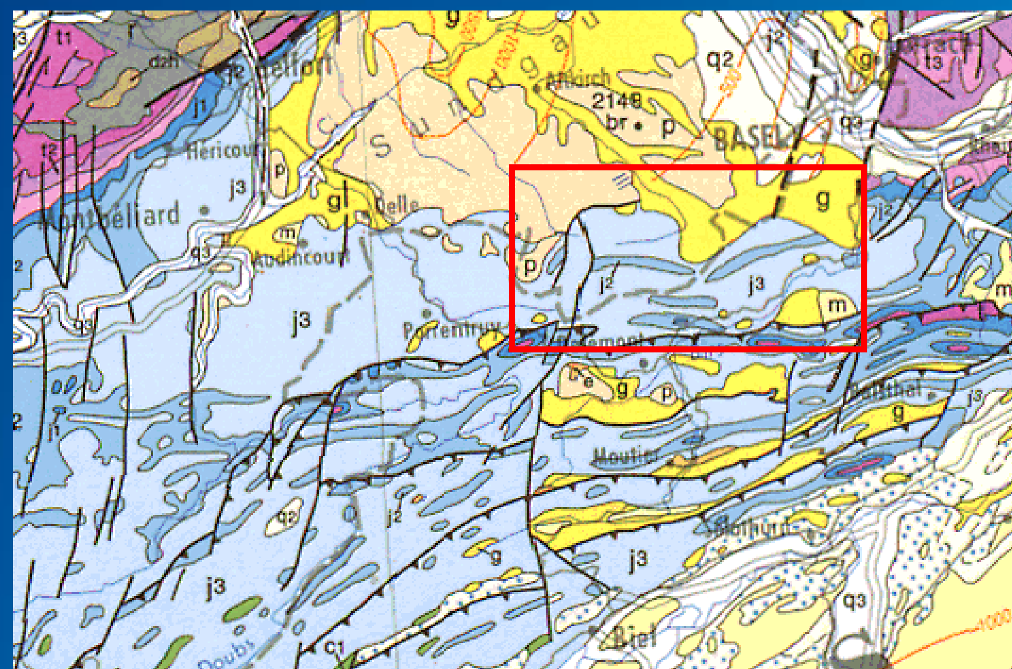
Montbéliard
Delle
Porrentruy
BASEL
2148
Moutier
Biel
Doubs

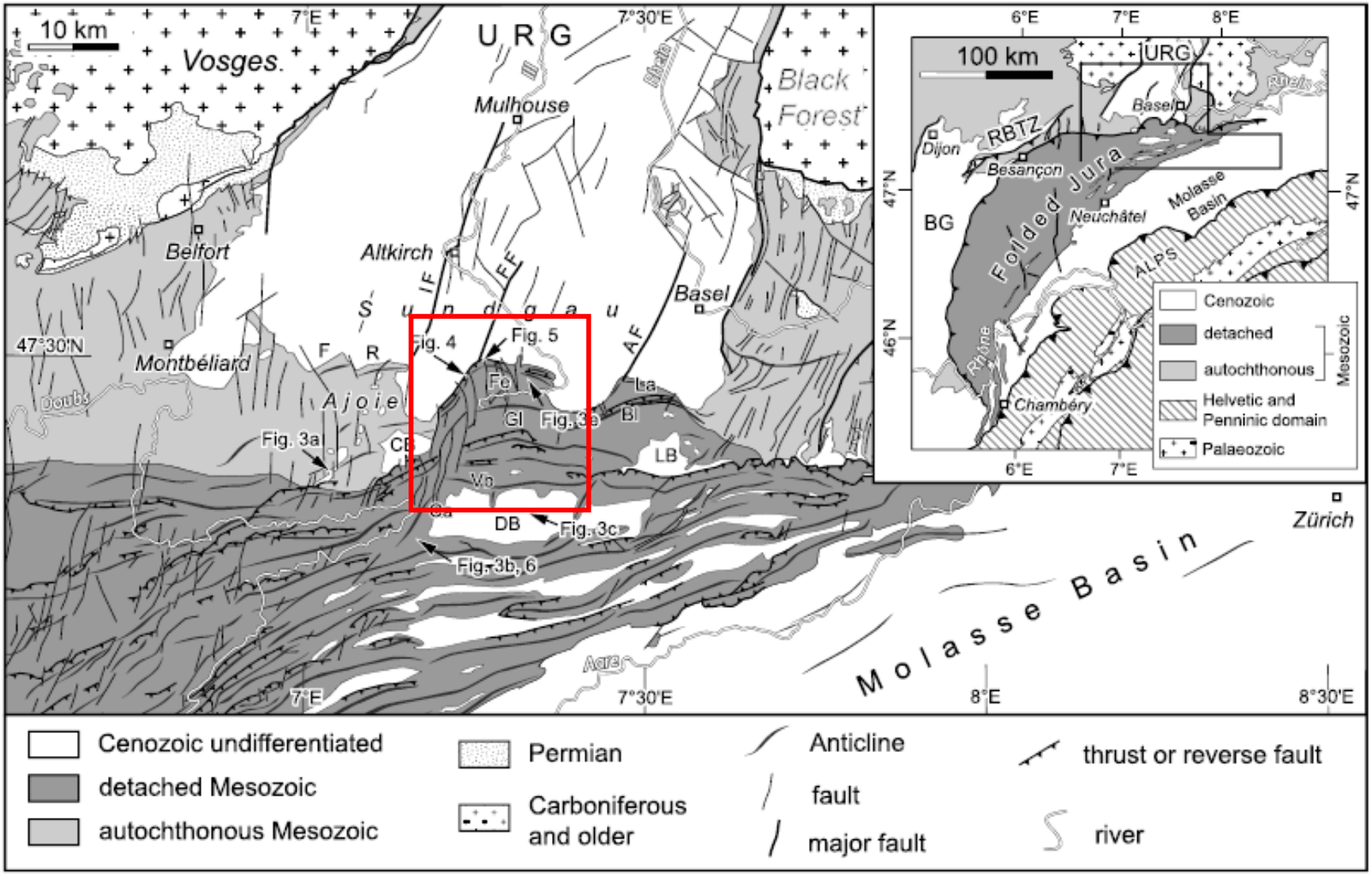

(Ustaszewski and Schmid, 2006)

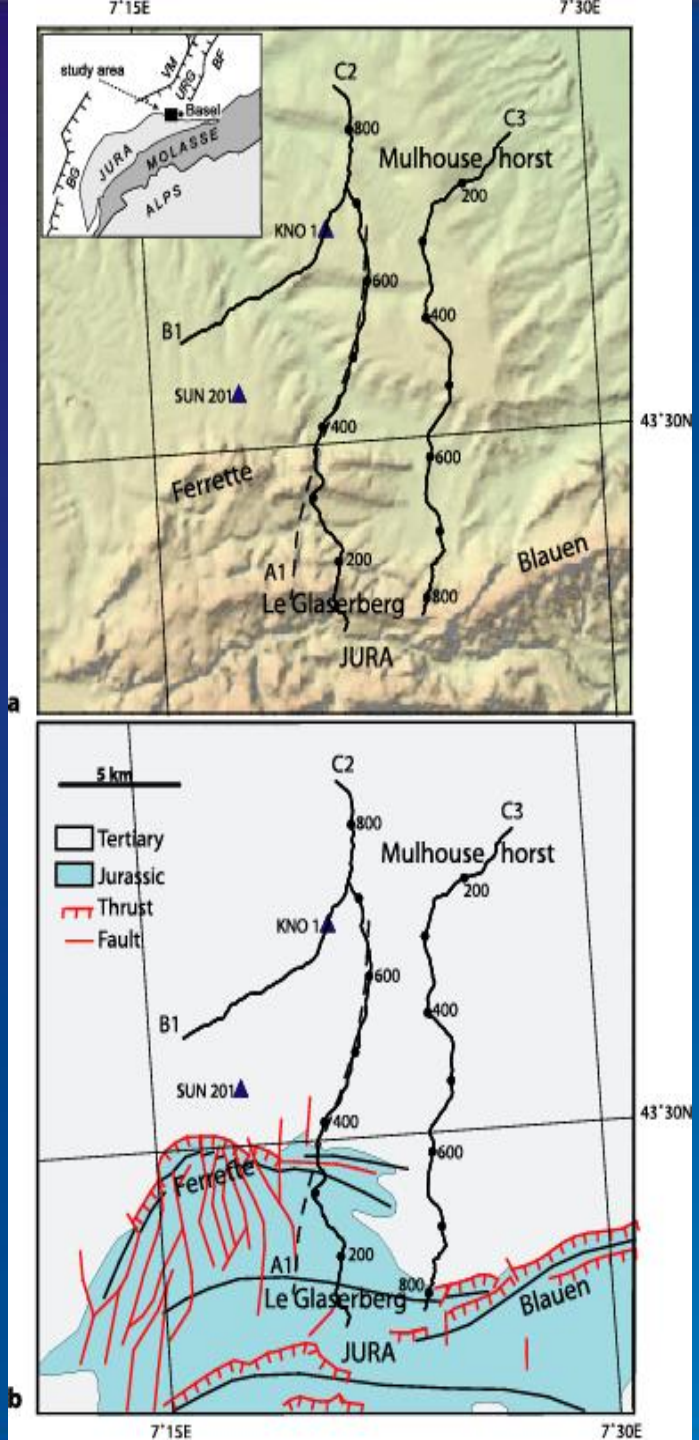

(Rotstein and Schaming, 2004)

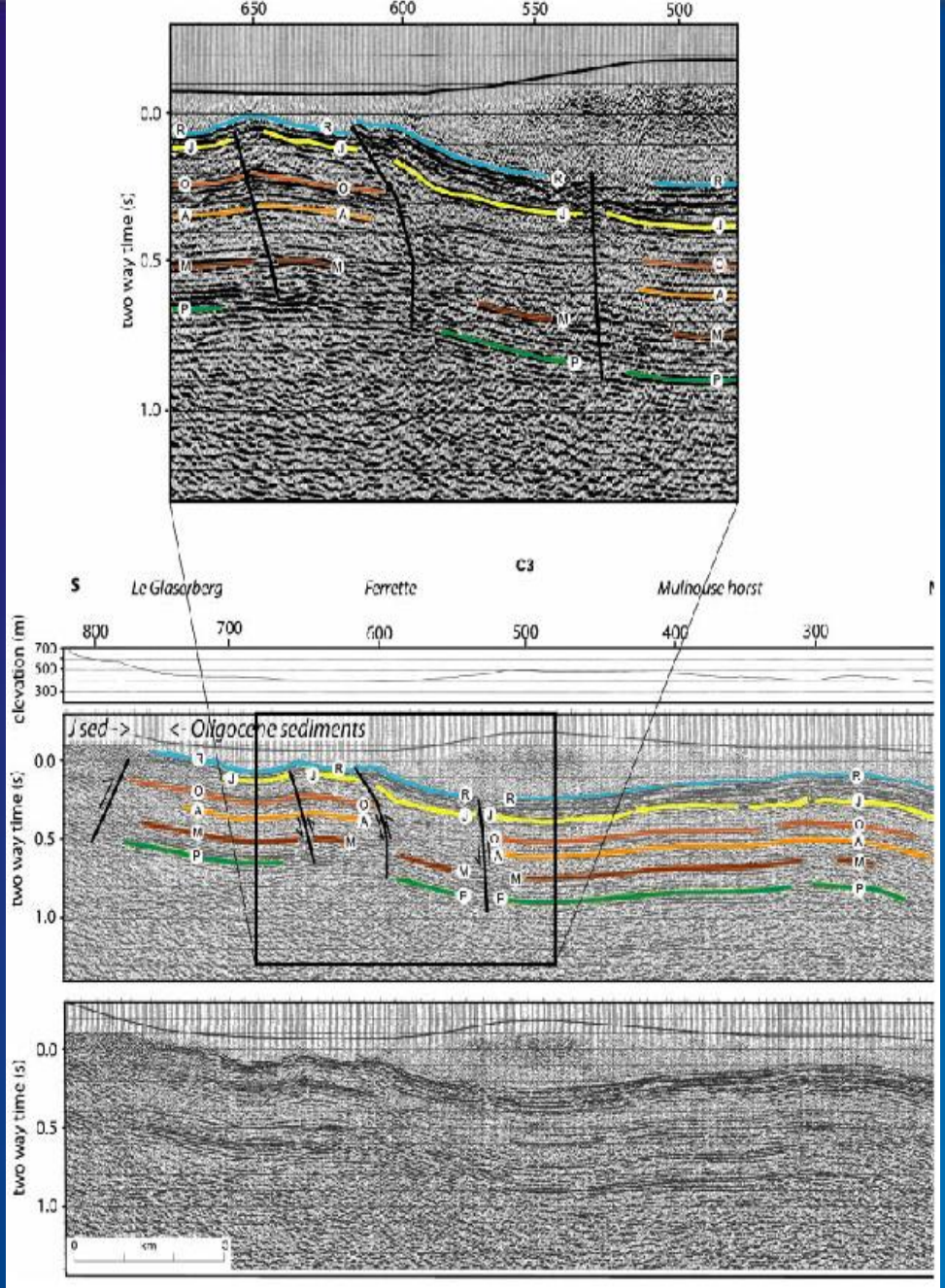

Fig. 3 Uninterpreted and interpreted part of migrated section C3. P, Top Permian; M, Muschelkalk (Triassic); A, Top Aalenian (Jurassic); O, Grande Oolithe (Jurassic); J, Top Jurassic; R, Rupelian. Zero reference is at 350 m above sea-level. Also shown are (1) the ages of the near-surface sediments that suggest thrusting, (2) the surface elevations, (3) the locations of the Ferrette and Le Glaserberg Jura anticlines, and (4) an enlargement of the main faulted area. For location, see Fig. 1.

(Rotstein and Schaming, 2004)

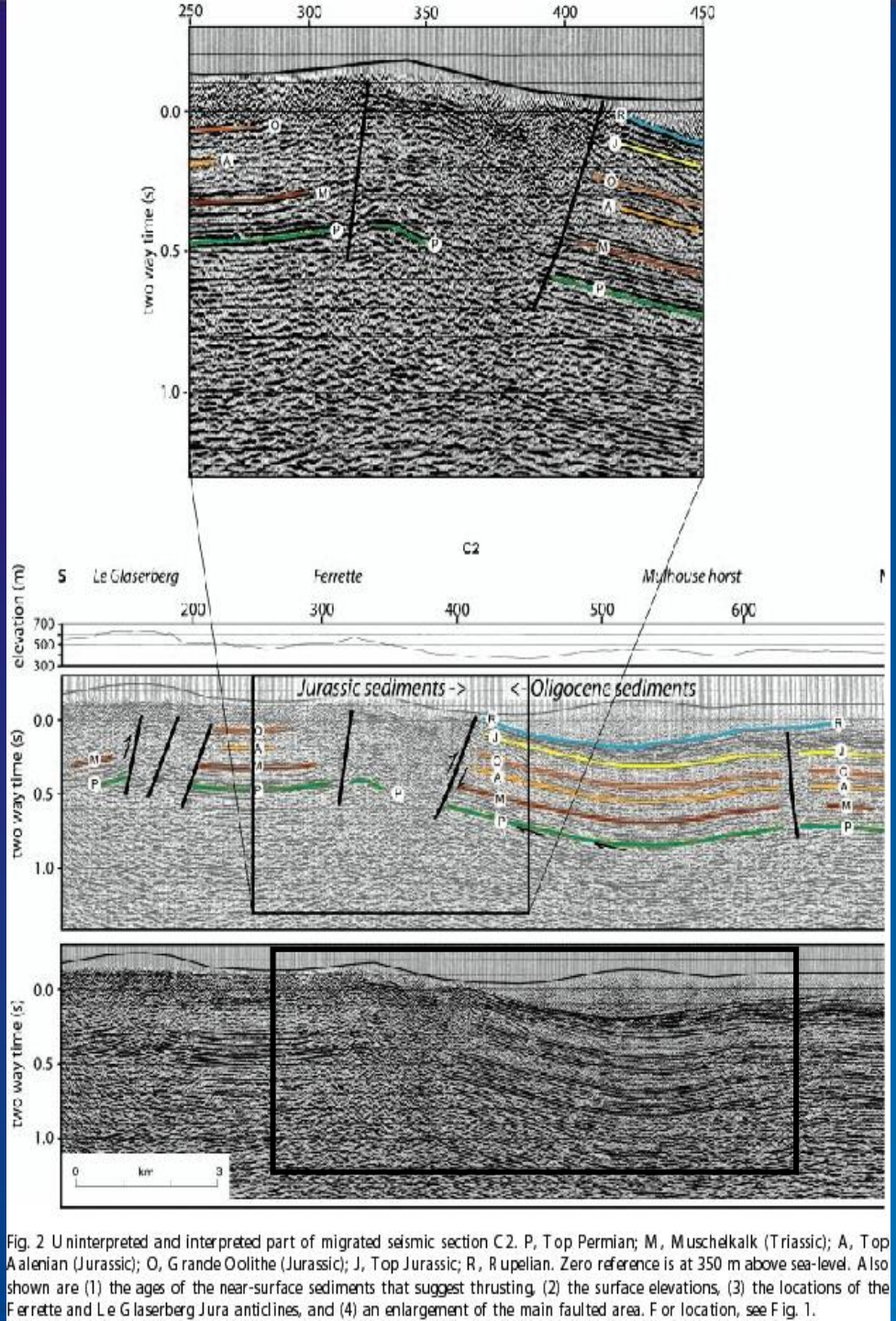

Fig. 2 Uninterpreted and interpreted part of migrated seismic section C2. P, Top Permian; M, Muschelkalk (Triassic); A, Top Aalenian (Jurassic); O, Grande Oolithe (Jurassic); J, Top Jurassic; R, Rupelian. Zero reference is at 350 m above sea-level. Also shown are (1) the ages of the near-surface sediments that suggest thrusting, (2) the surface elevations, (3) the locations of the Ferrette and Le Glaserberg Jura anticlines, and (4) an enlargement of the main faulted area. For location, see Fig. 1.

(Rotstein and Schaming, 2004)

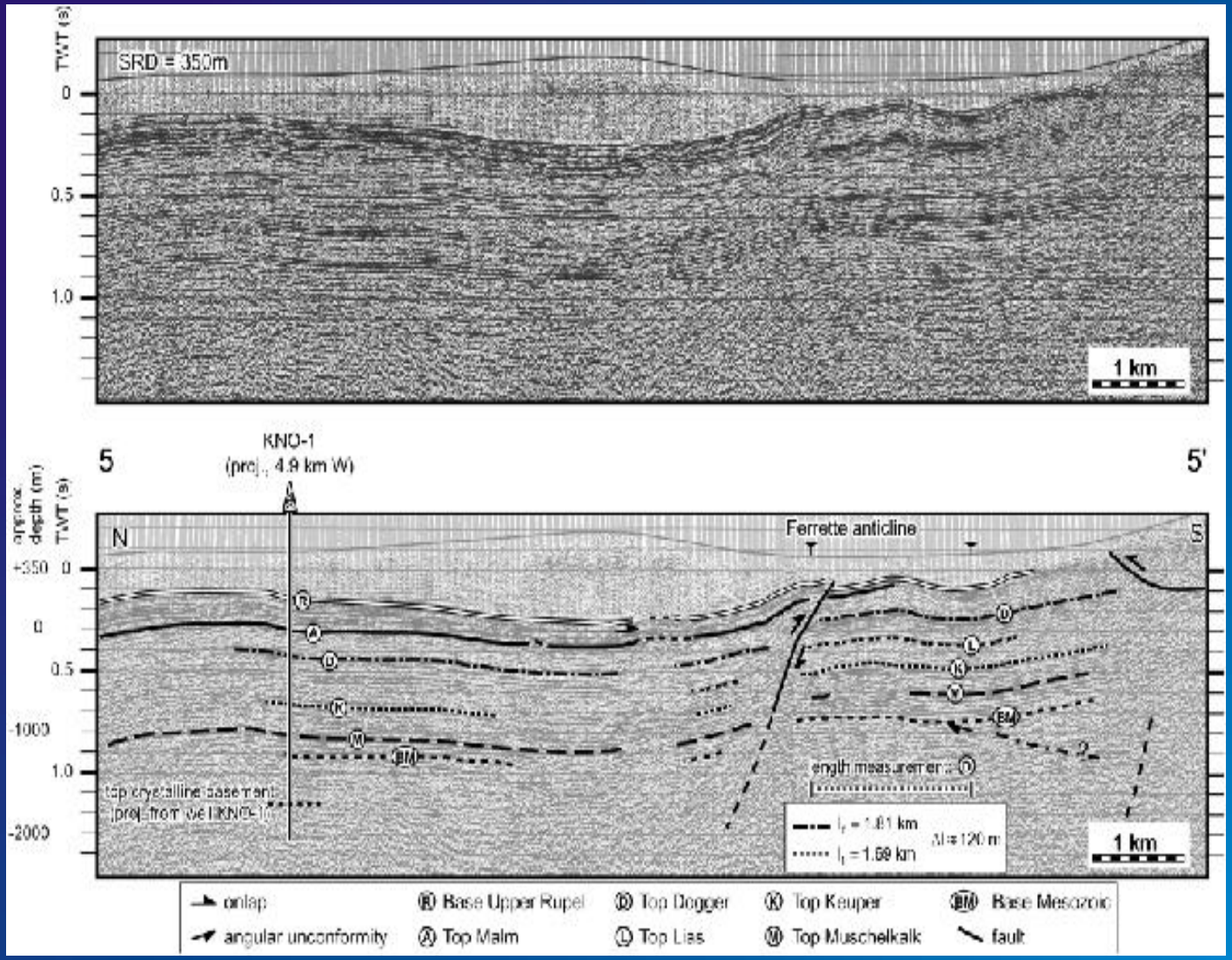

(Ustaszewski and Schmid, 2006)

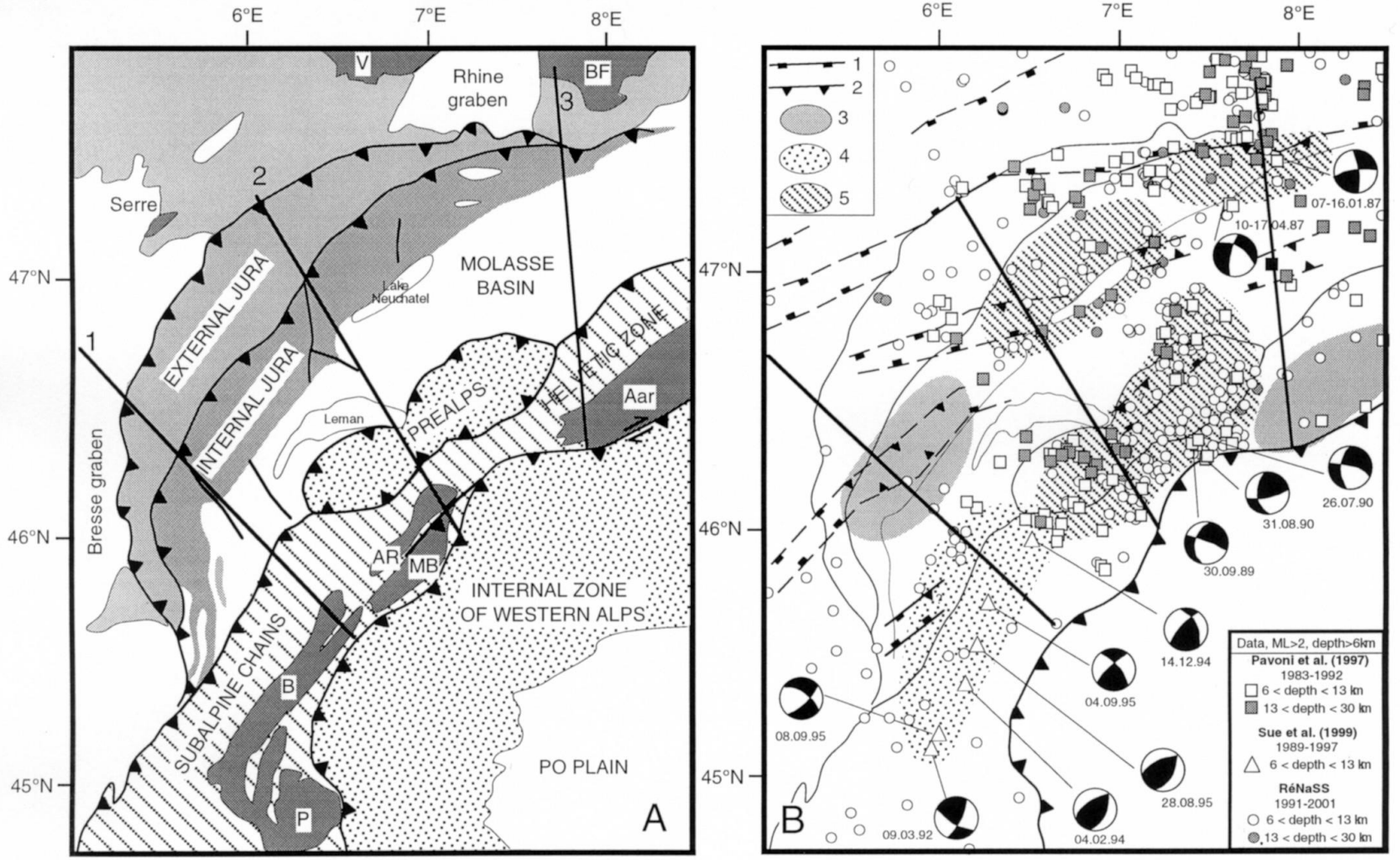

3, areas of present-day basement-involved shortening inferred from high present-day uplift rates 4, areas of present-day basement-involved shortening inferred from both high present-day uplift rates and seismicity; 5, areas of present-day basement-involved shortening inferred from seismicity.

(Lacombe and Mouthereau, 2002)

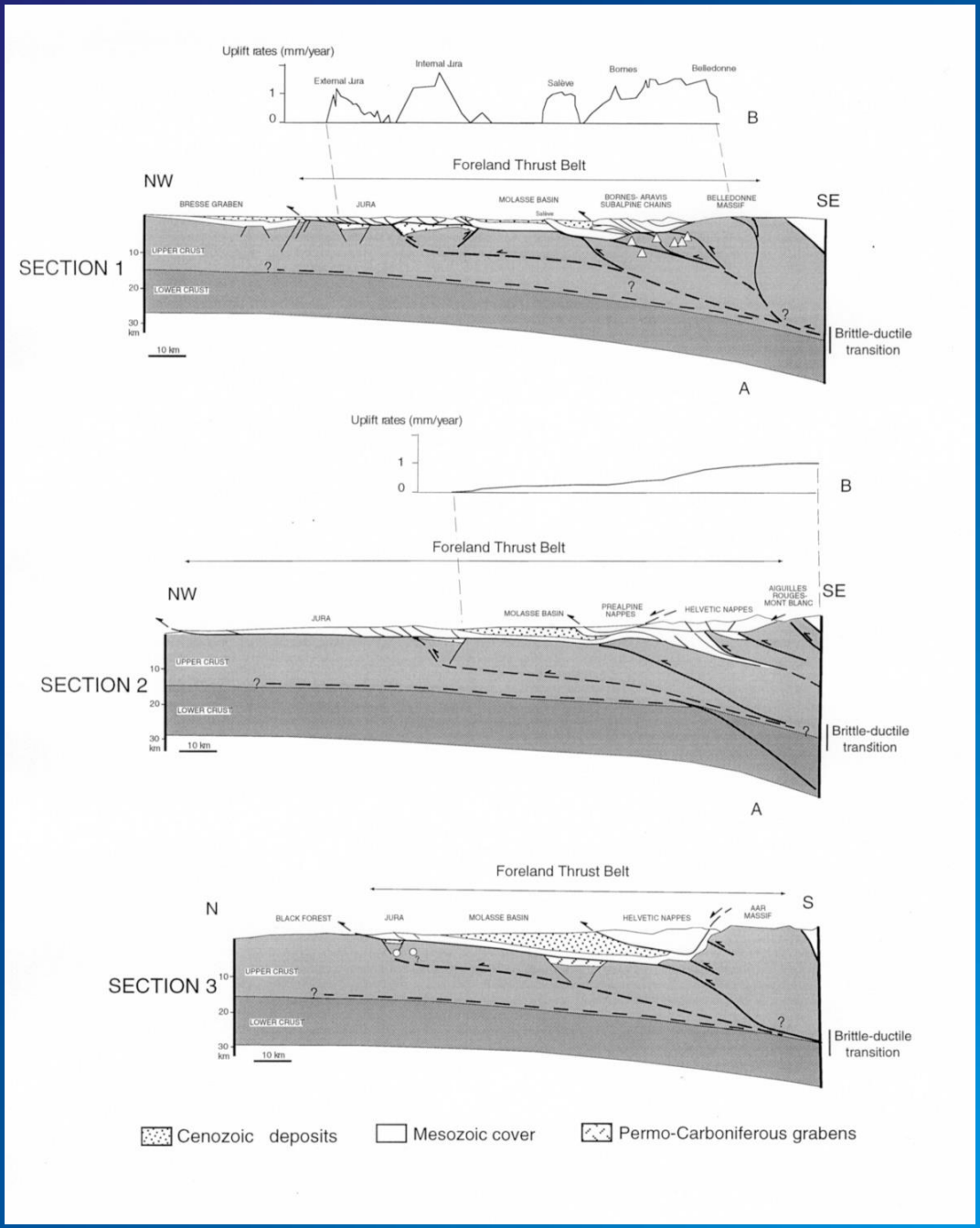

(Lacombe and Mouthereau, 2002)

(Meyer et al., 1994)

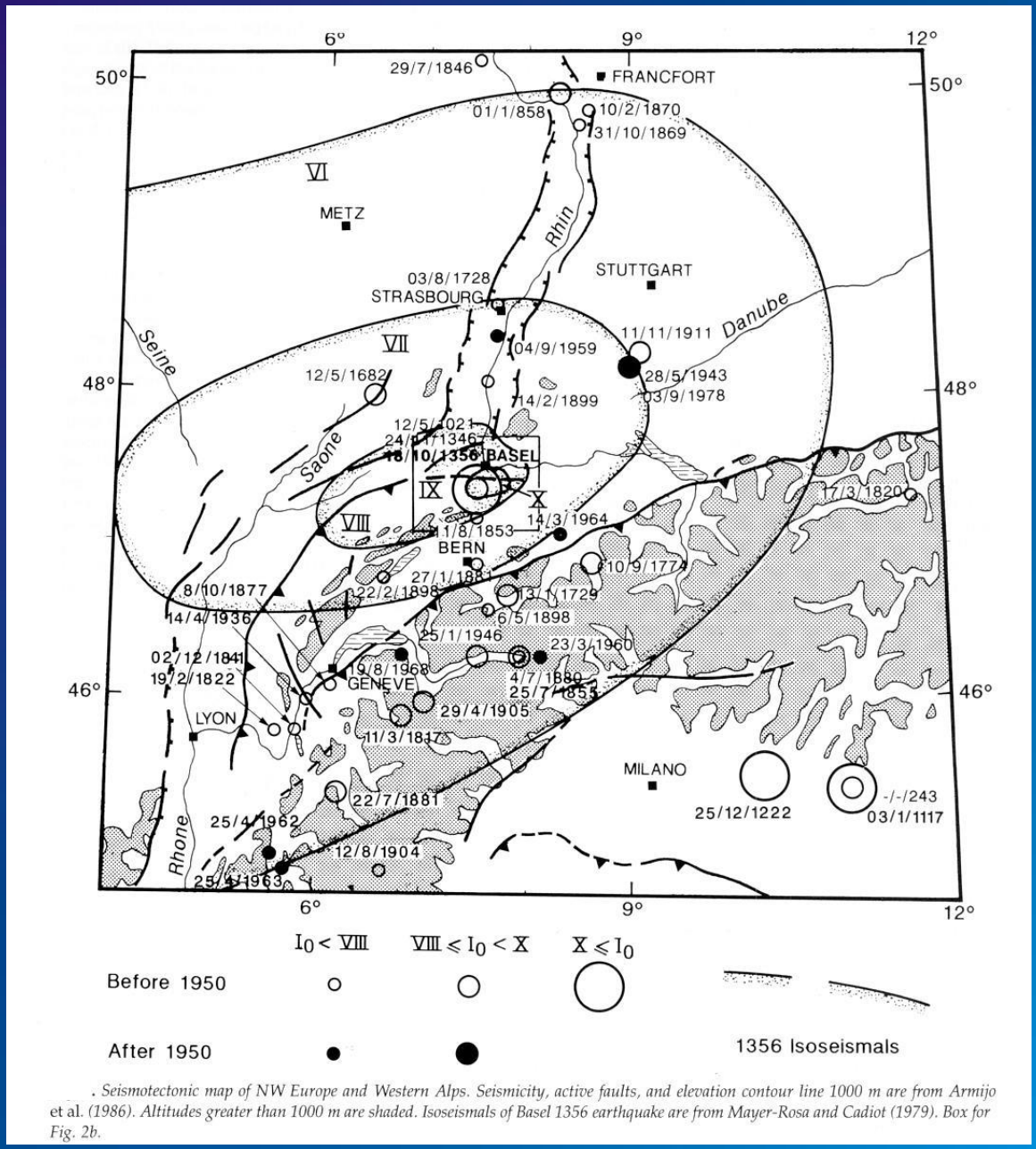

. Seismotectonic map of NW Europe and Western Alps. Seismicity, active faults, and elevation contour line 1000 m are from Armijo et al. (1986). Altitudes greater than 1000 m are shaded. Isoseismals of Basel 1356 earthquake are from Mayer-Rosa and Cadiot (1979). Box for Fig. 2b.

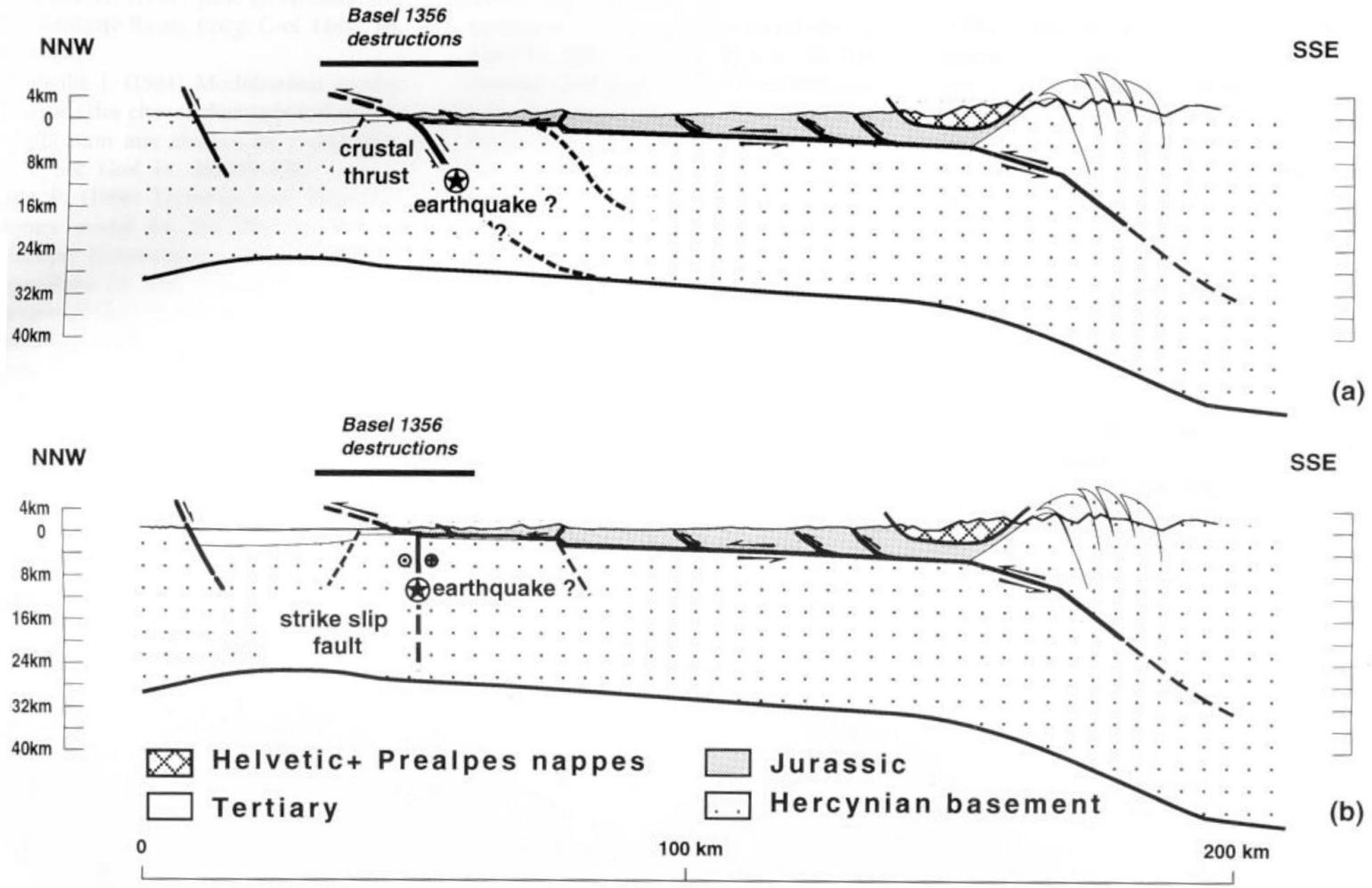

Plausible fault plane geometries for the Basel 1356 earthquake. (a) reactivation of a basement thrust fault beneath the detachment; (b) reactivation of a basement strike-slip fault beneath the detachment.

(Meyer et al., 1994)

Along-strike vatiations of deformation style and shortening : Western Alps and Pyrenees

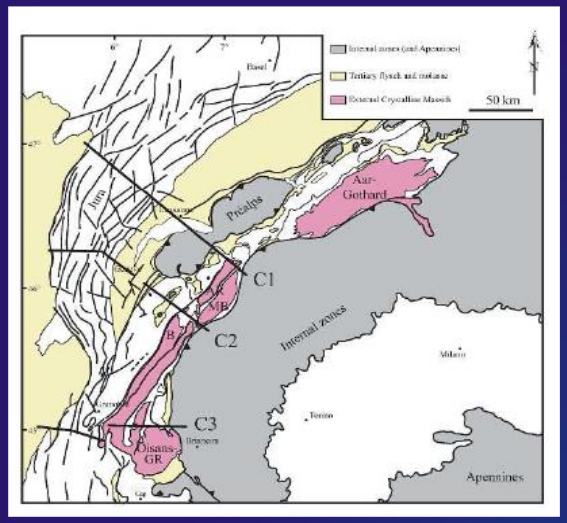

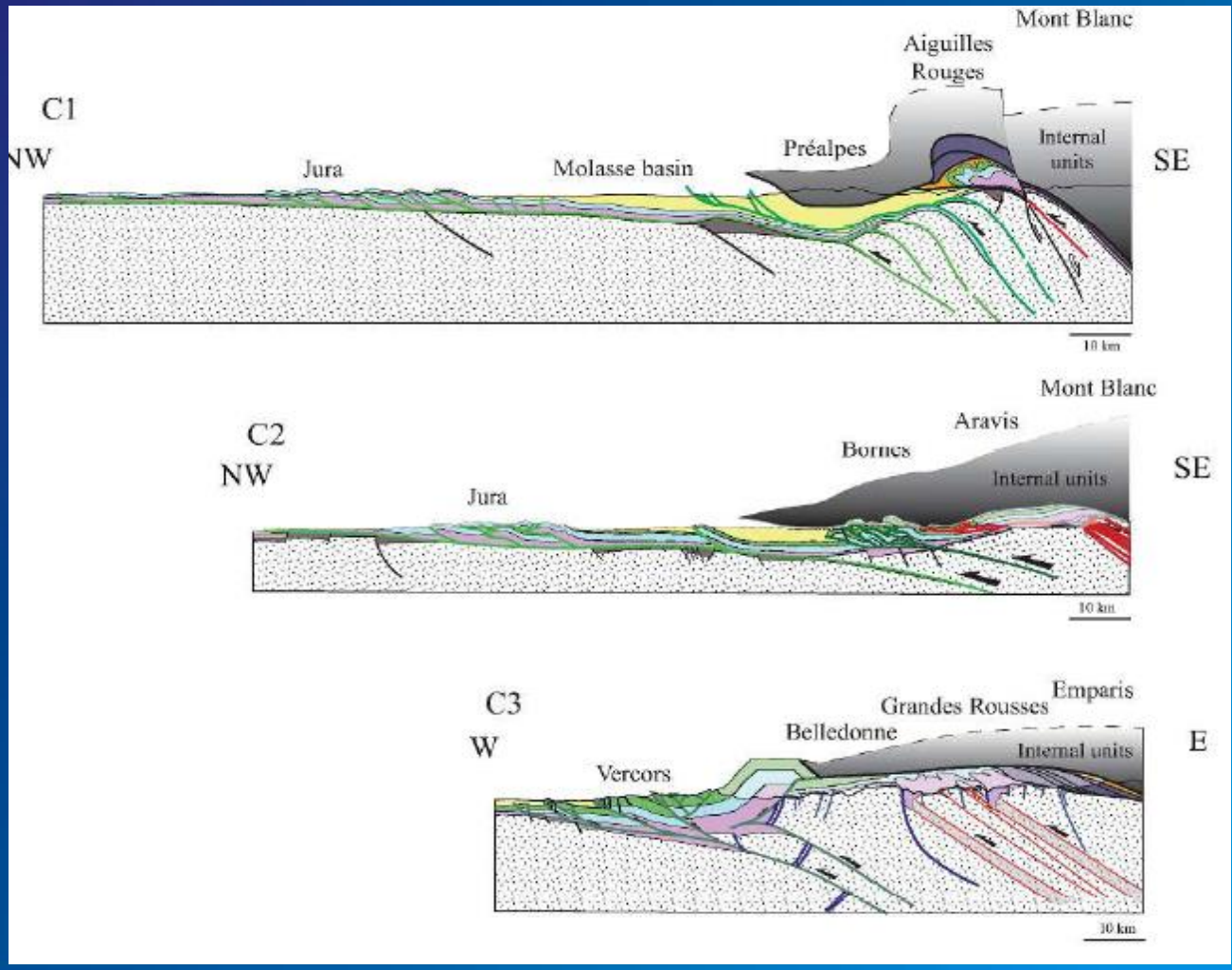

(Bellahsen et al., 2014)

Localization and style of basement-involved deformation varies along the strike of the western Alpine arc.

In the Oisans (section C3), basement was shortened in a distributed way during the Oligocene before deformation localized on the frontal ramp that activated the Vercors shallow decollement. Deformation there was thus first characterized by accretion and thrust stacking below the wedge (distributed underplating) without wedge widening, and later by frontal accretion hence orogenic wedge widening during Miocene times.

In contrast, along the Mont Blanc-Aiguilles Rouges section, basement shortened by underplating below the internal units during the Oligo-Miocene. During the late Miocene -early Pliocene, basement units were still underplated (lower Aiguilles Rouges) while a very wide cover domain was accreted in frontal parts (e.g., Jura and Molasse Basin) with the activation of large basement thrusts. Moreover, both amounts of shortening and shortening across the entire external zone increase from the Oisans section to the Mont Blanc section. The increase of the amount of shortening is most likely due to a wider inherited Mesozoic basin in the North (Ultra-Helvetic/Valaisan).

However, the increase of the shortening values probably has a rheological explanation. Along the Mont Blanc section, basement shortening remains localized, leading to stacking of basement slices (section C1). while it is distributed far toward the foreland along the Oisans section (section C3);
this can be related to the rheology of the crust during collision, the more buried and thermally weakened crust at the latitude of the Mont Blanc (400°C, 5kb) being more prone to localized shortening at the orogen-scale.

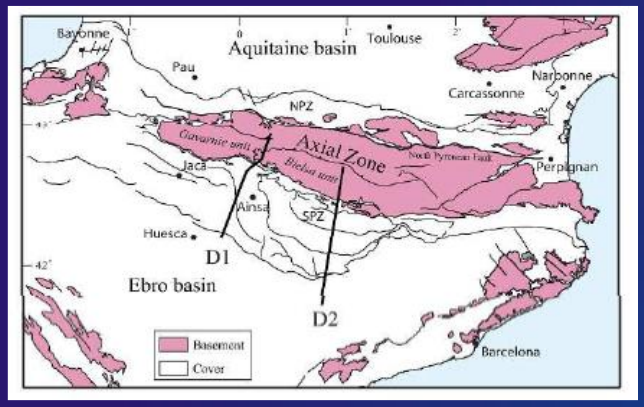
Bayonne
Aquitaine basin
Toulouse
Pau
Narbonne
Carcassonne
NPZ
Gavarnie unit
Axial Zone
North Pyrenean Fault
Bielsa unit
Jaca
Perpignan
Ainsa
SPZ
Huesca
D1
Ebro basin
D2
Basement
Cover
Barcelona

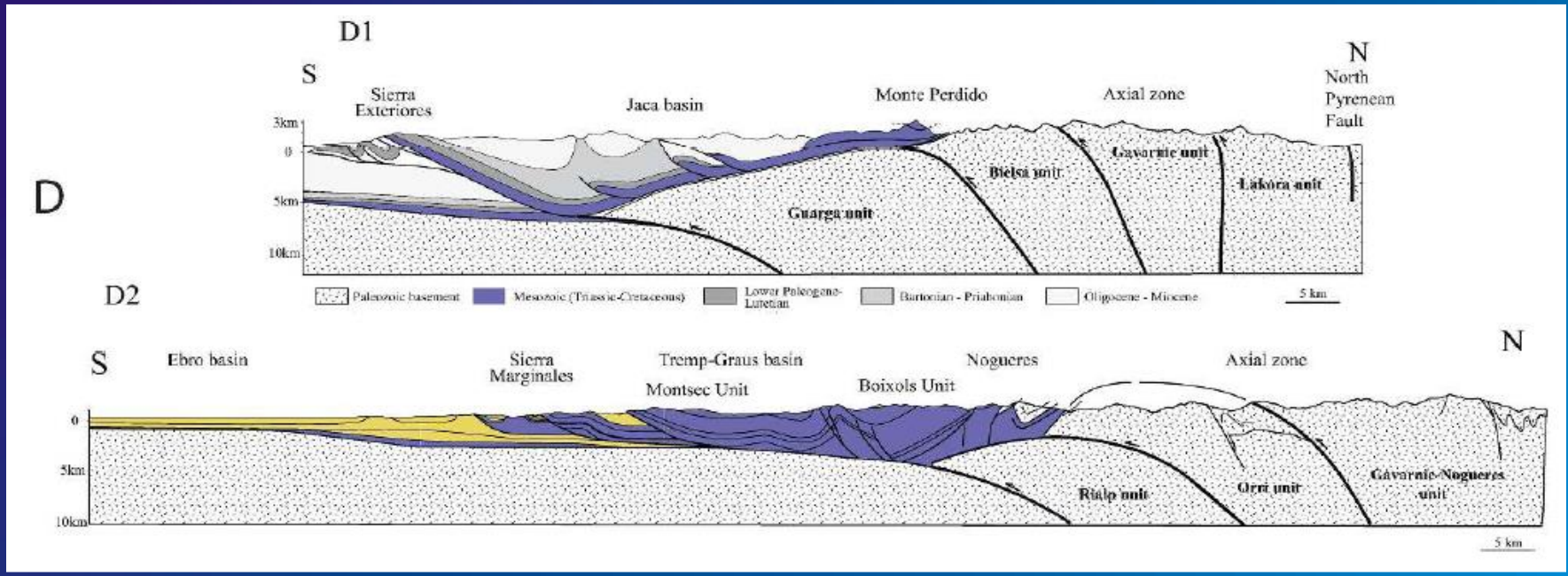
D1
S
N
Sierra Exteriores
Jaca basin
Monte Perdido
Axial zone
North Pyrenean Fault
3km
0
5km
10km
Gavarnie unit
Bielsa unit
Guarga unit
Lakora unit
D
D2
Paleozoic basement
Mesozoic (Triassic-Cretaceous)
Lower Paleogene-Lutetian
Bartonian - Priabonian
Oligocene - Miocene
5 km
S
Ebro basin
Sierra Marginales
Tremp-Graus basin
Montsec Unit
Nogueres
Boixols Unit
Axial zone
N
0
5km
10km
Riaño unit
Orri unit
Gavarnie-Nogueres unit
5 km

P-T conditions of deformation in the Pyrenees were very different from the western Alps, especially in term of burial which remained much shallower.

However, the striking similarity in term of basement shortening style between sections C1 and D2, and sections C2 and D1, suggests that along-strike variations in the structural style may also be controlled by difference in crustal thermicity, with temperature lower to the West than to the East.

This is consistent with the maximum temperature recorded by Raman Spectroscopy on Carbonaceous Material technique in the NPZ and related the Cretaceous extension and mantle denudation, higher to the East than to the West (Clerc & Lagabrielle, 2014). In this perspective, the crust was hotter and weaker in the East, where, as a consequence, shortening was more localized than in the West, although the total shortening is similar.

Low-Temperature thermochronology supports that the high geothermal gradient has lasted 30-50 Ma after extension, hence during convergence in the NPZ (Vacherat et al., 2014) and probably also in the Axial zone, which likely favored basement-involved shortening.

Basement control on the kinematics of fold-and-thrust belts : the Laramide belt case

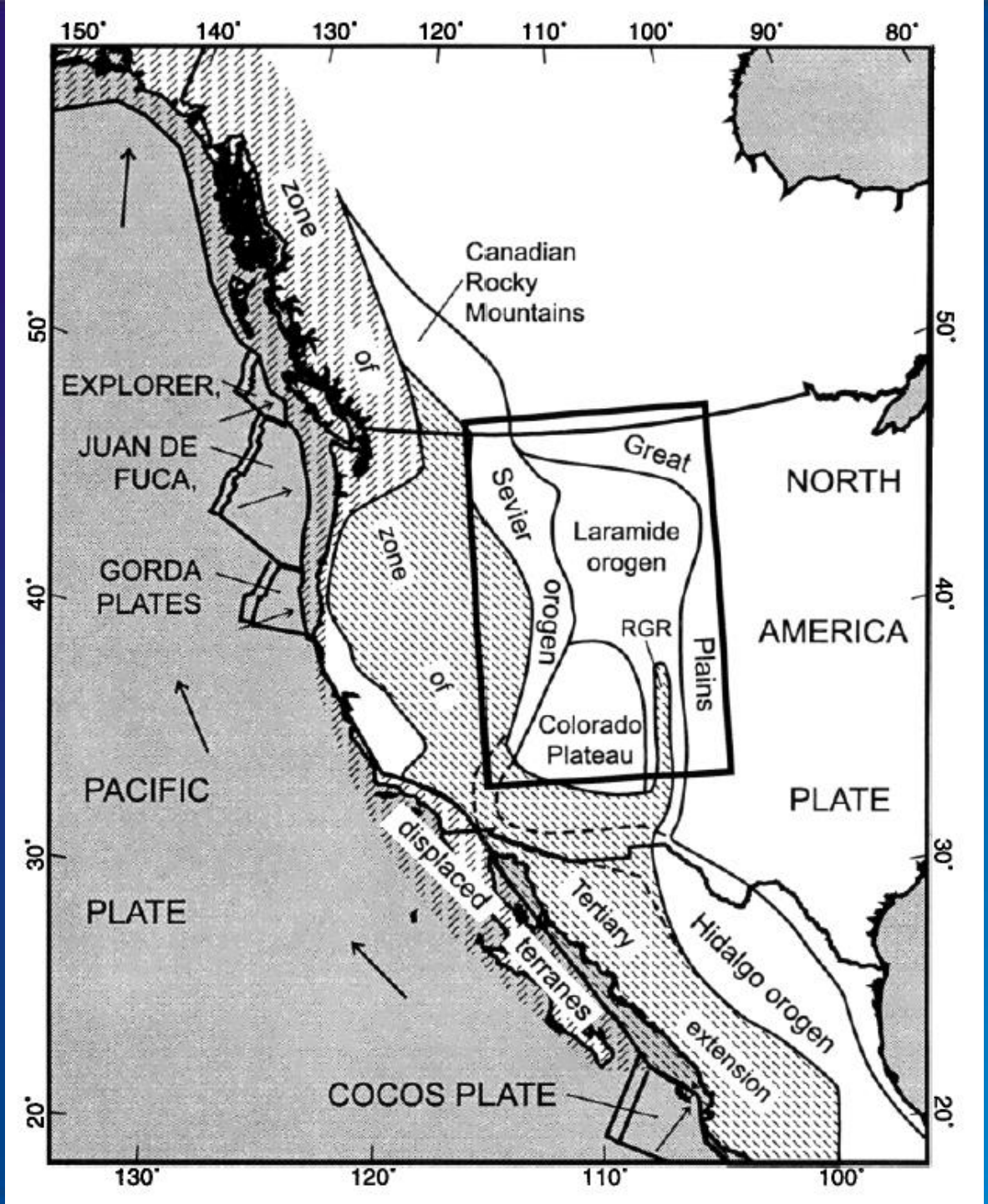
150°
140°
130°
120°
110°
100°
90°
80°
50°
40°
30°
20°
Canadian
Rocky
Mountains
zone
of
EXPLORER,
JUAN DE
FUCA,
GORDA
PLATES
PACIFIC
PLATE
Great
Sevier
orogen
Laramide
orogen
RGR
Plains
Colorado
Plateau
NORTH
AMERICA
PLATE
displaced
terranes
Tertiary
Hidalgo orogen
extension
COCOS PLATE
130°
120°
110°
100°

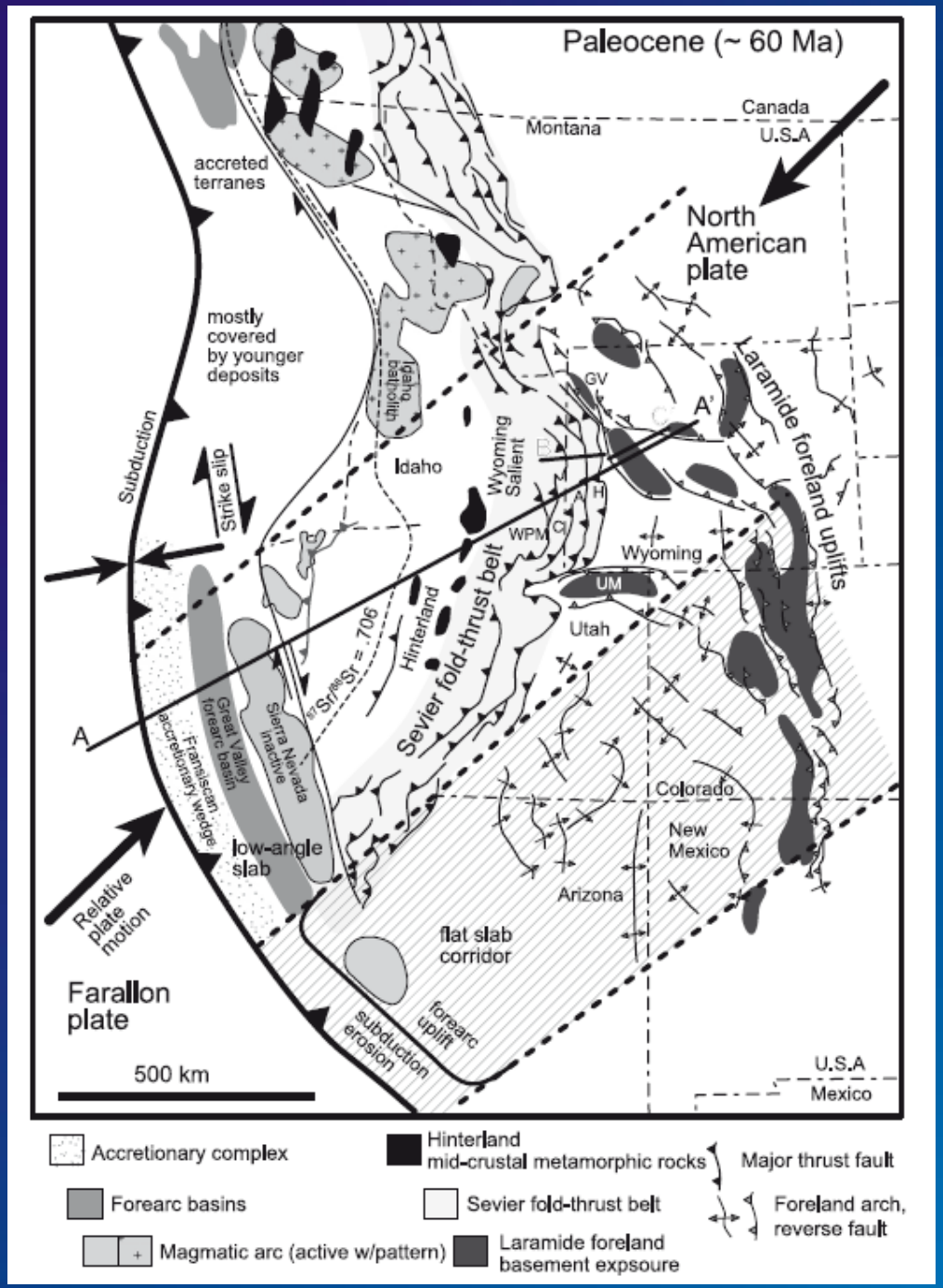

(Weil and Yonkee, 2012)

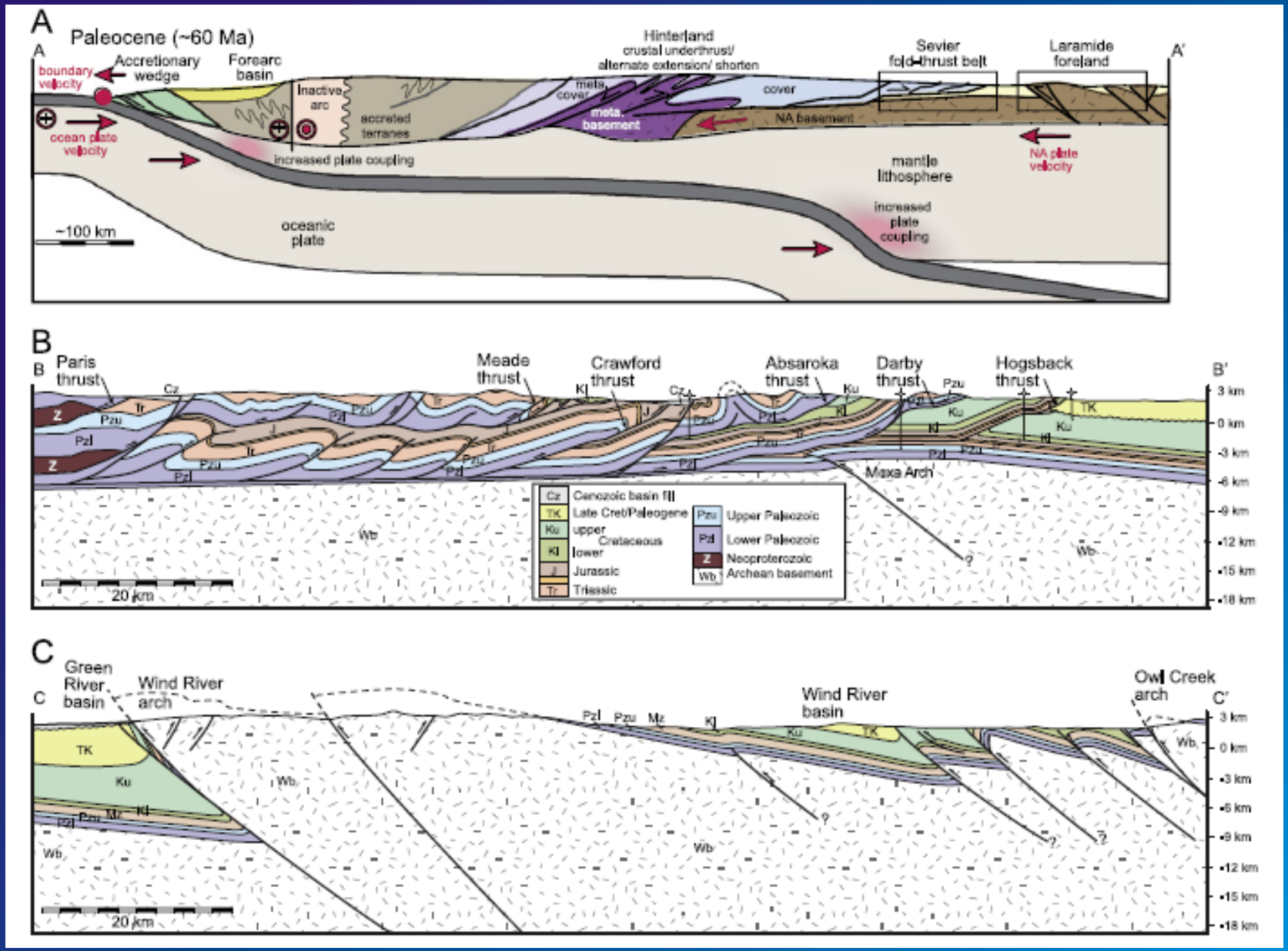

(Weil and Yonkee, 2012)

Bird (2002)

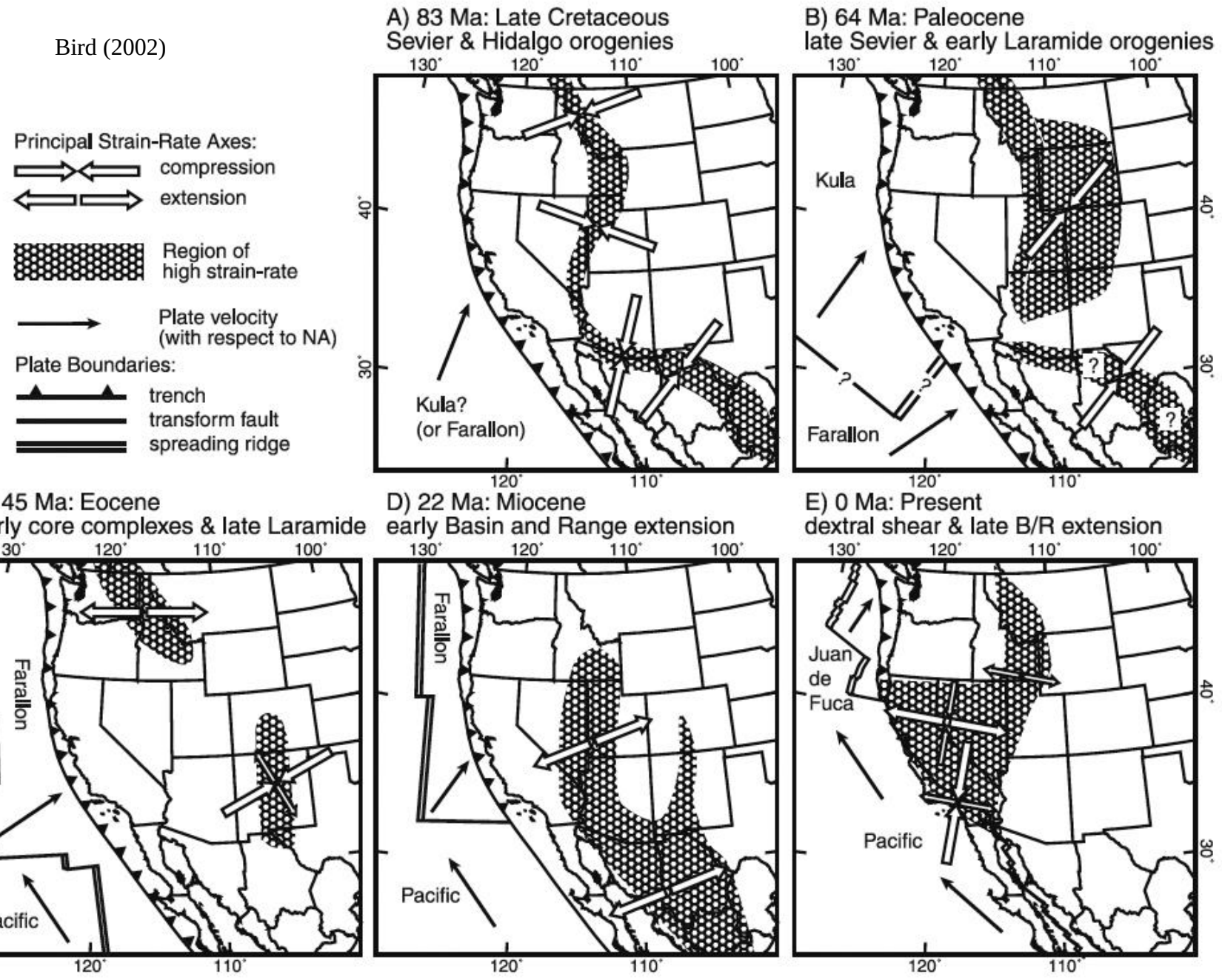
Principal Strain-Rate Axes:
compression
extension
Region of high strain-rate
Plate velocity (with respect to NA)
Plate Boundaries:
trench
transform fault
spreading ridge
A) 83 Ma: Late Cretaceous
Sevier & Hidalgo orogenies
Kula?
(or Farallon)
B) 64 Ma: Paleocene
late Sevier & early Laramide orogenies
Kula
Farallon
C) 45 Ma: Eocene
early core complexes & late Laramide
Farallon
Pacific
D) 22 Ma: Miocene
early Basin and Range extension
Farallon
Pacific
E) 0 Ma: Present
dextral shear & late B/R extension
Juan de Fuca
Pacific
130°
120°
110°
100°
40°
30°

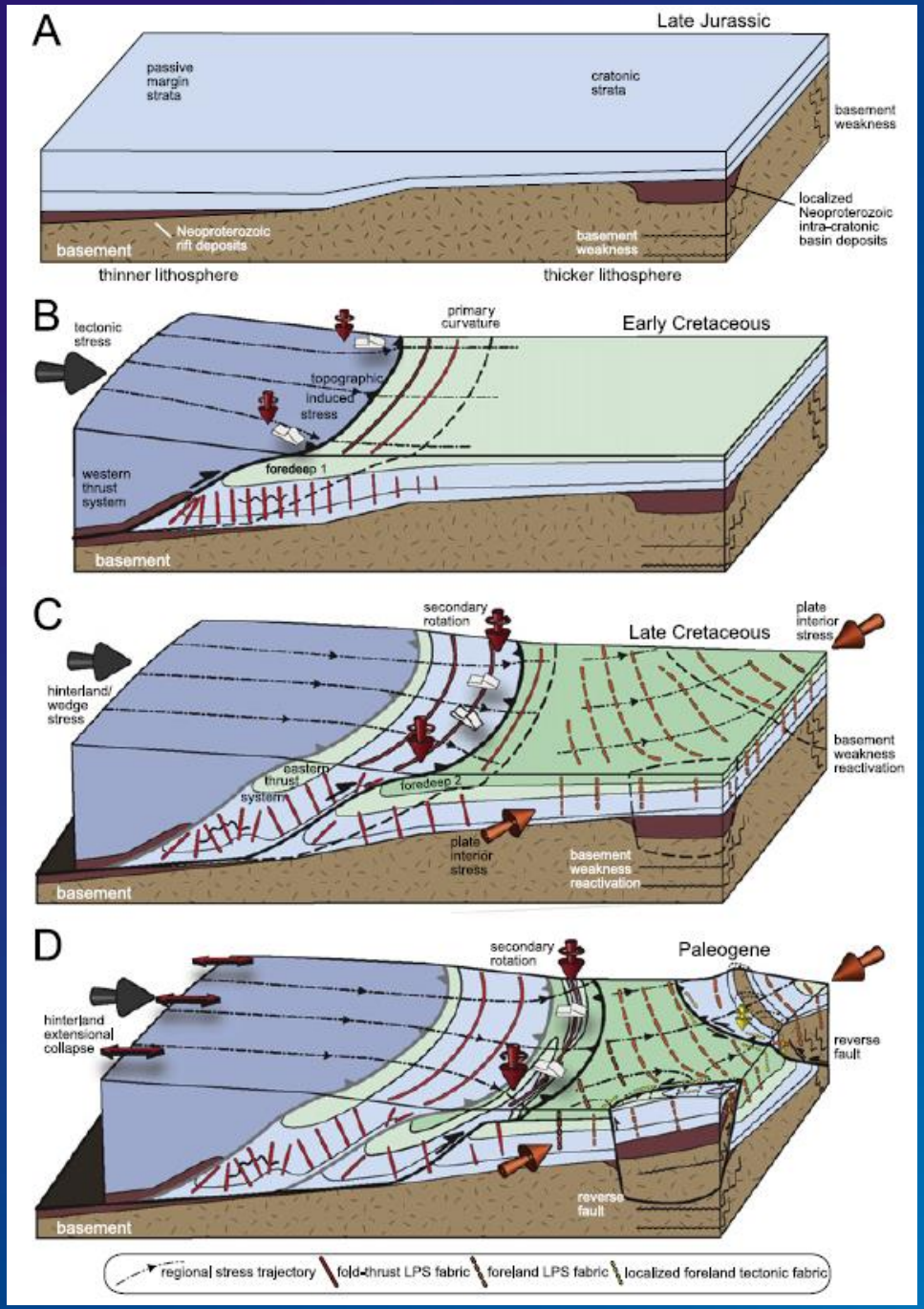

(Weil and Yonkee, 2012)

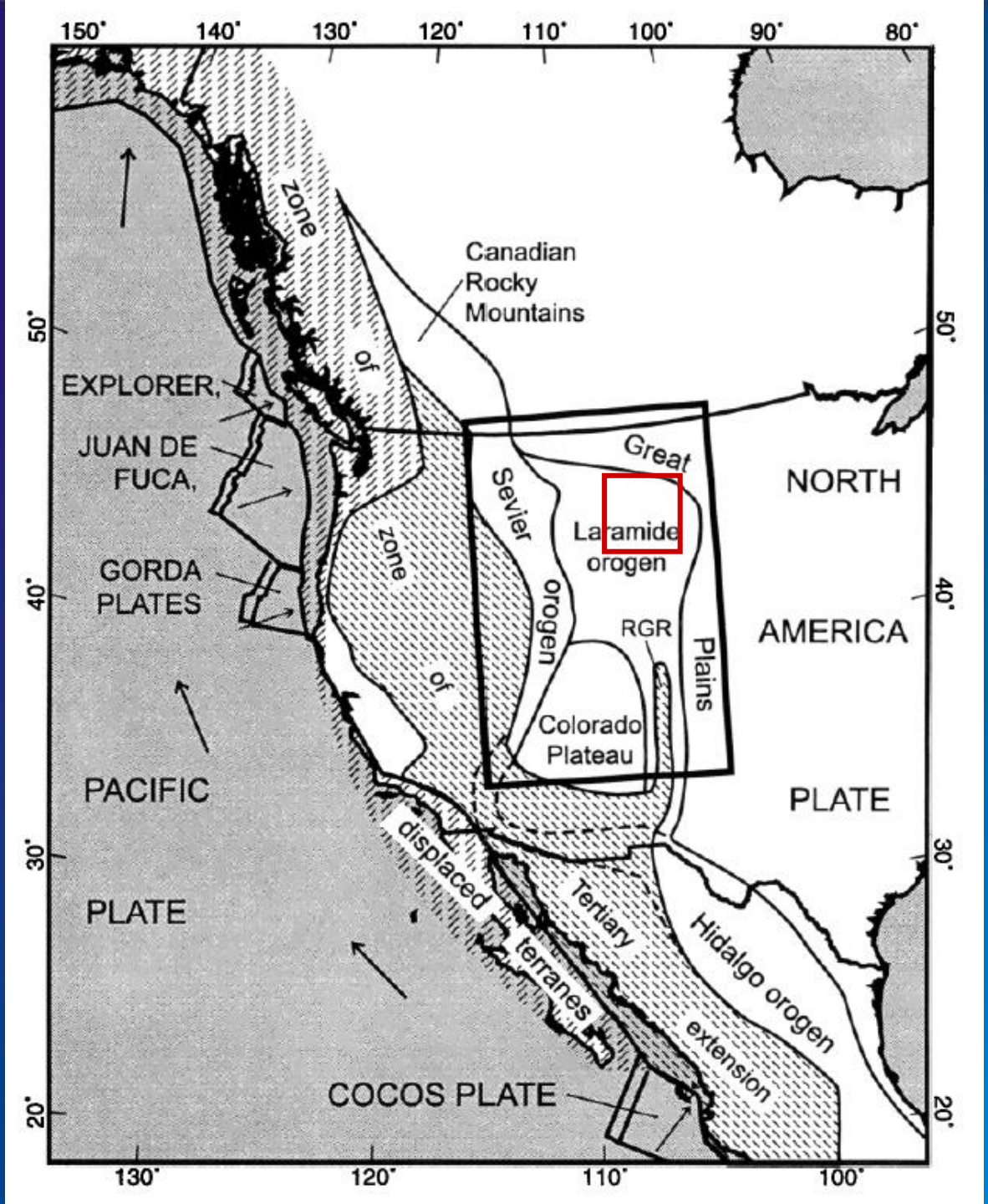
150°
140°
130°
120°
110°
100°
90°
80°
50°
40°
30°
20°
Canadian
Rocky
Mountains
EXPLORER,
JUAN DE
FUCA,
GORDA
PLATES
PACIFIC
PLATE
COCOS PLATE
zone
of
Great
Sevier
orogen
Laramide
orogen
zone
of
RGR
Plains
Colorado
Plateau
NORTH
AMERICA
PLATE
displaced
terranes
Tertiary
Hidalgo orogen
extension

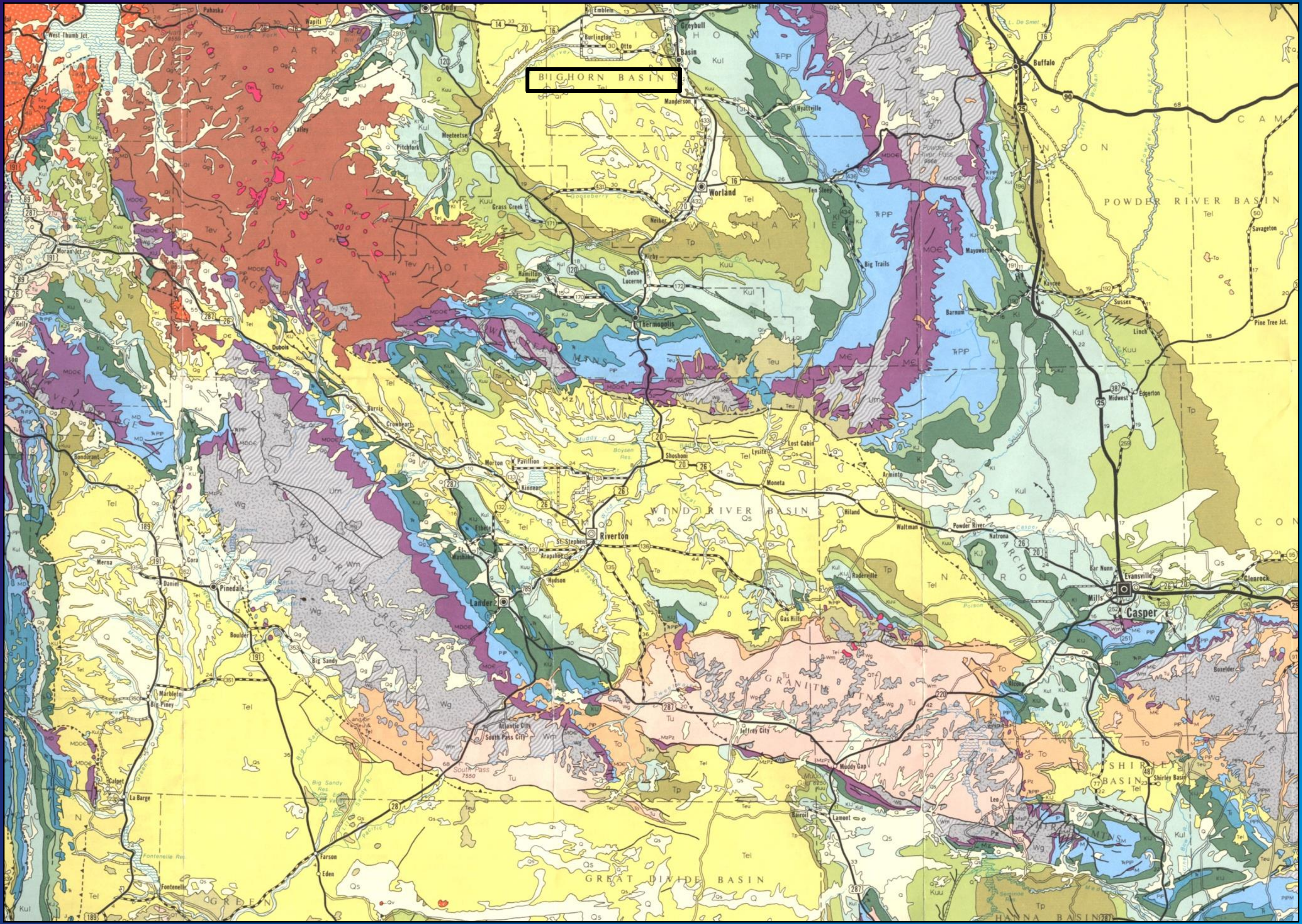

BIGHORN BASIN
WIND RIVER BASIN
POWDER RIVER BASIN
GREAT DIVIDE BASIN
HANNA BASIN
SHIRLEY BASIN
GRANITE MTNS
Cody
Greybull
Basin
Worland
Thermopolis
Riverton
Lander
Casper
Buffalo
Kaycee
Shoshoni
Pinedale
Dubois
South Pass City
Atlantic City
Jeffrey City
Muddy Gap
Farson
Eden
La Barge
Big Piney
Marbleton
Daniel
Boulder
Meeteetse
Ten Sleep
Manderson
Hyattville
Lost Cabin
Moneta
Waltman
Powder River
Mills
Evansville
Glenrock
Midwest
Edgerton

Jurassic – Cretaceous: The Western Interior Basin

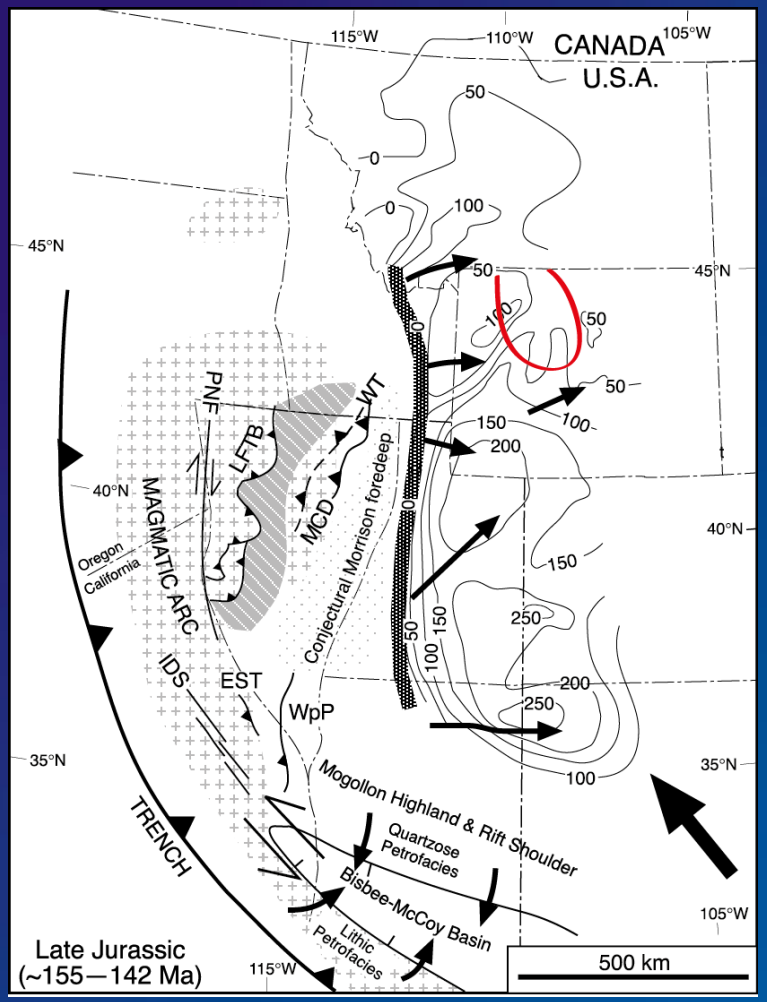

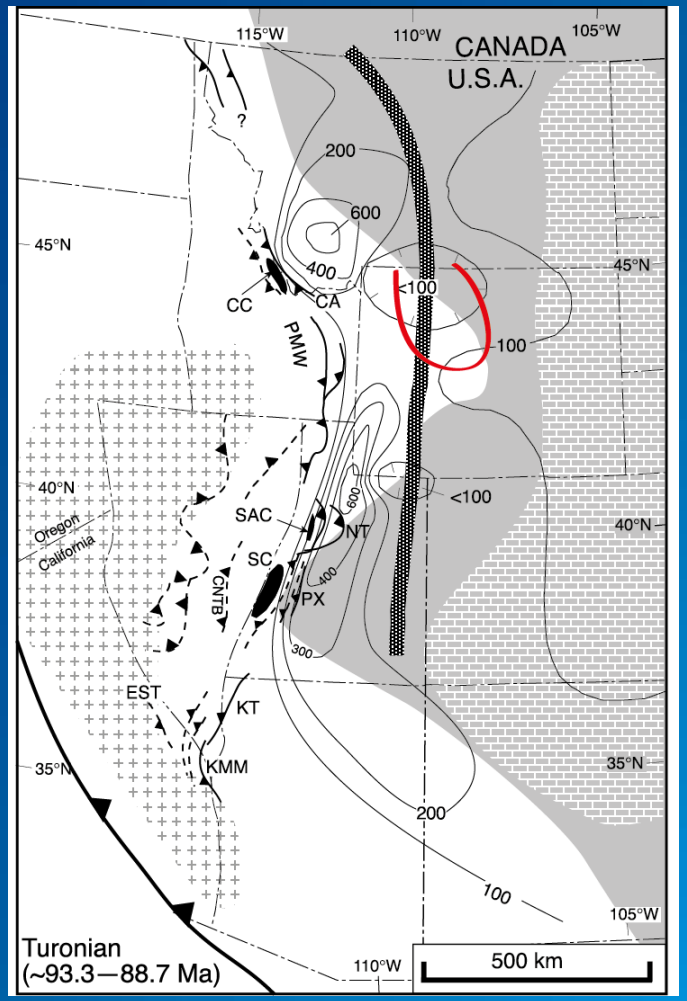

DeCelles, 2004

Late Cretaceous – Paleocene: The Bighorn Basin

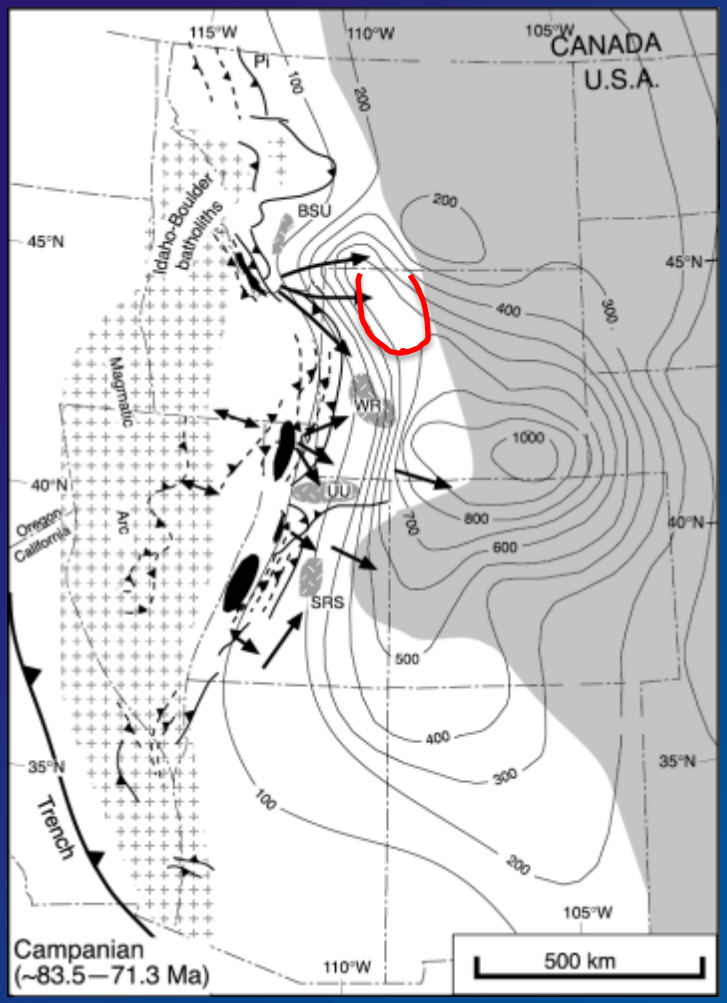

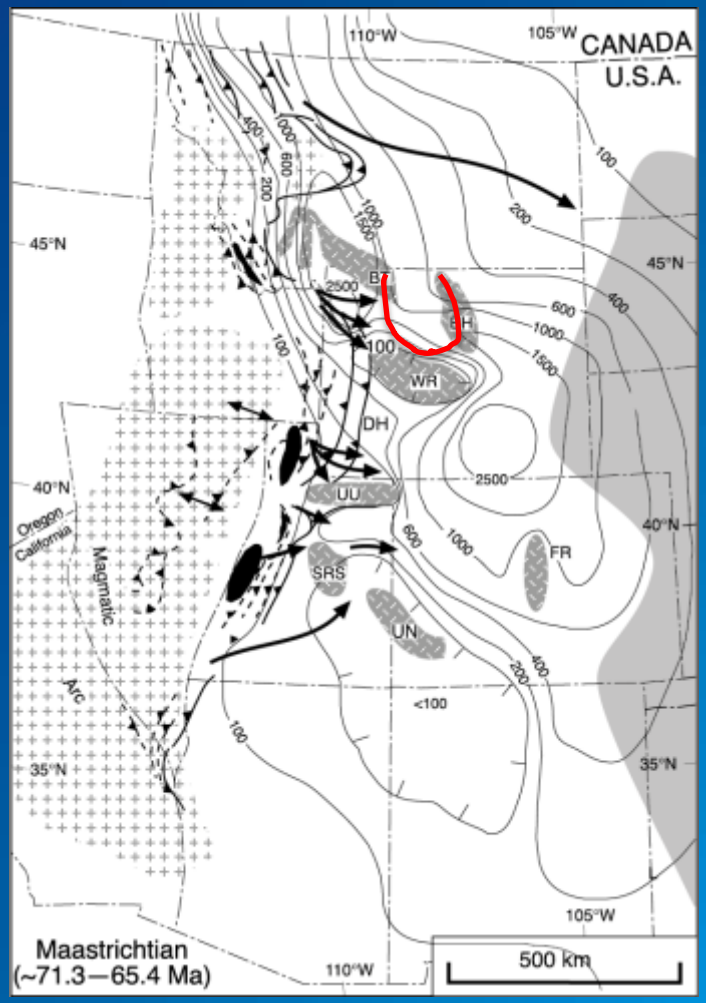

DeCelles, 2004

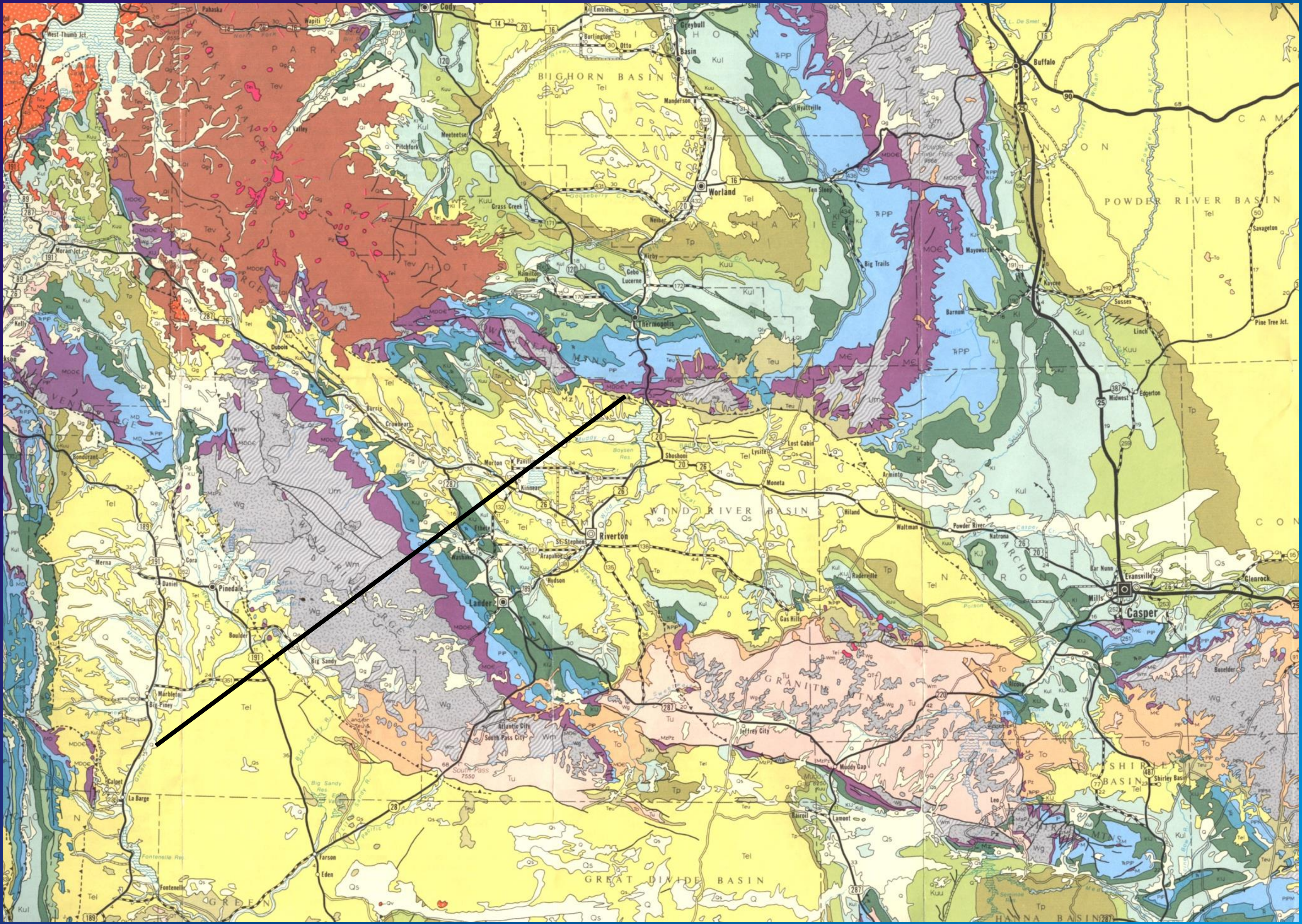

Cody
Greybull
Basin
BIGHORN BASIN
Worland
Buffalo
POWDER RIVER BASIN
Ten Sleep
Big Trails
Thermopolis
Shoshoni
Lost Cabin
Moneta
Riverton
WIND RIVER BASIN
Lander
Pinedale
Daniel
Boulder
Big Sandy
Marbleton
Big Piney
La Barge
Casper
Evansville
Mills
Natrona
Powder River
Waltman
Hiland
Arminto
Kaycee
Midwest
Edgerton
GRANITE MTNS
Jeffrey City
Atlantic City
South Pass City
Muddy Gap
Lamont
Bairoil
Farson
Eden
Fontenelle
GREAT DIVIDE BASIN
HANNA BASIN
SHIRLEY BASIN
Dubois
Burris
Crowheart
Kinnear
Pavillion
Morton
Hudson
Arapahoe
St. Stephens
Cora
Merna
Bondurant
Kelly
Moran Jct
Meeteetse
Pitchfork
Grass Creek
Hamilton Dome
Gebo
Lucerne
Kirby
Manderson
Hyattville
Barnum
Mayoworth
Linch
Sussex
Savageton
Pine Tree Jct.
Glenrock
Bar Nunn
Leo
Alcova
Gas Hills
Raderville
Lysite
Emblem
Burlington
Otto
Wapiti
Pahaska
West Thumb Jct.
Calpet

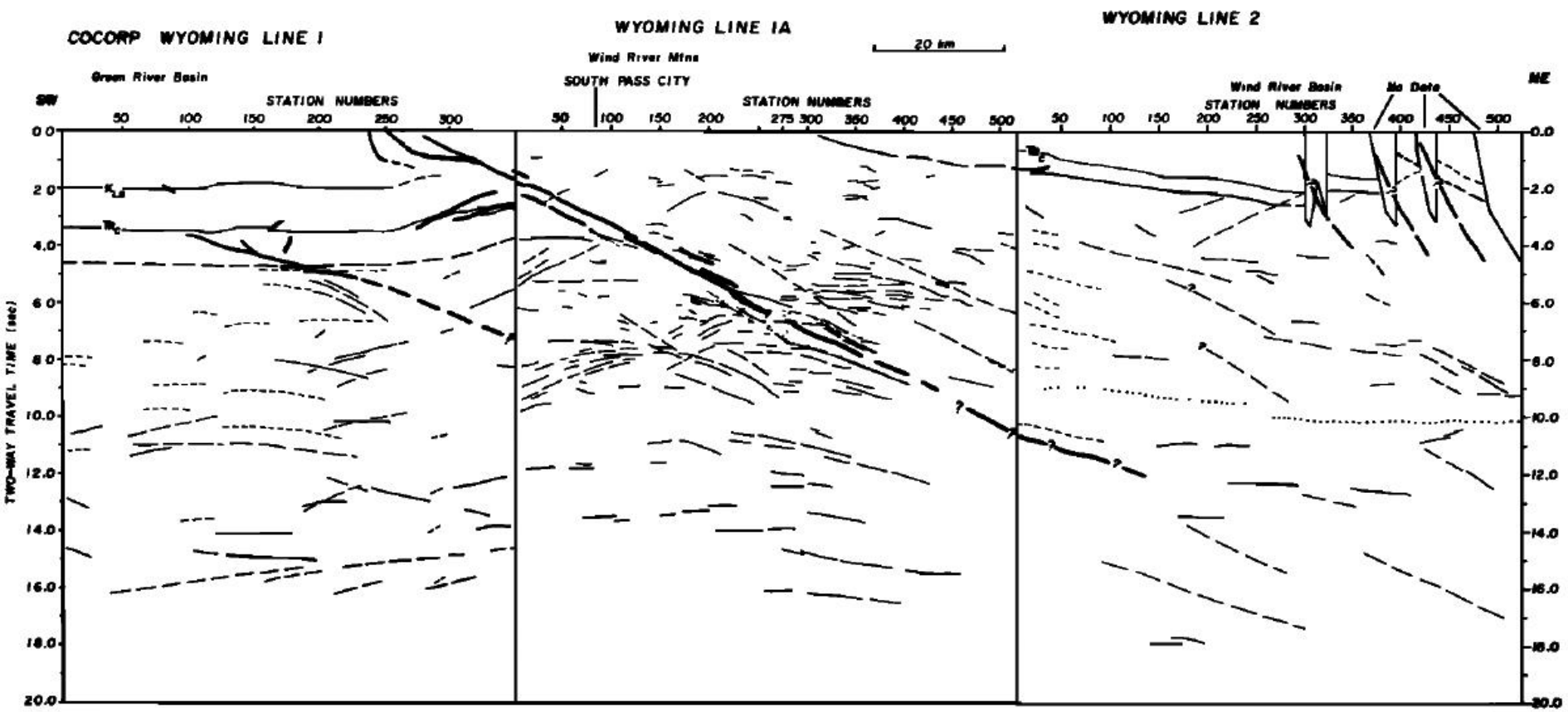

Smithson et al. (1979)

Beaudoin, PhD thesis, 2012

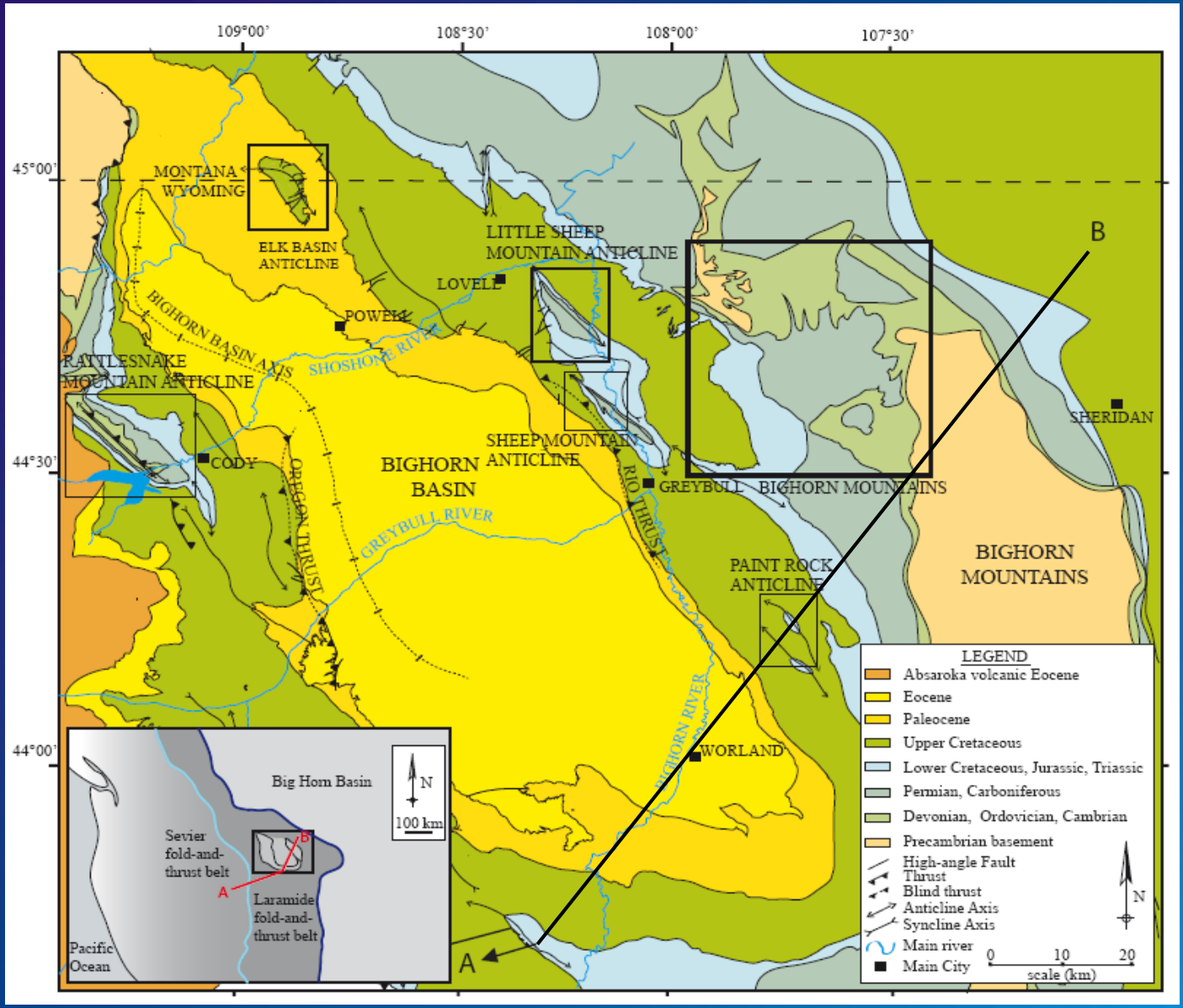

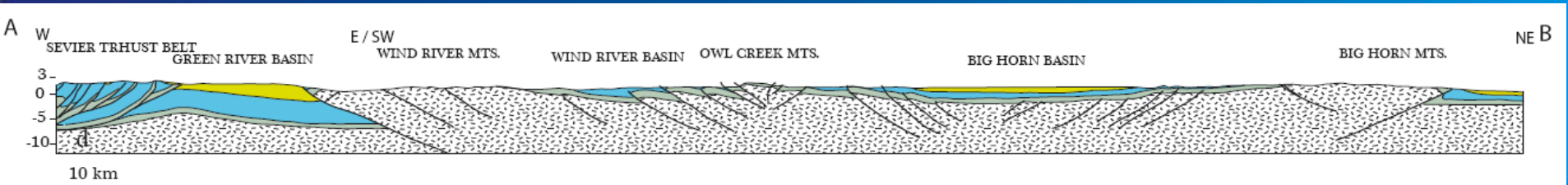

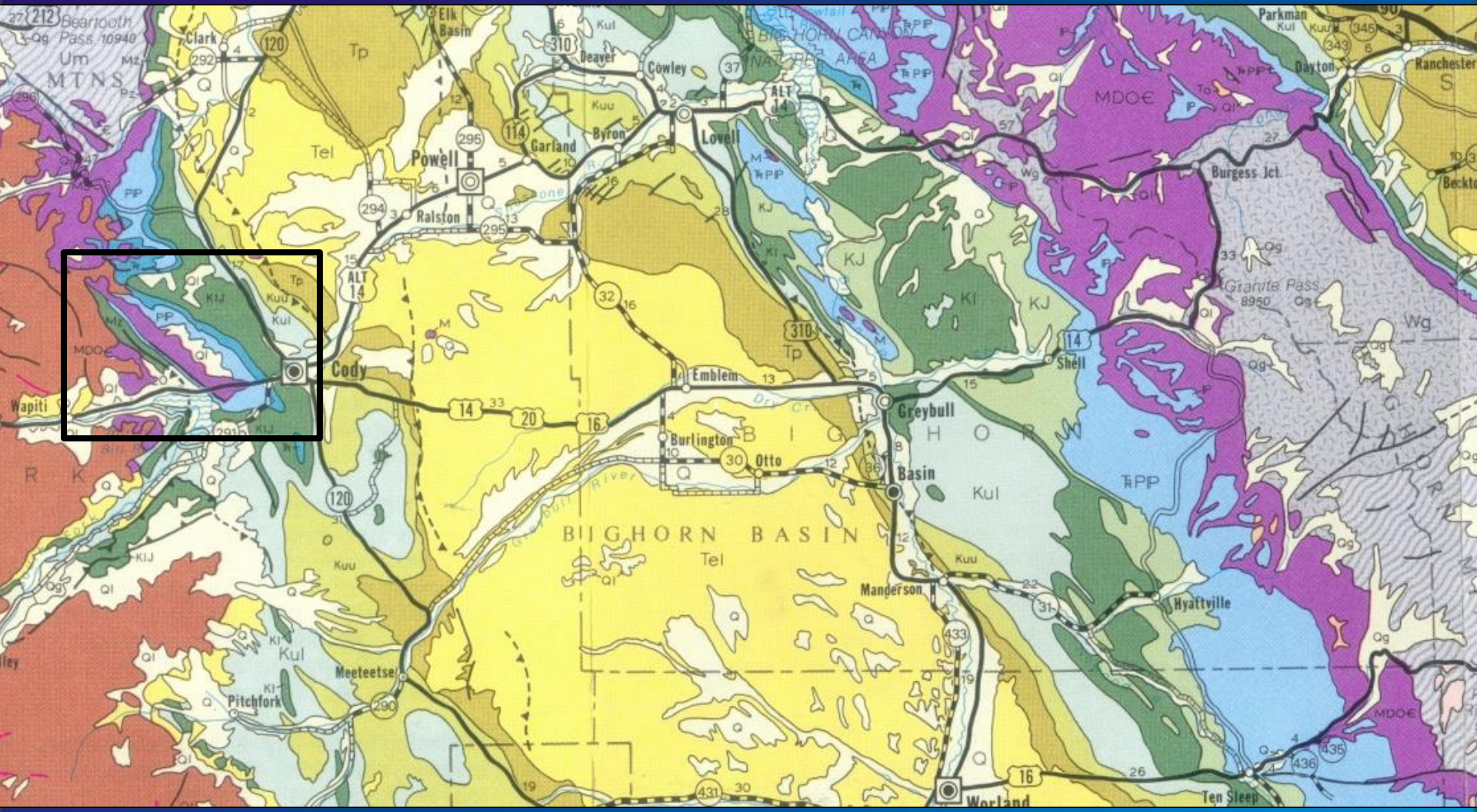
Clark
Elk Basin
Deaver
Cowley
Lovell
Byron
Garland
Powell
Ralston
Cody
Wapiti
Emblem
Burlington
Otto
Greybull
Basin
Shell
Burgess Jct.
Parkman
Dayton
Ranchester
Granite Pass
8950
BIGHORN BASIN
Manderson
Hyattville
Meeteetse
Pitchfork
Worland
Ten Sleep
Beartooth Pass 10940
MTNS
BIGHORN CANYON NATIONAL RECREATION AREA
Tp
Tel
Kul
Kuu
KJ
KI
KIJ
PP
PPP
MDOe
Wg
Og
Ql
Q
10 km

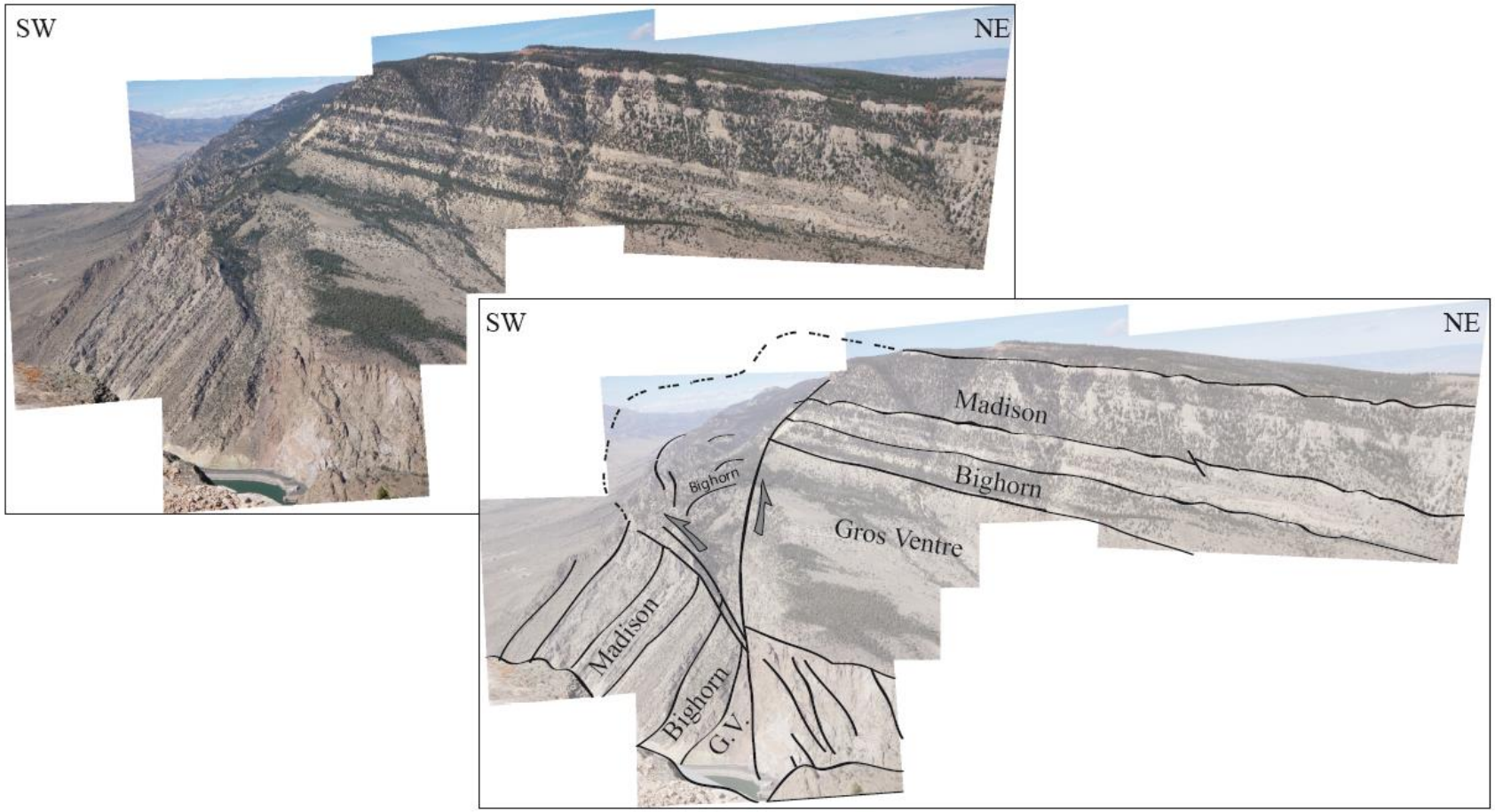

Beaudoin et al., 2012

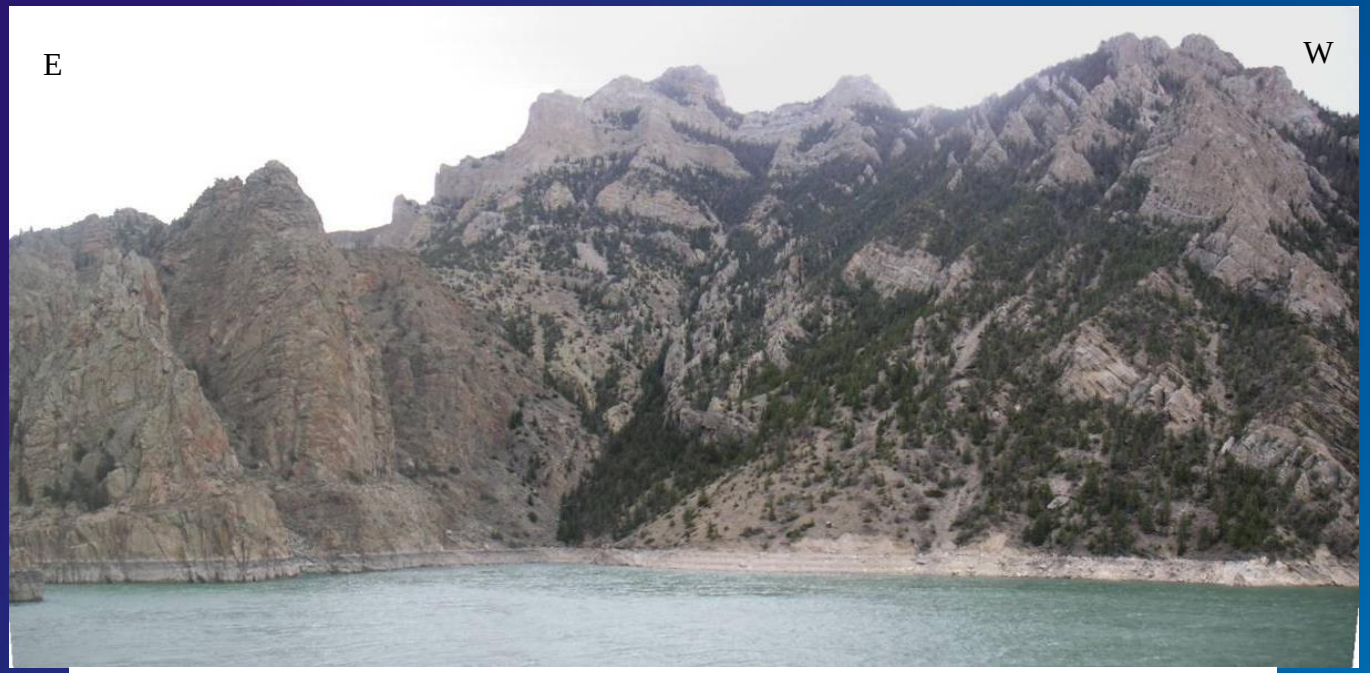
E
W

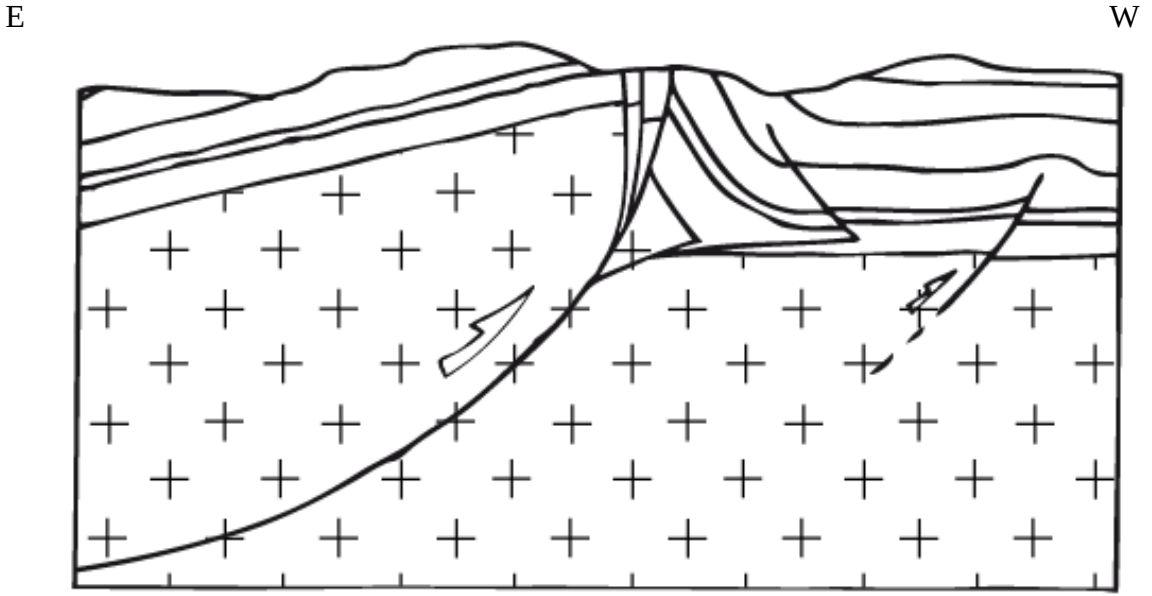
E
W

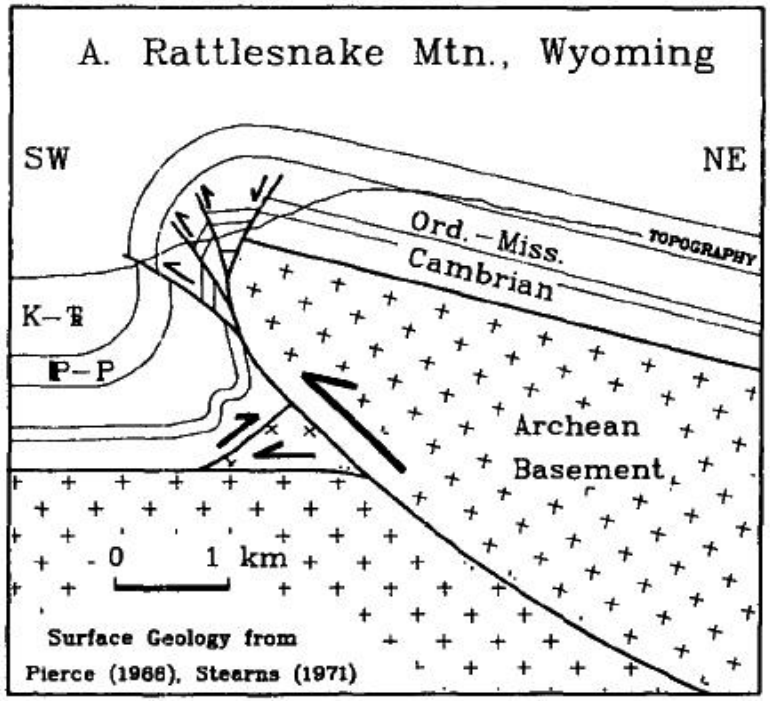
A. Rattlesnake Mtn., Wyoming
SW
NE
Ord.–Miss.
Cambrian
TOPOGRAPHY
K–T
P–P
Archean
Basement
0
1 km
Surface Geology from
Pierce (1966), Stearns (1971)

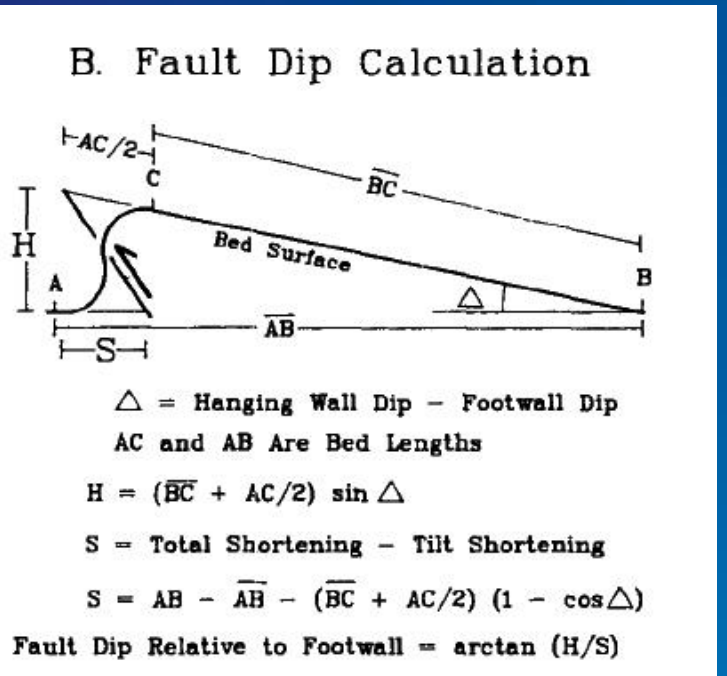
B. Fault Dip Calculation
AC/2
C
BC
H
Bed Surface
A
B
AB
S
△ = Hanging Wall Dip – Footwall Dip
AC and AB Are Bed Lengths
H = (BC + AC/2) sin △
S = Total Shortening – Tilt Shortening
S = AB – AB – (BC + AC/2) (1 – cos△)
Fault Dip Relative to Footwall = arctan (H/S)

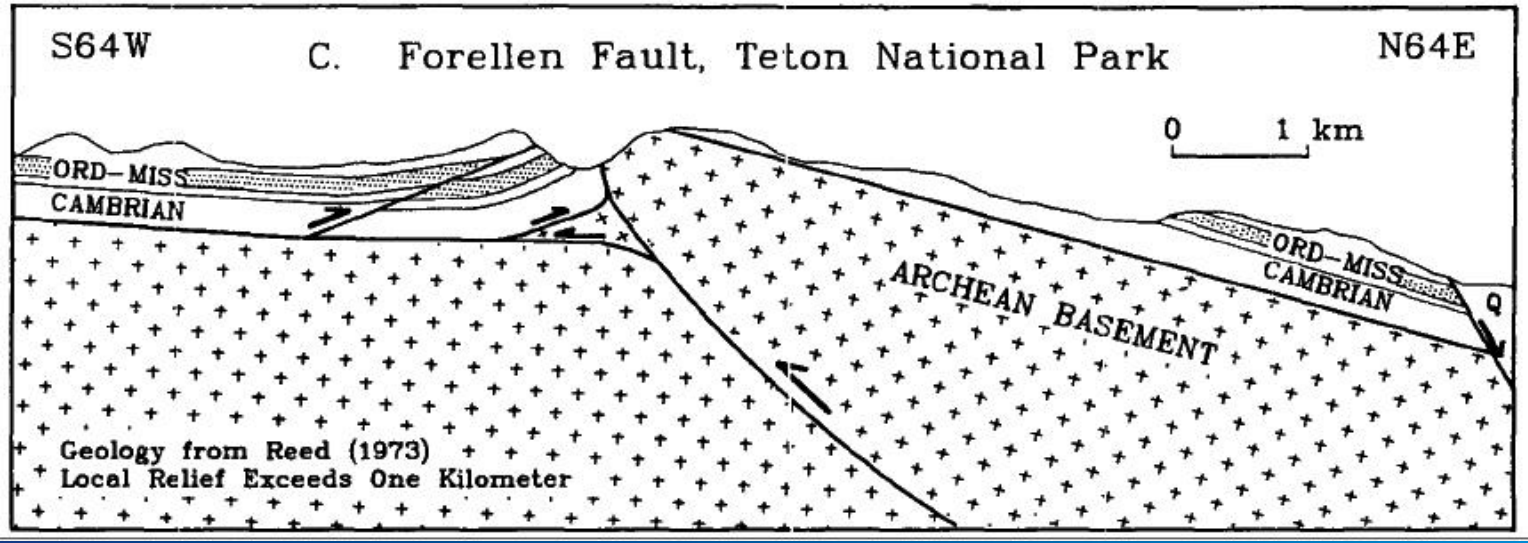
S64W
C. Forellen Fault, Teton National Park
N64E
0
1 km
ORD–MISS
CAMBRIAN
ARCHEAN BASEMENT
ORD–MISS
CAMBRIAN
Q
Geology from Reed (1973)
Local Relief Exceeds One Kilometer

Erslev (1986)

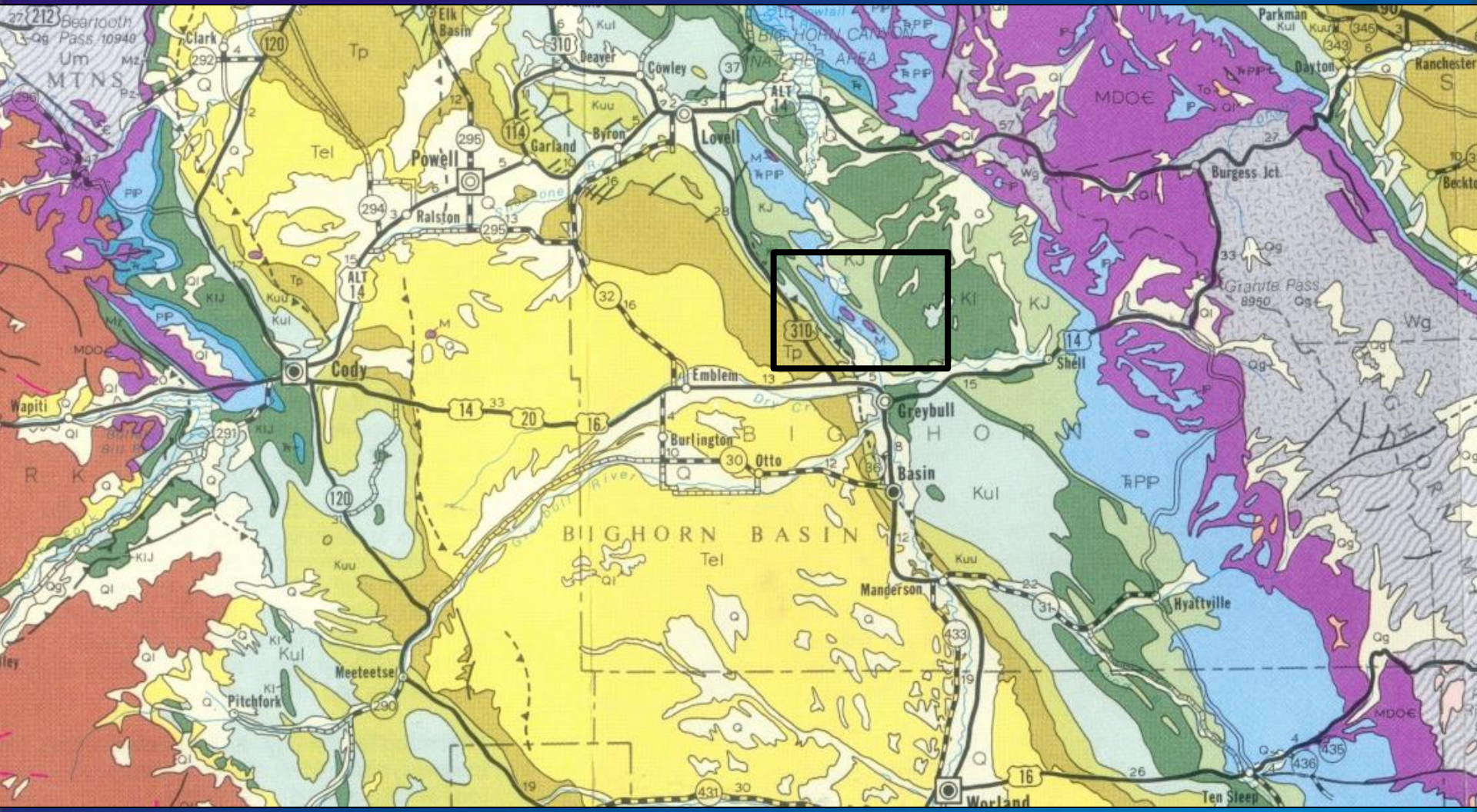
Cody
Powell
Ralston
Garland
Byron
Deaver
Cowley
Lovell
Elk Basin
Clark
Emblem
Burlington
Otto
Greybull
Basin
Shell
Burgess Jct.
Dayton
Parkman
Ranchester
Wapiti
Meeteetse
Pitchfork
Manderson
Hyattville
Worland
Ten Sleep
BIGHORN BASIN
Granite Pass
8950
Beartooth Pass 10940
MTNS
BIGHORN CANYON NATIONAL RECREATION AREA
Tel
Kul
Kuu
KJ
KI
MDOe
PPP
Wg
Tp
Qg
Qi
10 km

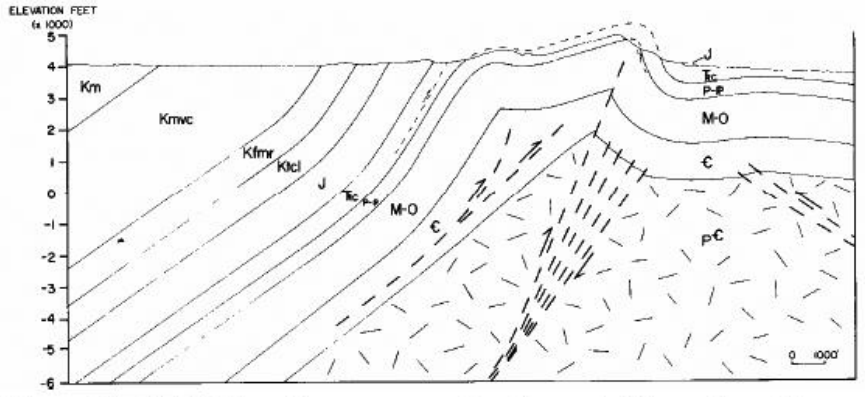

SW–NE trending cross section through Sheep Mountain anticline from Hennier and Spang, 1983. Bedding dips and Formation contacts are constrained by surface mapping and geologic markers from exploration wells. Hennier and Spang postulate a relatively undeformed basement with multiple thrust planes in an overall wedge shaped geometry to generate folding in the overlying sediments.

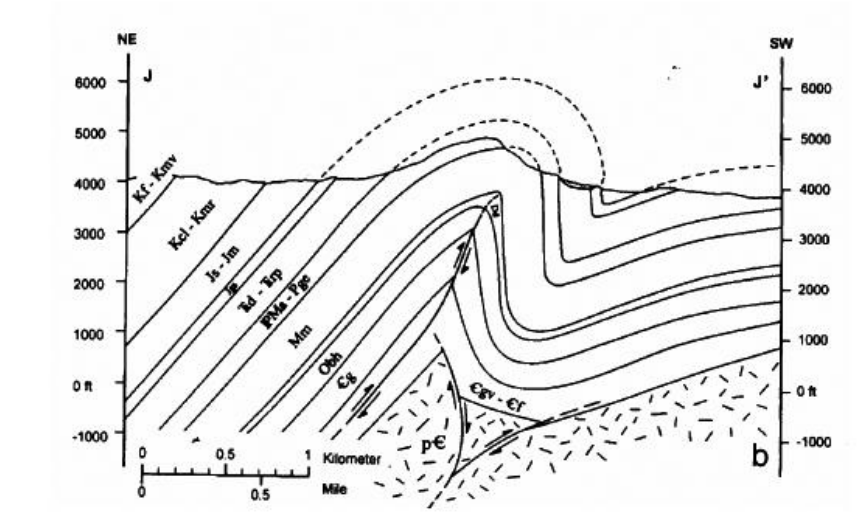

SW-NE trending cross-section through Sheep Mountain anticline from Forster et al., 1996. Bedding dips and Formation are constrained by surface mapping and geologic markers from exploration wells. A wedge shaped fault zone is hypothesized as the mechanism by which overlying strata fold.

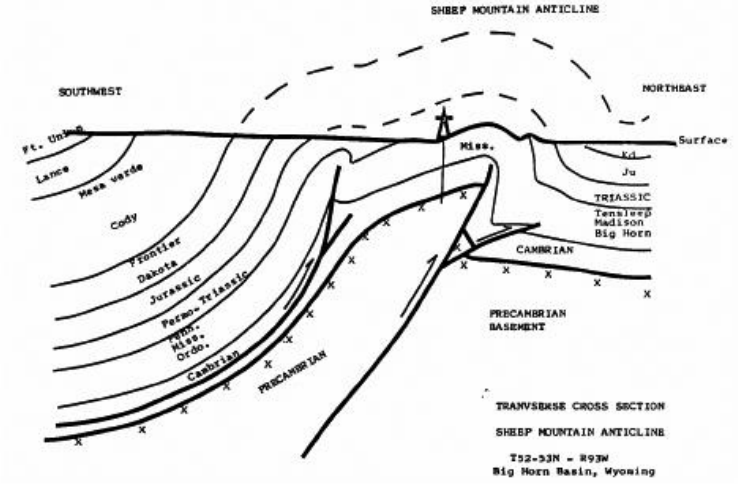

SW-NE trending cross-section through Sheep Mountain anticline from Brown, 1984. Geological constraints are not given, but are most likely surface dips and formation markers from wells. Brown proposes substantial basement folding and a wedge shaped fault zone beneath the forelimb of Sheep Mountain.

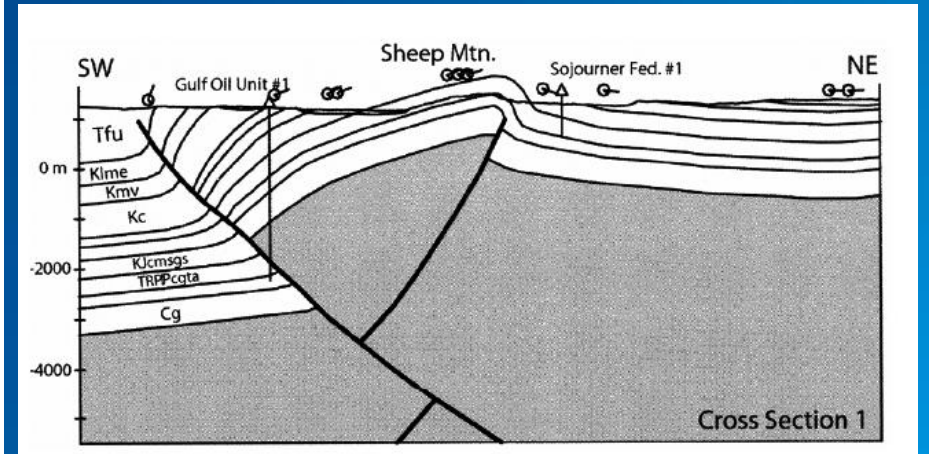

SW-NE trending cross-section through Sheep Mountain anticline from Stanton and Erslev, 2002. Geological constraints are surface dips, formation markers from wells, and three 2D seismic profiles. Stanton and Erslev propose a moderately folded basement. Their kinematic modeling suggests that the Rio thrust fault slipped after slip along the fault beneath Sheep Mountain Anticline had already uplifted the fold.

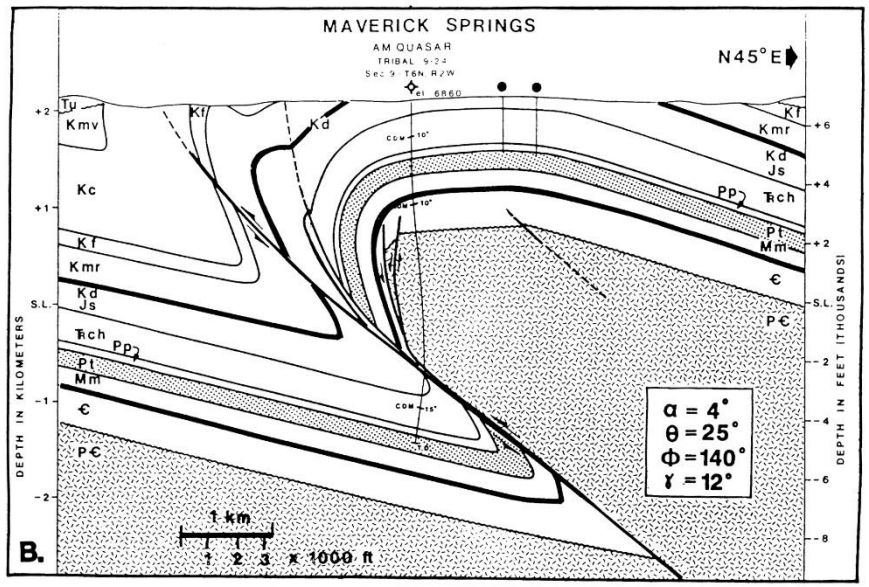

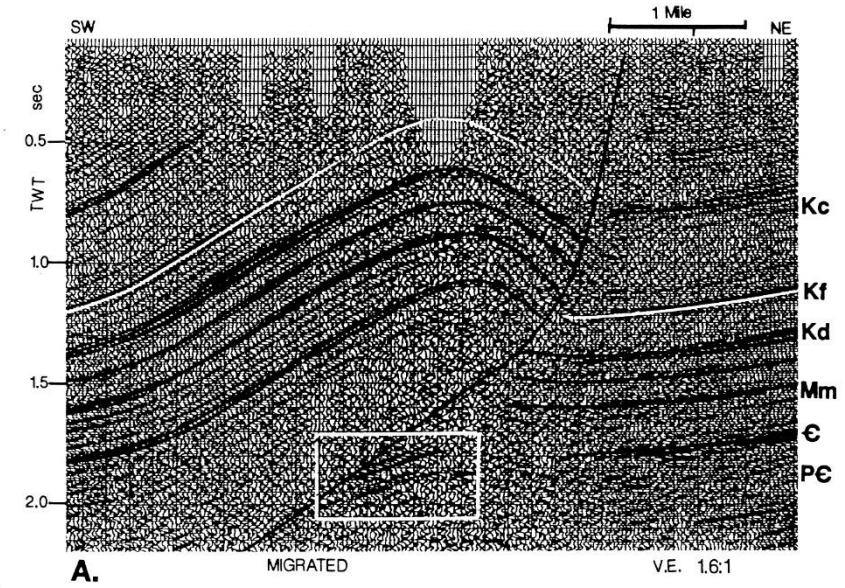

Stone (1993)

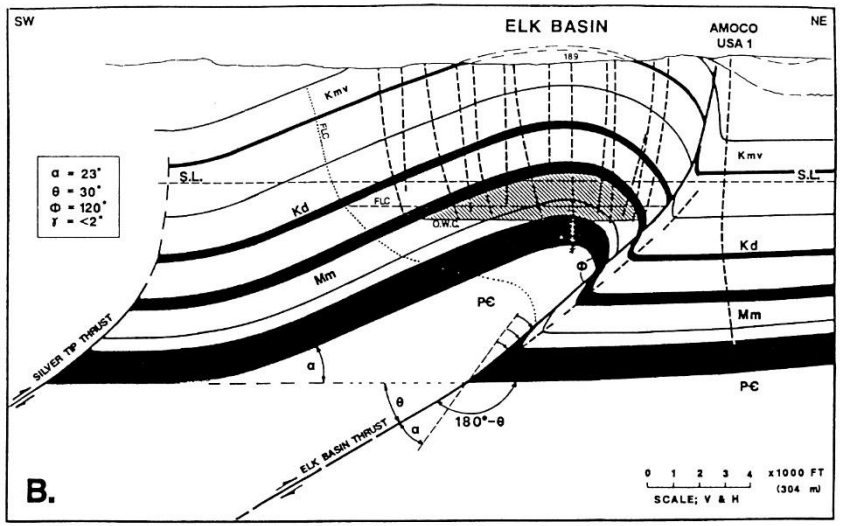

Elk Basin anticline, a mature thrust fold. A: Time-migrated, interpreted seismic profile (600% dynamite, 1969; modified from Weitzel, 1985). TWT is two-way traveltime. B: Structural cross section (see Fig. 15 C) showing well control, common Paleozoic oil pool (diagonally lined with oil-water contact (O.W.C.), a fault-limited chord (FLC) at the base of the Dakota (Kd) horizon, and values for the various angles (modified from Stone, 1983a). S.L. is sea level.

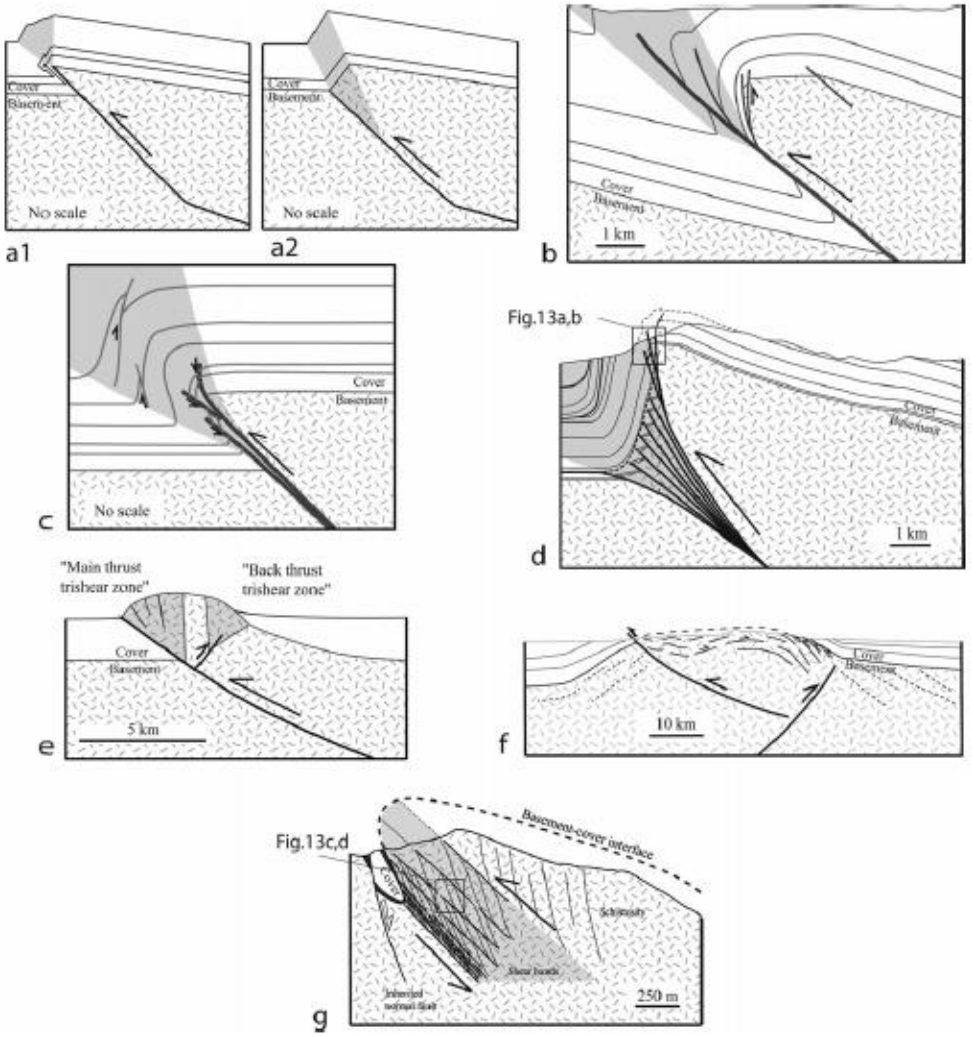

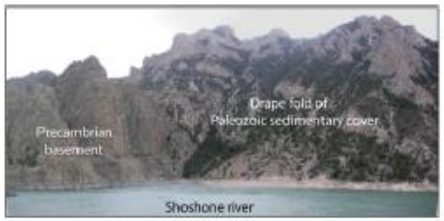

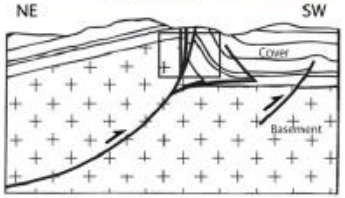

a

Rattlesnake Mountain anticline, Wyoming, USA

c Plan du Lac basement shear zones (Oisans Massif, Western Alps)

b

Rattlesnale Mountain anticline : high-angle reverse fault with a shaly gouge, in the Precambrian basement rocks. The fault is parallel to major fractures within the basement.

d

Mylonitic deformation associated with basement shear zones in the Oisans Massif (Western Alps)

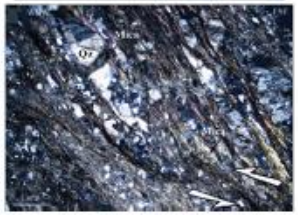

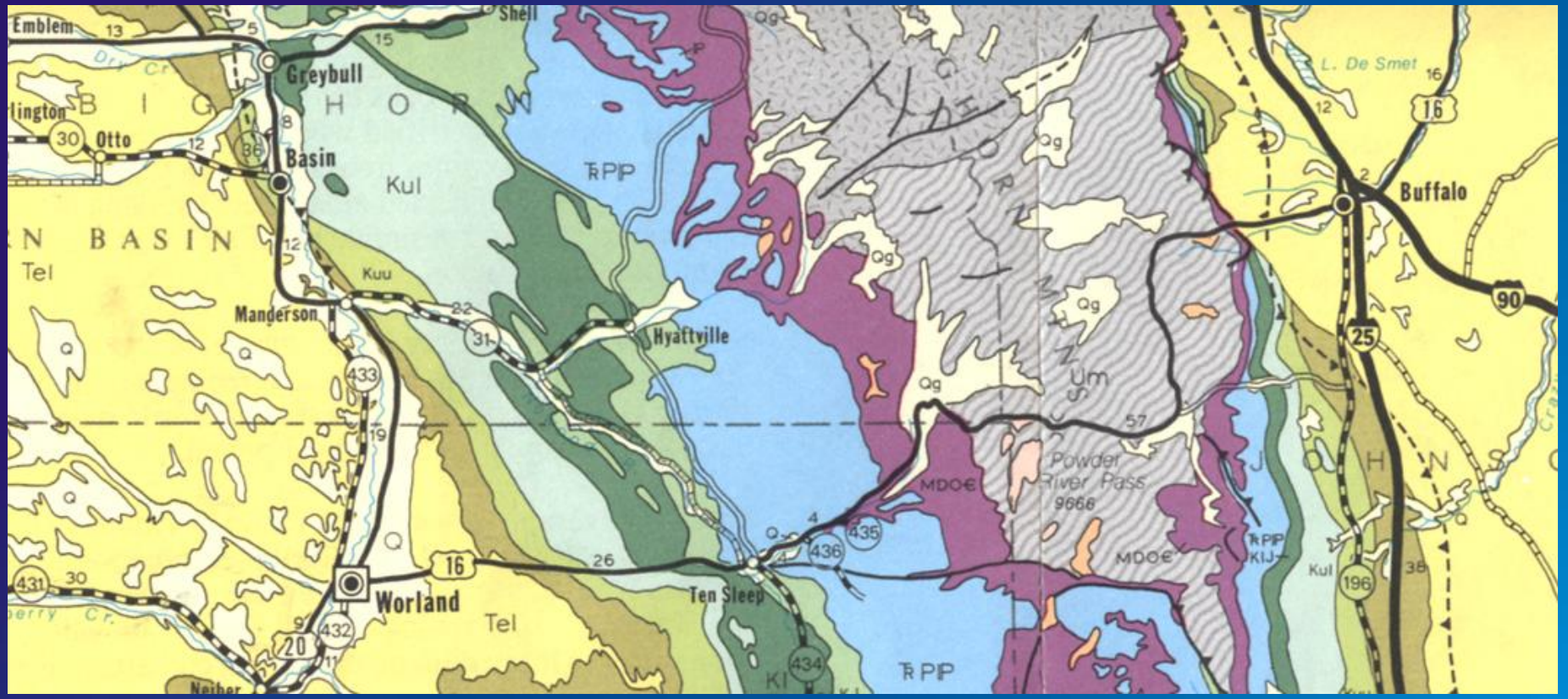
Emblem
Shell
Greybull
Otto
Basin
Kul
TrPP
Qg
L. De Smet
Buffalo
Tel
Kuu
Manderson
Hyattville
Um
Powder River Pass
9666
MDOe
Worland
Ten Sleep
TrPP KIJ
Kul
Tel
Kl
TrPP

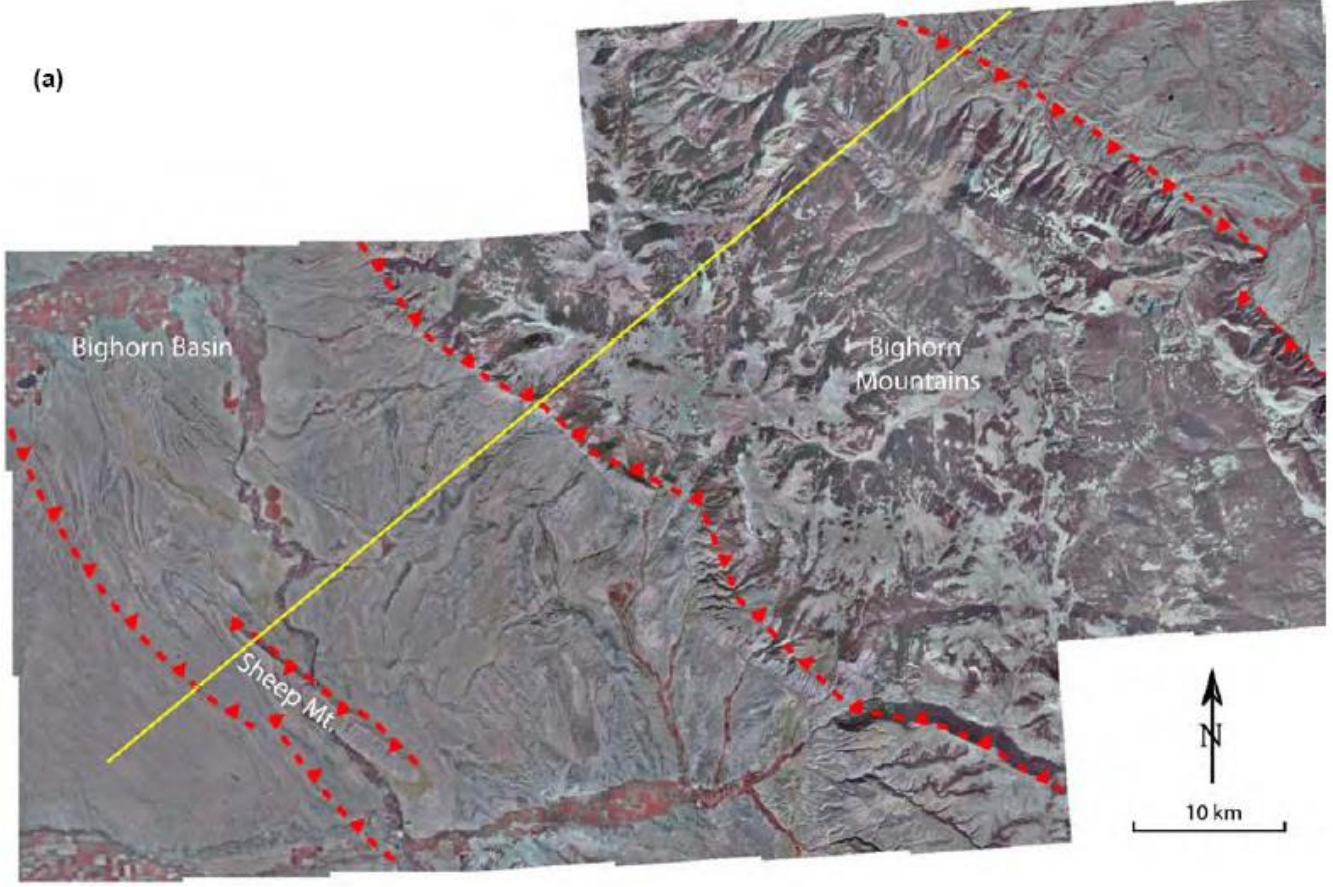
(a)
Bighorn Basin
Bighorn
Mountains
Sheep Mt.
N
10 km

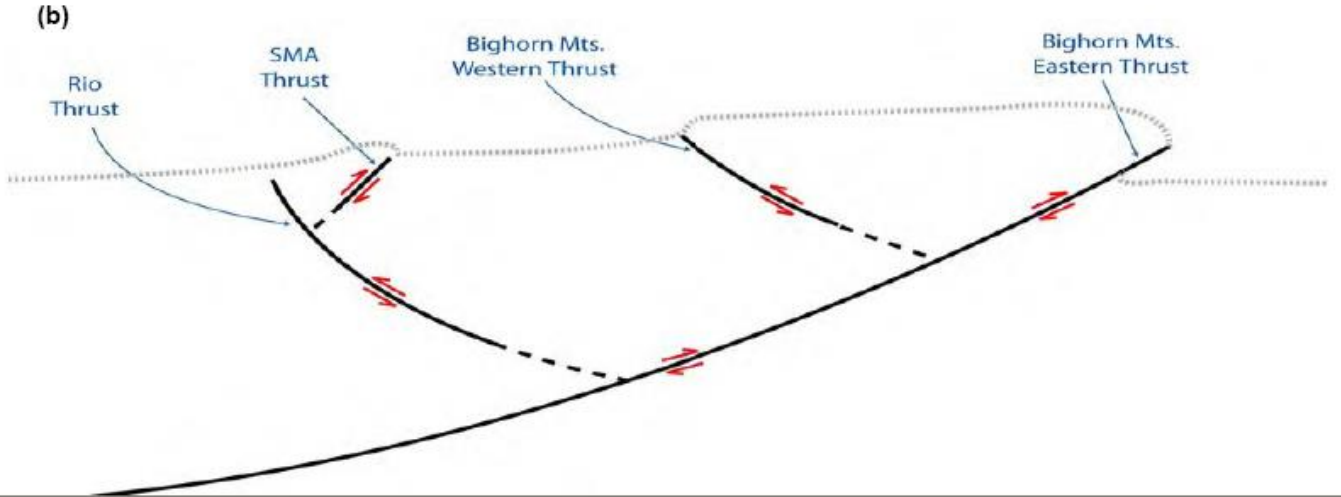
(b)
Rio
Thrust
SMA
Thrust
Bighorn Mts.
Western Thrust
Bighorn Mts.
Eastern Thrust

Basement-Involved, Second-Order Anticlinal Structures

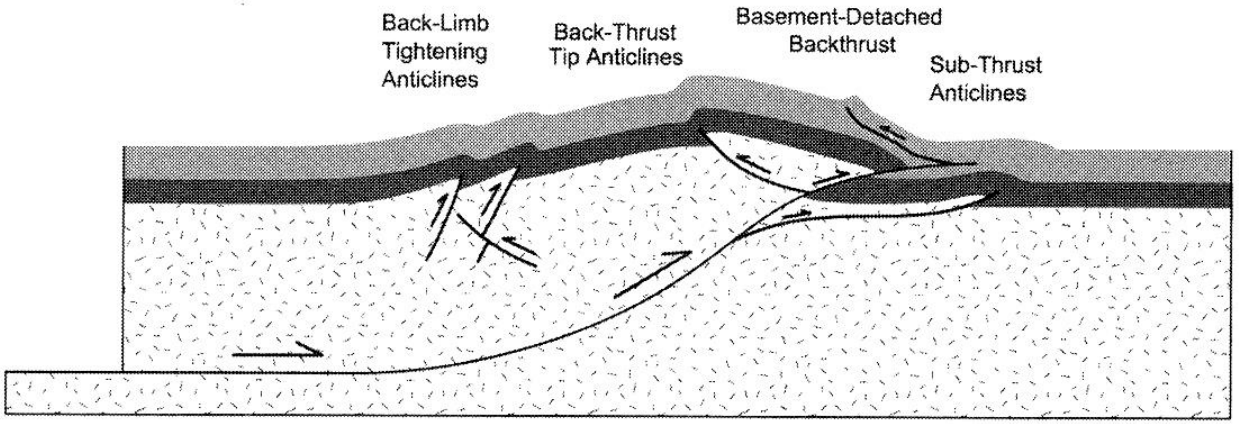

Restored Section

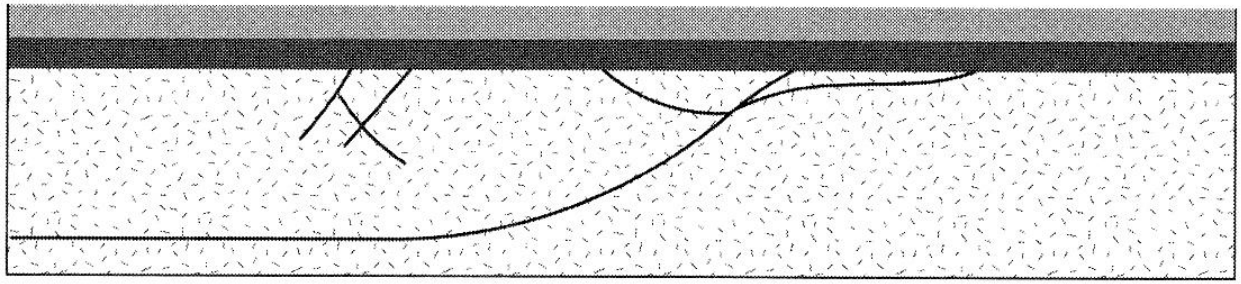

Erslev (2005)

Marshak et al. (2000)

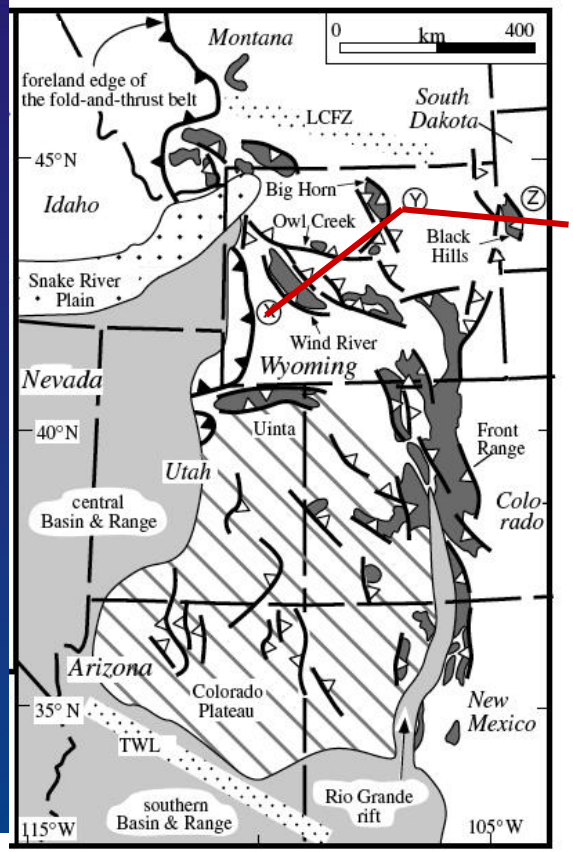

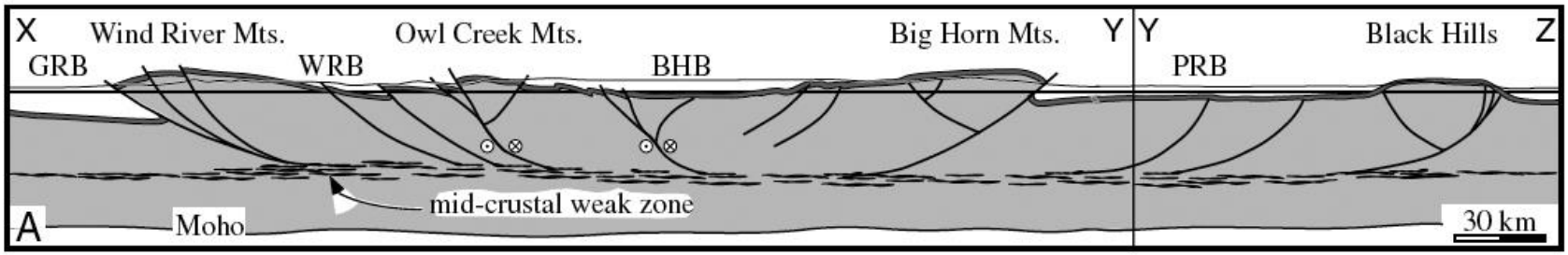

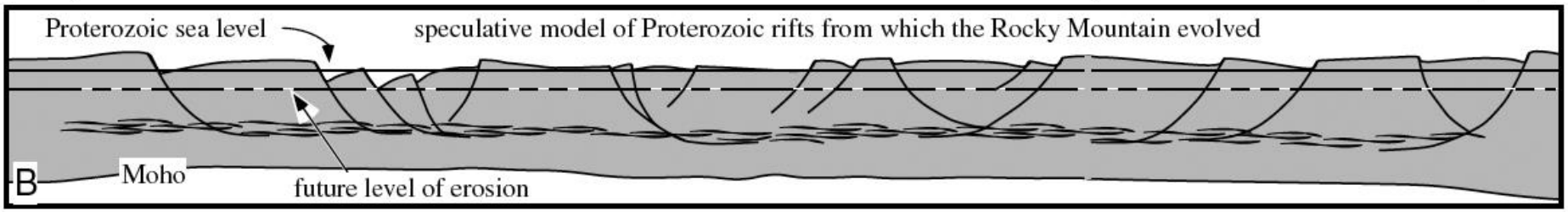

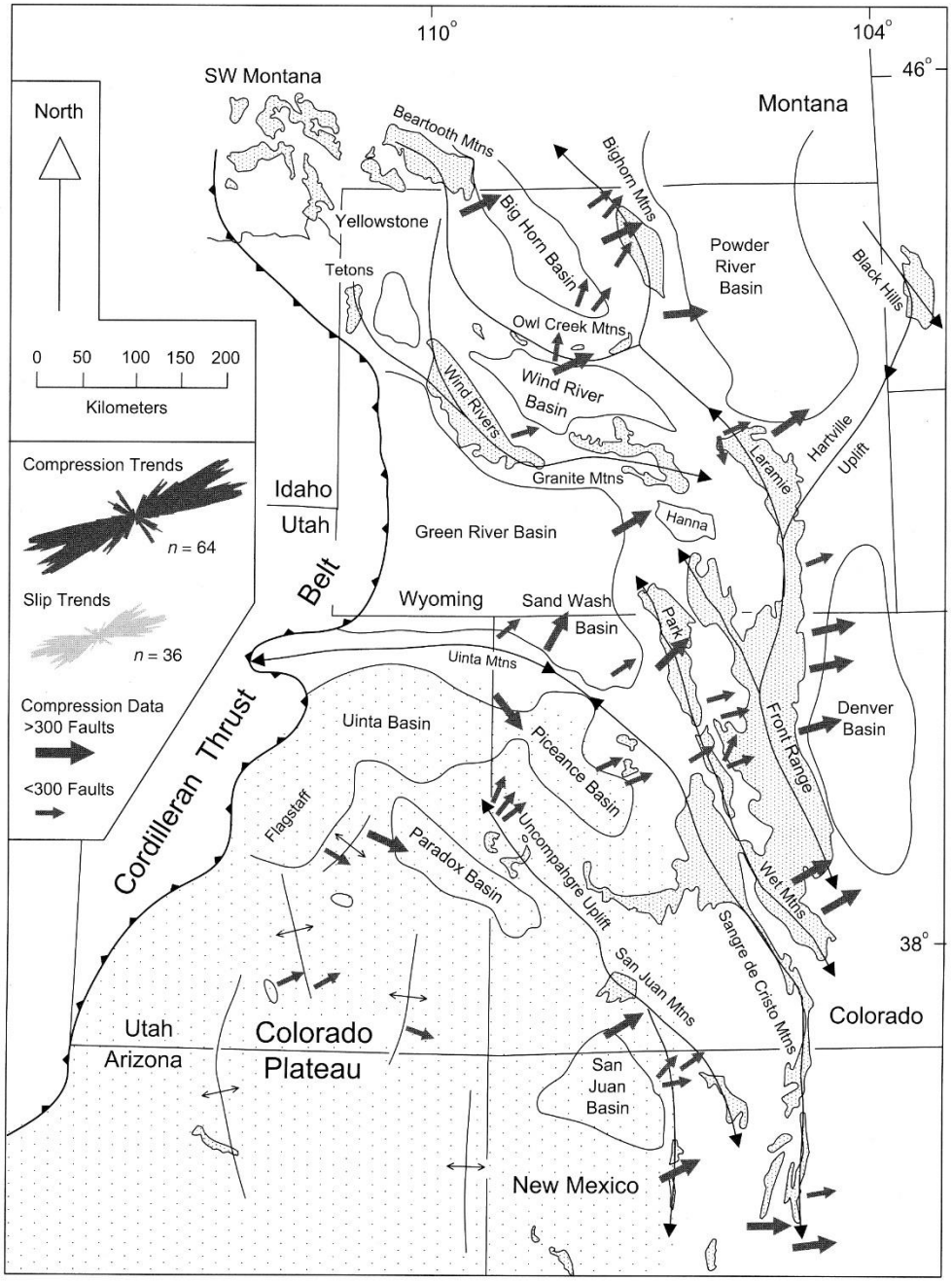

Figure 1. Tectonic map of the Rocky Mountain region showing the major Laramide arches, which are commonly cored by Precambrian crystalline basement exposures (fine stipple), as well as the adjoining Colorado Plateau (coarse stipple) and Cordilleran thrust belt. Average compression directions from minor faults are shown as arrows; smoothed (10°) rose diagrams show all compression and slip directions from Table 2.

Erslev (2009)

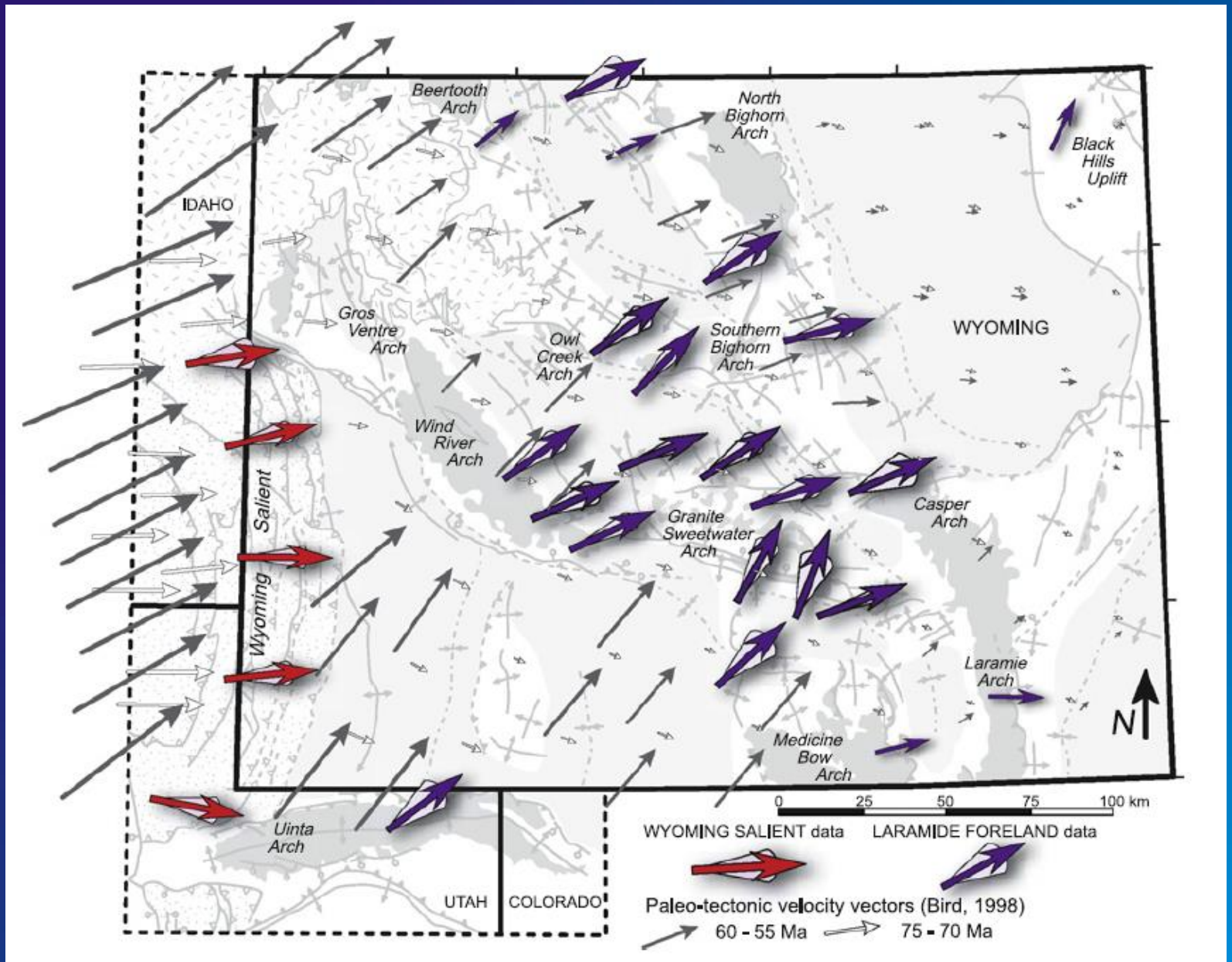

(Weil and Yonkee, 2012)

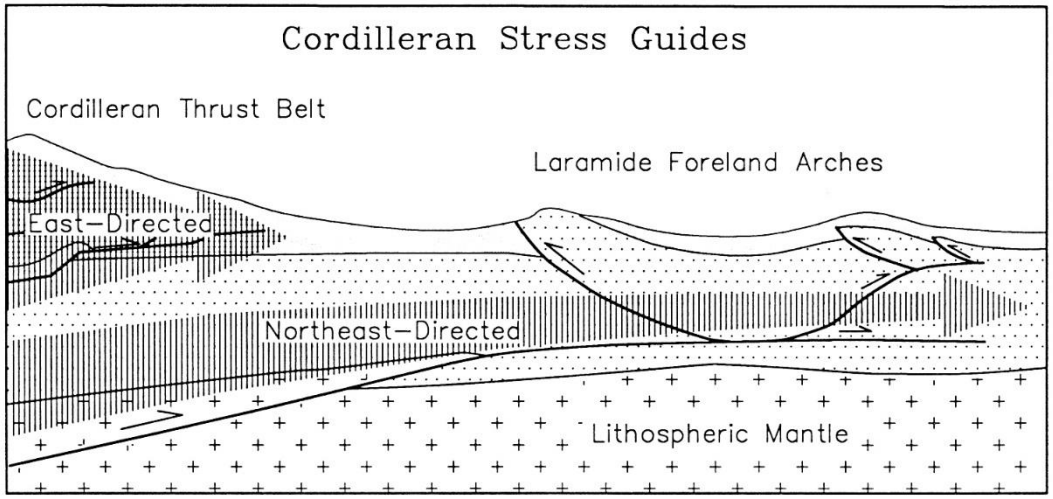

Schematic cartoon showing multiple stress guides and multilevel detachment during Cordilleran-Laramide lateral compression.

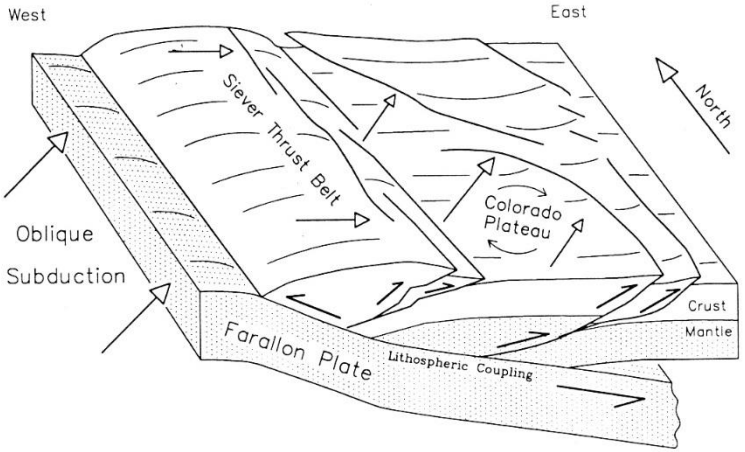

Schematic block diagram showing the development of Laramide structures by crustal detachment during lithospheric coupling in a low-angle subduction west of the Rockies. Note that variable slip on the detachment could explain the rotation of the Colorado Plateau.

Erslev (1993)

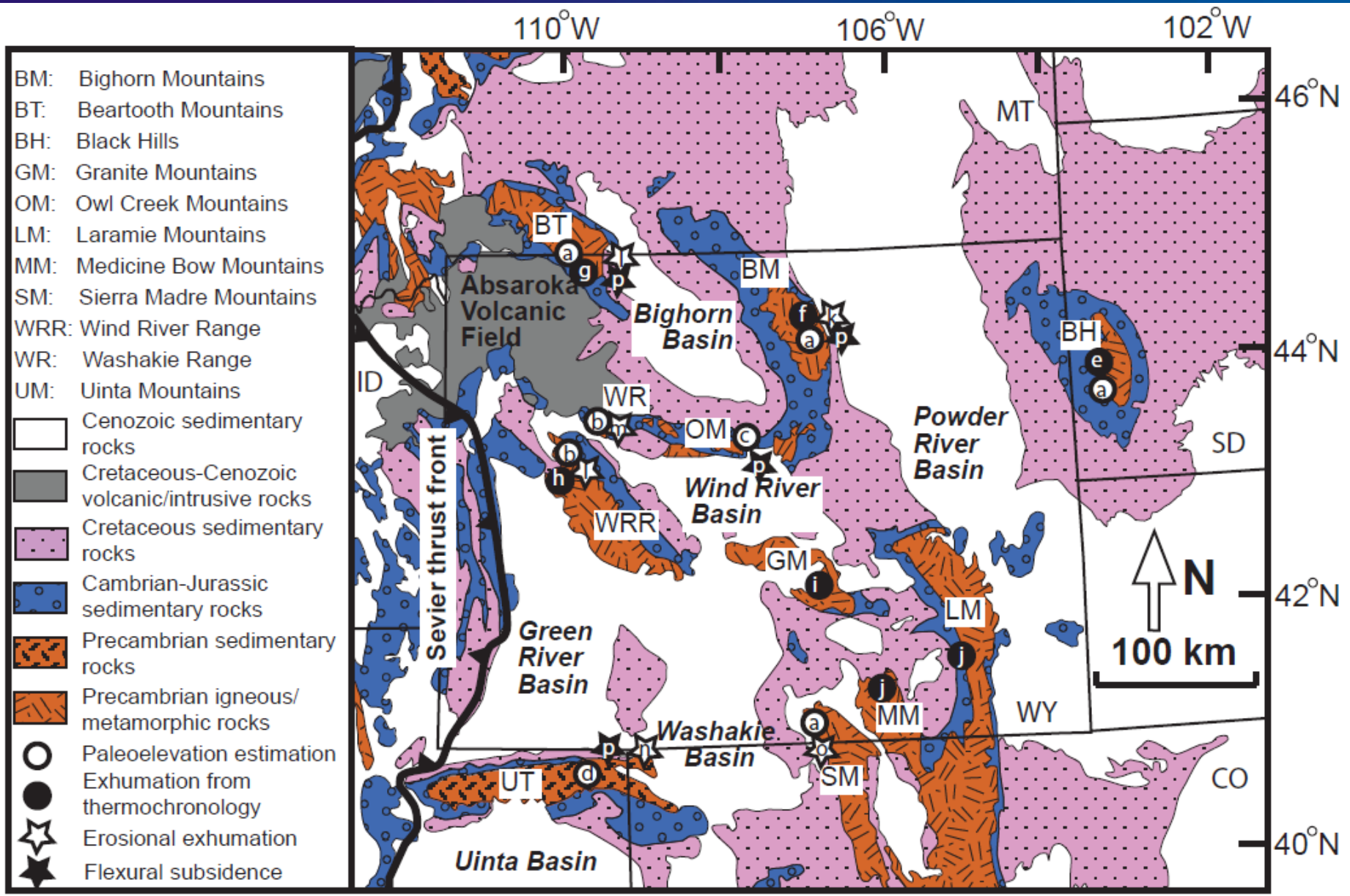
BM: Bighorn Mountains
BT: Beartooth Mountains
BH: Black Hills
GM: Granite Mountains
OM: Owl Creek Mountains
LM: Laramie Mountains
MM: Medicine Bow Mountains
SM: Sierra Madre Mountains
WRR: Wind River Range
WR: Washakie Range
UM: Uinta Mountains
Cenozoic sedimentary rocks
Cretaceous-Cenozoic volcanic/intrusive rocks
Cretaceous sedimentary rocks
Cambrian-Jurassic sedimentary rocks
Precambrian sedimentary rocks
Precambrian igneous/ metamorphic rocks
Paleoelevation estimation
Exhumation from thermochronology
Erosional exhumation
Flexural subsidence
110°W
106°W
102°W
46°N
44°N
42°N
40°N
MT
SD
WY
CO
ID
BT
BM
BH
WR
OM
WRR
GM
LM
MM
SM
UT
Absaroka Volcanic Field
Bighorn Basin
Powder River Basin
Wind River Basin
Green River Basin
Washakie Basin
Uinta Basin
Sevier thrust front
N
100 km

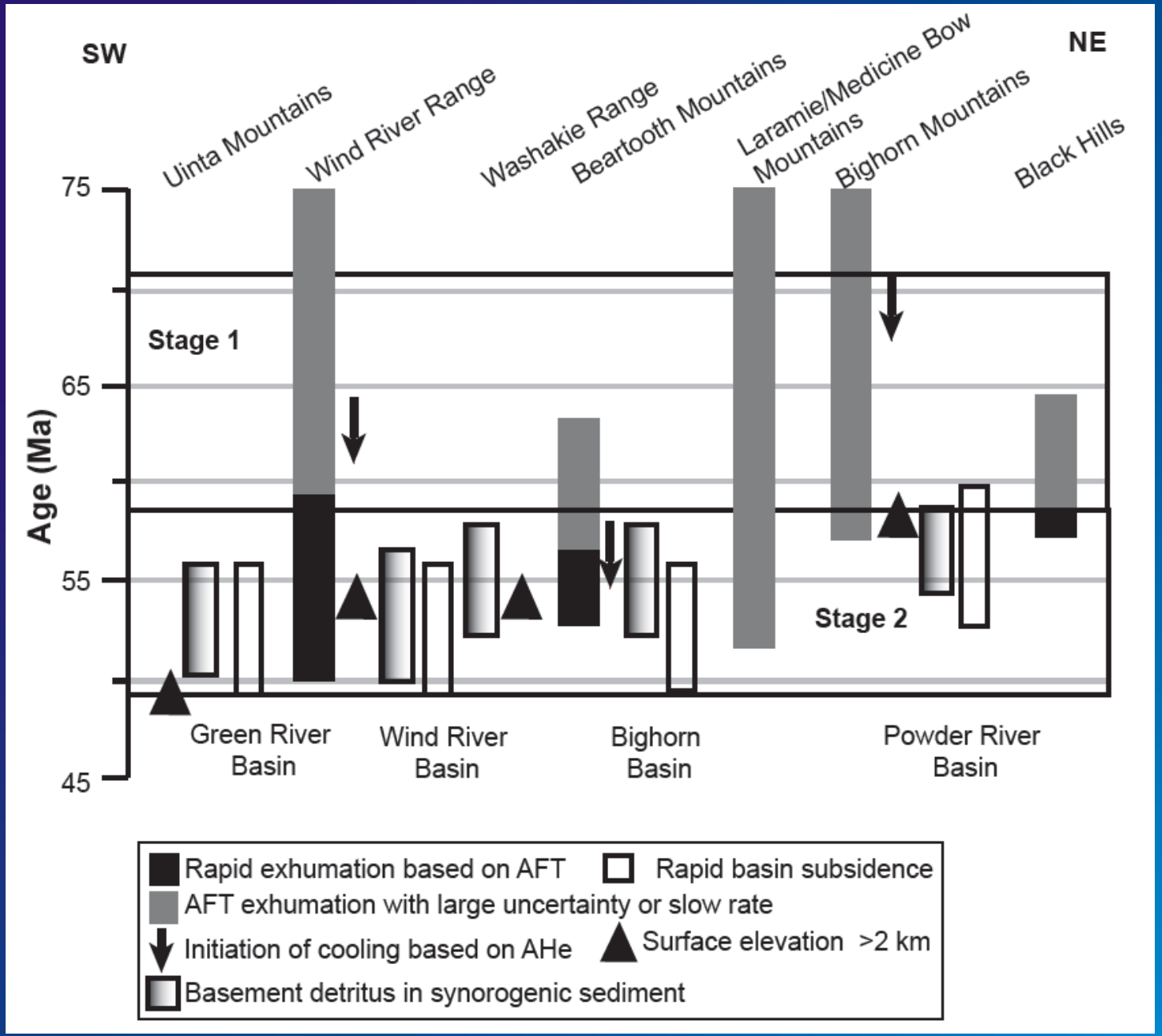

Fan and Carrapa, 2014

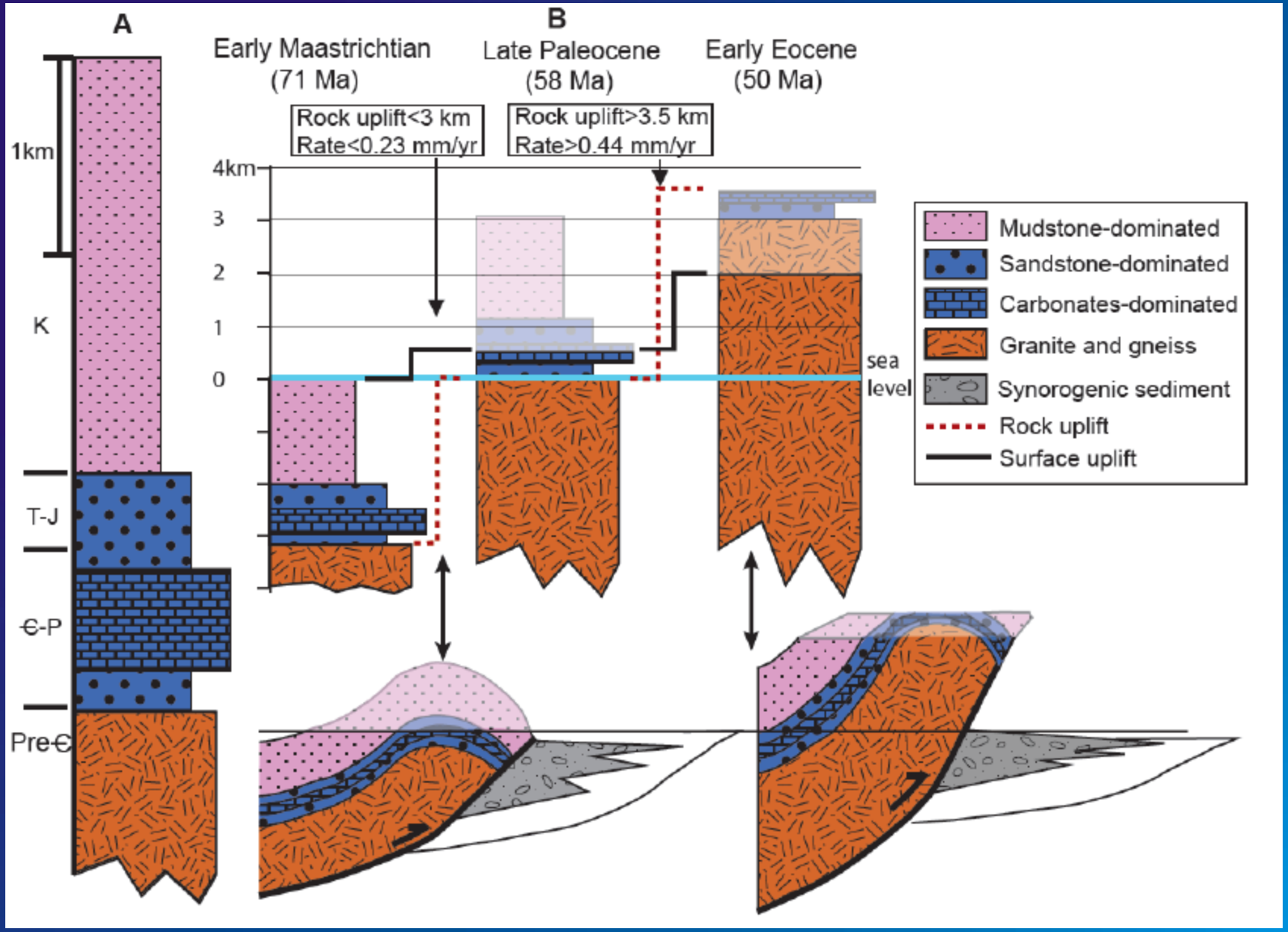

Fan and Carrapa, 2014

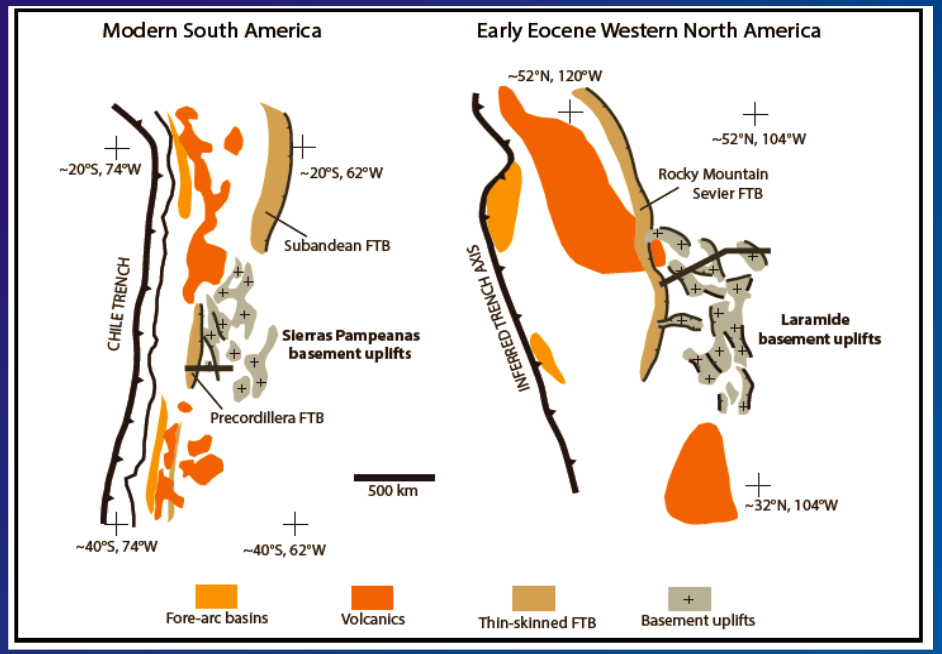
Modern South America
Early Eocene Western North America
~20°S, 74°W
~20°S, 62°W
Subandean FTB
CHILE TRENCH
Sierras Pampeanas basement uplifts
Precordillera FTB
500 km
~40°S, 74°W
~40°S, 62°W
~52°N, 120°W
~52°N, 104°W
Rocky Mountain Sevier FTB
INFERRED TRENCH AXIS
Laramide basement uplifts
~32°N, 104°W
Fore-arc basins
Volcanics
Thin-skinned FTB
Basement uplifts

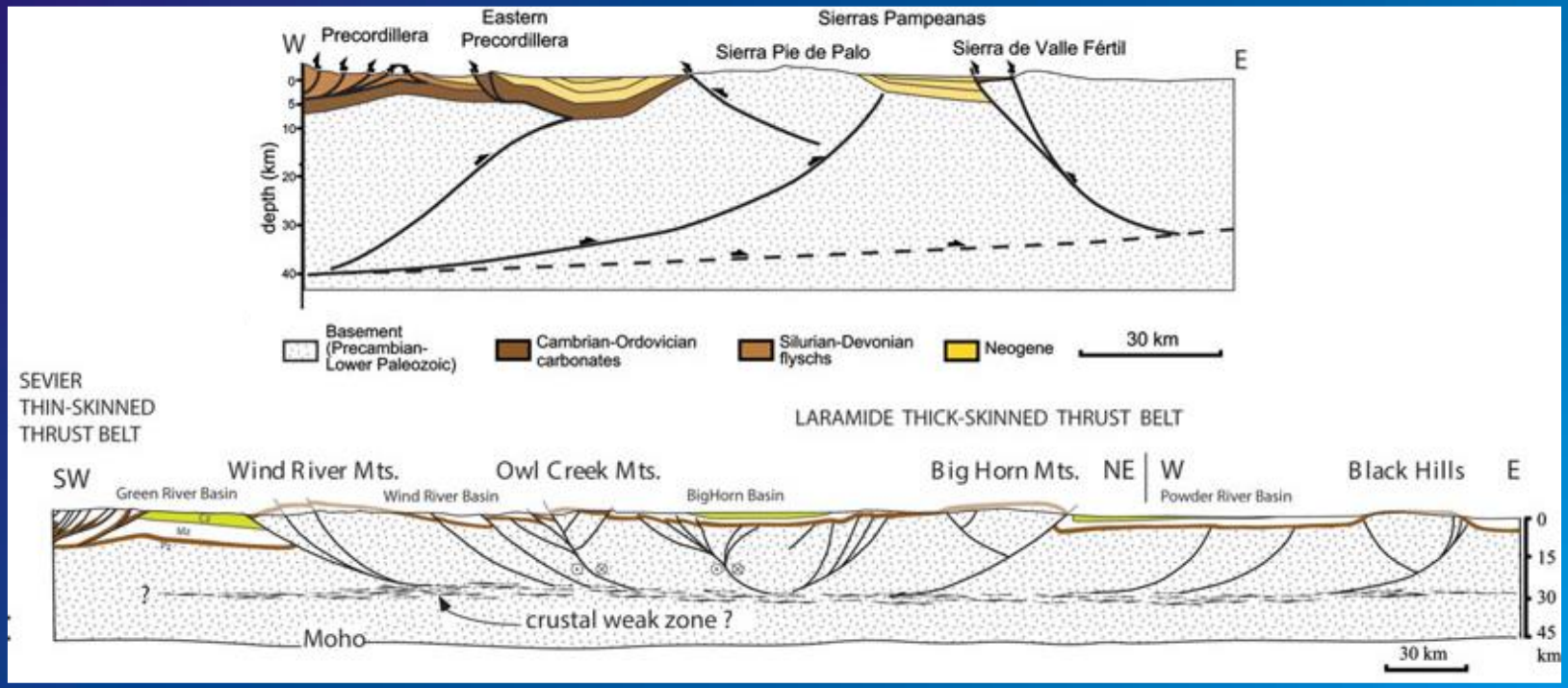
W
Precordillera
Eastern Precordillera
Sierras Pampeanas
Sierra Pie de Palo
Sierra de Valle Fértil
E
depth (km)
0
5
10
20
30
40
Basement (Precambian-Lower Paleozoic)
Cambrian-Ordovician carbonates
Silurian-Devonian flyschs
Neogene
30 km
SEVIER THIN-SKINNED THRUST BELT
LARAMIDE THICK-SKINNED THRUST BELT
SW
Wind River Mts.
Owl Creek Mts.
Big Horn Mts.
NE
W
Black Hills
E
Green River Basin
Wind River Basin
BigHorn Basin
Powder River Basin
?
crustal weak zone ?
Moho
0
15
30
45
km
30 km

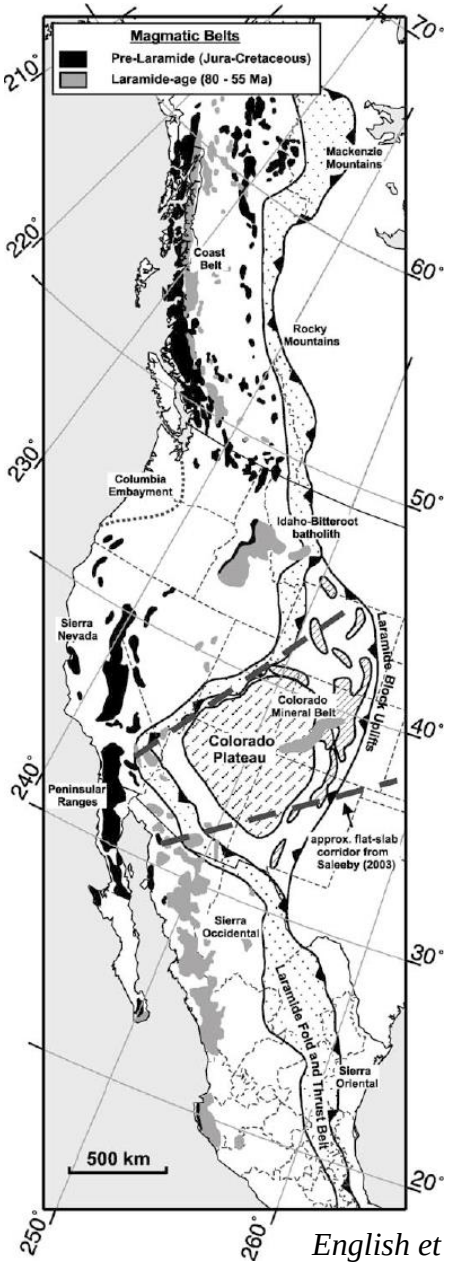

English et al., 1993

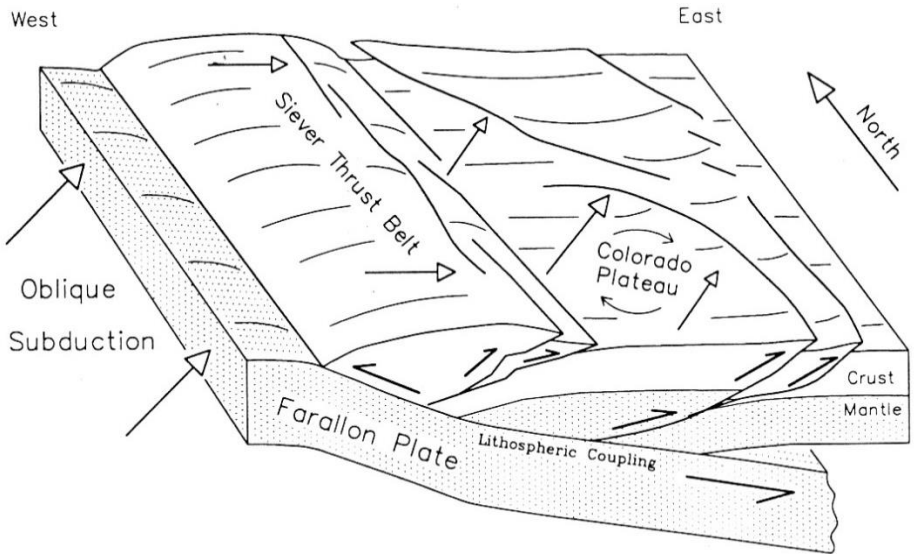

Erslev, 1993

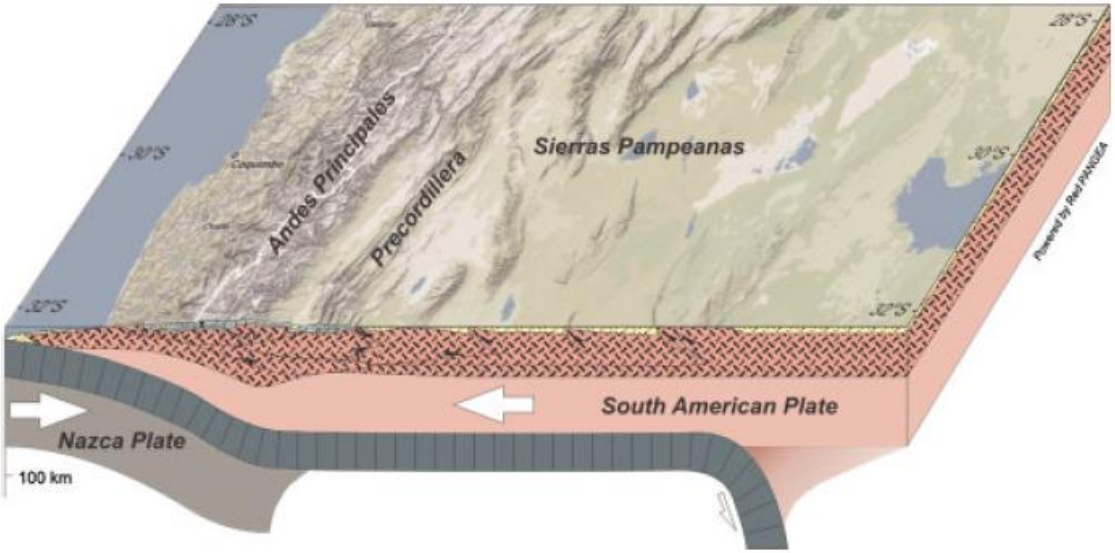

Ramos, 2010

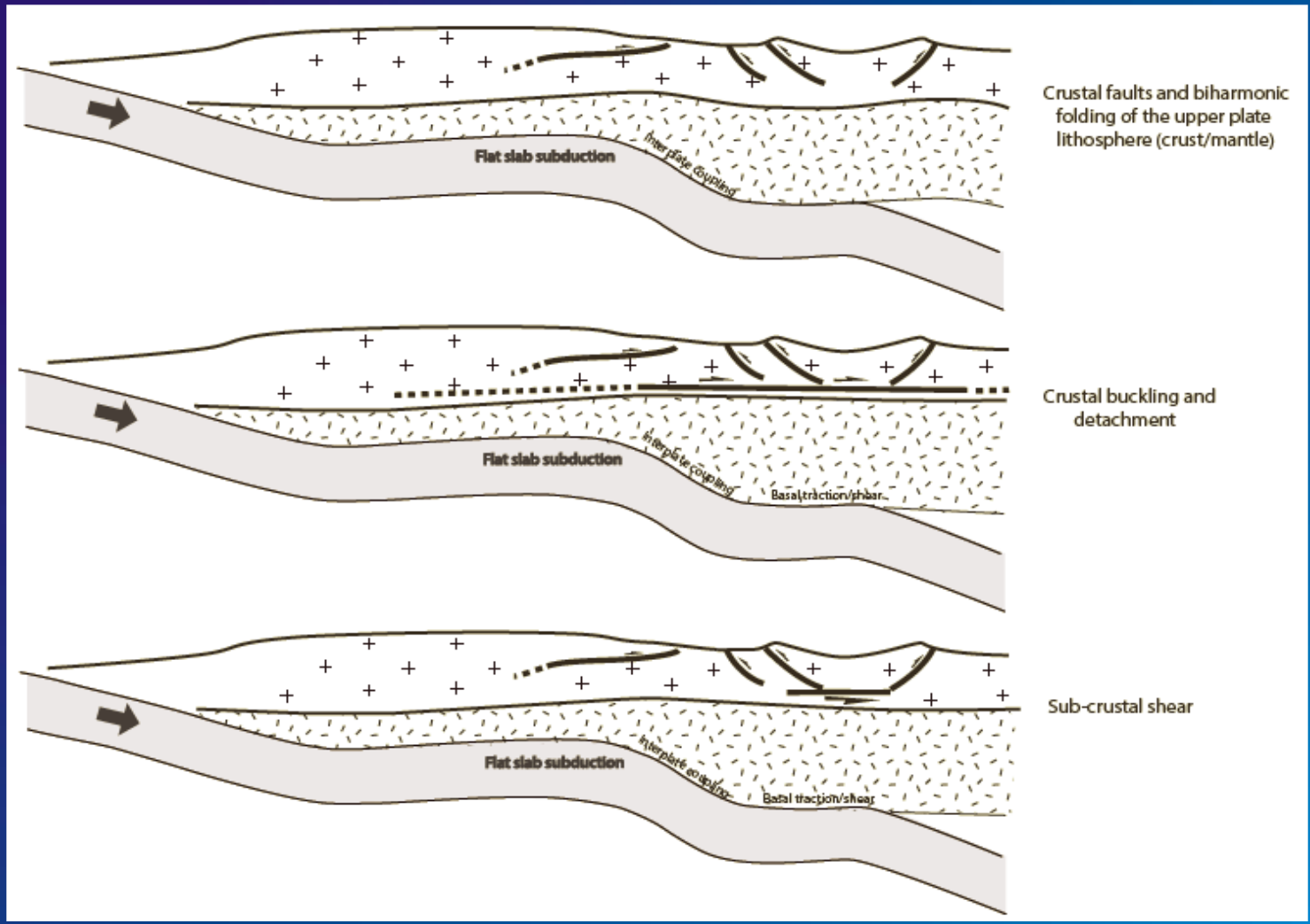
Flat slab subduction
Interplate coupling
Crustal faults and biharmonic folding of the upper plate lithosphere (crust/mantle)
Flat slab subduction
Interplate coupling
Basal traction/shear
Crustal buckling and detachment
Flat slab subduction
Interplate coupling
Basal traction/shear
Sub-crustal shear

Basement control on along-strike variations of fold-and-thrust belts : the Taiwan case

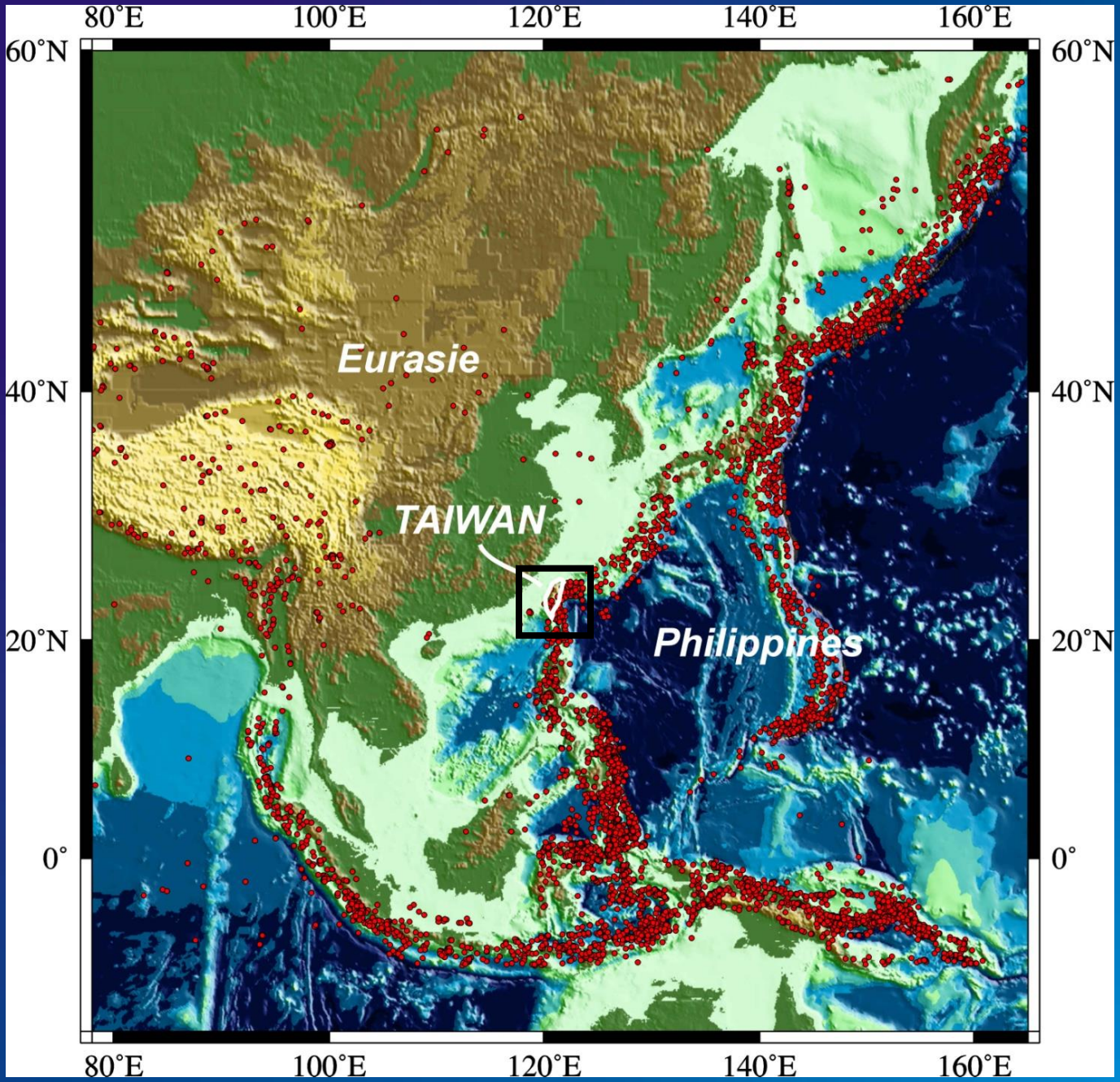
80°E
100°E
120°E
140°E
160°E
60°N
40°N
20°N
0°
Eurasie
TAIWAN
Philippines

A Plio-Pleistocene collision between the N-S Luzon volcanic arc and the ENE Paleogene chinese continental passive margin

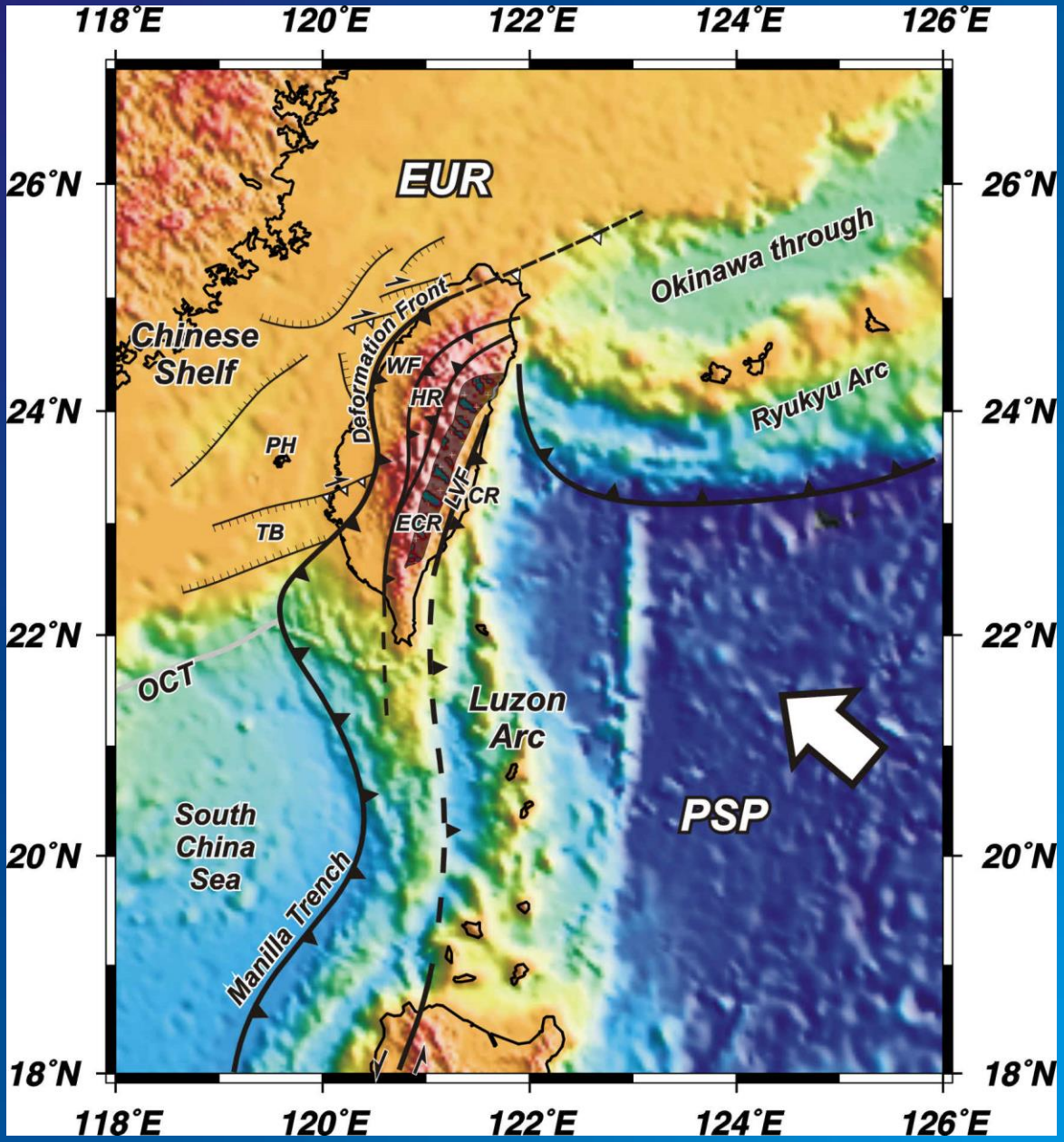

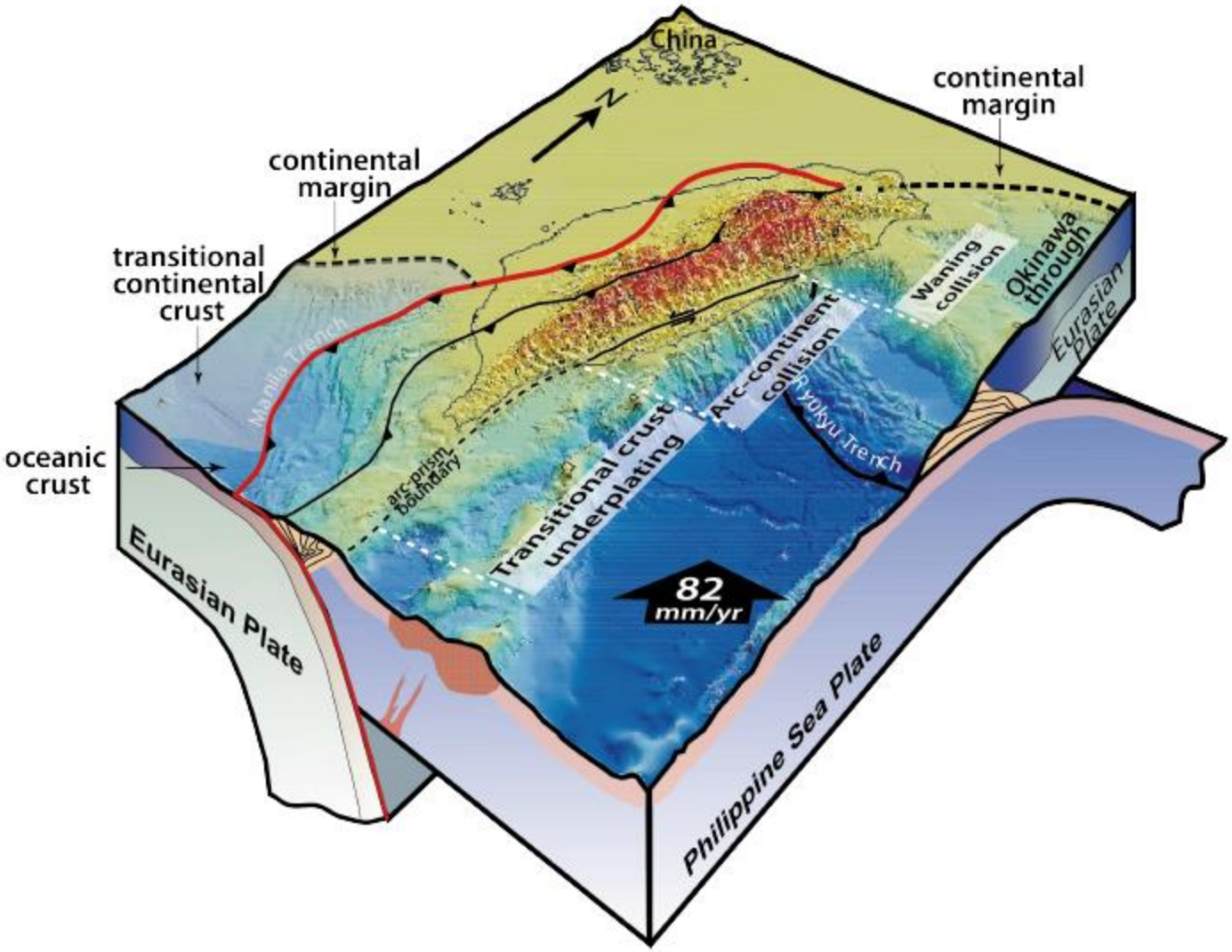
China
continental margin
continental margin
transitional continental crust
oceanic crust
Manila Trench
arc-prism boundary
Transitional crust underplating
Arc-continent collision
Waning collision
Okinawa through
Eurasian Plate
Ryukyu Trench
82 mm/yr
Eurasian Plate
Philippine Sea Plate

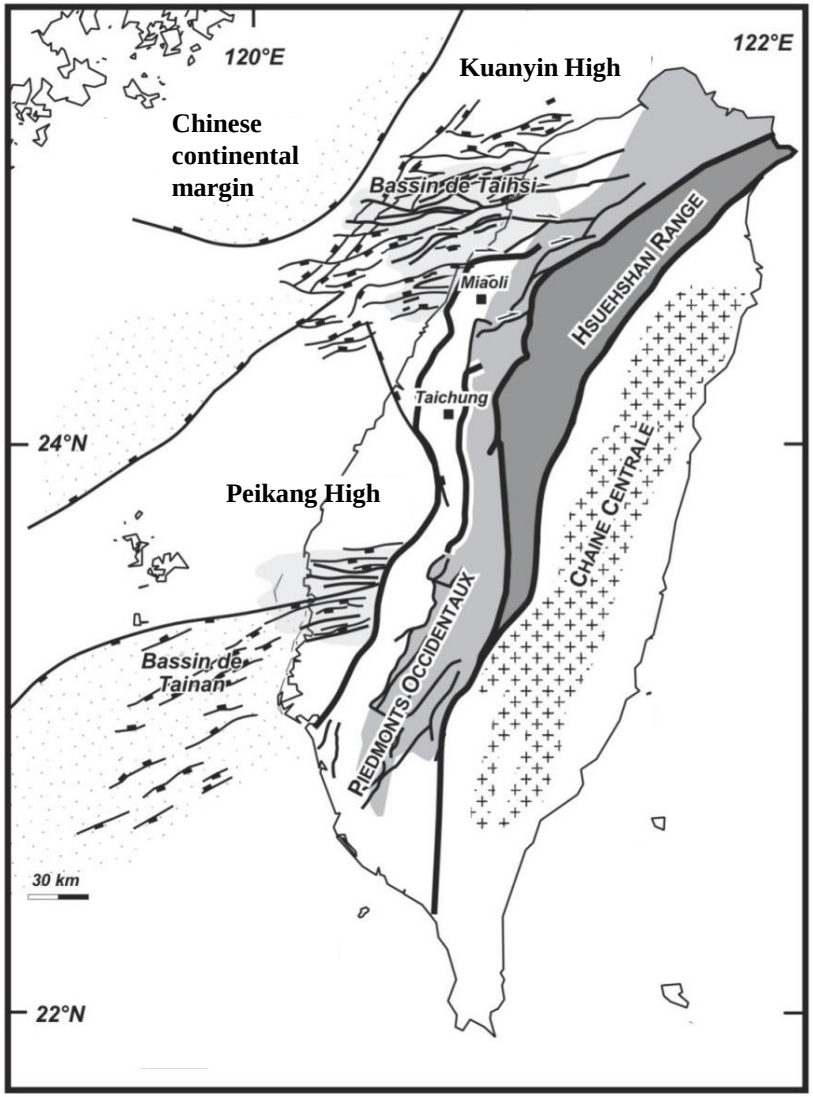
120°E
122°E
Kuanyin High
Chinese continental margin
Bassin de Taihsi
HSUEHSHAN RANGE
Miaoli
Taichung
24°N
Peikang High
CHAINE CENTRALE
PIEDMONTS OCCIDENTAUX
Bassin de Tainan
30 km
22°N

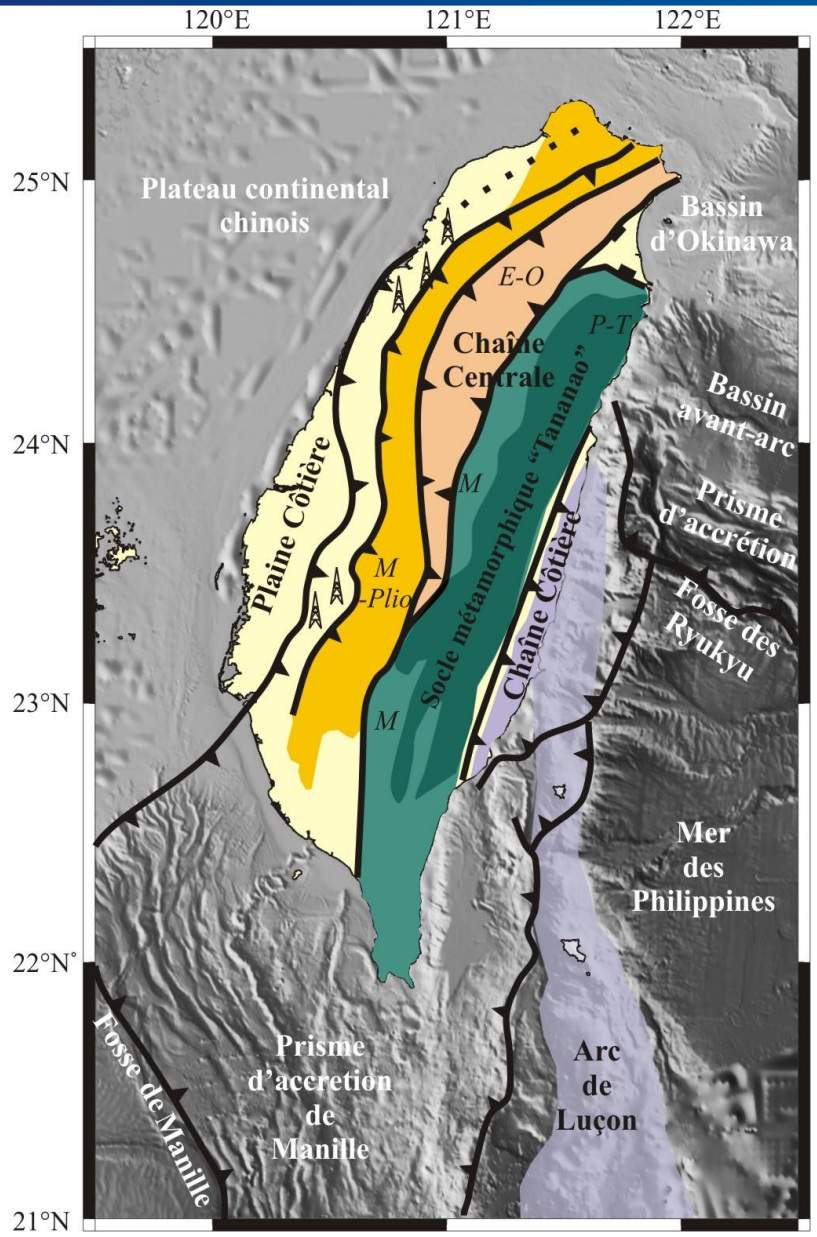
120°E
121°E
122°E
25°N
24°N
23°N
22°N
21°N
Plateau continental chinois
Bassin d'Okinawa
E-O
P-T
Chaîne Centrale
Bassin avant-arc
Plaine Côtière
M
M -Plio
M
Socle métamorphique "Tananao"
Chaîne Côtière
Prisme d'accrétion
Fosse des Ryukyu
Mer des Philippines
Fosse de Manille
Prisme d'accretion de Manille
Arc de Luçon

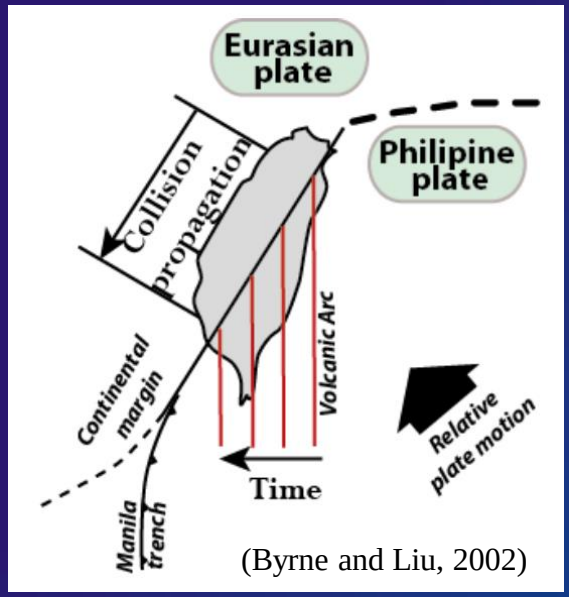

(Byrne and Liu, 2002)

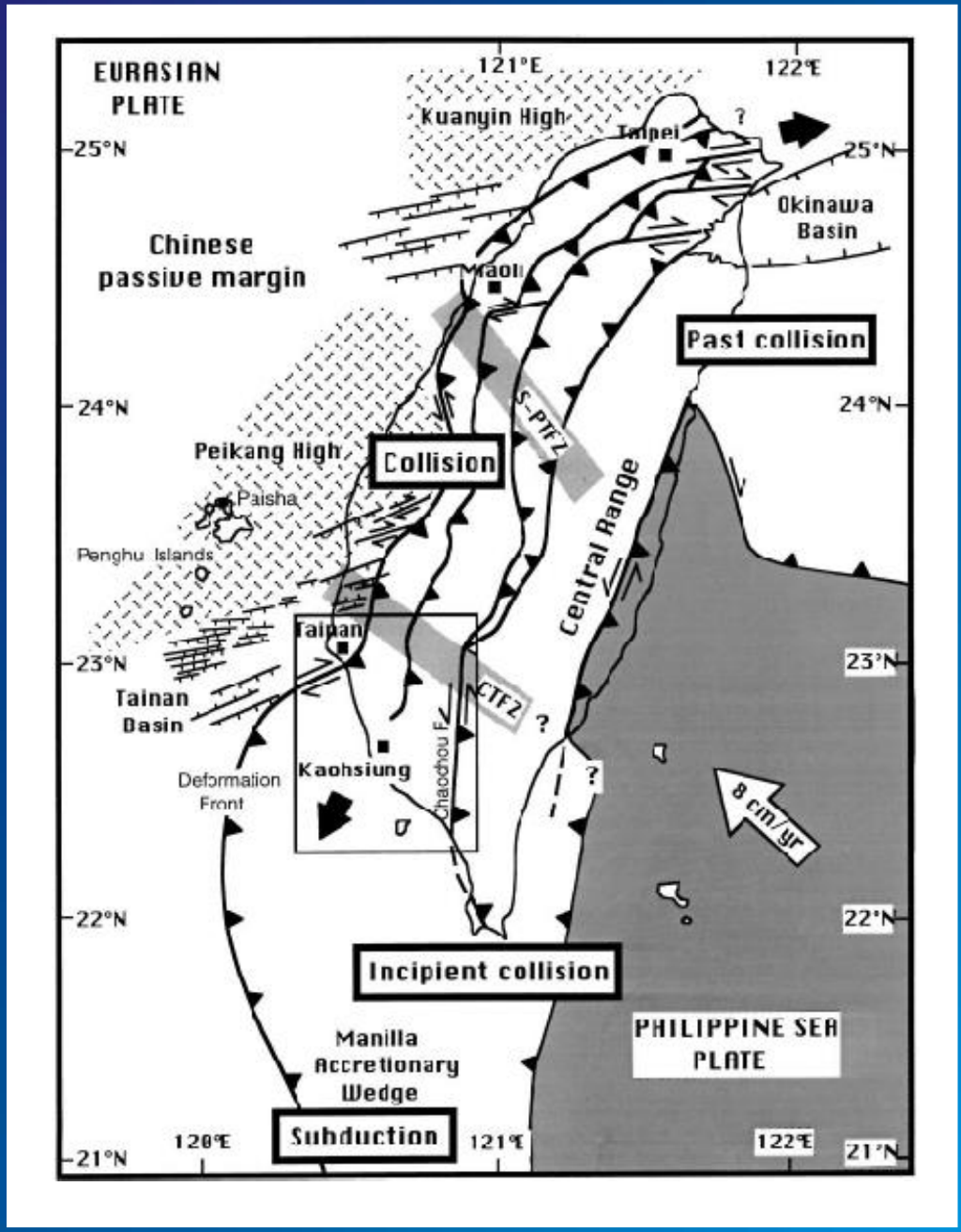

(Lacombe et al., 2001; Modified after Lallemand and Tsien, 1997)

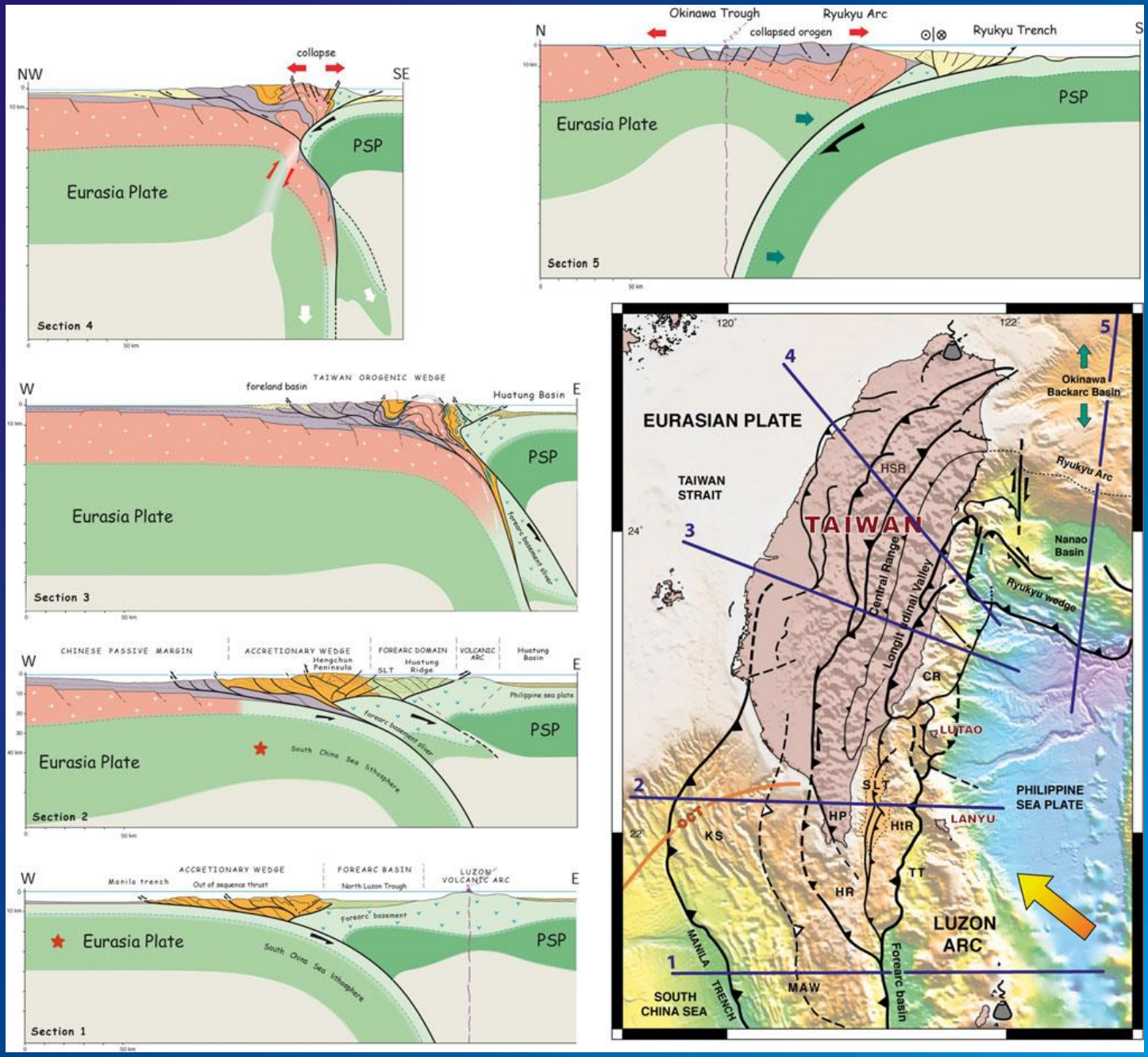

(Molli and Malavieille, 2011)

Steady critical wegde model for Taiwan

Critically tapered wegde (with thin-skinned approximation)

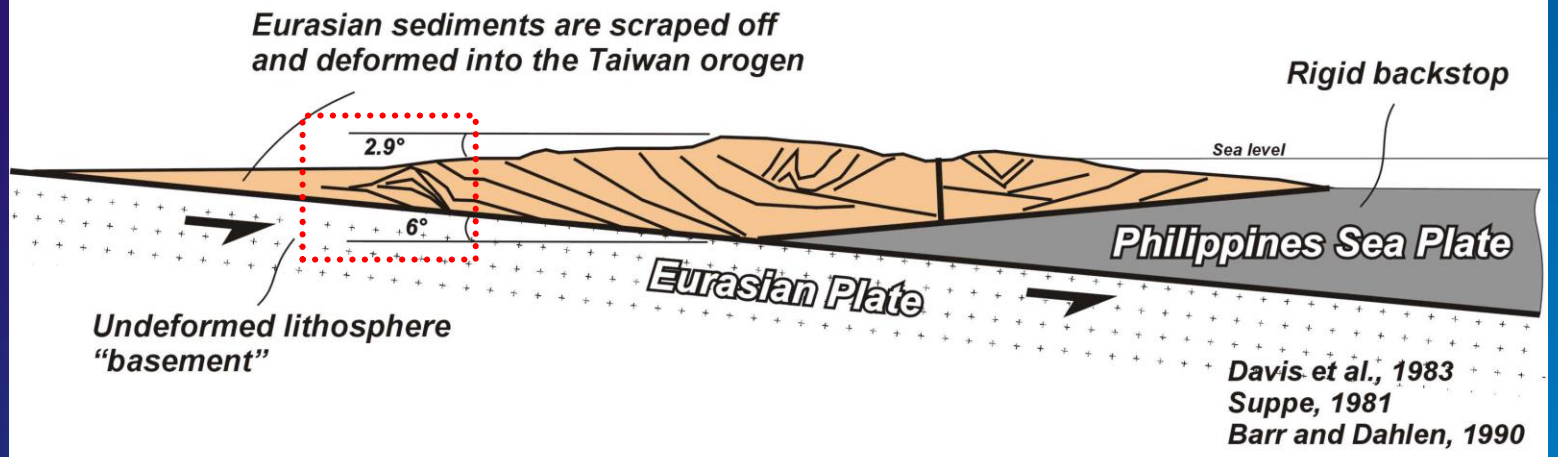

+

Wedge shape (taper) unchanged through time

Steady development

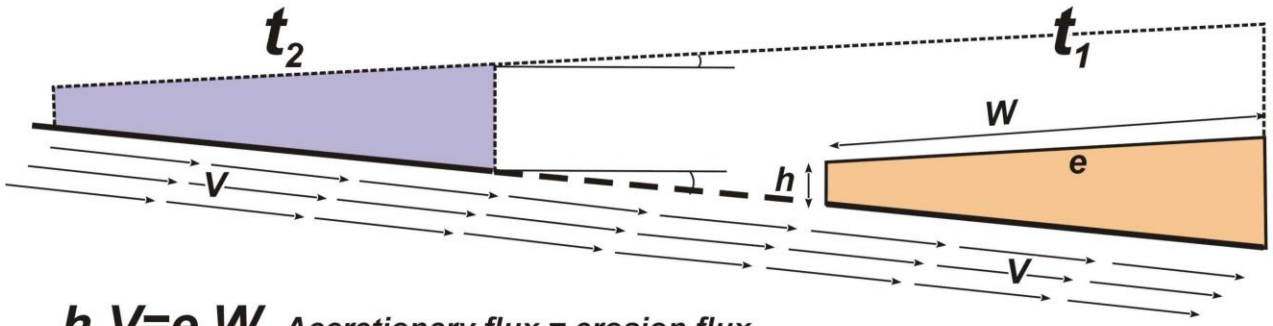

$h.V=e.W$ Accretionary flux = erosion flux

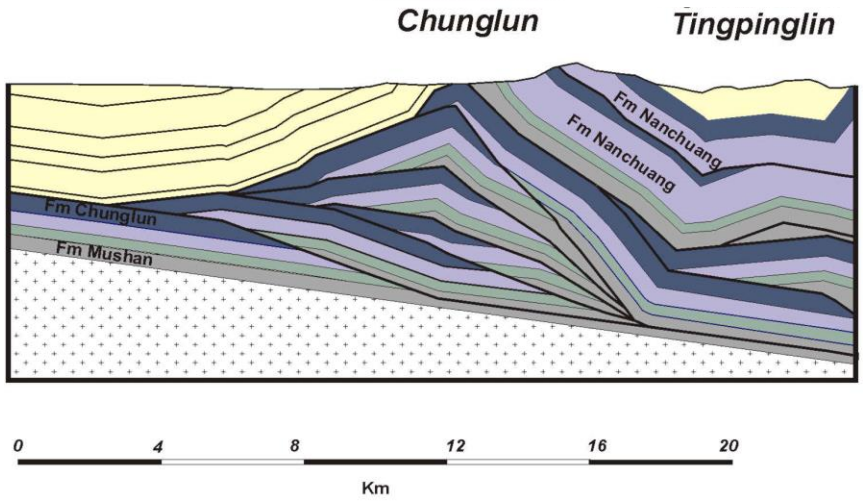

Thin-skinned hypothesis

Large shortening
of the sedimentary cover

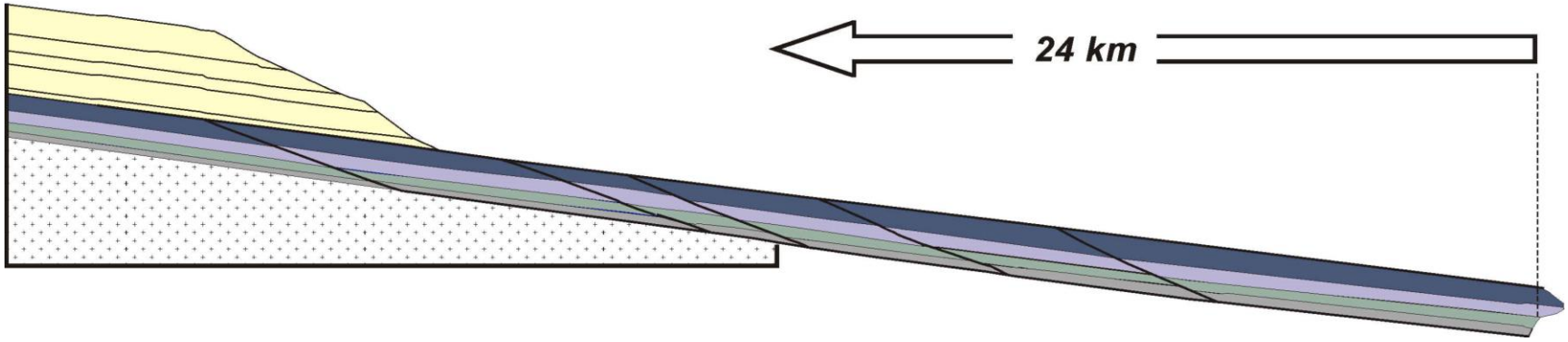

Basement topography

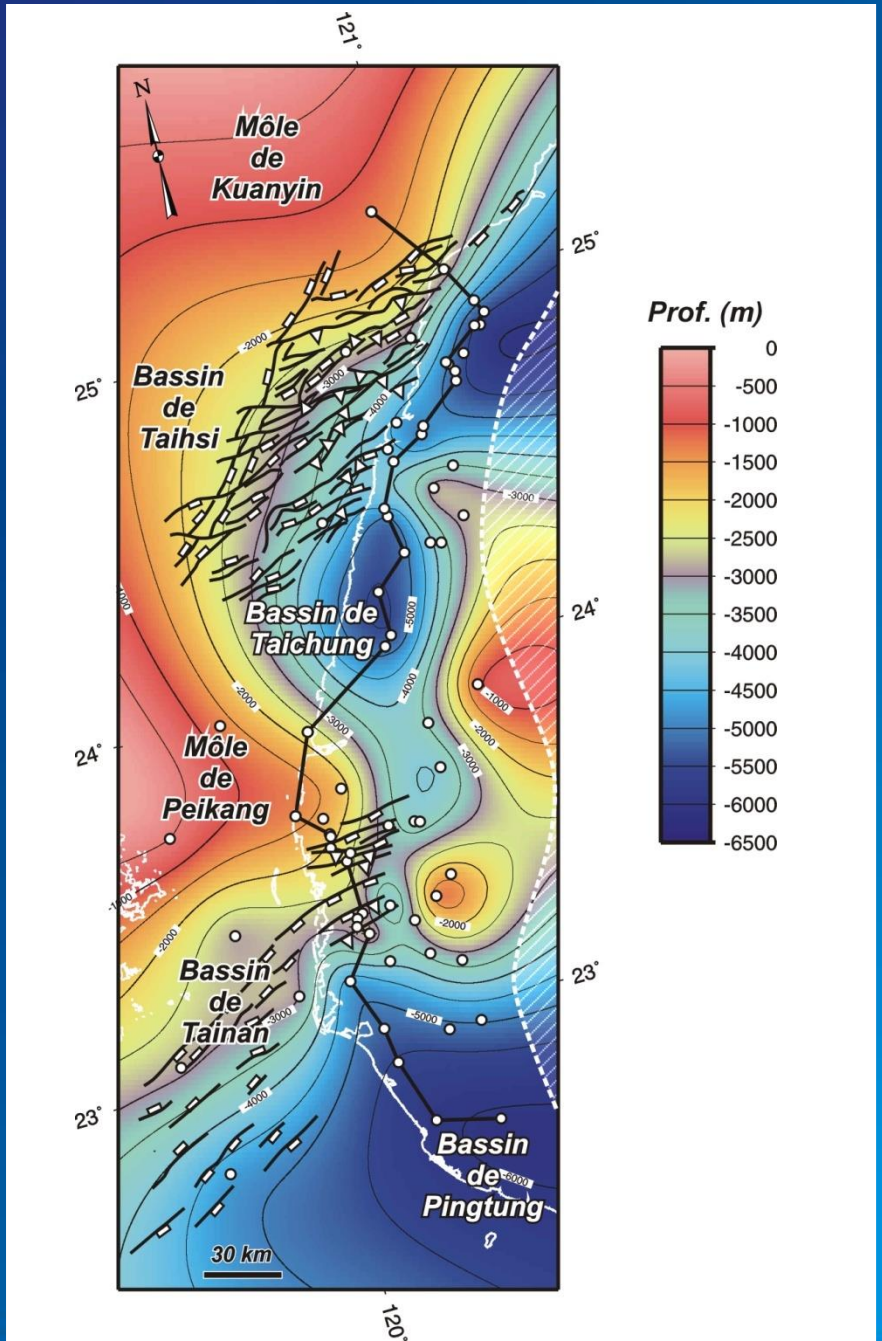

(Mouthereau et al., 2002)

Structural inheritance and inversion south of the basement highs

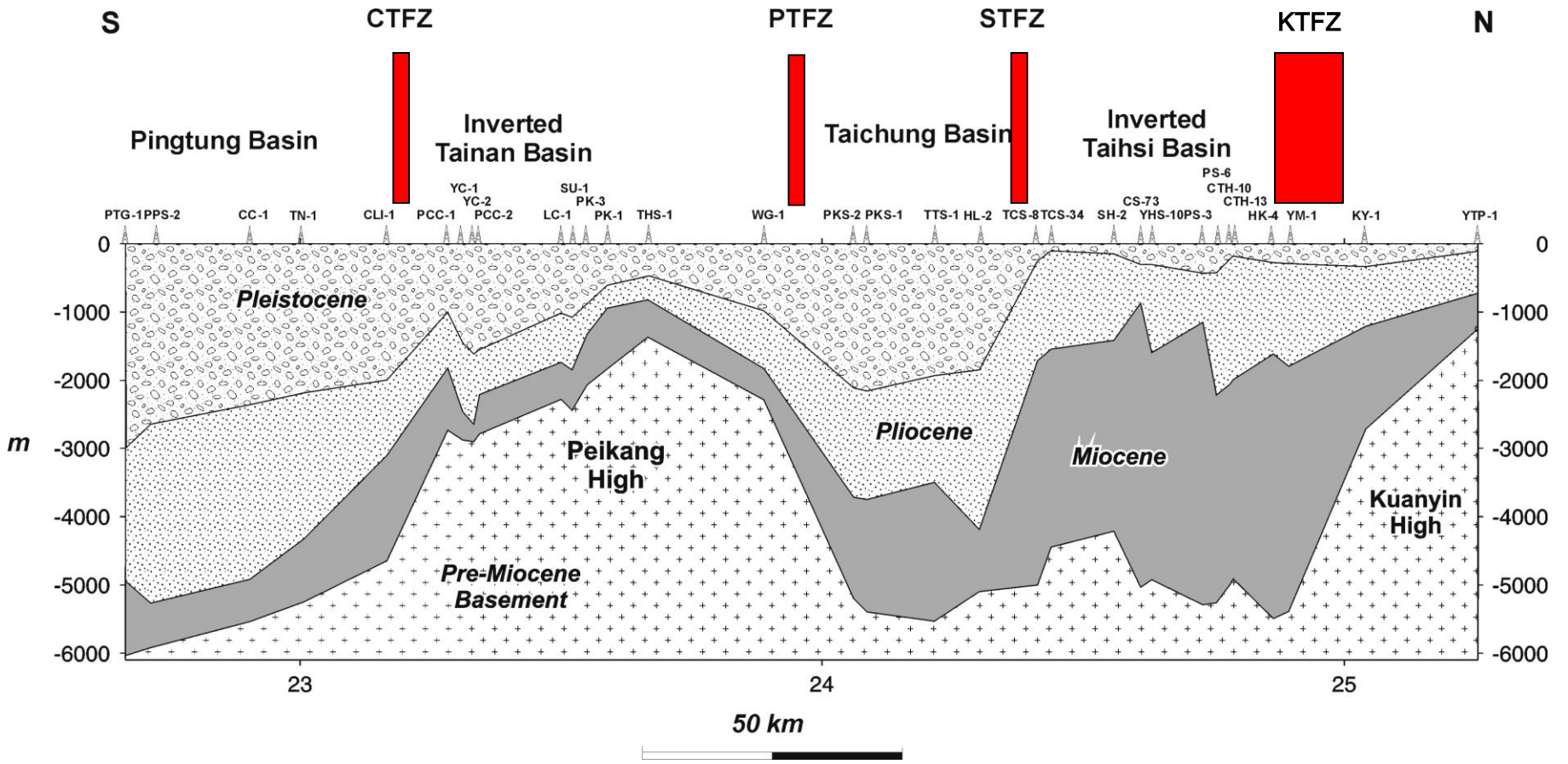

(Mouthereau et al., 2002)

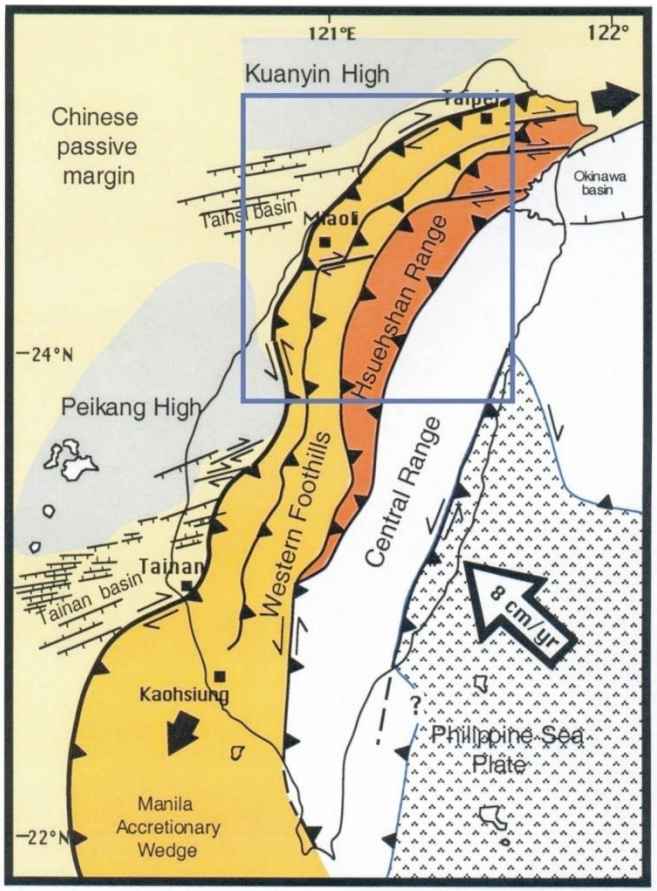

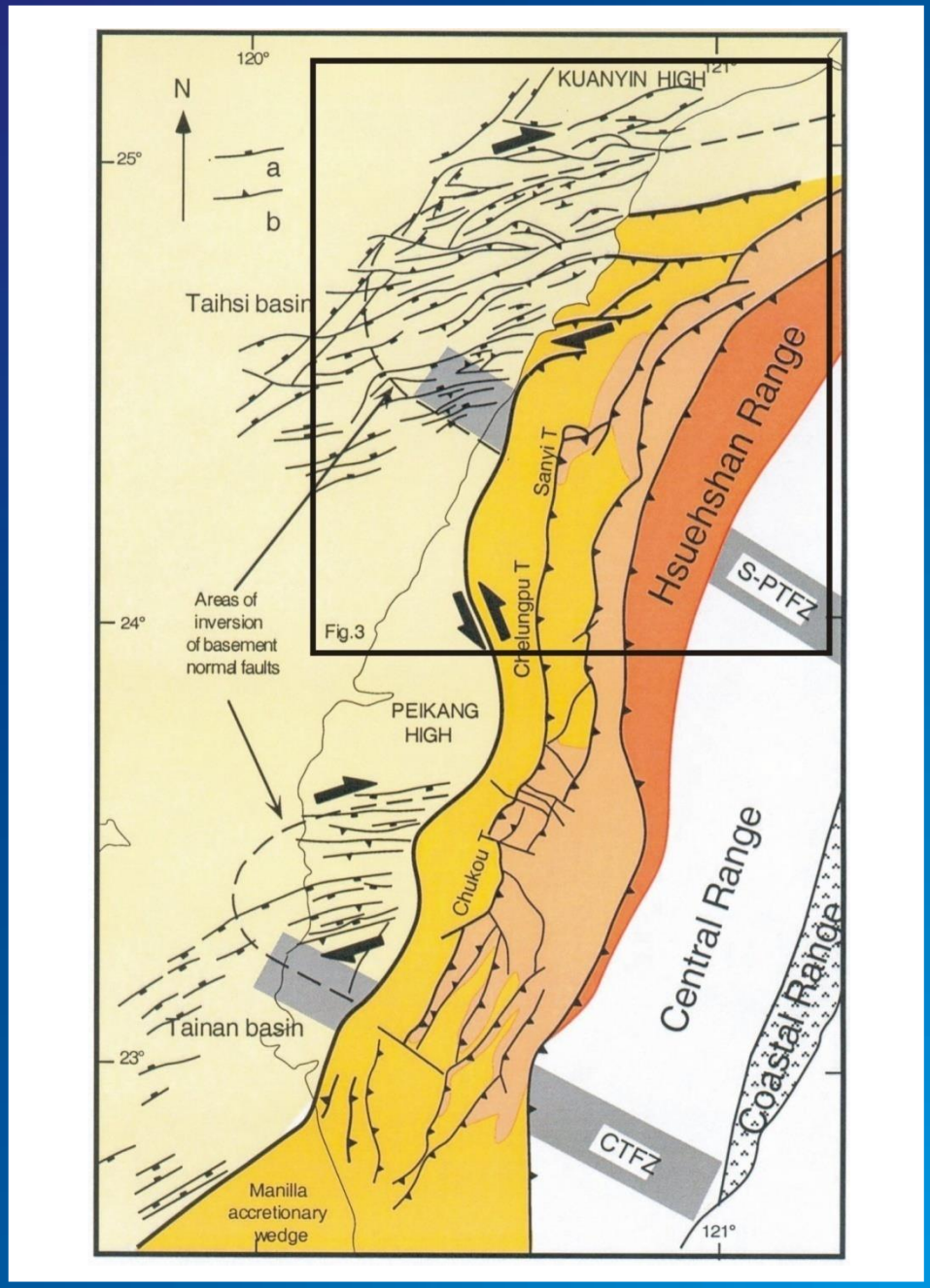

(Lacombe and Mouthereau, 2002)

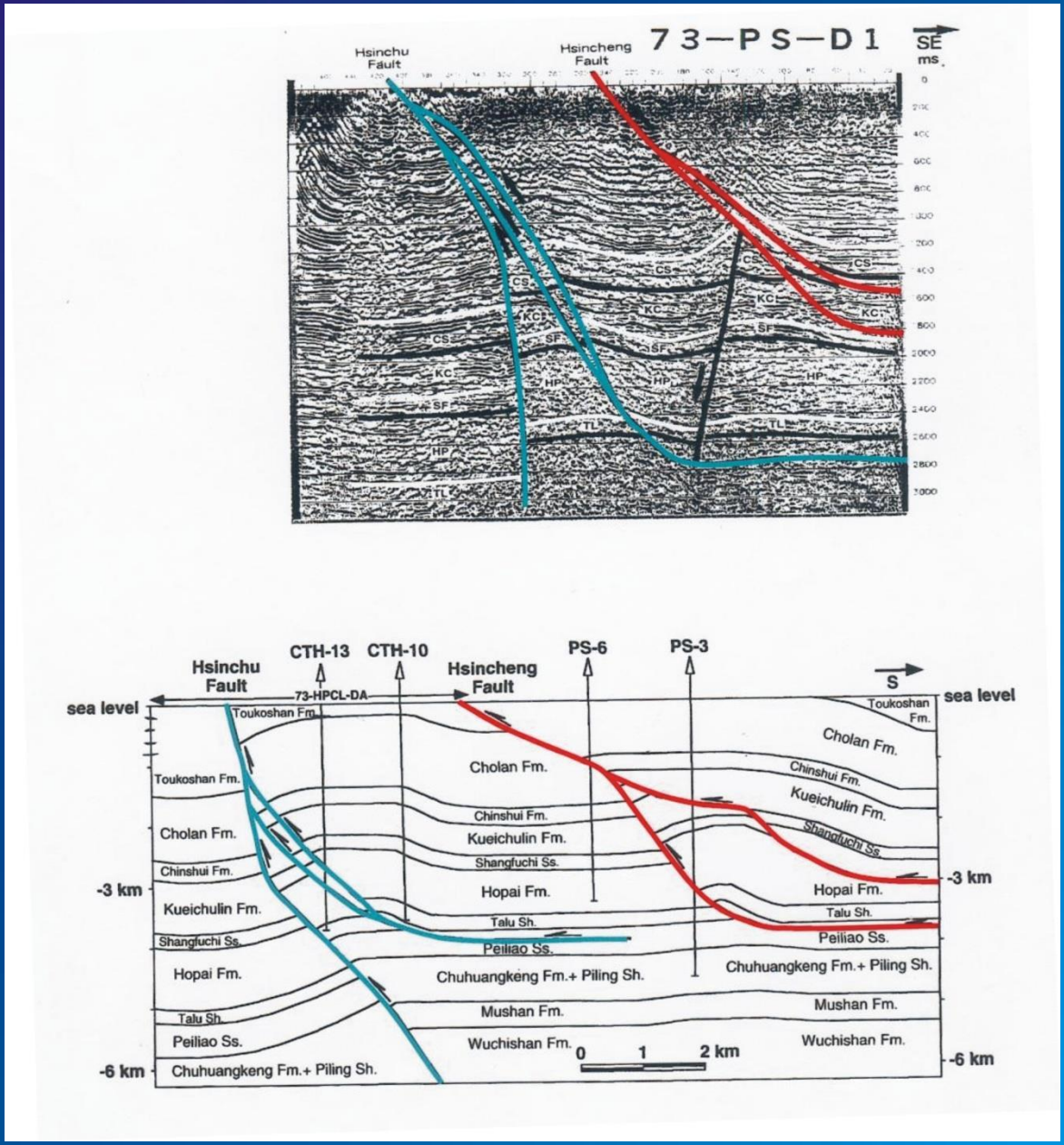

(Yang et al., 1996)

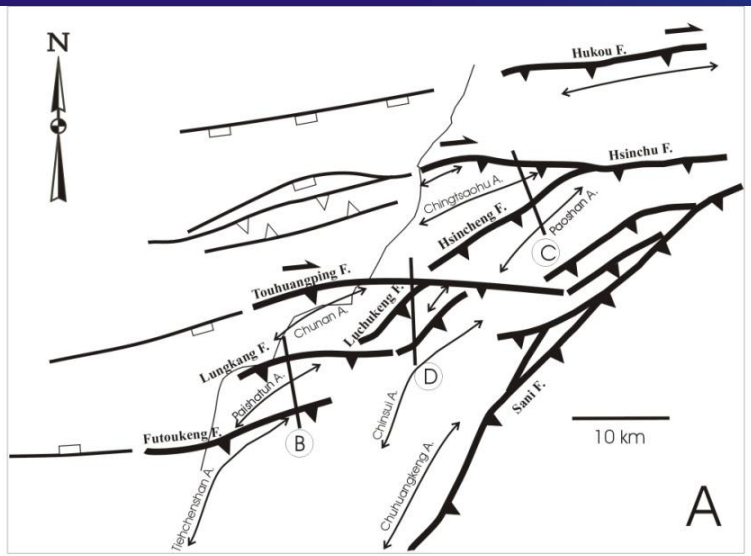

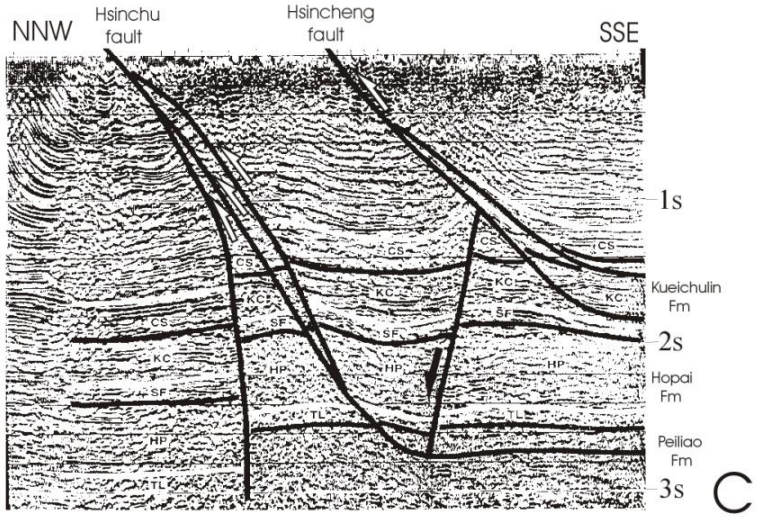

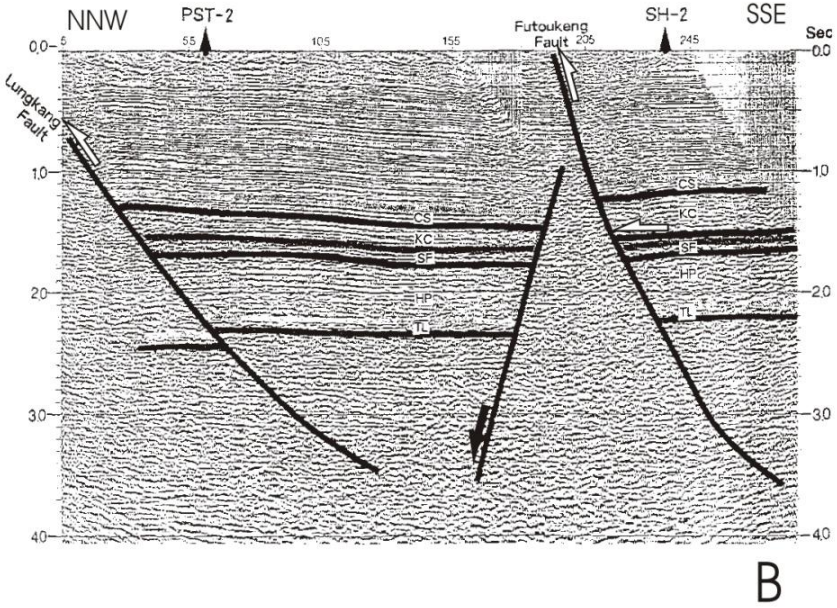

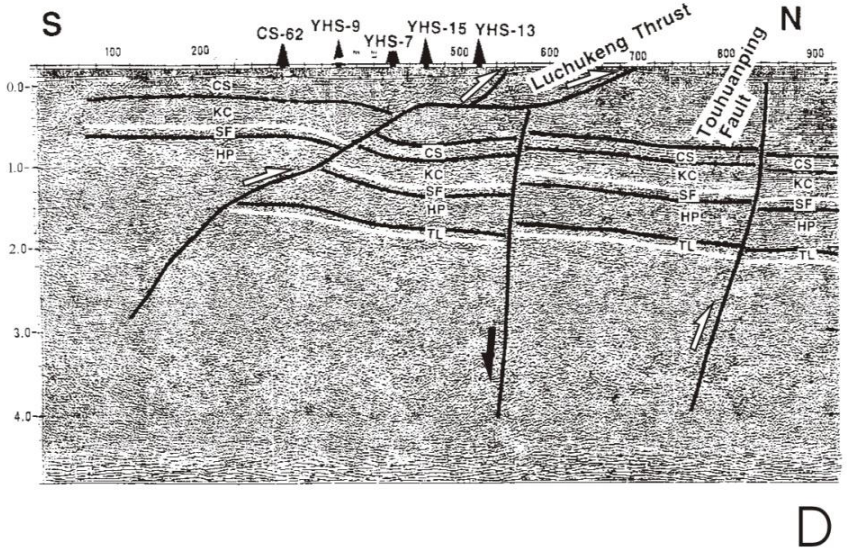

(Lacombe et al., 2003; profiles from Yang et al., 1994, 1996, 1997)

2 very different visions of the structural style in northern Taiwan

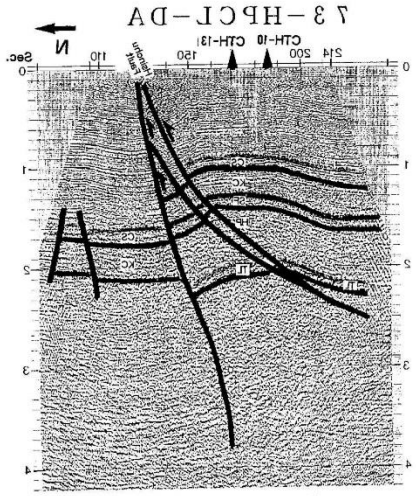

(*Yang et al.*, 1996)

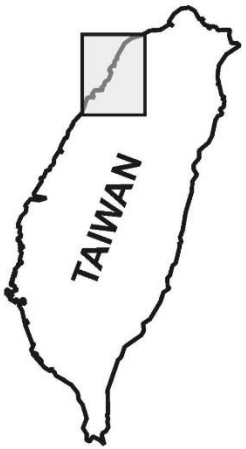

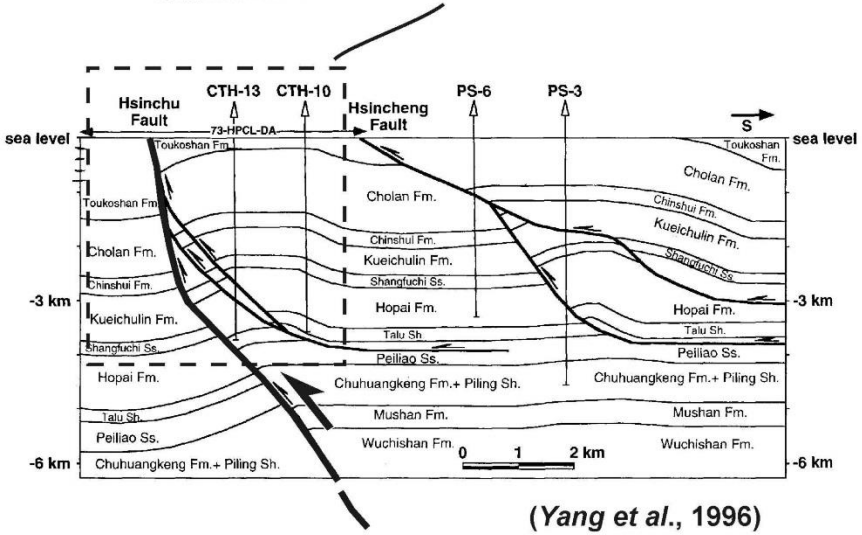

(*Yang et al.*, 1996)

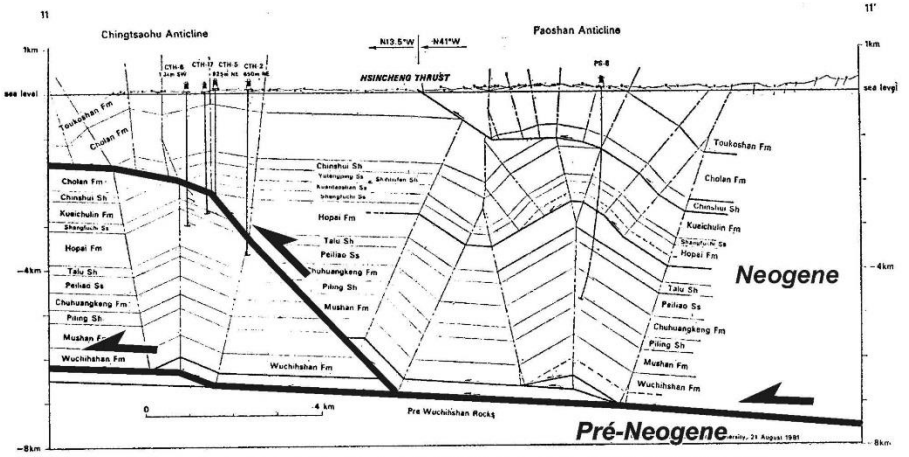

Figure 2. Structural interpretation through section 11-11′ in the northern part of the Miaoli-Hsinchu area.

(Namson, 1981)

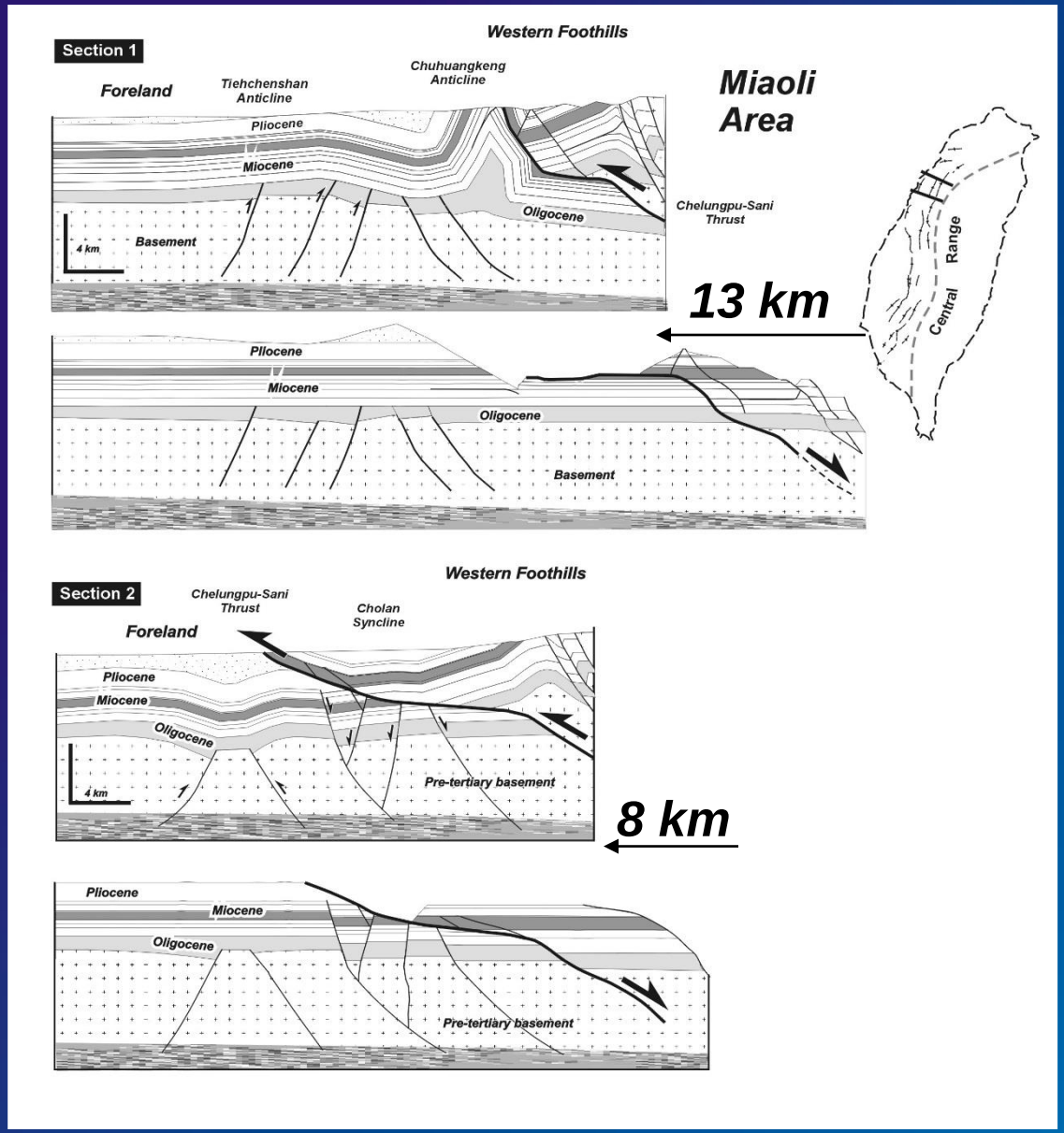

(Mouthereau and Lacombe, 2006)

Superimposed decoupling in the sedimentary cover and basement controlled by structural inheritance

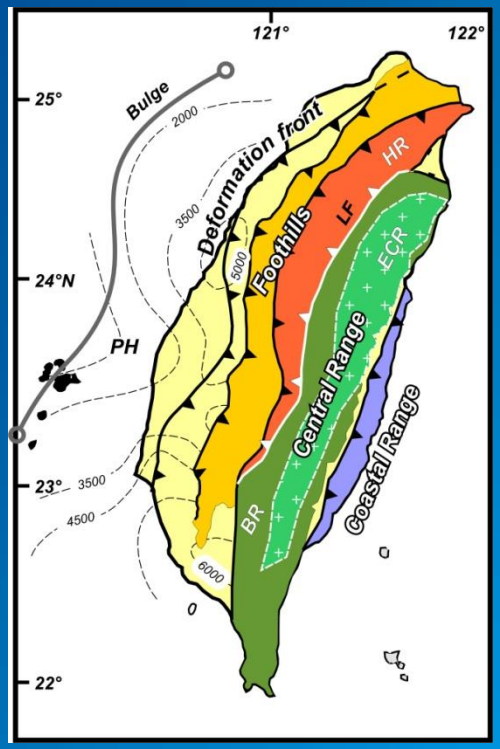

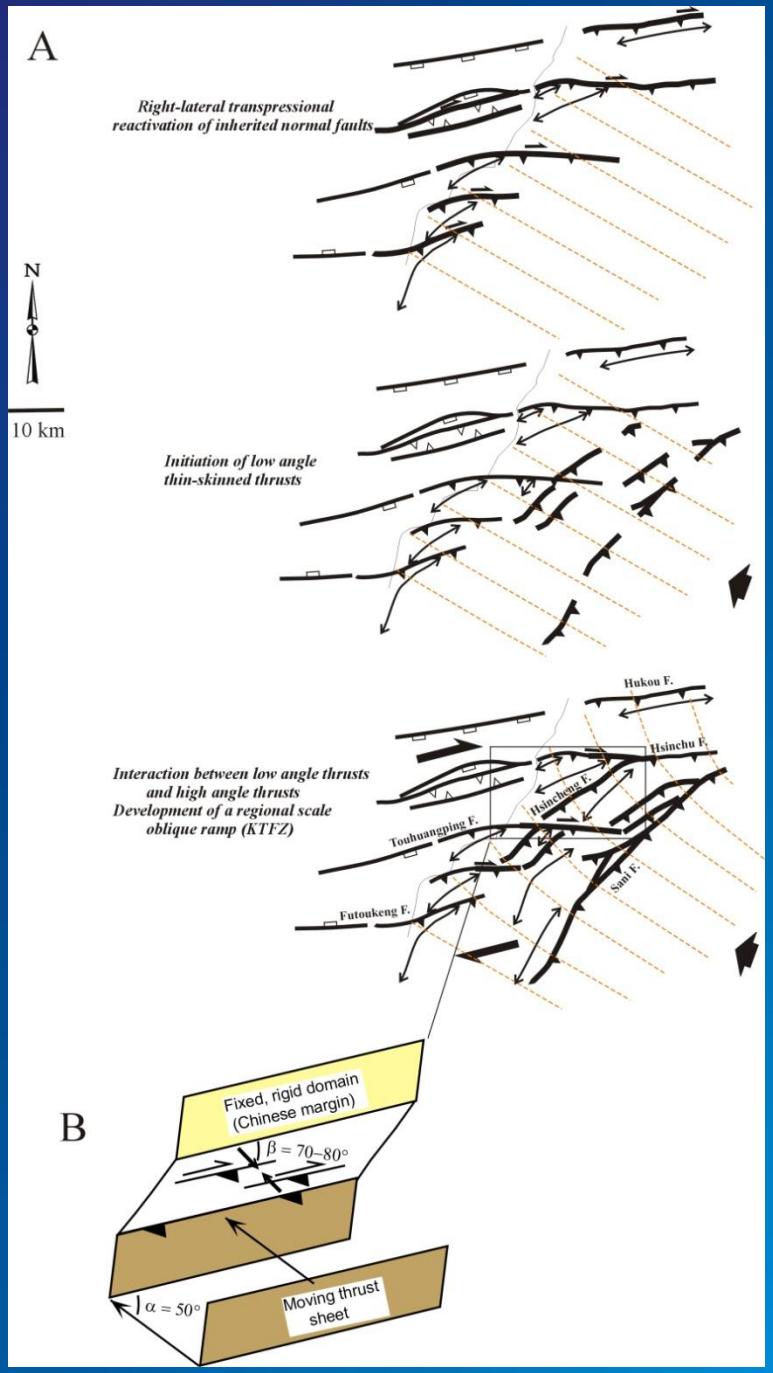

(Lacombe et al., 2003)

(Lacombe et al., 2003)

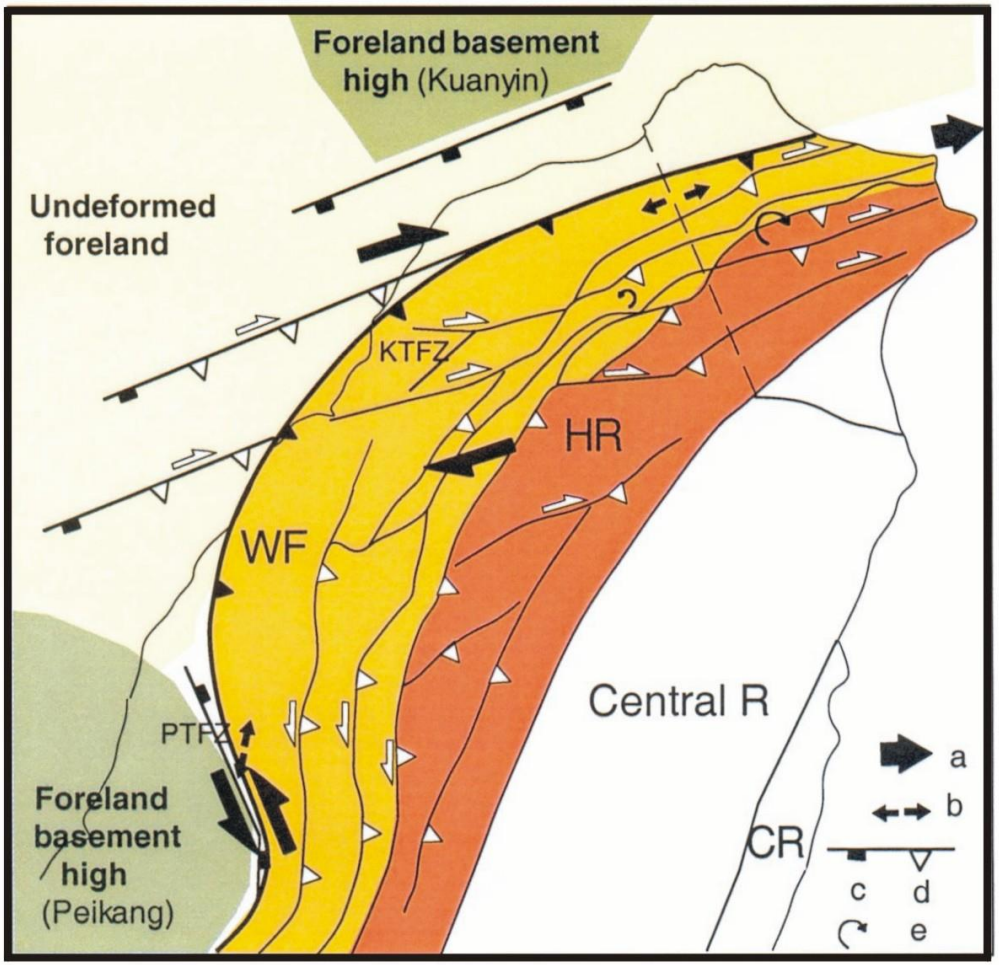

NW Taiwan : the position of the salient's apex coincides with the location of the precollisional depocenter (thickest strata) in the basin from which the salient formed.

The NW Taiwan salient mainly formed in response to the along-strike variation in the pre-orogenic basin thickness, leading to recognize this salient as a basin-controlled salient.

It differs from arcs formed in thin-skinned orogens in that deformation was accommodated by both thin-skinned shallow thrusts and basement faults and therefore that both the cover and the basement are involved in collisional shortening.

→ « Passive » and/or « active » basement control on geometry (segmentation, curvature,) and kinematics of fold-thrust belts

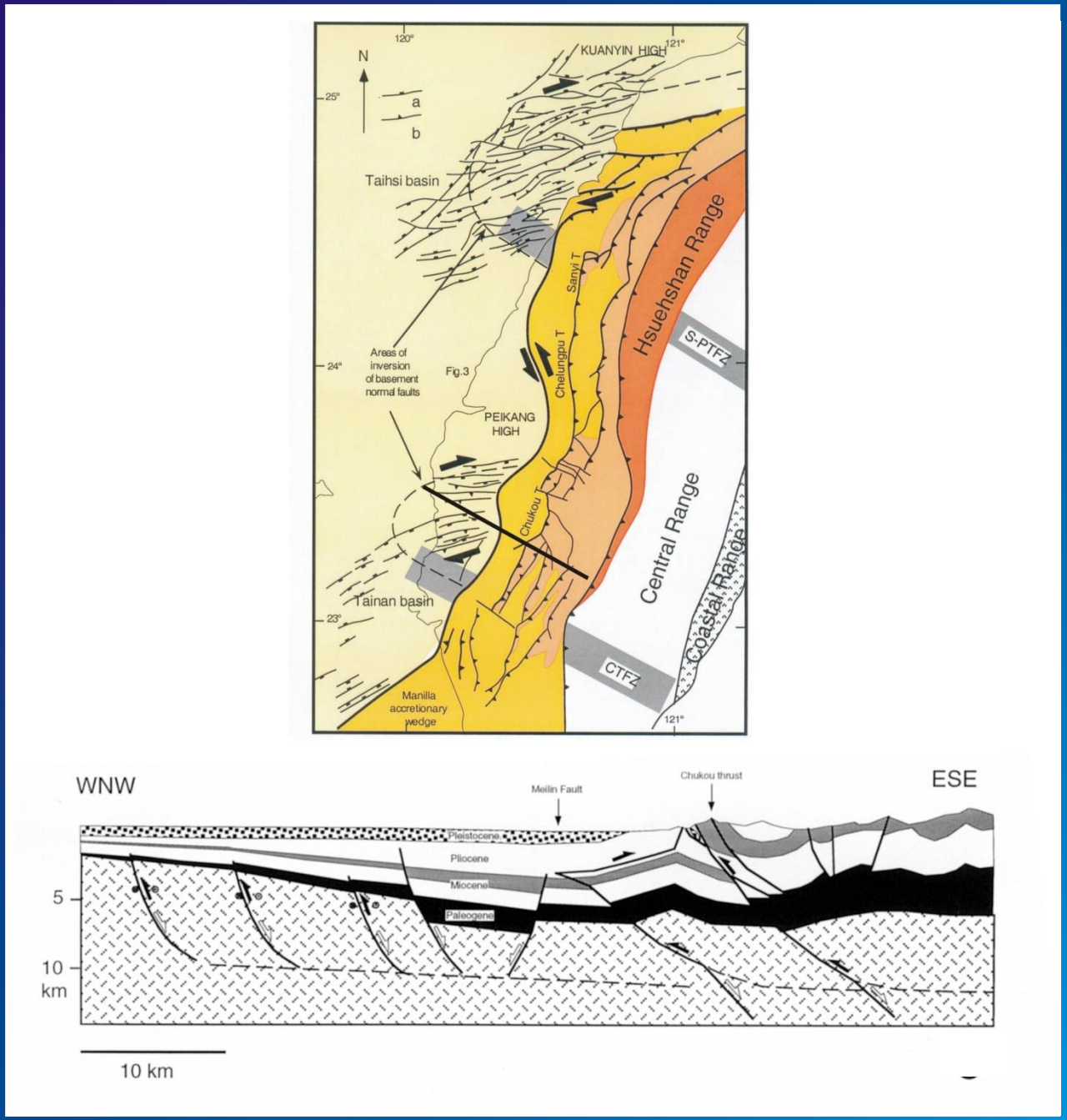

(Lacombe and Mouthereau, 2002)

2 very different visions of the structural style in central Taiwan

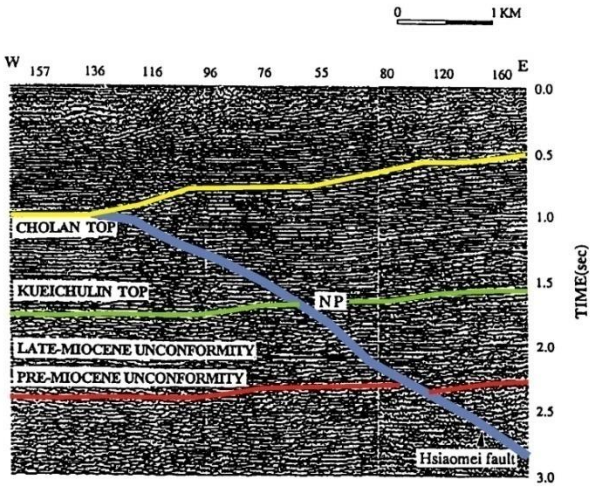

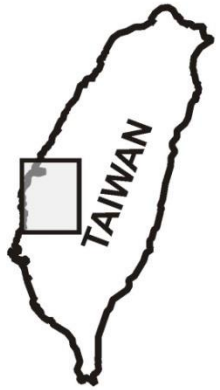

Hung et al., 1999

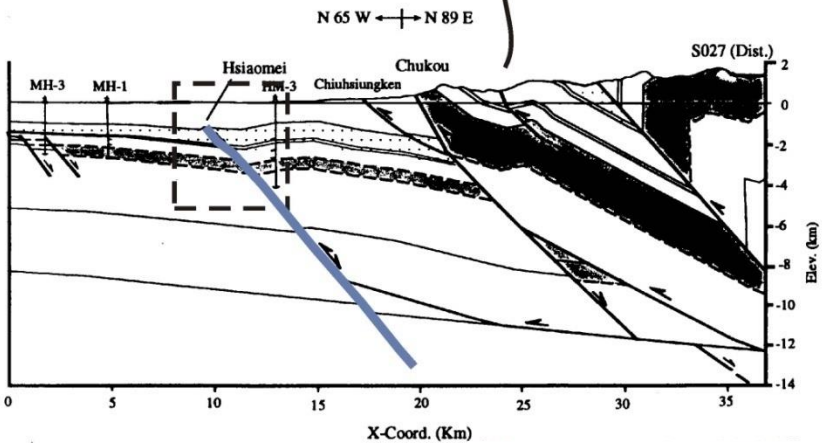

Suppe and Namson, 1979

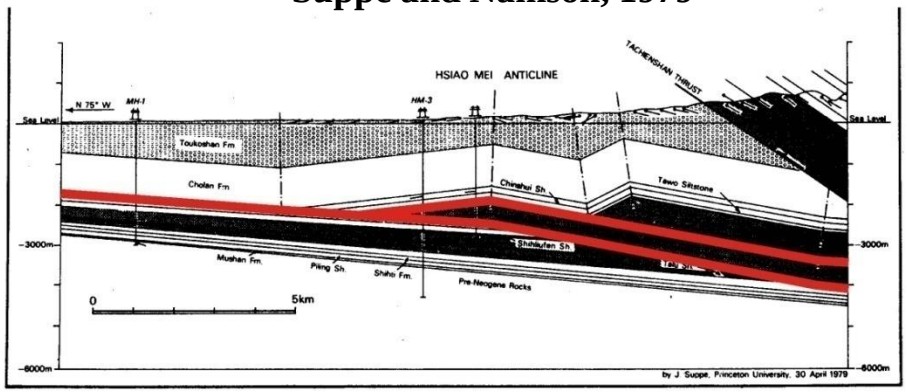

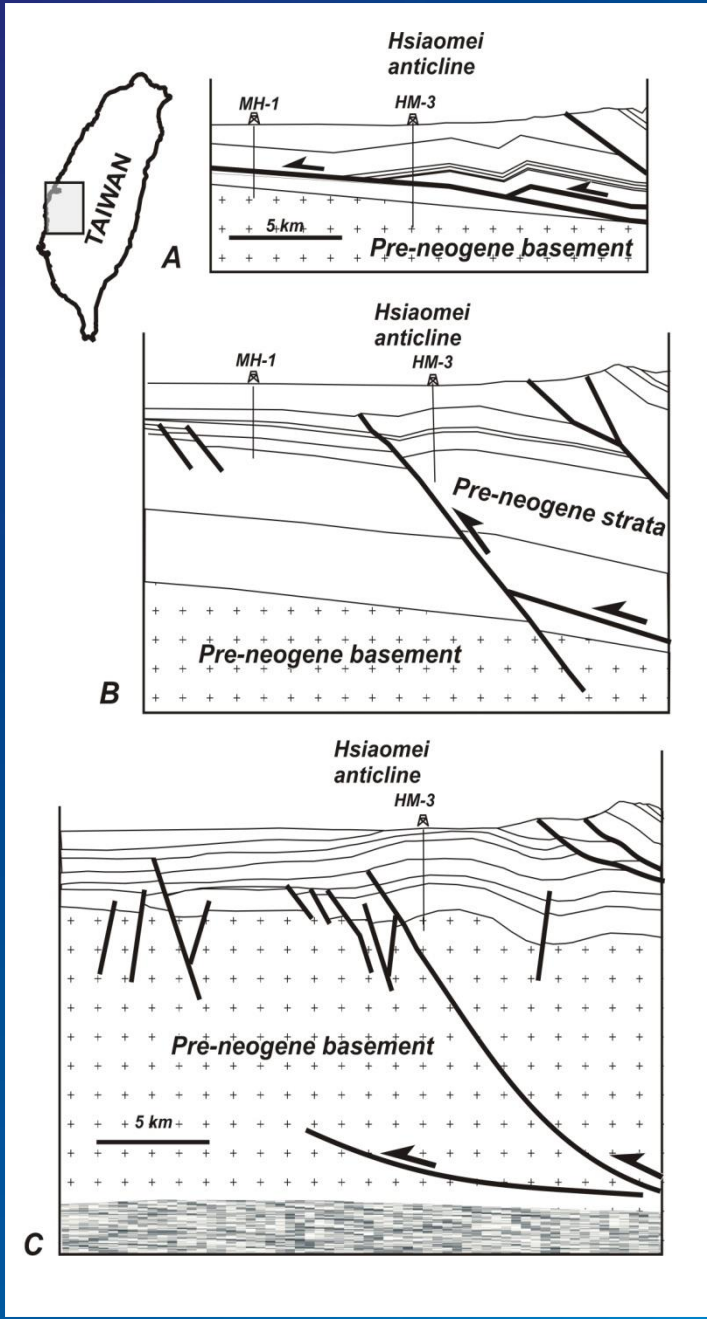

(Mouthereau and Lacombe, 2006)

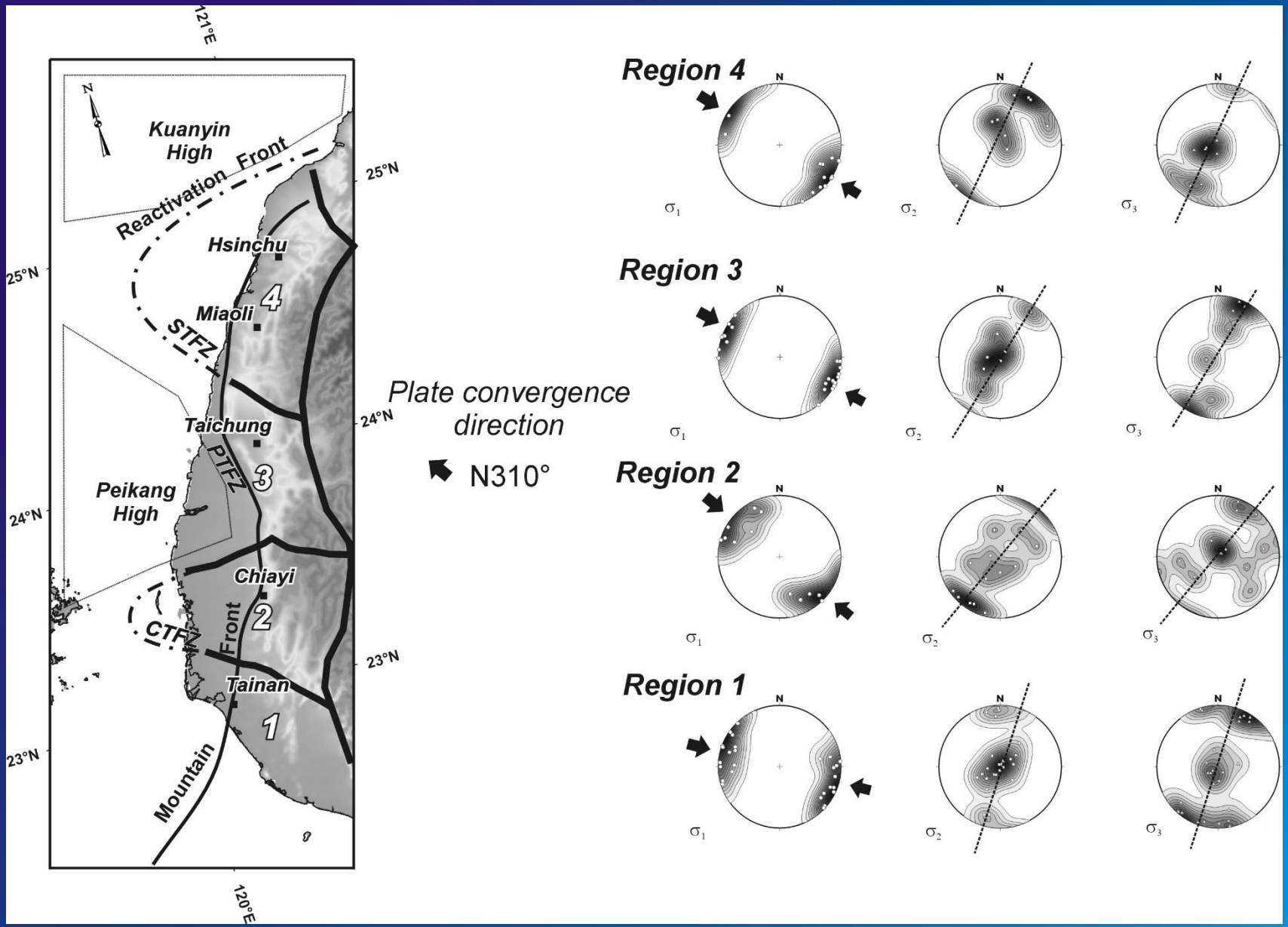

(Mouthereau et al., 2002)

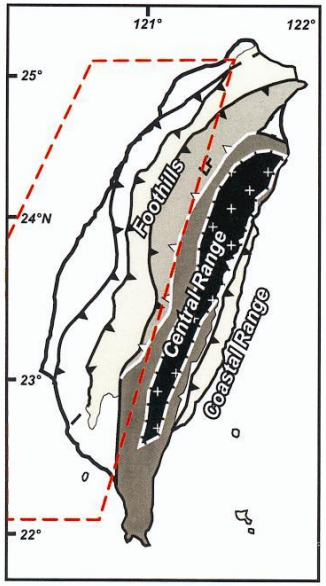

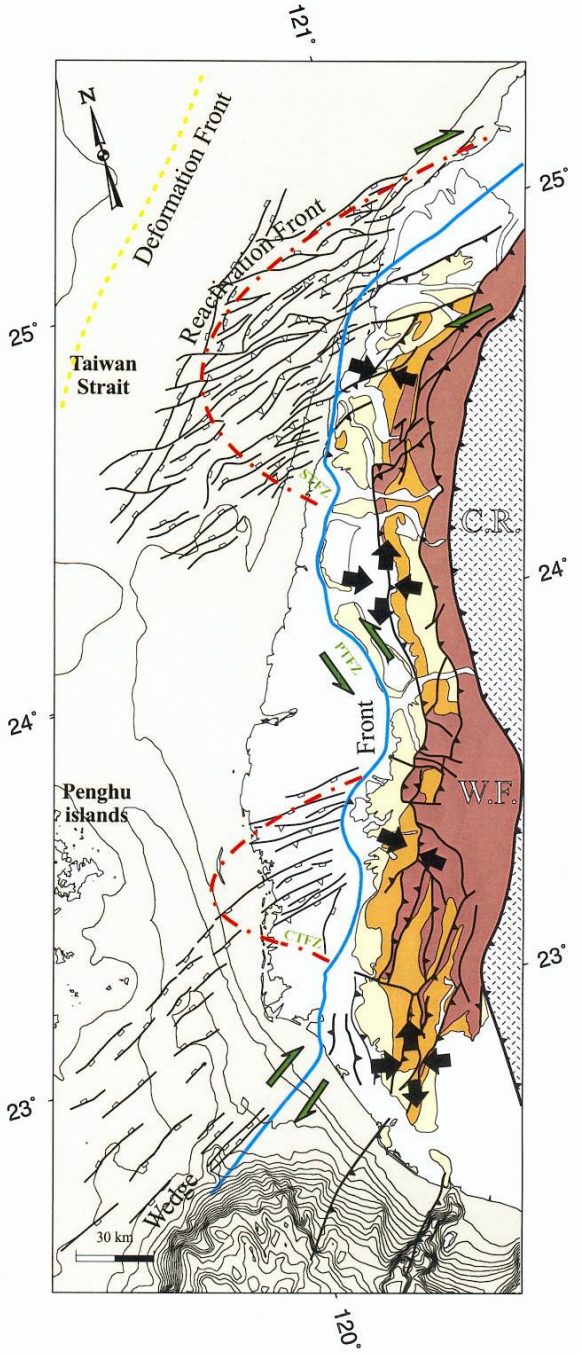

(Mouthereau et al., 2002)

(Lacombe and Mouthereau, 2002)

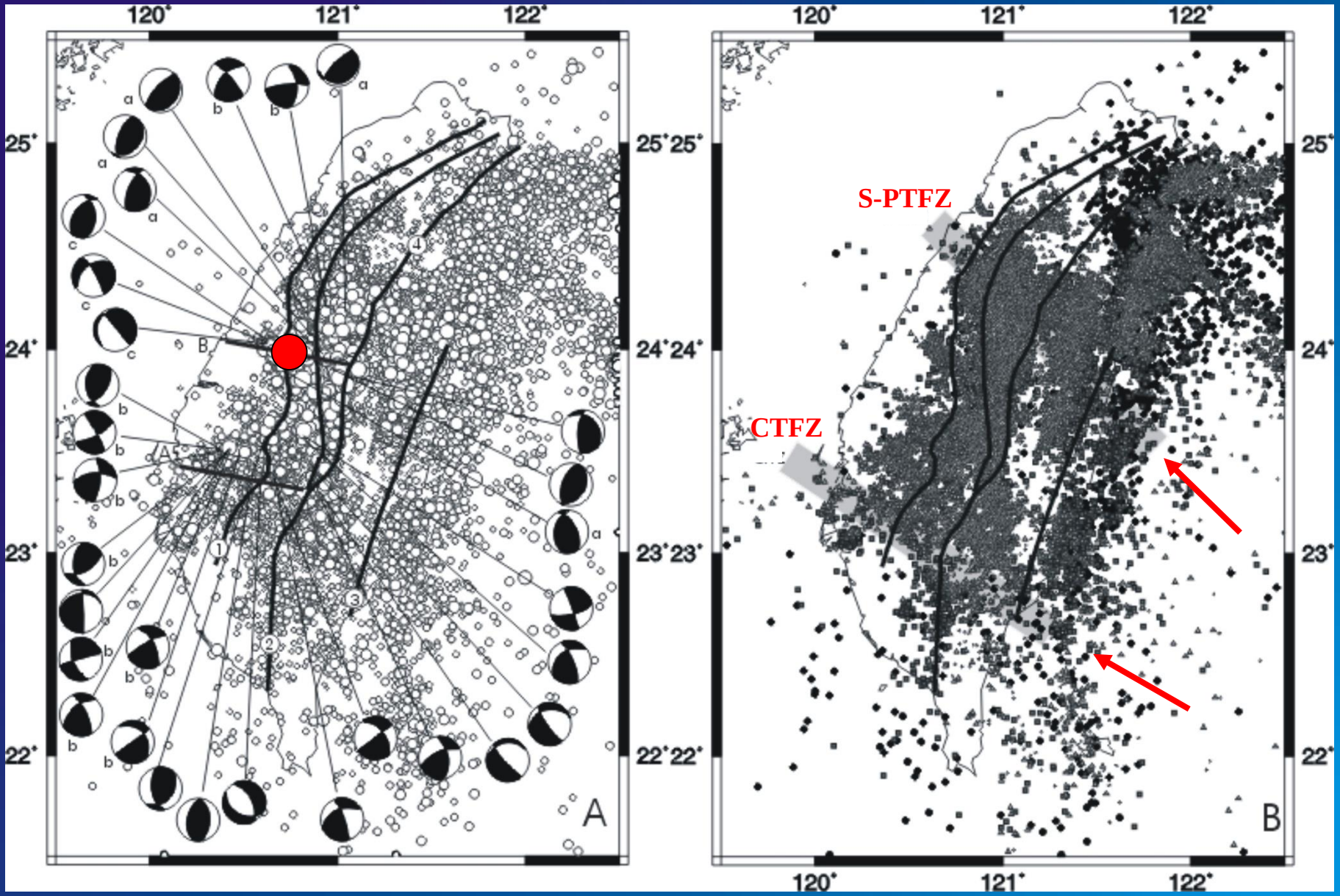

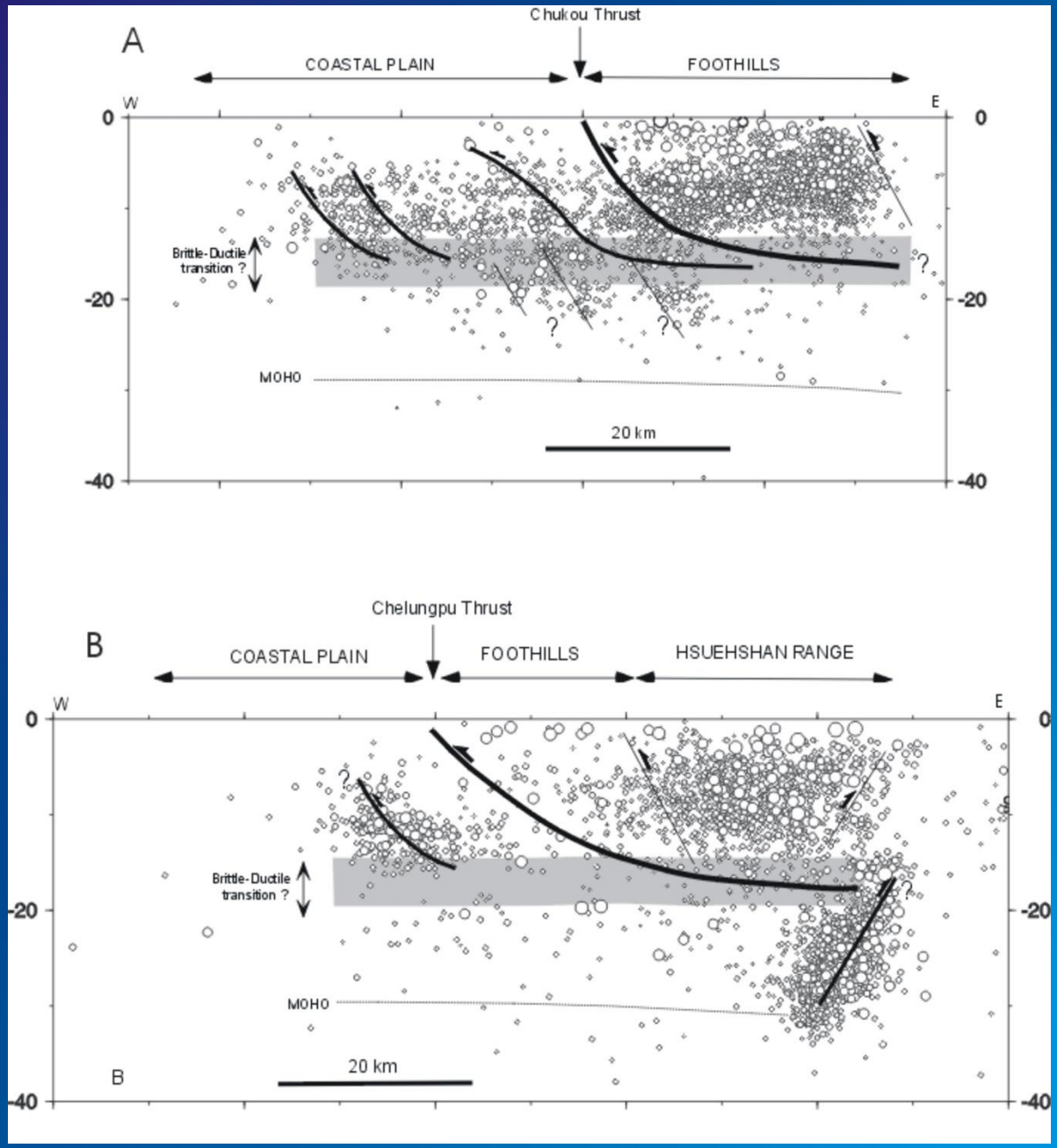

(Lacombe and Mouthereau, 2002)

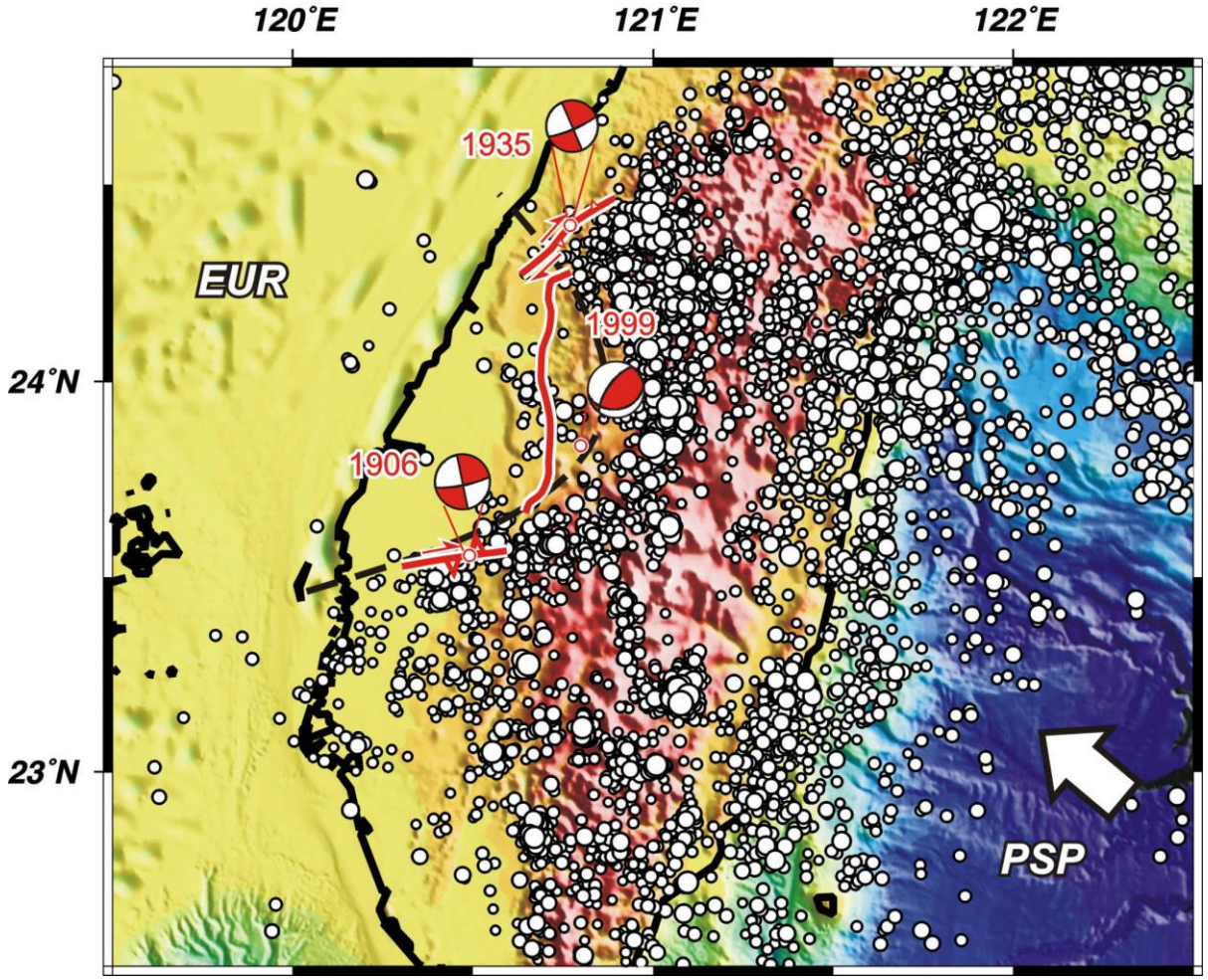
120˚E
121˚E
122˚E
24˚N
23˚N
1935
1999
1906
EUR
PSP

Chichi (Mw=7.9)

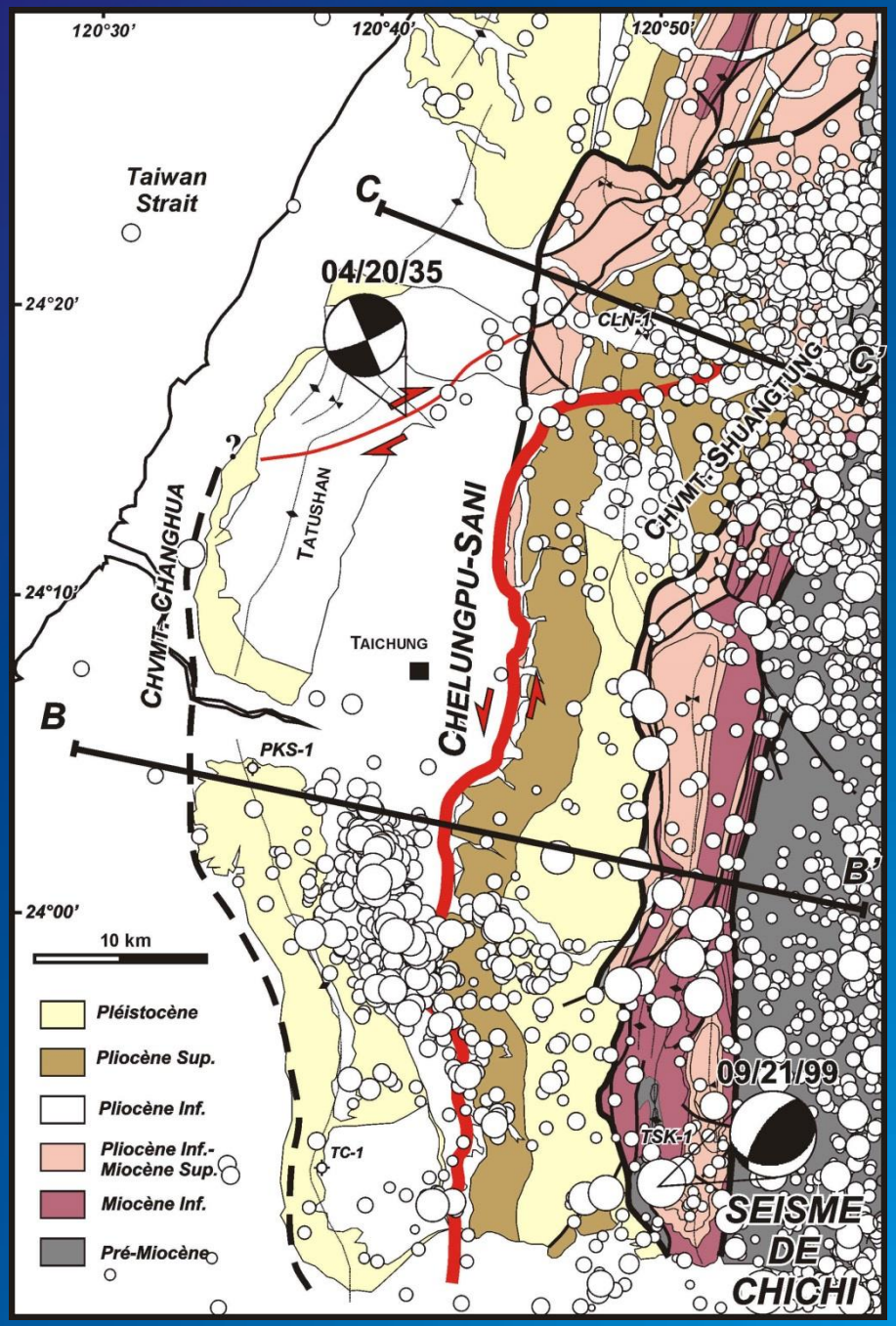
120°30'
120°40'
120°50'
Taiwan Strait
C
C'
04/20/35
24°20'
CLN-1
CHVMT-SHUANGTUNG
?
TATUSHAN
CHVMT-CHANGHUA
24°10'
TAICHUNG
CHELUNGPU-SANI
B
PKS-1
B'
24°00'
10 km
Pléistocène
Pliocène Sup.
Pliocène Inf.
Pliocène Inf.-Miocène Sup.
Miocène Inf.
Pré-Miocène
TC-1
09/21/99
TSK-1
SEISME DE CHICHI

The Chichi earthquake :
initiation of a thrust ramp dipping 30° at 11-12 km which connects to the Chelungpu thrust (an inherited normal fault)

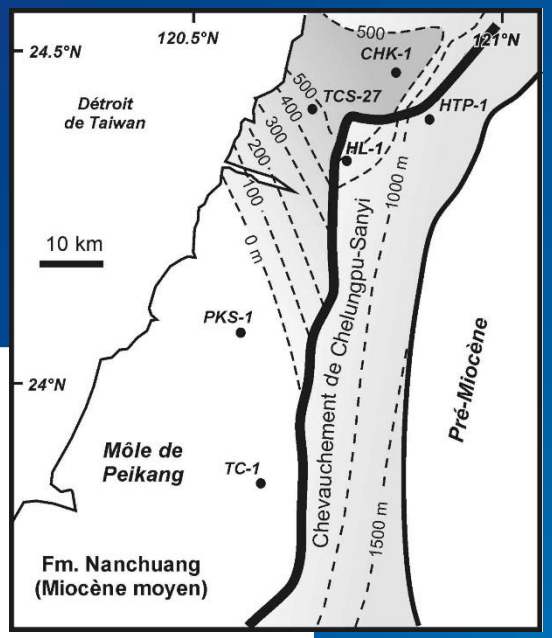

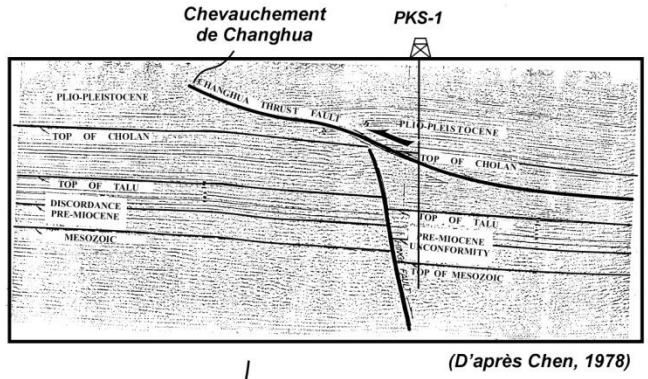

(D'après Chen, 1978)

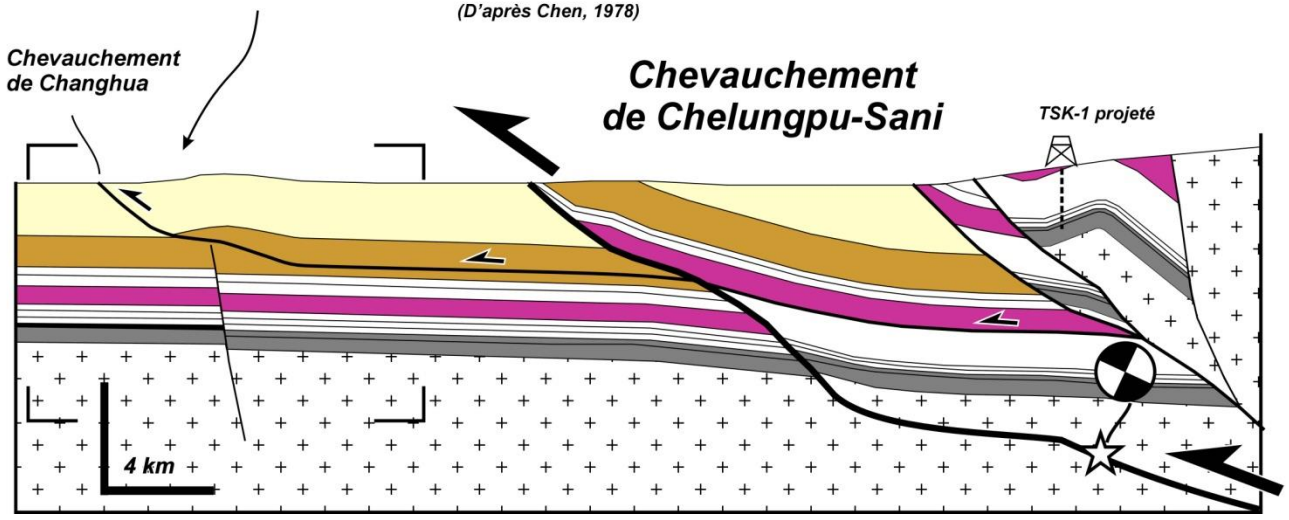

(Mouthereau et al, 2001)

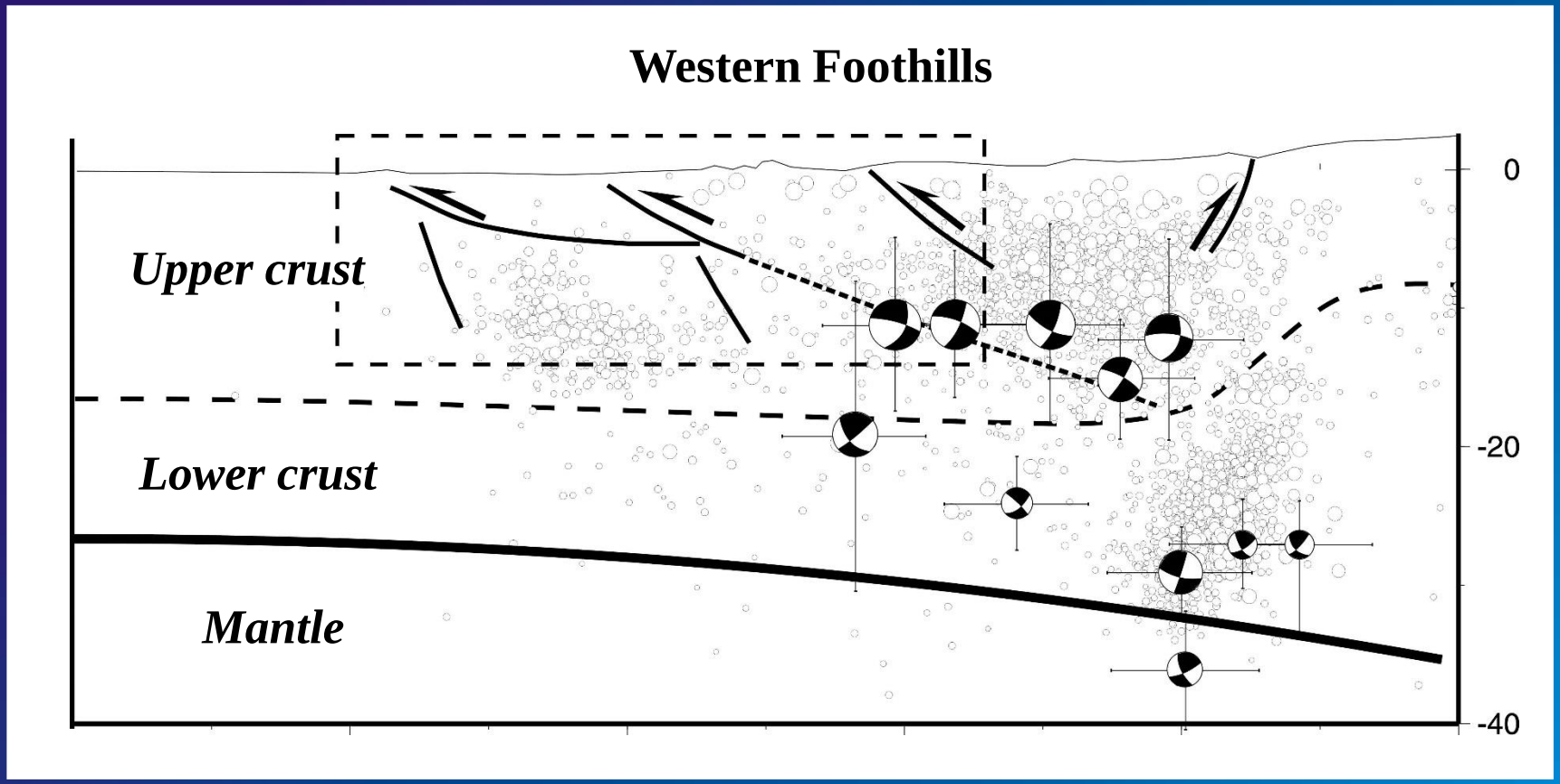

(Kao et al., 2000)

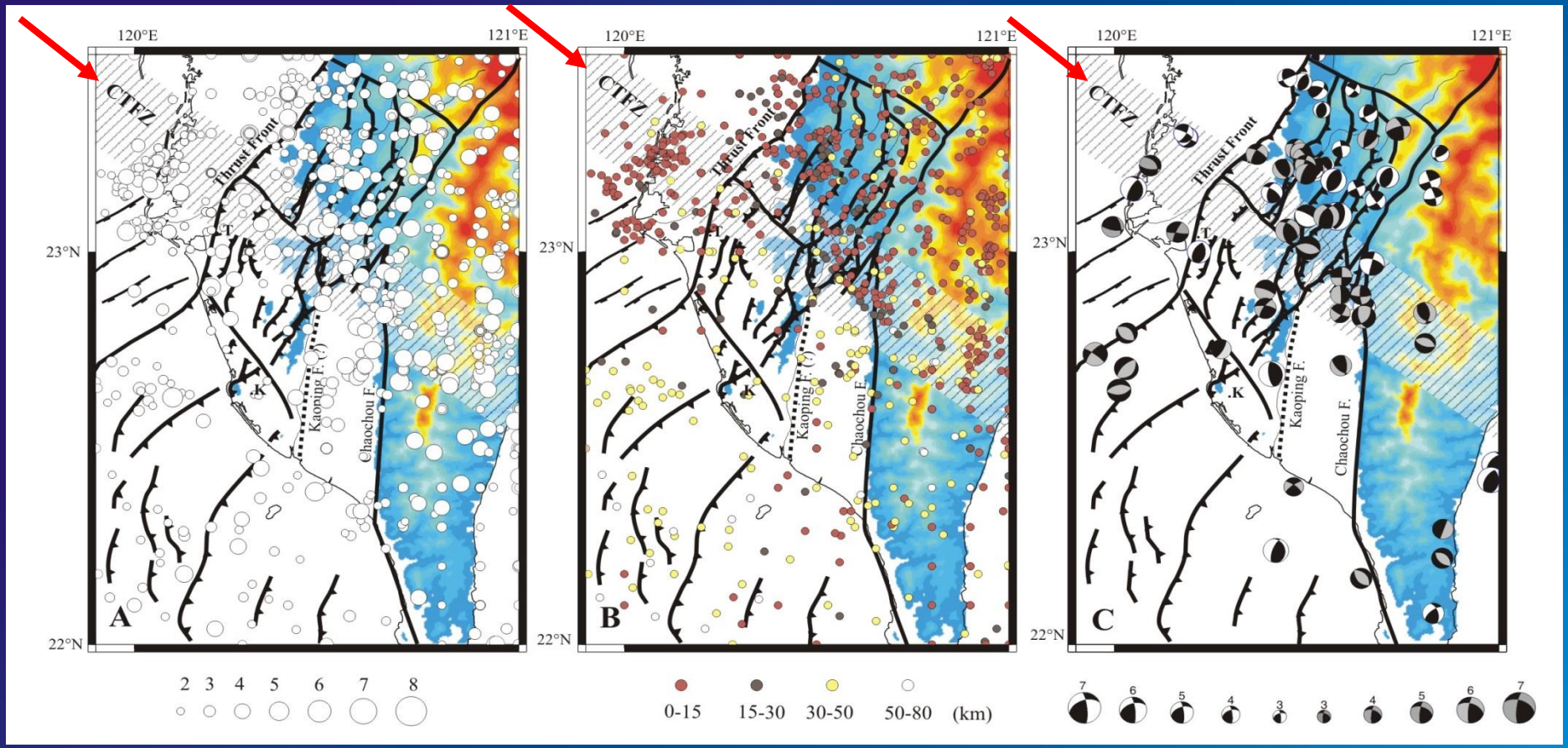

(Lacombe et al., 2001)

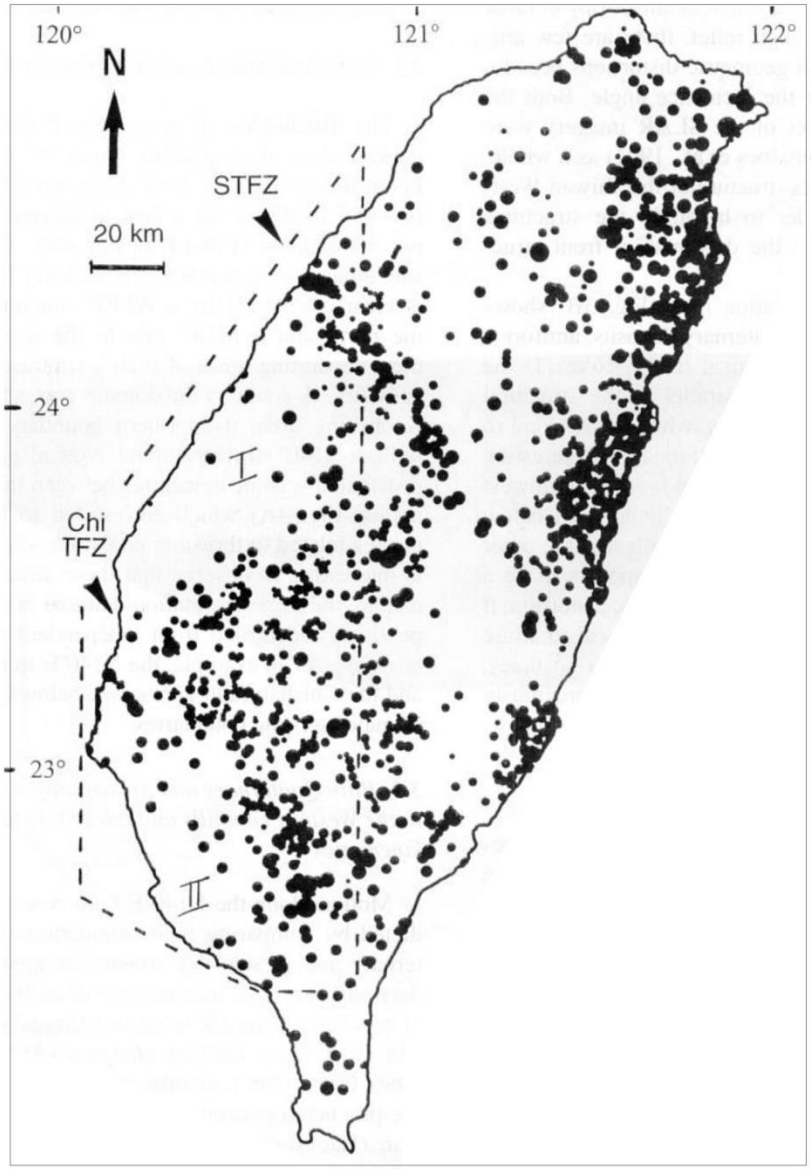

(Deffontaines et al., 1997)

(Rau et al, 2013)

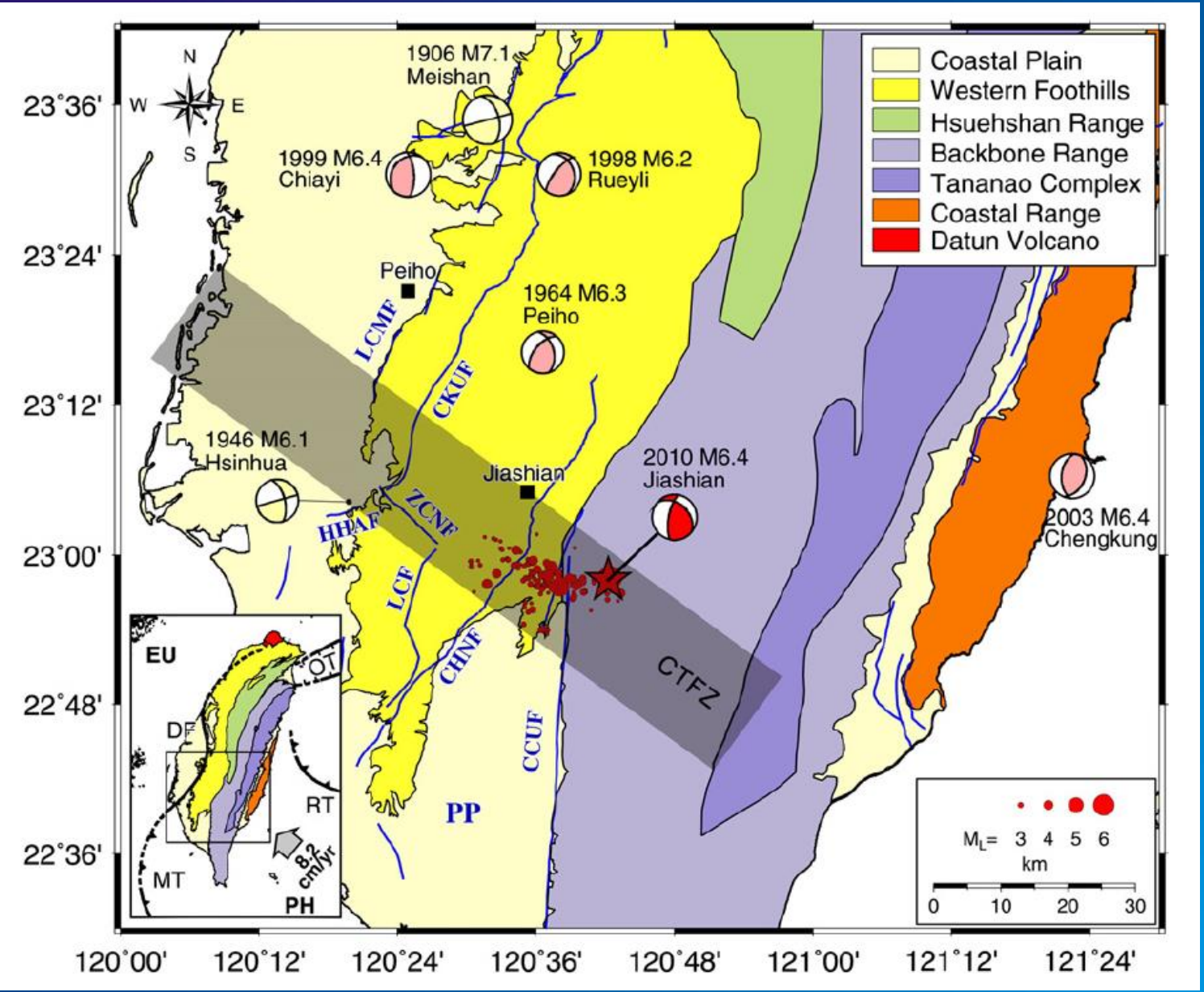

2010 March 4, Mw 6.3 Jia-Shian earthquake

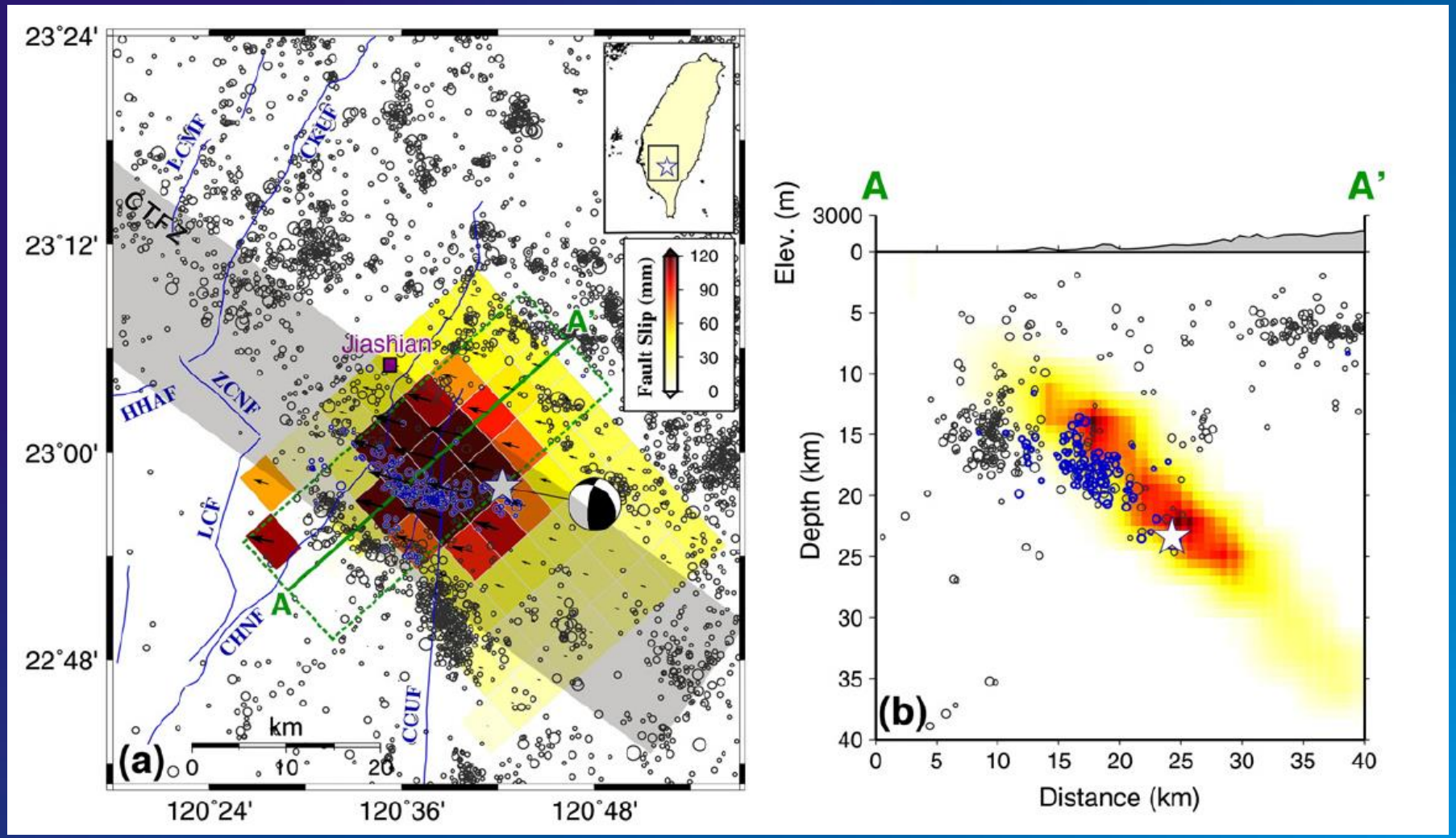

(Rau et al, 2013)

2010 March 4, Mw 6.3 Jia-Shian earthquake

ML 6.2 and ML 6.5 2013 Nantou earthquakes

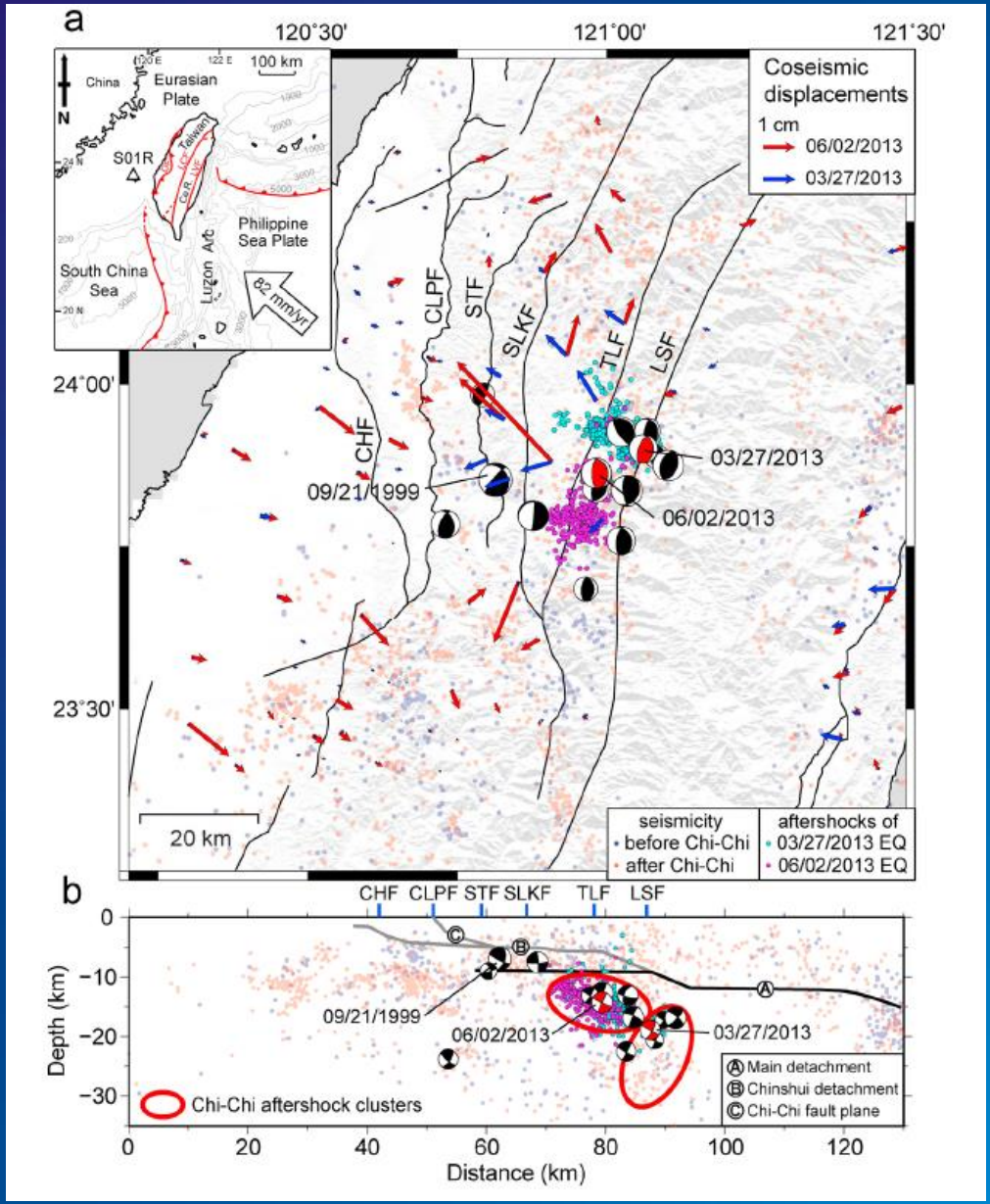

(Chuang et al, 2013)

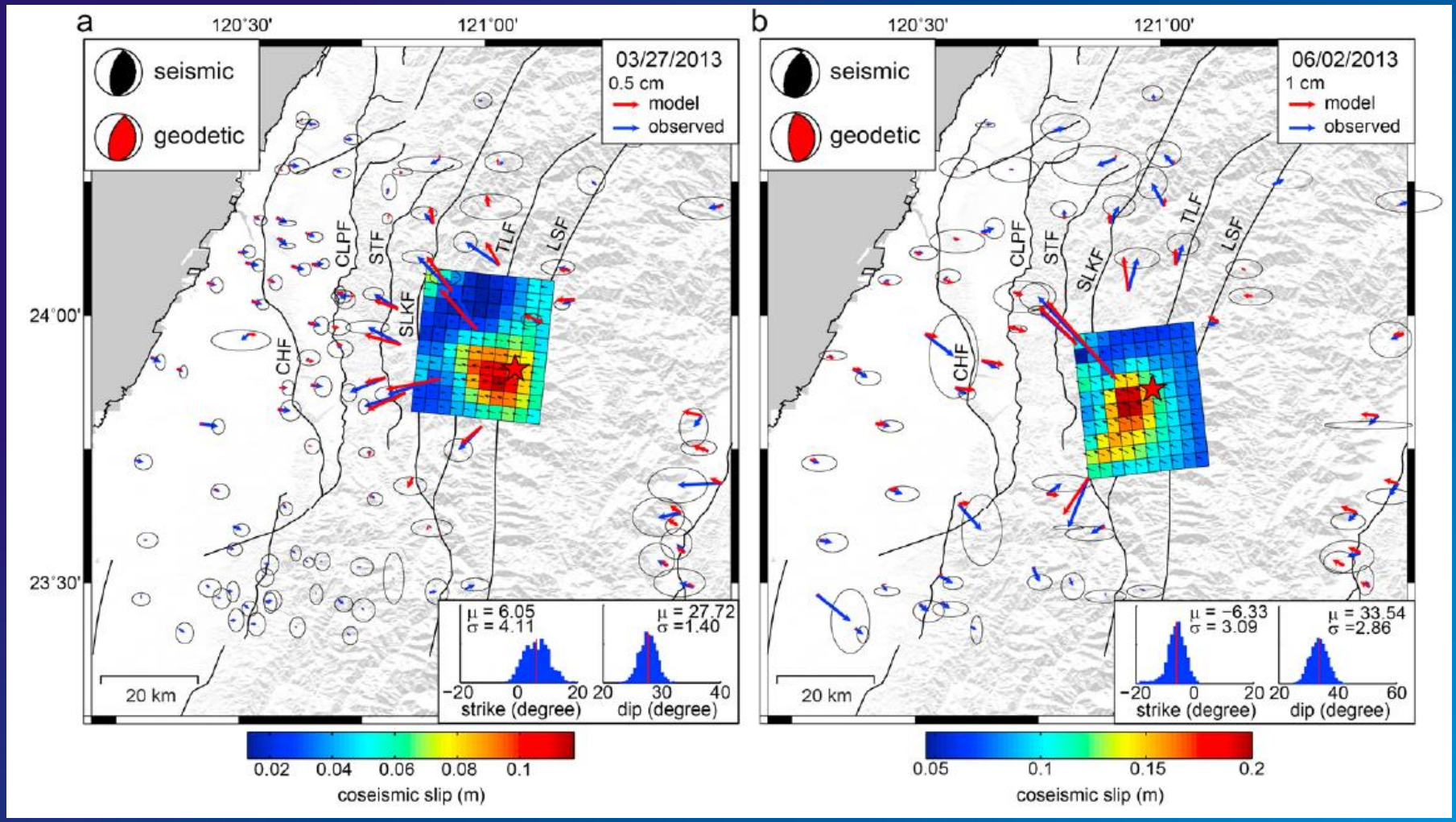

(Chuang et al, 2013)

ML 6.2 and ML 6.5 2013 Nantou earthquakes

ML 6.2 and ML 6.5 2013 Nantou earthquakes

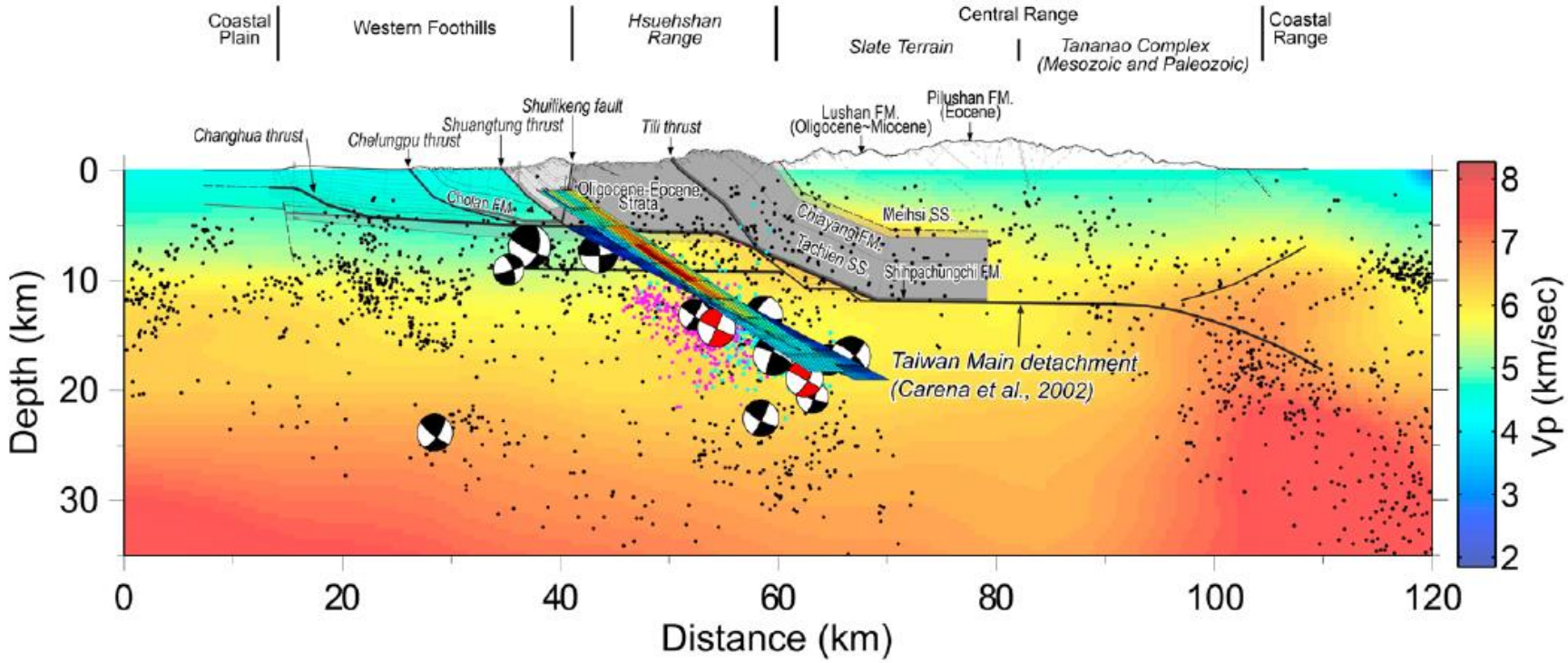

(Chuang et al, 2013)

The earthquakes occur on essentially the same 30° dipping fault plane ramping up from ~20 km depth near a cluster of 1999 Chi-Chi earthquake aftershocks to the shallow detachment and the Chi-Chi fault plane.

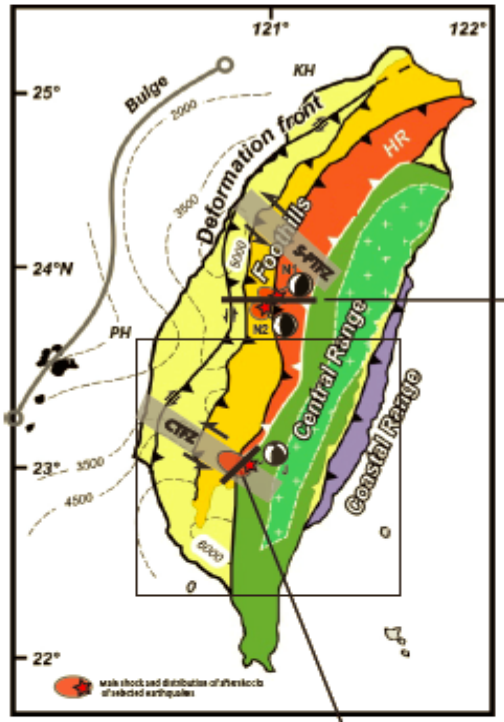
121°
122°
25°
24°N
23°
22°
Bulge
KH
Deformation front
HR
Foothills
5-PFFZ
N1
N2
PH
CTFZ
Central Range
Coastal Range
2000
3500
4500
5000
6000
main shock and distribution of aftershocks of selected earthquakes

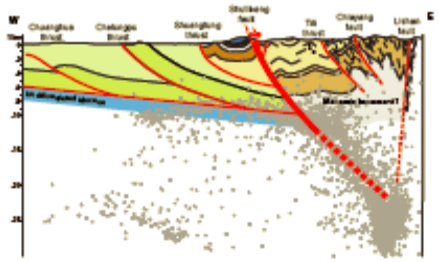

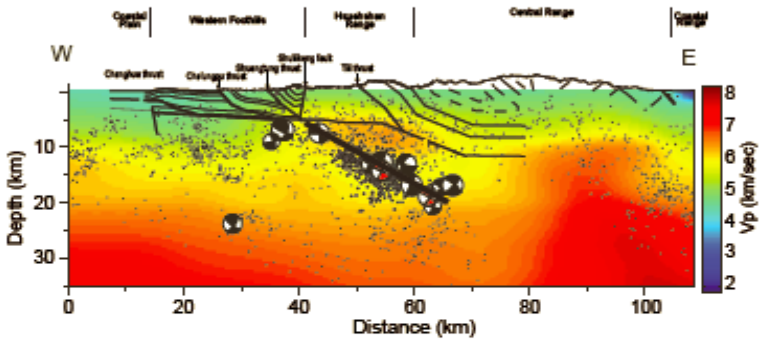
W
E
Depth (km)
10
20
30
0
20
40
60
80
100
Distance (km)
Vp (km/sec)
8
7
6
5
4
3
2

SW NE

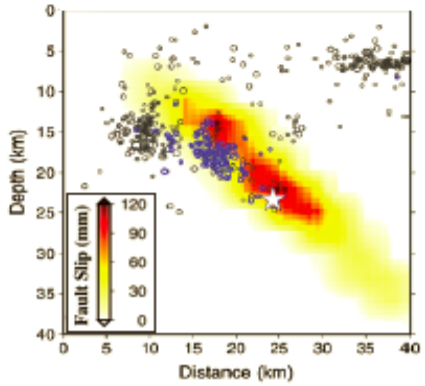
Depth (km)
0
5
10
15
20
25
30
35
40
Fault Slip (mm)
120
90
60
30
0
0
5
10
15
20
25
30
35
40
Distance (km)

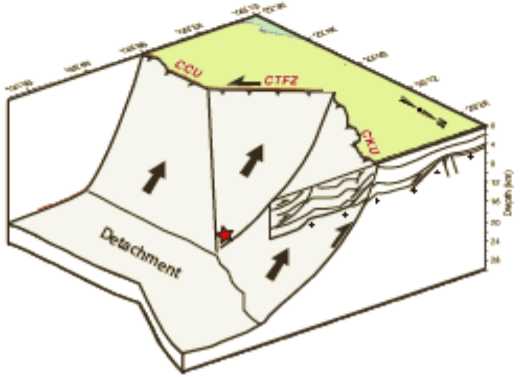
CCU
CTFZ
CKU
Detachment

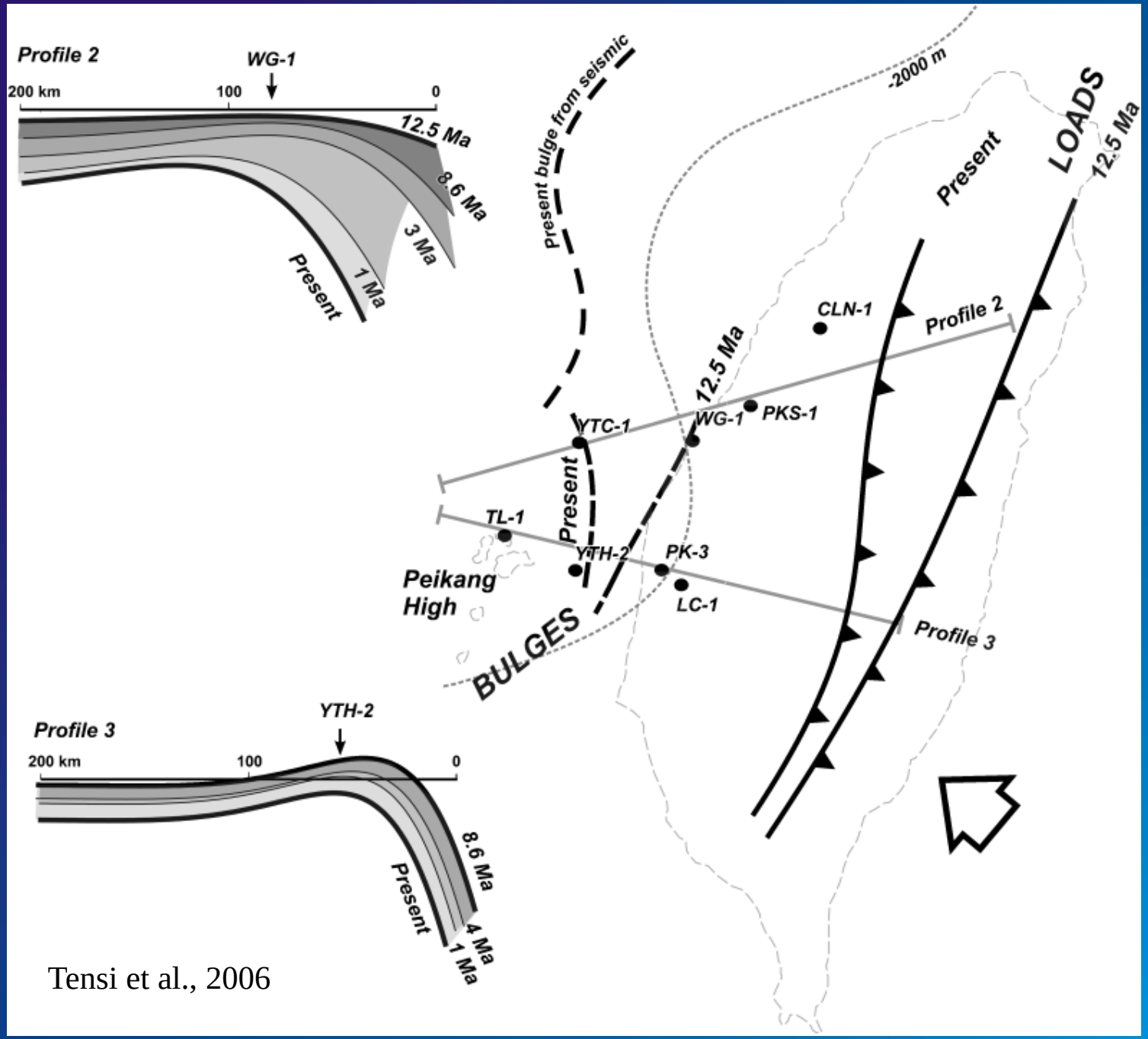

Tensi et al., 2006

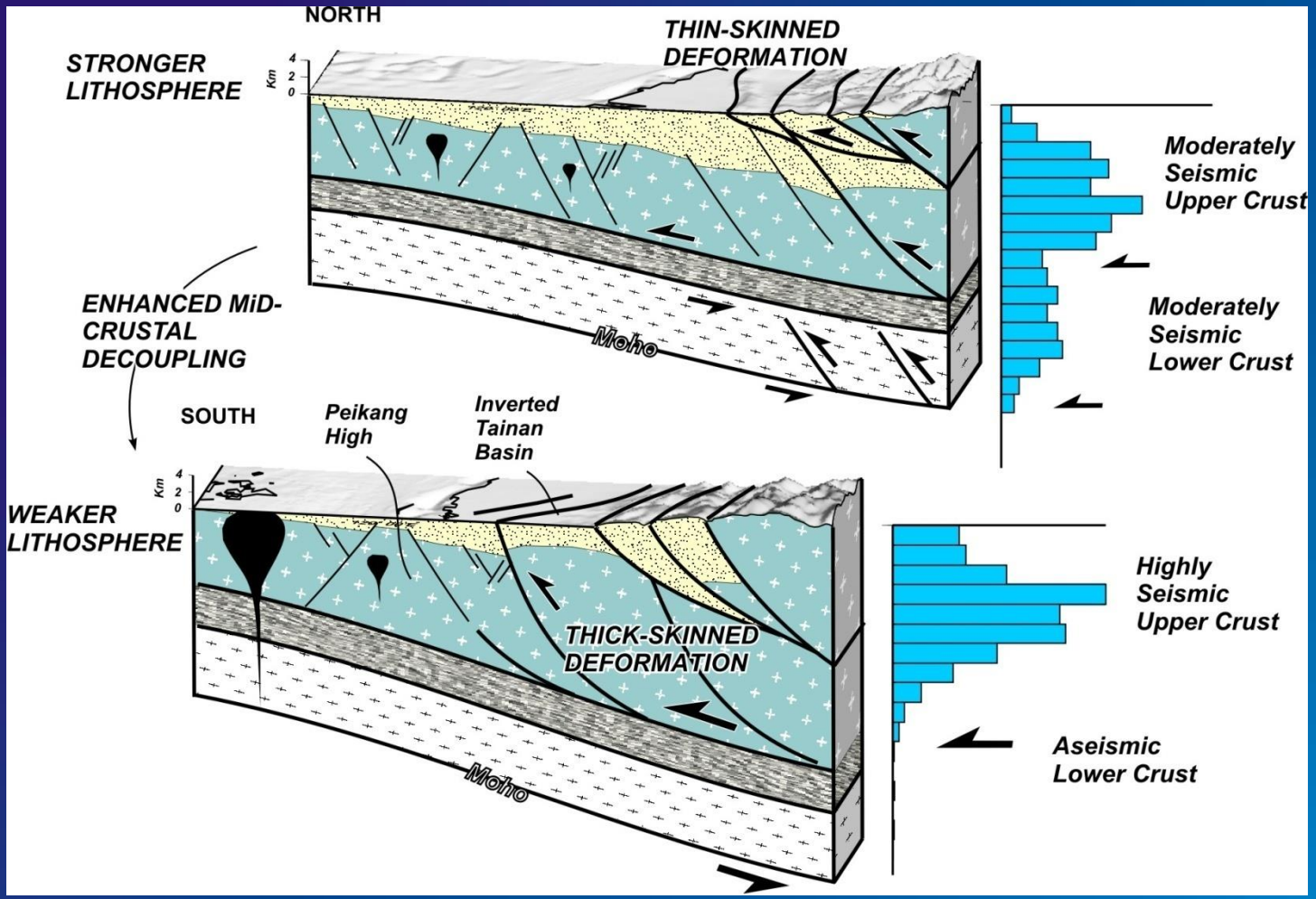

The degree of basement involvement *vs* thin-skinned deformation increases as the lithosphere weakens (rheology of the lower crust)

(Mouthereau and Petit, 2003)

Taiwan : inverted Tertiary rifted margin
Shortening : ~35 %

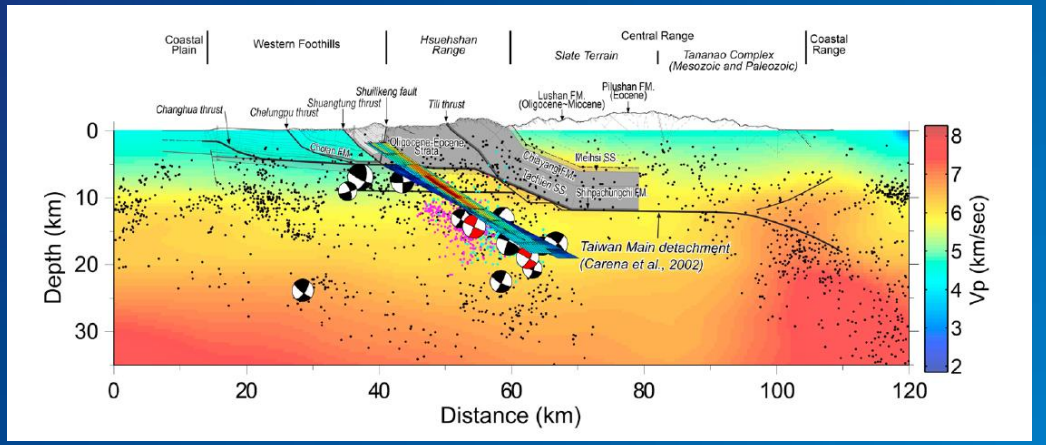

Convergence 80 km/Ma
Erosion rate 6-8 km/Ma

Thick-skinned tectonic style
"pure-shear"

Decoupling within middle-lower crust
h ~ 20 km

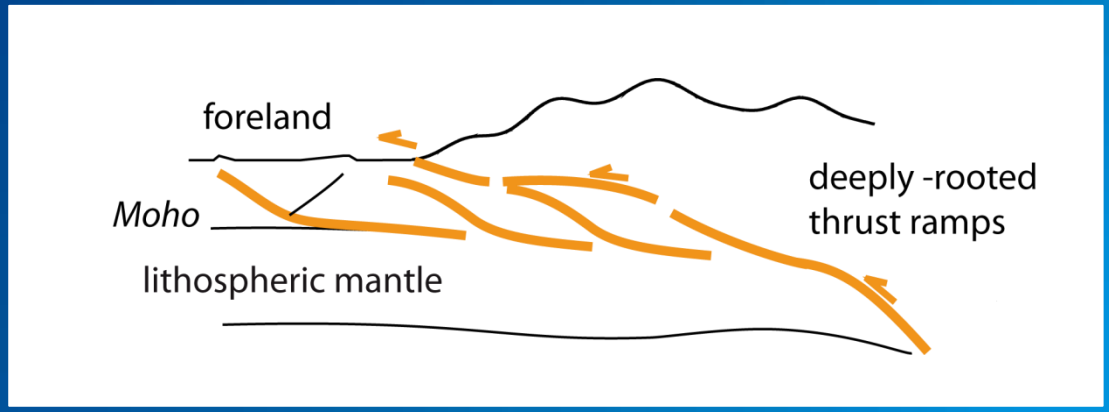

Early inversion of inherited normal faults / early high angle basement thrusting in the foreland (Zagros, Taiwan)

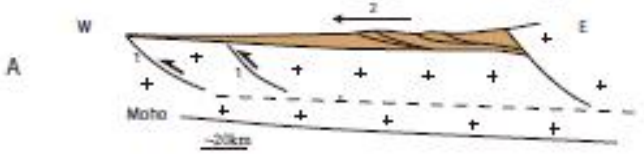

Basement shortening at the rear than exhumation and forelandward propagation above basement ramps activating cover shallow decollement (Western Alps)

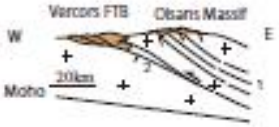

Coeval thin-skinned and thick-skinned tectonics.
The cover is detached mainly above the low-viscosity Hormuz salt layer while the basement deforms by both seismogenic faulting and ductile aseismic shearing (Zagros)

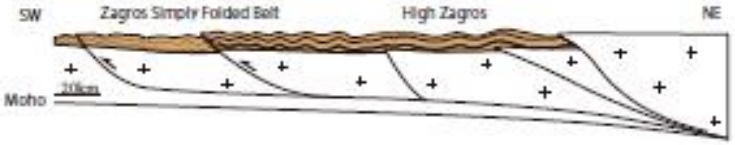

Late basement thrusting : refolding of shallow nappes by high angle thrusts reactivating inherited normal faults (e.g. Jura, Provence) /out-of-sequence seismogenic basement thrusting

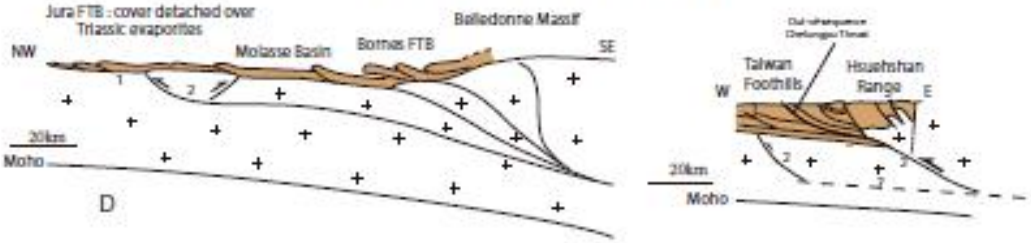

Basement-involved shortening occuring forelandward after thin-skinned tectonics : Laramide uplifts / Sevier FTB and Sierras Pampeanas / Pre-Cordillera FTB of Argentina

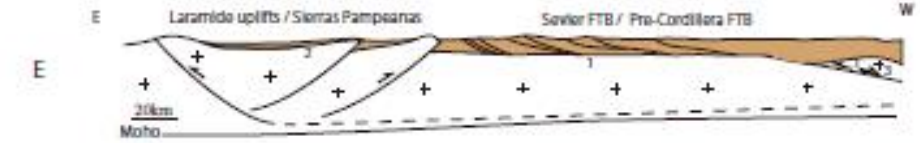

Some first-order rheological controls of the structure of fold-and-thrust belts

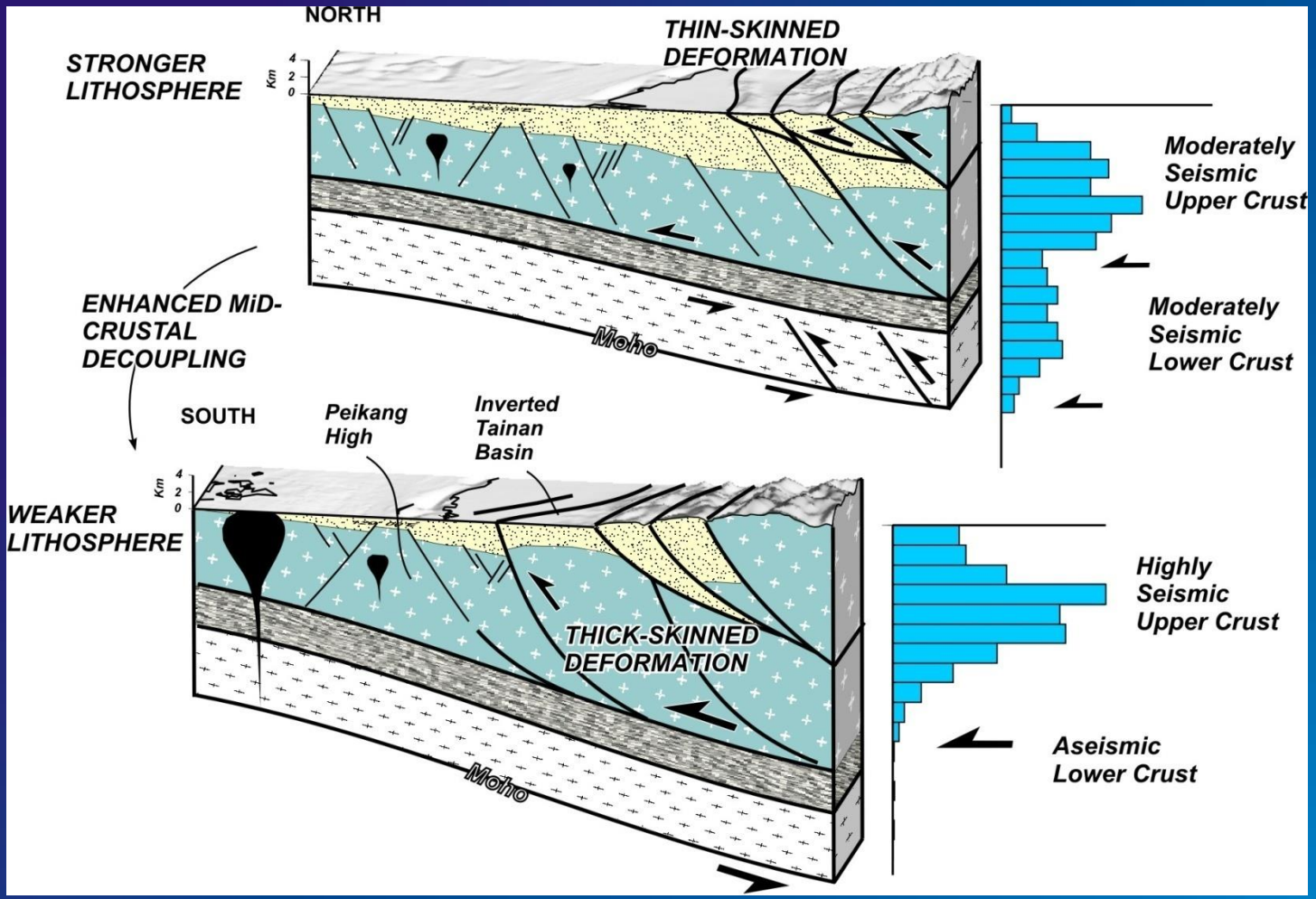

The degree of basement involvement *vs* thin-skinned deformation increases as the lithosphere weakens (rheology of the lower crust)

(Mouthereau and Petit, 2003)

Correlation between spatial variations of the flexural rigidity of the lithosphere and the nature and amount of foreland deformation has been suggested for the Andes FTB (Watts et al., 1995) and Taiwan (Mouthereau & Petit, 2003).

These authors documented that regions with low Equivalent Elastic Thickness (Te) correlate with thick-skinned deformation whereas regions with high Te correlate with thin-skinned deformation. The idea behind is that a strong lithosphere is less easily deformed so that shortening is localized in a narrow zone at shallow depth, while a weaker lithosphere enables crust-mantle decoupling and shortening of the whole crust.

Mouthereau & Petit (2003) emphasized that the local increase of plate coupling and inhomogeneities in a prefractured margin as in Taiwan can affect the rigidity of the layered continental lithosphere, supporting a mechanical relationship between its strength and the structural style.

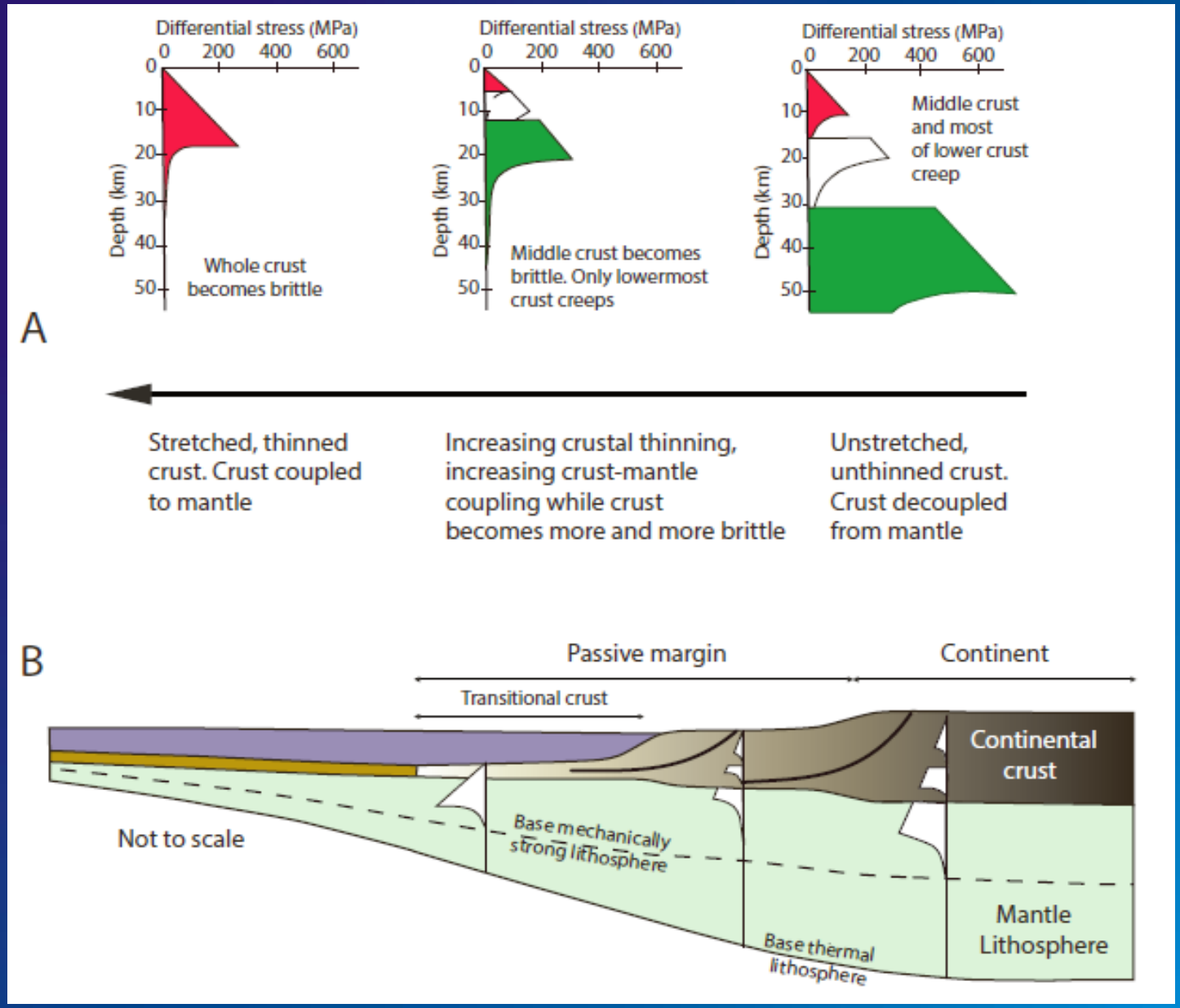

(Reston and Manatschal, 2011; Cloetingth et al., 2005)

Passive margins are key players in the collisional processes as the arrival of theirproximal, poorly thinned parts into the subduction zone mark the onset of collision. The transition between continental and oceanic crusts is often marked by a wide domain of progressively thinner continental crust, with occasional locally exhumed sub-continental mantle.

Differential stretching of the lithosphere modifies its rheological properties which will subsequently control deformation style during collision (Cloetingh et al., 2005). As the crust thins and cools during progressive rifting, the reduction in overburden pressure and temperature makes the rocks which originally deformed by plastic creep gradually become more prone to brittle failure. The result is that the initial weak zones in the middle crust and deep crust disappear and that the entire crust becomes brittle. The important consequences of the progressive embrittlement of originally ductile rocks during lithospheric extension are (1) that lateral flow or displacement of particular layers within the crust should become progressively more difficult as rifting proceeds, and (2) that the upper crust becomes coupled to the mantle (Reston & Manatschal, 2011).

→ For thick-skinned FTBs that developed from former passive margins, the occurrence of weak mechanical layers within the proximal margin lithosphere (the middle and most of the lower crust are expectedly ductile) may explain thatcontractional deformation be distributed within most of the crust, giving rise to basement- involved tectonic style. In contrast, because these weak crustal levels are usually lacking indistal parts of the margins as a result of thinning, these stronger lithospheric domains are more prone to localized deformation in a continental subduction style.

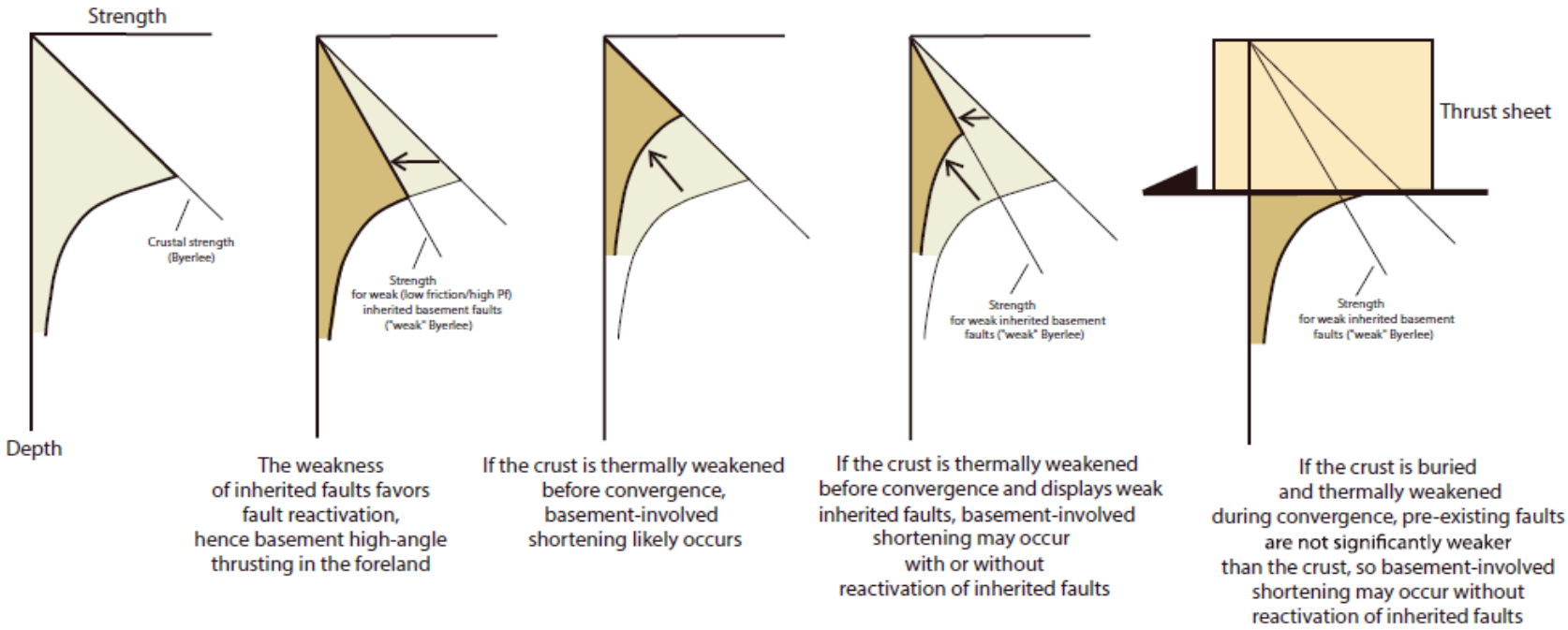

The weakness of inherited faults favors fault reactivation, hence basement high-angle thrusting in the foreland

If the crust is thermally weakened before convergence, basement-involved shortening likely occurs

If the crust is thermally weakened before convergence and displays weak inherited faults, basement-involved shortening may occur with or without reactivation of inherited faults

If the crust is buried and thermally weakened during convergence, pre-existing faults are not significantly weaker than the crust, so basement-involved shortening may occur without reactivation of inherited faults

Deformation in orogens

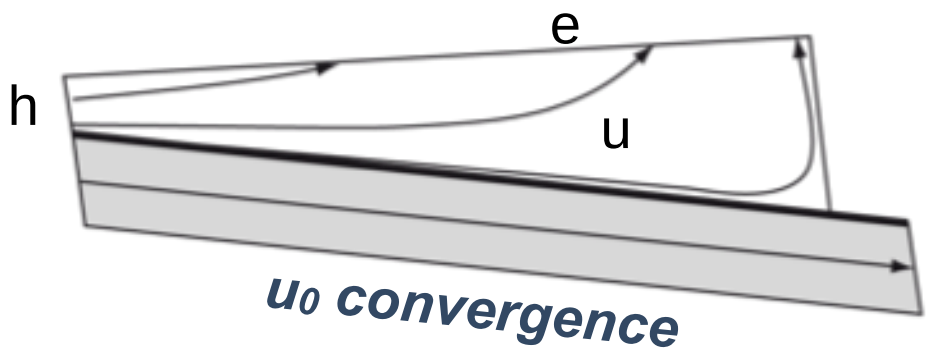

Displacement

Erosion

$$u(x,z) = \frac{1}{h(x)} \int_0^x \epsilon(x)\,dx$$

Accreted thickness

h(x) ⇨ inheritance

Shortening (%)

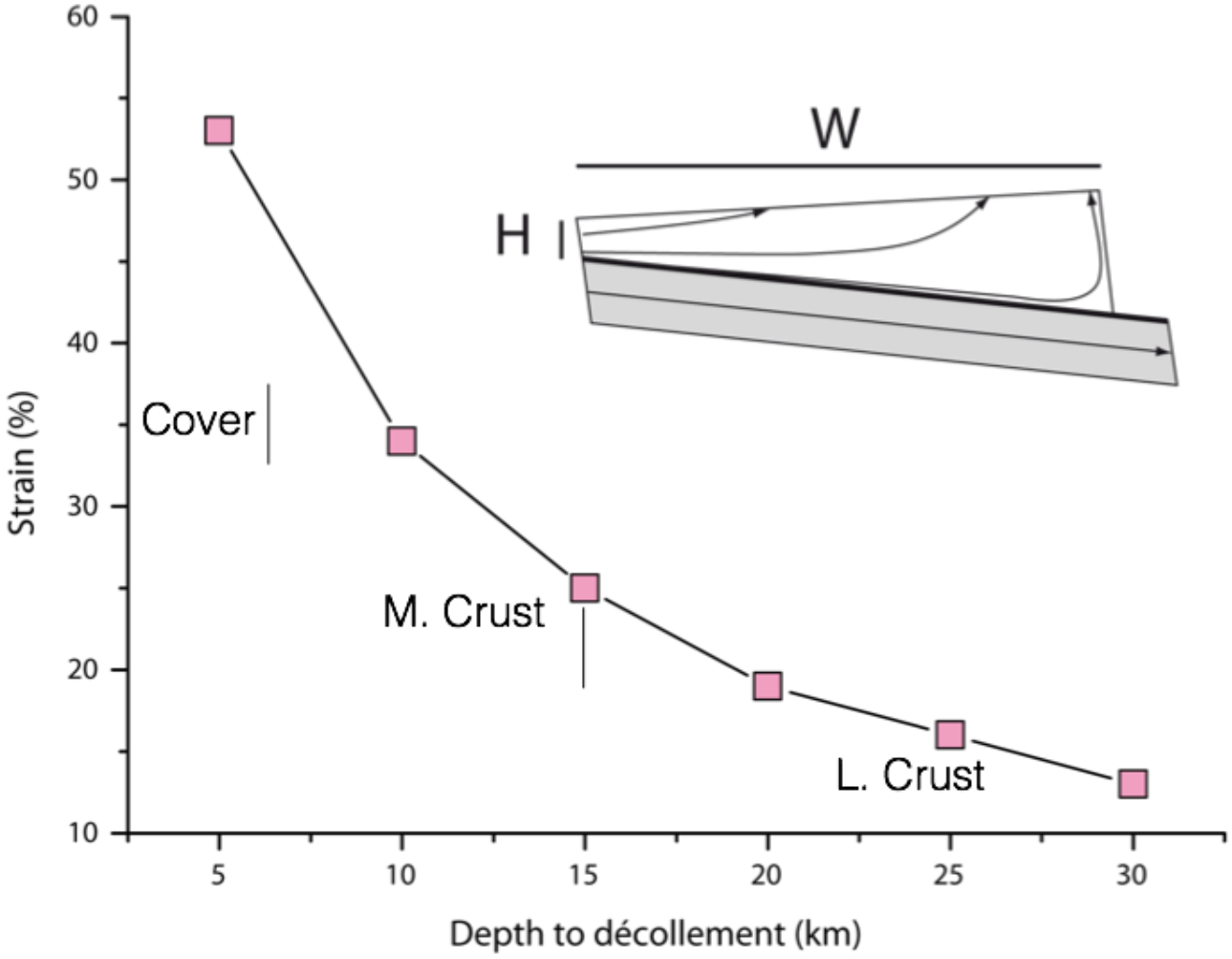

Shortening
→ DL/L (%)

Linear erosion
0 →5.5 km/Myr

Convergence =
4.6 km/Myr

Décollement → 3°

Taiwan : inverted Tertiary rifted margin

Shortening : ~35 %

Convergence 80 km/Ma
Erosion rate 6-8 km/Ma

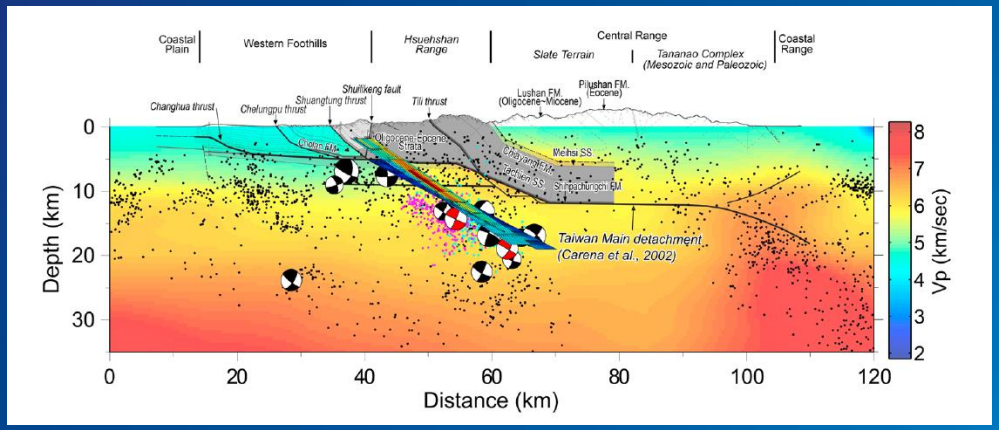

Chuang et al. (2013)

thick-skinned tectonics style
"pure-shear"

Decoupling within middle-lower crust
h ~ 20 km

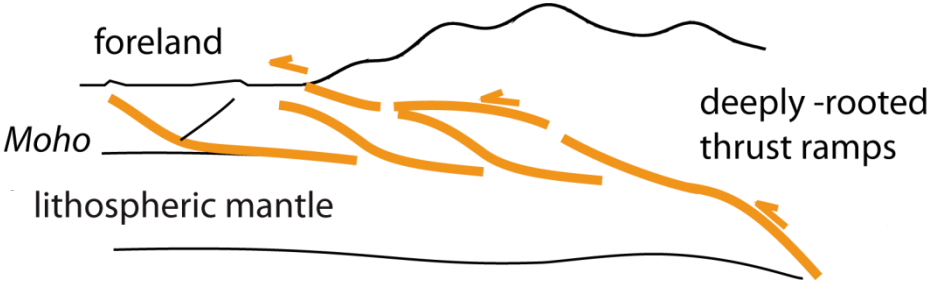

Zagros : inverted Mesozoic rifted margin

Shortening : ~37 %

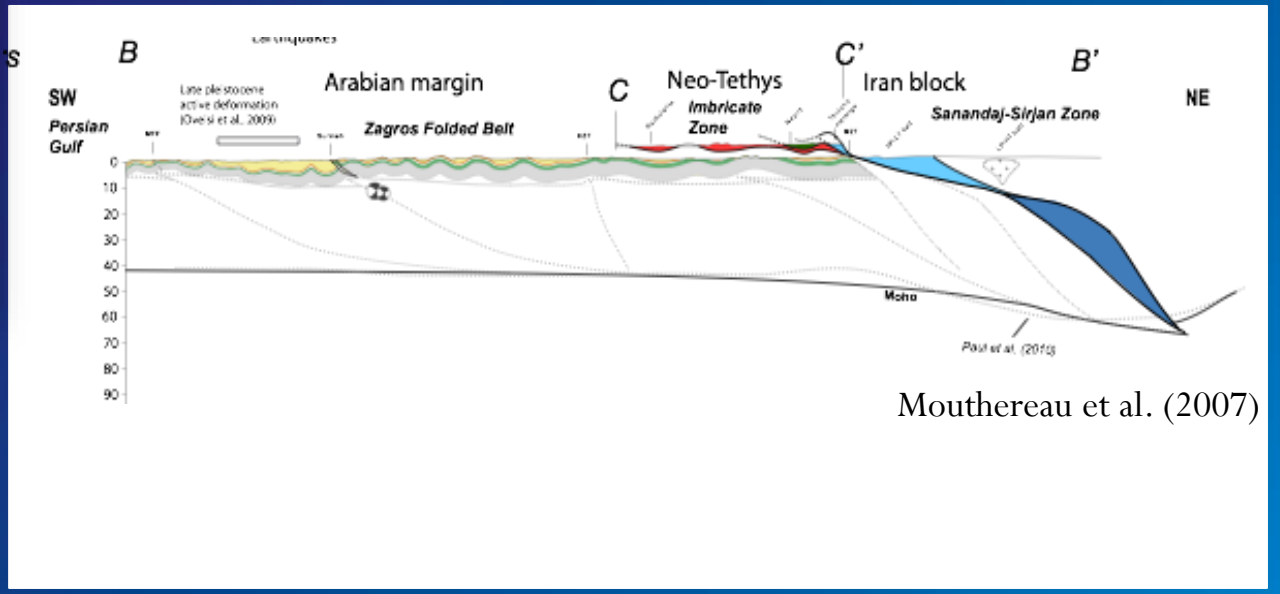

Mouthereau et al. (2007)

Convergence 7km/Ma
Erosion rate <2 km/Ma

Thick-skinned tectonic style
"pure-shear"

Decoupling within middle-lower crust
h ~ 15-20 km

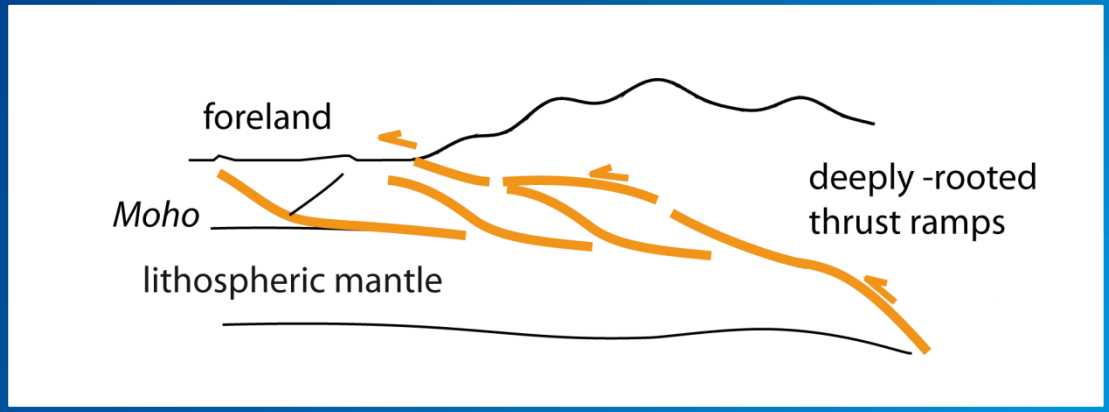

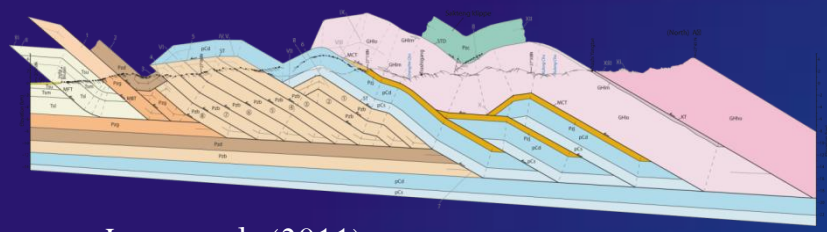

Long et al. (2011)

Himalaya : « underthrusting of a paleo-proterozoic craton

Shortening : ~ 70 %

Convergence 50 km/Ma
Erosion rate3-5 km/Ma

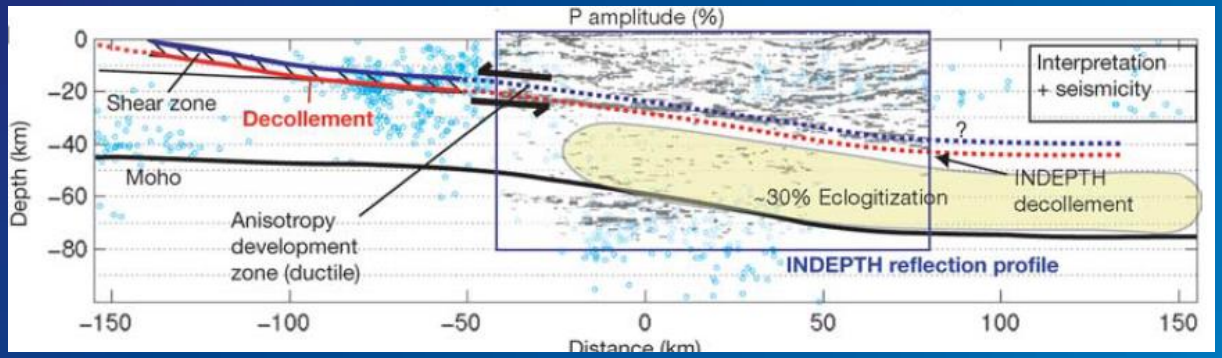

Schulte-Pelkum et al. (2005)

Thin-skinned tectonics style
"simple shear"

Décollement
h <10 km

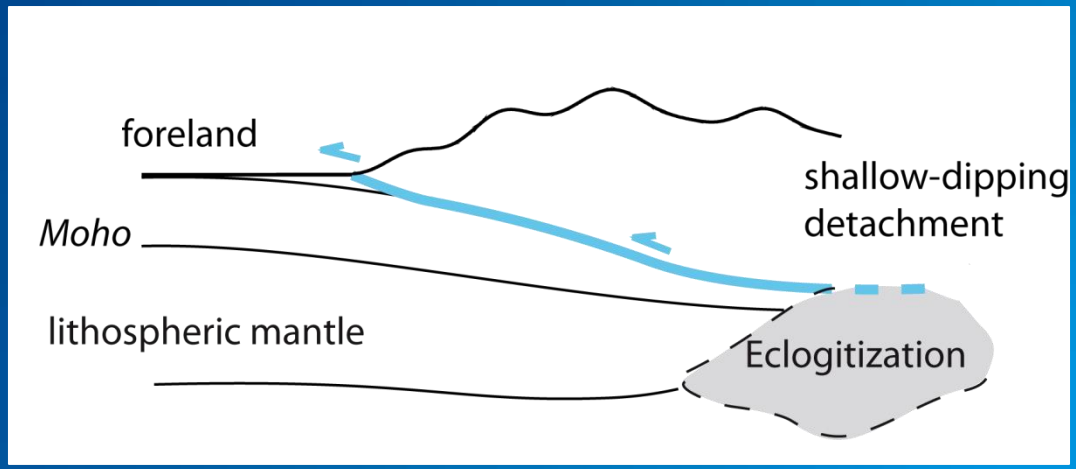

Two main modes of accretion - why?

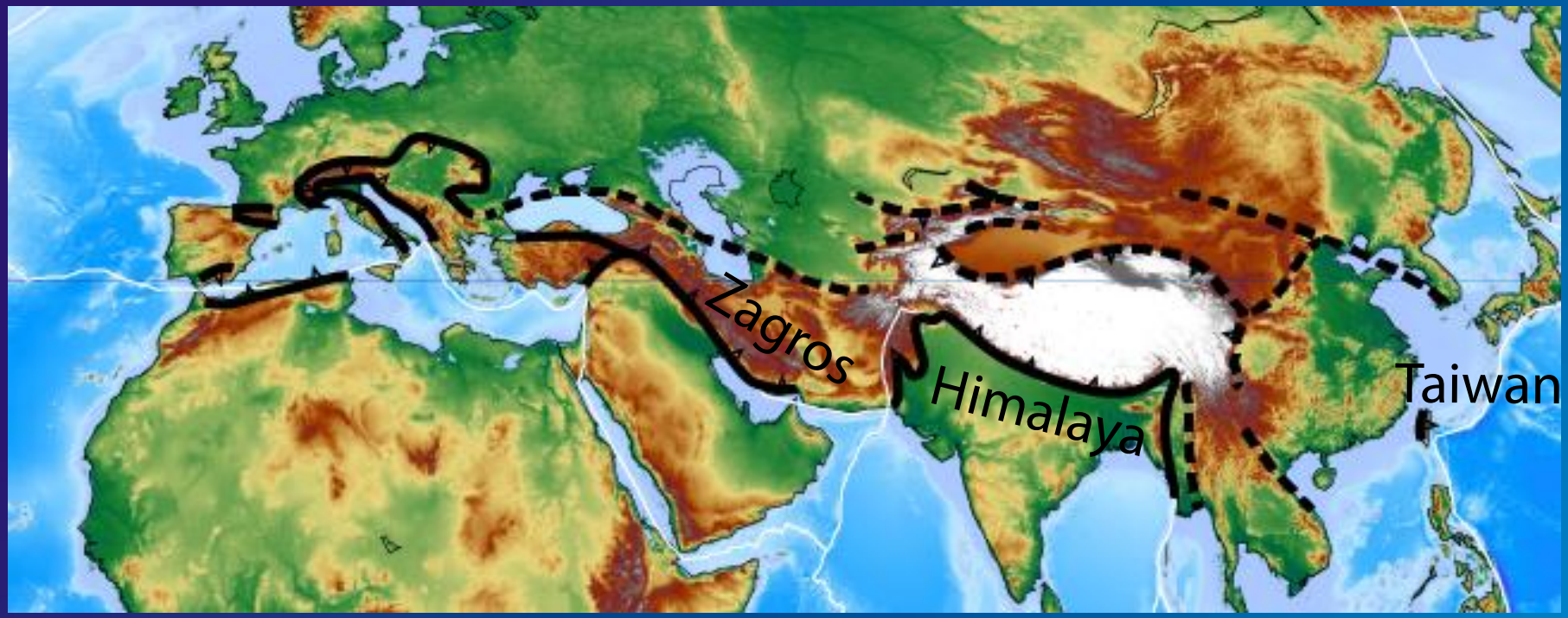

h < 10 km

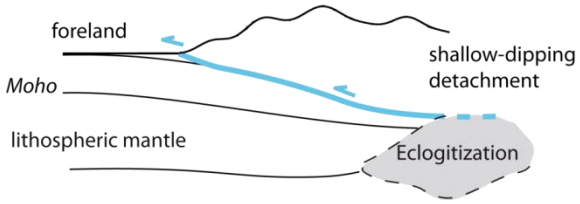

h > 15-20 km

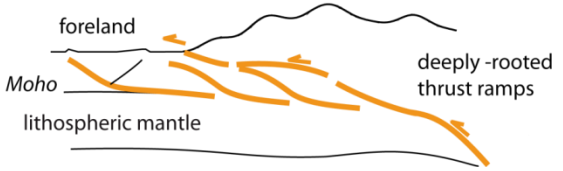

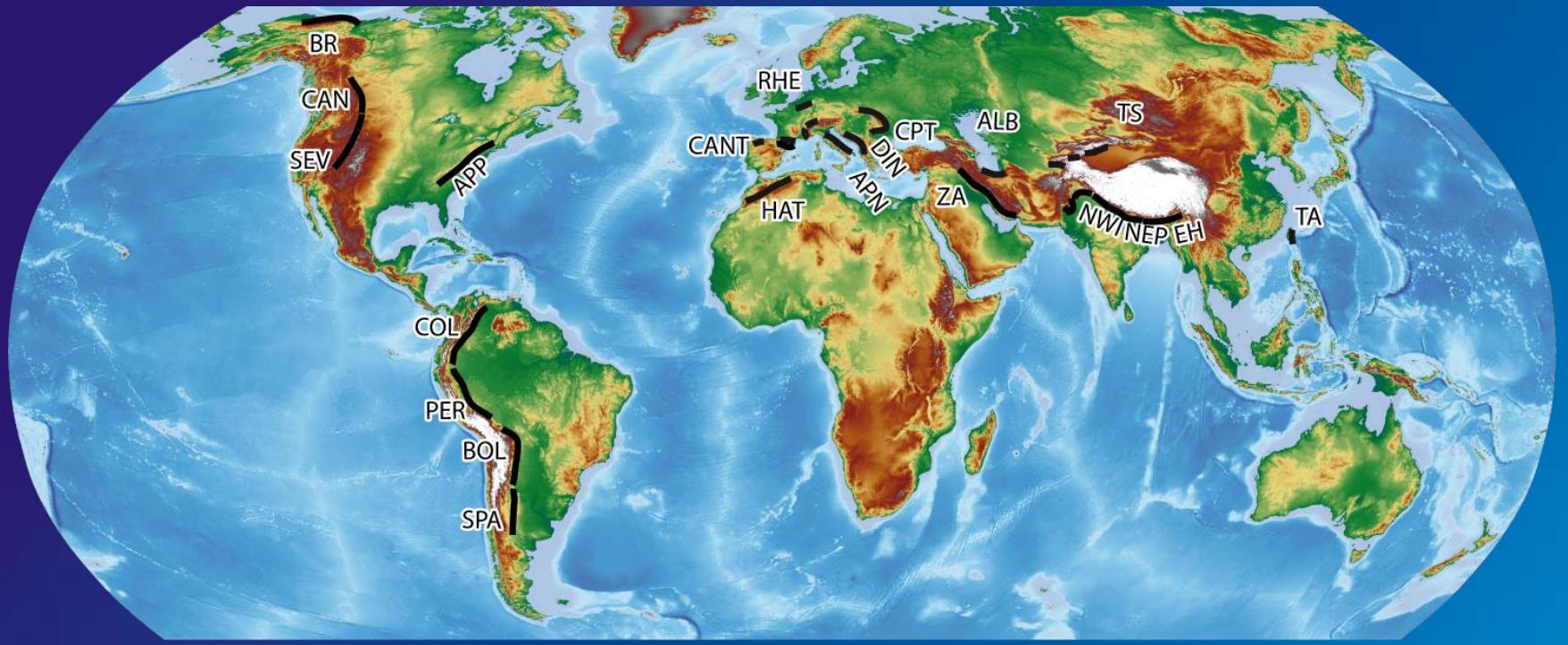

Estimates of shortening in 30 fold-and-thrust belts worldwide

Courtesy of F. Mouthereau

Shortening /structure

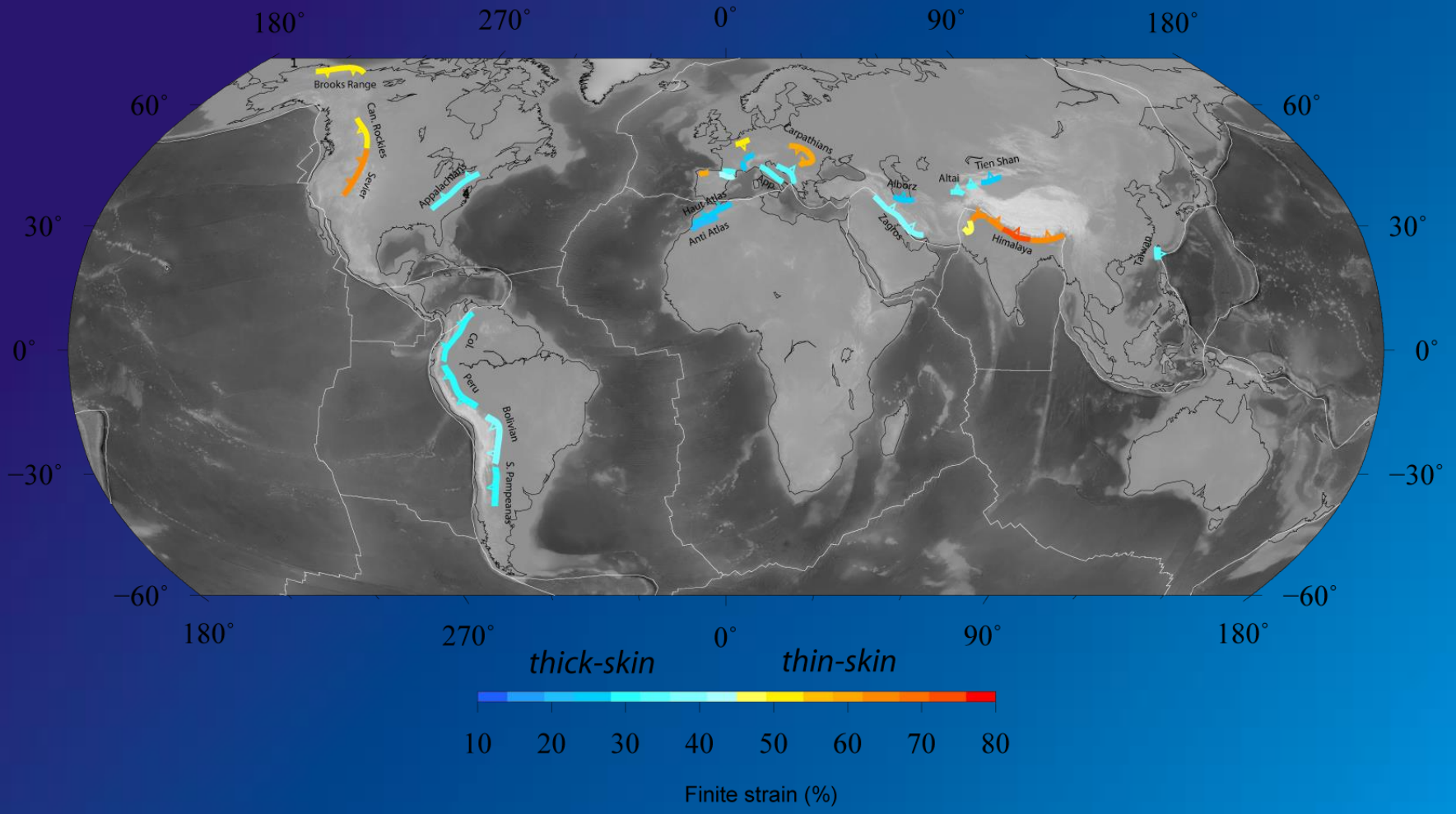

Thin-skinned ~40-75%
Thick-skinned ~20-40%

Long-term strength of continents

(18,633 Te values)

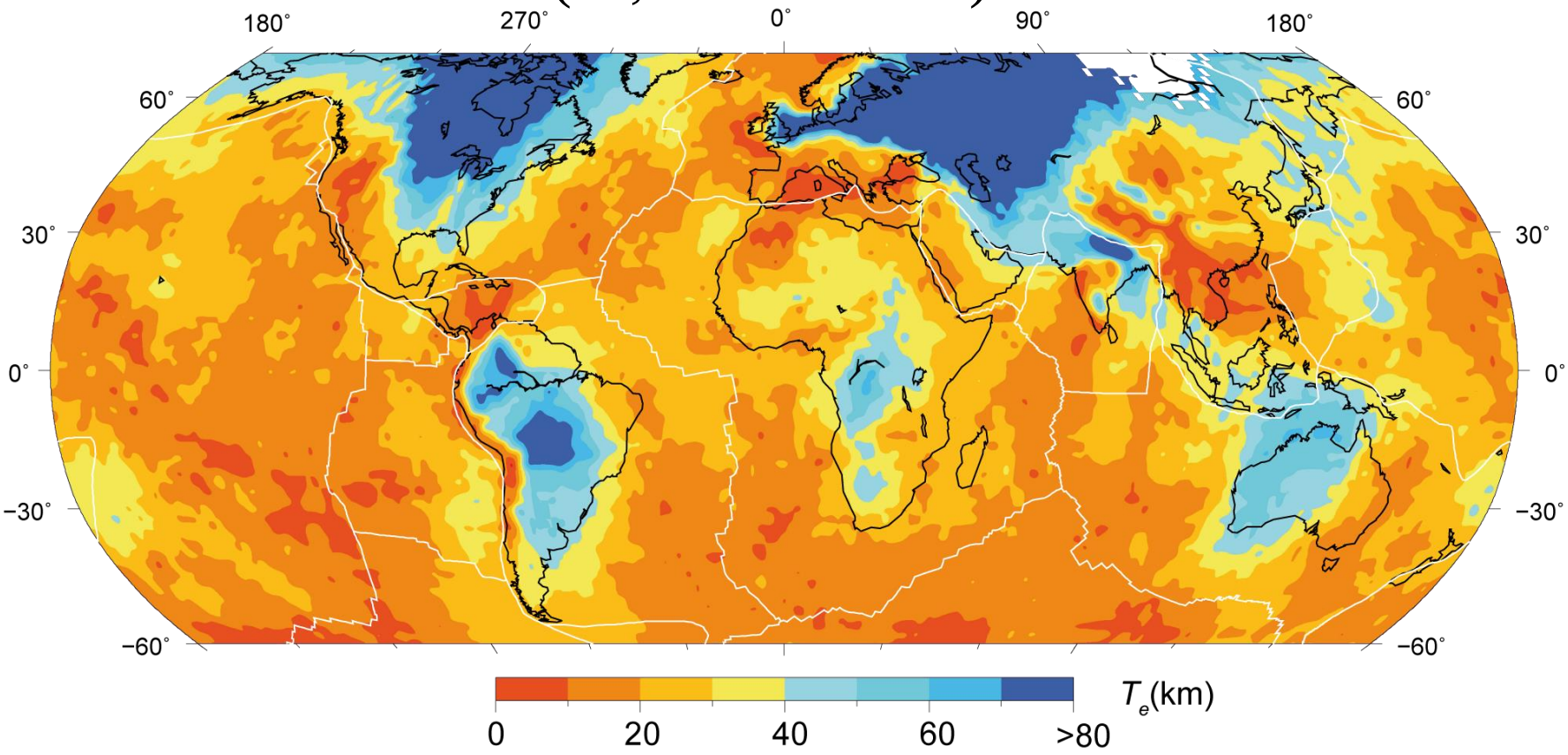

Gravimetry + flexure analysis

Mouthereau et al. (2013)

Thermotectonic age of continents
= age of the last tectono-magmatic event

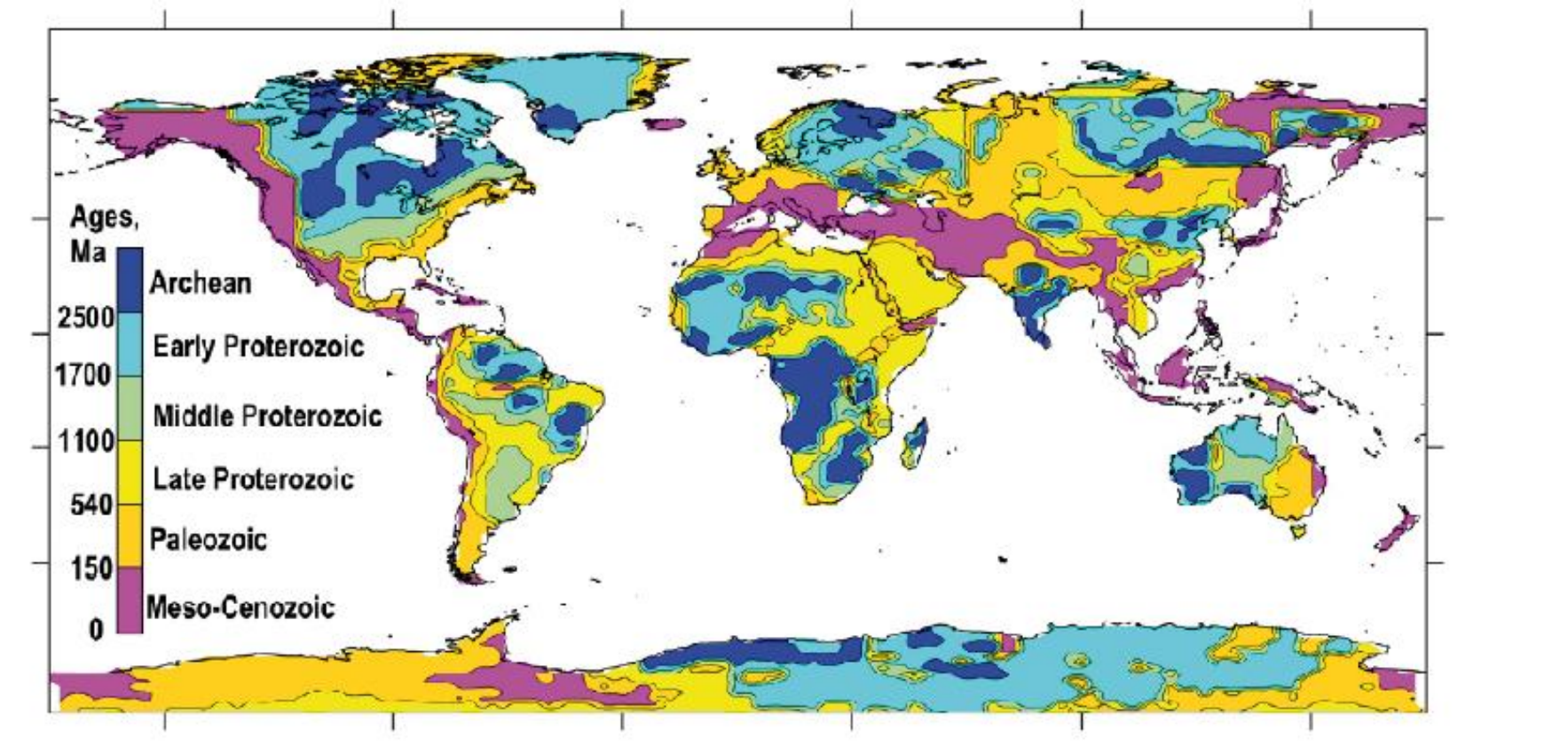

Artemieva (2006)

Mouthereau et al. (2013)

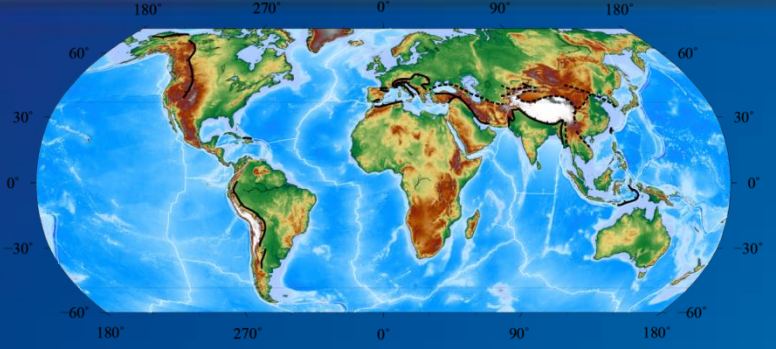

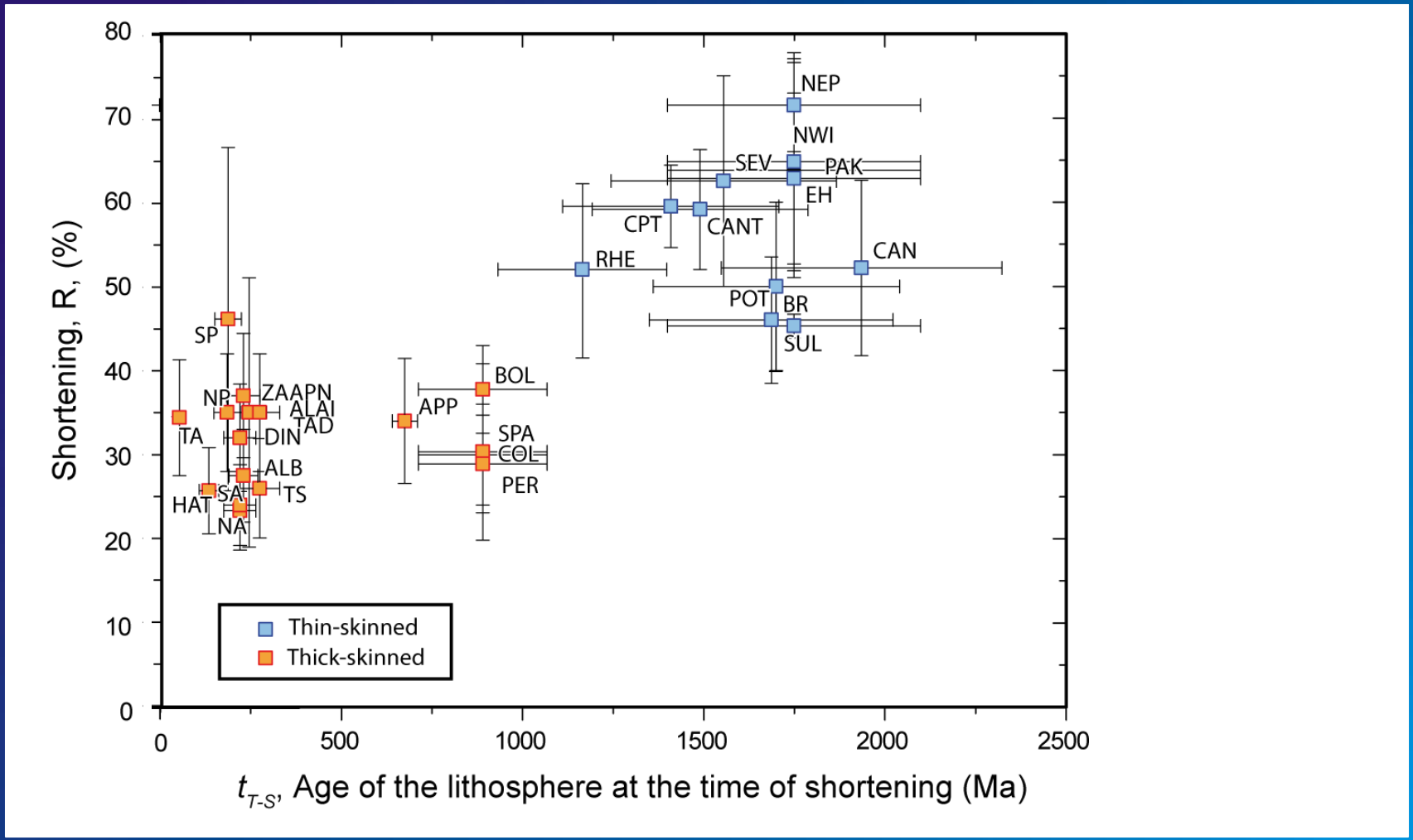

Thick-skinned fold-thrust belts

Pure-shear ('inversion/ collision') style

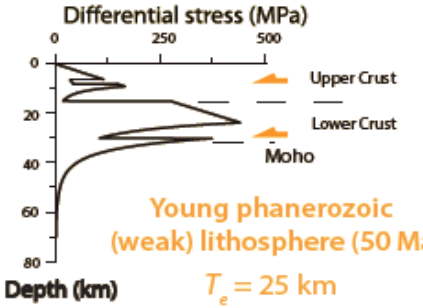

Young phanerozoic (weak) lithosphere (50 Ma)

T_e = 25 km

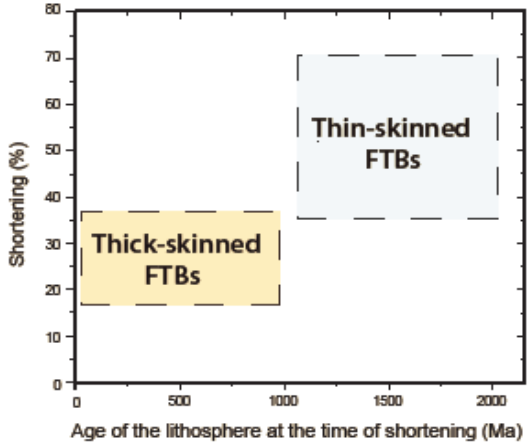

Thin-skinned fold-thrust belts

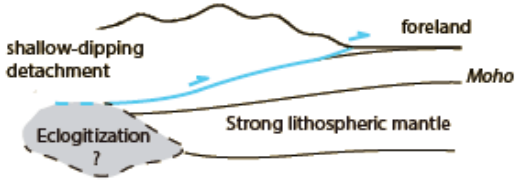

Simple-shear ('subduction') style

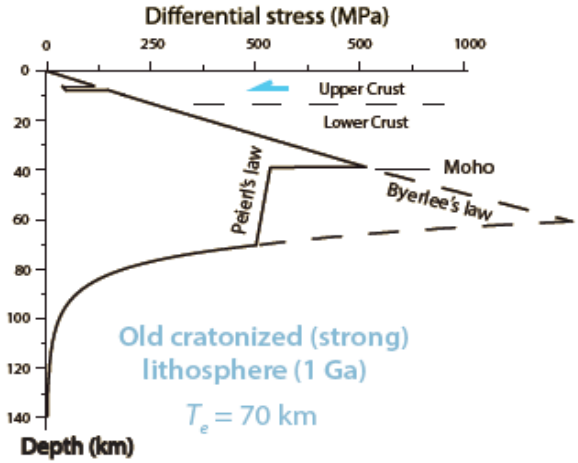

Old cratonized (strong) lithosphere (1 Ga)

T_e = 70 km

There are increasing lines of evidence of basement-involved shortening in FTBs, even in the 'archetypal' thin-skinned belts. This basement involvement is often associated with basement inversion tectonics.

The pre-orogenic deformation of the basement may control the geometry, kinematics and mechanics of FTBs, either at the scale of the whole belt (e.g., belt curvature, segmentation and along-strike variations of structural styles, sequence of deformation, localization of contractional deformation and % of shortening) or at the scale of tectonic units (reactivation of inherited basement faults, basement-cored folding). In some cases however, inherited basement (normal) faults are not reactivated whereas newly-formed compressional shear zones develop, which brings into question the bulk rheology of the crust vs the rheology of preexisting fault zones available for reactivation.

In basement-involved, thick-skinned FTBs, shortening is distributed throughout the whole crust and is usually lower than in their thin-skinned counterparts, which likely requires/reflects a specific thermo-mechanical behavior of the underlying lithosphere (e.g, hot and young, hence weak). In FTBs resulting from inversion of former proximal passive margins, basement thrusting that occurs in a rather localized way in their inner parts requires structural inheritance and/or a hot crustal temperature either inherited from a recent (pre- orogenic) rifting event or resulting from syn-orogenic underthrusting and heating.

Basement-involvement in FTBs raises the question of the way the orogen is mechanically coupled to the foreland and how orogenic stresses are transmitted through the heterogeneous basement of the foreland/plate interior. Development of thick-skinned belts within cratons remains somewhat enigmatic and likely requires specific boundary conditions (strong interplate coupling, such as provided by flat-slab subduction) ensuring efficient transmission of stresses (crustal/lithospheric stress guide) and propagation of deformation in the pro- and retro-foreland by crustal/lithospheric buckling or deep crustal decollement, in addition to local structural and/or possible physical/compositional weakening.

Thank you
for your attention…

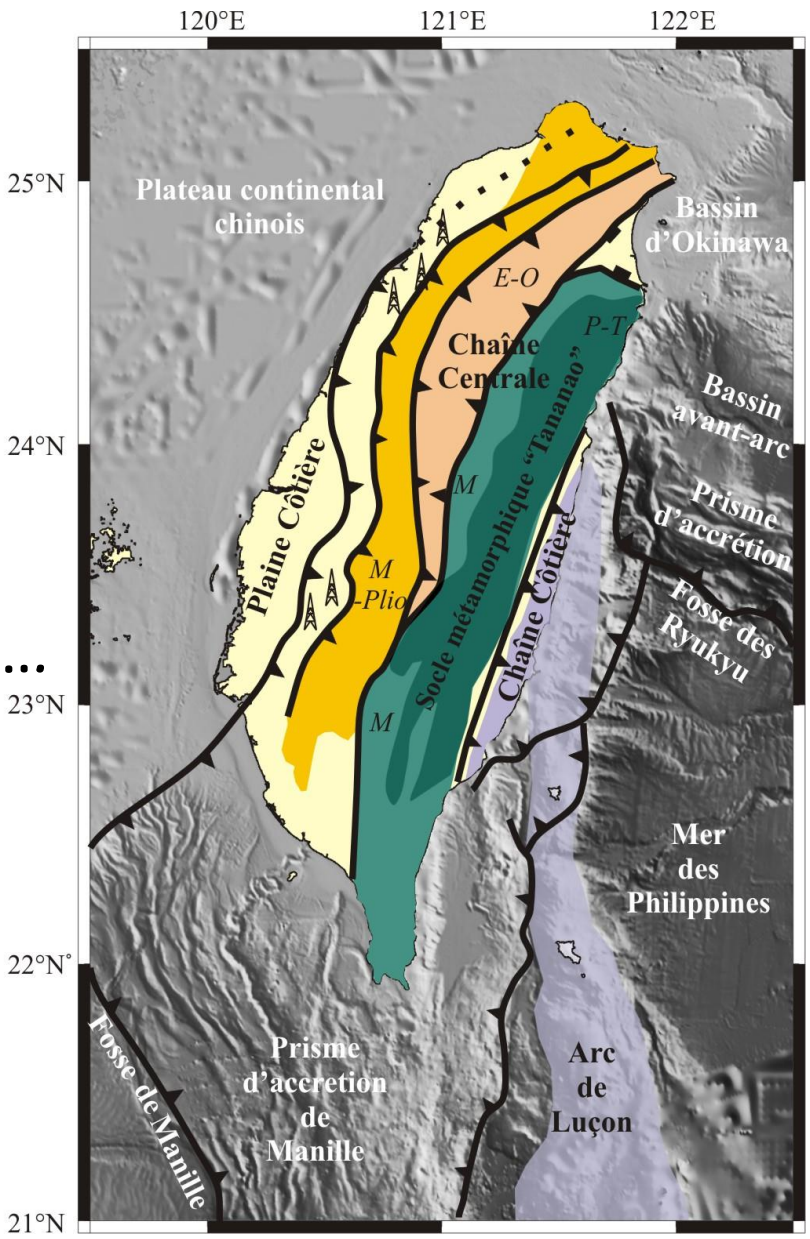

Suggested readings :

Lacombe O. & Mouthereau F., 2002. Basement-involved shortening and deep detachment tectonics in forelands of orogens : insights from recent collision belts (Taiwan, western Alps, Pyrenees). ***Tectonics****, 21, 4, 1030*

Lacombe O. & Bellahsen N., 2016. Thick-skinned tectonics and basement-involved fold-thrust belts. Insights from selected Cenozoic orogens. ***Geological Magazine****, 153, 5-6, 763-810*

Mouthereau F. & Lacombe O., 2006, Inversion of the Paleogene Chinese continental margin and thick-skinned deformation in the western foreland of Taiwan, ***J. Struct. Geol.****, 28, 1977-1993*

Mouthereau F., Deffontaines B., Lacombe O. & Angelier J., 2002. Variations along the strike of the Taiwan thrust belt : Basement control on structural style, wedge geometry and kinematics. In Byrne T.B., and Liu C.-S., eds, Geology and Geophysics of an Arc-Continent Collision, Taiwan, Republic of China, Boulder, Colorado, ***Geol. Soc. Am. Spec. Pap.****, 358, chapter 3, 35-58*

Mouthereau, F.,Watts, A.B., & Burov, E., 2013. Structure of orogenic belts controlled by lithosphere age. ***Nature Geosciences****, 6 (9), 785-789*